OPTIMAL CAPACITOR PLACEMENT TO MINIMISE HARMONICS IN POWER SYSTEMS AND SOFTWARE TOOLS

Prepared by: Helmuth Victor Hitzeroth

Prepared for: The Department of Electrical and Electronic Engineering
University of Cape Town
Private Bag
Rondebosch / Cape Town
7700
Republic of South Africa

Supervisor: Professor Alexander Petroianu
Corporation Chair: Power System Engineering

Date: December 1995

This thesis is prepared in fulfilment of the requirements for the Master of Science Degree in Electrical and Electronic Engineering (MSc (Eng)).

Acknowledgements

Throughout my studies at the University of Cape Town I received help and support in many ways, from various people. I would like to take this opportunity of thanking the following persons in particular:

- Prof. A. Petroianu for having set aside time for this research project, for his generous support and for his checking of the thesis.

- Eskom for providing financial support for conducting this research project.

- Mr. R. G. Koch for acting as mediator between Eskom and the University of Cape Town in all matters regarding this project, as well as for his personal interest concerning it.

- Prof. M. Braae for the useful discussions with him, in particular as regards the sections on the state space model in chapter 6.

- My colleagues at the Department of Electrical and Electronic Engineering for the useful discussions, criticisms, ideas and encouragement.

- My family and friends for their constant support and understanding.

Terms of Reference

In 1993 Eskom approached the Department of Electrical and Electronic Engineering of the University of Cape Town with the request to investigate the effects of harmonics in power systems. Following an informal agreement to this effect, two final year BSc (Eng) students investigated this topic, which resulted in two BSc (Eng) theses in the same year.

1. The one thesis [1 - 3], developed a power system harmonic analysis software programme for students. This programme was also verified by way of comparison with other commercial software packages.

2. The other thesis [4], investigated harmonic phenomena in power systems, with the aid of specific power system harmonic analysis software packages. The results obtained with the different software packages were subsequently analysed and compared.

However, the completion of the two theses showed that the amount of work required for an exhaustive and adequate investigation of the effects of harmonics in power systems was far more than could be expected by way of two BSc(Eng) theses. A formal agreement was therefore reached between Eskom and the Department of Electrical and Electronic Engineering of the University of Cape Town in 1994, to extend the project and to conduct more particular research into the effects of harmonics in power systems. The topics for this purpose were identified in consultation with Eskom and were meant to cover their particular requirements and priorities. The scope of this more comprehensive project was meant to cover the following specific topics:

1. A comprehensive review of the theory of harmonics in power systems.

2. An investigation of the algorithms that are used for harmonic analysis in power systems, particularly the companion circuit method, the Newton-Raphson method, the Gauss-Seidel method and the current injection method.

3. A study and comparison of harmonic analysis software programmes for power systems. In particular this comparison should cover the advantages and disadvantages, facilities, user-friendliness, interfaces and a sensitivity analysis of modelling parameters of the various harmonic analysis programmes.

4. An investigation and quantification of sensitive parameters in the simulation of harmonics in power systems, with special reference to the modelling of different network elements, namely: transformers, distribution lines, transmission lines and loads.

5. The investigation of a theoretical foundation for addressing the problems associated with harmonics in radial and meshed power systems.

6. The mitigation or possible elimination of the undesirable effects of harmonics in radial and meshed power systems.

Given the wide scope and complexity of the research project (as set out above, items 1. to 6.), it was thought appropriate to make it the research topic of one MSc (Eng) thesis and several supplementary BSc (Eng) theses. The present MSc (Eng) thesis was therefore commissioned by prof. A. Petroianu in January 1994 and I was given the task of addressing the research topics as listed above (items 1. to 6.), which included co-supervising the planned supplementary BSc (Eng) theses. The specific topics that were set aside for final year BSc (Eng) theses were the following:

- An investigation into the algorithms used for harmonic analysis (item 2. above).
- A comparison of power system harmonic analysis software programmes (item 3. above).
- The modelling of networkelements (item 4. above).

The envisaged research work on these topics was conducted during 1994 and 1995 under my co-supervision. This entailed discussions with the students concerned, analysing the problems and objectives, formulating steps to address the problems and continued support in the execution of the research work. All of the envisaged BSc (Eng) theses have already been completed, as follows:

- The first thesis [5], deals mainly with the modelling of transformers.
- The second thesis [6], discusses the modelling of a 22 kV distribution line.
- The third thesis [7], investigates the modelling of a 400 kV transmission line.
- The fourth thesis [8], deals with the harmonic modelling of loads in power systems.

Overall there are now six undergraduate theses and one masters degree thesis available, that deal with the above mentioned topics.

The present MSc (Eng) thesis therefore will not present the detailed work and results covered in all the supplementary BSc (Eng) theses (mentioned above), but will merely refer to their major findings and conclusions.

References

[1] P. G. Mbuyazi, " Prestudy: Harmonic Load Flow Analysis", *BSc (Eng) Thesis*, University of Cape Town, Republic of South Africa, 1993.

[2] P. G. Mbuyazi, " The Voltage Prediction Tool: User's Manual", *BSc (Eng) Thesis*, University of Cape Town, Republic of South Africa, 1993.

[3] P. G. Mbuyazi, "The Investigation of Power System Harmonic Voltages and the Development of a Teaching Tool for Undergraduate Students", *BSc (Eng) Thesis*, University of Cape Town, Republic of South Africa, 1993.

[4] M. W. Roberts, " Analysis of the Harmonic Impedance of a Transmission Network using the ATP and V-Harm Software Packages", *BSc (Eng) Thesis*, University of Cape Town, Republic of South Africa, 1993.

[5] R. Hawkins, " Study of Transformer Modelling in Harmonic Analysis and the Ability of Various Software Packages to Implement the Different Models", *BSc (Eng) Thesis*, University of Cape Town, Republic of South Africa, 1994.

[6] G. W. Rowse, "A Harmonic Parametrical Study of a 22kV Transmission Line using EMTP and V-Harm", *BSc (Eng) Thesis*, University of Cape Town, Republic of South Africa, 1994.

[7] V. Maharaj, "A Harmonic Parametrical Study of a 400kV Transmission Line using Harmonic Simulation Tools", *BSc (Eng) Thesis*, University of Cape Town, Republic of South Africa, 1995.

[8] R. Abrahams, "Power System Load Analysis for Harmonic Studies", *BSc (Eng) Thesis*, University of Cape Town, Republic of South Africa, 1995.

Synopsis

Harmonics in power systems is a relatively new area of research. In view of this and the growing awareness of the quality of the electricity supply, the theory of harmonics in power systems is reviewed. The sources and the effects of harmonics are investigated. The algorithms that are used for the frequency analysis of power systems are investigated and compared. These algorithms comprise the companion circuit method, the Gauss-Seidel method, the Newton-Raphson method and the current injection method. In addition various freely and commercially available software packages for the harmonic analysis of power systems are studied and compared. For this purpose a questionnaire was sent out to software developers and suppliers. This questionnaire as well as the results of the comparative investigation are presented.

A power system has many configurations due to the switching of power capacitors on to and off the power grid. Some of these configurations can result in unacceptable distortion levels. An existing state space method is investigated to analyse these configurations and an example is worked through, to illustrate how this method works. However, this state space model is only applicable to radial power systems and there have to be power capacitors at the end of every feeder amongst others. Because of these significant disadvantages of this method, a new analytical approach or theoretical foundation for the analysis of power capacitors in radial as well as meshed power systems is developed in this thesis. For this purpose the branch current and nodal voltage equations are determined. Redundant nodal voltages are eliminated from the set of branch current equations. The remaining equations and the nodal voltage equations are then combined to form a system realisation. This system realisation is still overspecified and a further reduction is done to obtain a minimal realisation of the power system. This approach is demonstrated analytically and numerically by way of five case studies. This approach is also verified by comparing it with the current injection method. Identical results are obtained with the state space approach and with the current injection method, demonstrating that the state space approach is indeed valid.

Finally methods for the mitigation and elimination of the undesirable effects of harmonics in power systems are addressed. A new method of achieving the reduction of harmonics is developed. This method makes use of a neighbourhood search algorithm in order to optimally place power capacitors so that they cause minimal distortion and also filter out harmonics. A new specific objective function subject to constraints, making use of pole / zero placement is developed for this purpose. An example is worked through to illustrate the application of the method. This objective function is improved upon, resulting in a new specific objective function subject to constraints, making use of H_2 and $H\infty$ norm principles. This objective function is combined with the simulated annealing optimisation algorithm. Once again a case study is done to demonstrate the application of the method.

Table of Contents

		Page
Acknowledgements		II
Terms of Reference		III
Synopsis		VII
Table of Contents		IX
List of Illustrations		XIII
List of Tables		XVI
Chapter 1: Introduction		1
1.1	Overview	1
1.2	Accomplishments	2
1.3	References	3
Chapter 2: Literature Review of the Theory of Harmonics in Power Systems		5
2.1	Introduction	5
2.2	Power Quality	5
2.3	Harmonics	7
2.4	Subharmonics	9
2.5	Interharmonics	9
2.6	Characteristic and Non-Characteristic Harmonics	9
2.7	Fundamental and Harmonic Power	9
2.8	Composition and Decomposition of Periodic Waves	10
2.9	Distorted Wave Shapes	12
2.10	Harmonics and Sequence Components	13
2.11	Causes of Voltage and Current Wave Distortion in Power Systems	15
2.12	Harmonic Penetration	18
2.13	Resonance	19
2.14	The Effects of Harmonics on Equipment in a Power System	24
2.15	Mitigation or Elimination of Harmonics	25

2.16 References 26

Chapter 3: Literature Review of the Theory of Algorithms used for Harmonic Analysis in Power Systems and Comparison thereof 33

3.1 Introduction 33

3.2 Companion Circuit Method 33

3.3 Gauss-Seidel Method 35

3.4 Newton-Raphson Method 38

3.5 Comparison of the Gauss-Seidel and Newton-Raphson Methods 47

3.6 The Current Injection Method 49

3.7 Comparison of Harmonic Analysis Methods 51

3.8 Discussion 52

3.9 Case Study 53

3.10 References 60

Chapter 4: Comparison of Harmonic Analysis Software Packages for Power Systems 63

4.1 Introduction 63

4.2 Questionnaire on Harmonic Analysis Software Programmes for Power Systems 63

4.3 Evaluation of the Results of the Survey on Harmonic Analysis Programmes for Power Systems 64

4.4 Harmflo 66

4.5 V-Harm 66

4.6 The Harmflo+ Workstation 66

4.7 Hi_Wave 70

4.8 Harmonique 70

4.9 ETAP 70

4.10 CYMHARMO 71

4.11 PCFLO 71

4.12 ERACS 71

4.13 Electrical Distribution System Analysis Programs (EDSA) 71

4.14 DigSilent 72

4.15 EMTP 73

4.16 Matlab 75
4.17 Maple 76
4.18 Conclusion and Recommendations 76
4.19 References 77

Chapter 5: Analysis of an Existing State Space Model for Radial Power Systems and the Development of a New State Space Model for Radial and Meshed Power Systems 81

5.1 Introduction 81
5.2 Existing State Space Model for Radial Power Systems 81
5.2.1 Case Study Using the Existing State Space Model 84
5.3 Derivation of a New State Space Model for Radial and Meshed Power Systems 86
5.3.1 Obtaining the equations 86
5.3.2 Reducing equation (5.3.1.1) 87
5.3.3 Derivation of a Reduction Formula for a Node to be Eliminated, Adjacent to Nodes with Capacitors 88
5.3.4 Derivation of a Reduction Formula for Two Adjacent Nodes to be Eliminated, Adjacent to Nodes with Capacitors 89
5.3.5 Derivation of a Reduction Formula for Three or More Adjacent Nodes to be Eliminated, Adjacent to Nodes with Capacitors 91
5.3.6 Developing the New State Space Model 91
5.3.7 Obtaining a Minimal Realisation of the System 93
5.3.8 Flowchart for the Derivation of the State Space Model 94
5.3.9 Case Studies 95
5.4 References 111

Chapter 6: New Methods of Mitigating or Eliminating Harmonics by Optimal Capacitor Placement 114

6.1 Introduction 114
6.2 Configuration Space 114
6.3 Move Set 114
6.4 Objective Function or Cost Function 115

6.4.1 Case Study 1 115

6.4.2 Case Study 2 116

6.5 Exhaustive Search 118

6.6 Greedy Search 118

6.7 Neighbourhood Search 118

6.7.1 Case Study 3 119

6.8 Simulated Annealing 126

6.8.1 Case Study 4 128

6.9 References 132

Chapter 7: Conclusions and Future Research 135

Appendix A Questionnaire on Harmonic Analysis Programmes for Power Systems 138

Appendix B Results of the Survey of Harmonic Analysis Programmes for Power Systems 146

Appendix C Paper submitted to the 1996 Power Systems Computation Conference, Dresden, Federal Republic of Germany, August 1996 163

Appendix D Summary and Paper to be submitted to the 1996 IEEE Summer Meeting and Transactions, Denver, United States of America, July 1996 171

Appendix E Paper presented at the South African Universities Power Engineering Conference, Pretoria, Republic of South Africa, January 1995 179

Appendix F Summary of the Paper submitted to the South African Universities Power Engineering Conference, Johannesburg, Republic of South Africa, January 1996 184

Appendix G Matlab Programmes written for this thesis 186

List of Illustrations

Page

Chapter 2

Figure 2.3.1	The fundamental sinusoid with its second harmonic.	7
Figure 2.3.2	The fundamental sinusoid with its third harmonic.	8
Figure 2.3.3	The fundamental sinusoid with its fourth harmonic.	8
Figure 2.3.4	The fundamental sinusoid with its fifth harmonic.	8
Figure 2.8.1	The fundamental sinusoid and its third harmonic.	10
Figure 2.8.2	Superposition of the fundamental sinusoid and its third harmonic.	10
Figure 2.8.3	Superposition of the fundamental sinusoid, its third and its fifth harmonic.	11
Figure 2.8.4	The fundamental sinusoid, its third and its fifth harmonic.	11
Figure 2.8.5	A square wave.	12
Figure 2.10.1	Balanced three phase voltage or current with the third harmonics.	15
Figure 2.11.4.1	Arc furnace waveshapes, phase current drawn and the resulting voltage on the bus.	17
Figure 2.12.1	Propagation of harmonic voltages and currents through a power system.	19
Figure 2.13.1.1	One-line diagram of a plant utilising several static converter motor drives.	21
Figure 2.13.1.2	Equivalent circuit of the plant shown in figure 2.13.1.1.	21
Figure 2.13.1.3	Impedance *versus* frequency curve, for the plant shown in figure 2.13.1.1.	21
Figure 2.13.1.4	Current amplification *versus* frequency curve for the plant shown in figure 2.13.1.1, illustrating the effect of an increase in the resistance of the tank circuit.	22
Figure 2.13.1.5	Current amplification *versus* frequency curve for the plant shown in figure 2.13.1.1, illustrating the effect of an increase	

	in the load, due to additional low impedance paths.	22
Figure 2.13.2.1	A plant prone to series resonance.	23
Figure 2.13.2.2	Equivalent circuit for the plant shown in figure 2.13.2.1.	23
Figure 2.13.2.3	Impedance *versus* frequency curve for the plant shown in figure 2.13.2.1.	24
Chapter 3		
Figure 3.2.1	Companion circuit for an inductor.	34
Figure 3.9.1	Three bus network.	54
Figure 3.9.2	Voltage frequency response at bus 1.	55
Figure 3.9.3	Voltage frequency response at bus 2.	55
Figure 3.9.4	Voltage frequency response at bus 3.	56
Figure 3.9.5	Current injected by the harmonic current source.	56
Figure 3.9.6	Current frequency response through C2.	57
Figure 3.9.7	Current frequency response through C3.	57
Figure 3.9.8	Current frequency response through L1,2.	58
Figure 3.9.9	Current frequency response through L1,3.	58
Figure 3.9.10	Current frequency response through L2,3.	59
Figure 3.9.11	Current frequency response through L2.	59
Figure 3.9.12	Current frequency response through L3.	60
Chapter 4		
Figure 4.18.1	Overview of algorithms used by the different packages.	77
Chapter 5		
Figure 5.2.1.1	Two bus radial power system.	84
Figure 5.3.6.1	Block diagram of the state space model.	92
Figure 5.3.8.1	Flowchart for the derivation of the state space model.	94
Figure 5.3.9.1.1	3 bus meshed network.	95
Figure 5.3.9.2.1	3 bus meshed network.	99
Figure 5.3.9.3.1	Output voltage at bus 1.	103
Figure 5.3.9.3.2	Output voltage at bus 2.	103
Figure 5.3.9.3.3	Output voltage at bus 3.	104
Figure 5.3.9.3.4	Output voltage at bus 1.	104
Figure 5.3.9.3.5	Output voltage at bus 2.	105

Figure 5.3.9.3.6	Output voltage at bus 3.	105
Figure 5.3.9.4.1	16 bus meshed network.	108
Figure 5.3.9.5.1	Magnitude *versus* frequency diagram of the voltage at bus 9.	111
Chapter 6		
Figure 6.7.1.1	Flowchart of the neighbourhood search optimisation algorithm.	120
Figure 6.7.1.2	Positive sequence representation of the 18 bus radial network.	121
Figure 6.7.1.3	V-Harm output response before the optimisation.	123
Figure 6.7.1.4	Value of the objective function for each iteration.	124
Figure 6.7.1.5	V-Harm output response with the optimal capacitor assignment.	125
Figure 6.8.1.1	Linear frequency response of the 16 bus network before the optimal placement of capacitors.	129
Figure 6.8.1.2	Logarithmic frequency response of the 16 bus network before the optimal placement of capacitors.	129
Figure 6.8.1.3	Flowchart of the simulated annealing algorithm.	130
Figure 6.8.1.4	Linear frequency response of the 16 bus network after the optimal placement of capacitors.	131
Figure 6.8.1.5	Logarithmic frequency response of the 16 bus network after the optimal placement of capacitors.	132

List of Tables

		Page
Chapter 2		
Table 2.8.1	Fourier components of a square wave.	12
Table 2.10.1	Harmonics and their sequence components.	13
Chapter 3		
Table 3.5.1	Comparison of the Gauss-Seidel and Newton-Raphson methods for the fundamental frequency loadflow [13].	47
Table 3.5.2	Comparison of the Newton-Raphson fundamental loadflow and harmonic loadflow methods [13].	48
Table 3.7.1	Comparison of the current injection, Gauss-Seidel and Newton-Raphson methods [13].	52
Table 3.9.1	Data for the three bus power system.	54
Chapter 4		
Table 4.6.2.1	Device libraries for the different versions of SuperHarm [7].	69
Chapter 5		
Table 5.3.9.3.1	Numerical data for the case studies in sections 5.3.9.1 and 5.3.9.2.	102
Table 5.3.9.4.1	Generator data in per unit for the 16 bus network.	106
Table 5.3.9.4.2	Transformer data in per unit for the 16 bus network.	106
Table 5.3.9.4.3	Line data in per unit for the 16 bus network.	107
Table 5.3.9.4.4	Capacitor data in per unit for the 16 bus network.	107
Table 5.3.9.4.5	Coefficients of the A matrix.	109
Table 5.3.9.4.6	Coefficients of the B matrix transposed.	110
Table 5.3.9.4.7	Coefficients of the C matrix.	110
Table 5.3.9.4.8	Coefficients of the D matrix.	110
Chapter 6		
Table 6.7.1.1	Line and transformer data in percent of per unit for the 18 bus network.	122
Table 6.7.1.2	Lower system poles and zeros in per unit before the optimisation.	123
Table 6.7.1.3	Lower system poles and zeros in per unit with the optimal capacitor assignment.	125

Chapter 1

Introduction

1.1 Overview

The quality of the power supply has become increasingly more important in power system planning and operation, especially because of, on the one hand the recent boom in the computer industry and the increased sensitivity of equipment in general; and on the other hand because loads themselves also produce harmonics on the power grid [1, 2]. Disturbances on a power grid can be caused by any consumer and these disturbances can also propagate to remote branches of the power grid, causing problems at unexpected locations [3]. Harmonic problems arise when resonances are excited by harmonic currents. Resonance conditions lead to current multiplication and high harmonic voltage levels [4].

In order to ensure that supply quality does not deteriorate beyond acceptable limits, utilities and consumers have found it necessary to draw up injection contracts, according to which agreement is reached between the two parties involved (i.e. the consumer and the utility), as to who is responsible for certain disturbances on the power system. Once this has been established, the guilty party is required to correct the situation [5, 6].

Not only are various algorithms employed to analyse the effect of harmonic problems in power systems, but it is also necessary to have a proper understanding of the problem situations. As slight changes in the network configuration can cause huge improvements in the quality of the supply, it is necessary to utilise this optimally. In order to analyse a given situation it is necessary to choose a programme that is suitable for the given situation and also utilises an appropriate algorithm.

The installation of power capacitors on power systems causes a reduction of active power losses, a release in system capacities and a reduction of the voltage drop along a feeder. The

extent of these improvements depends greatly on the location, type and size of the power capacitors. However, the use of these power capacitors unfortunately also increases the potential for resonance conditions to arise. Most studies only consider the effects on the fundamental frequency and neglect the effects of harmonics [7 - 9]. Optimal capacitor sizes determined without considering their harmonic effects can result in unacceptable voltage distortion levels.

1.2 Accomplishments

In the first part of the thesis the theory of harmonics is reviewed and the different algorithms used for the harmonic analysis of power systems are investigated and compared. A software comparison of existing commercial and public domain software packages is also reported upon.

In the second part of the thesis, an existing state space model for the analysis of power systems is investigated. As this approach has significant disadvantages, a new system realisation for the analysis of harmonics in power systems is developed, which applies to radial as well as meshed power systems.

In the third part of the thesis the existing state space model method is used for the optimal placement of power capacitors. An objective function with constraints utilising pole / zero placement methods is specifically developed for this purpose. A neighbourhood search algorithm is used to determine the optimal power capacitor locations. This process is subsequently improved upon, by utilising the newly developed state space model approach. Another objective function with constraints is developed specifically for this purpose and is implemented with the aid of the simulated annealing algorithm. In this way the power capacitors are used in three ways, namely:

1. To keep the voltage profile of the bus that they are connected to within ±5% of one per unit.
2. To filter out unwanted harmonics.
3. To minimise harmonics, by placing them in strategic positions.

References

[1] G. T. Heydt, *Electric Power Quality*, Stars in a Circle Publications, West LaFayette, 1991.

[2] W. E. Kazibwe and M. H. Sendaula, *Electric Power Quality Control Techniques*, van Nostrand Reinhold, New York, 1993.

[3] IEEE Tutorial Course, *Power System Harmonics*, Course Text, 84 EH0221-2-PWR, 1984.

[4] J. Arrillaga, D. Bradley and D. Bodger, *Power System Harmonics*, John Wiley & Sons, New York, 1985.

[5] T. Deflandre, S. Arson and P. Rioual, "Working out a rule for connecting industrial customers generating harmonics", *Collection de notes internes de la Direction des Etudes et Recherches*, Electricite de France: Direction des Etudes et Recherches, 95NR00010, Juillet 1994.

[6] Eskom Quality of Supply Group, *Eskom Handbook on Quality of Supply*, Revision 1, August 1994.

[7] S. H. Lee and J. J. Grainger, "Optimum Placement of Fixed and Switched Capacitors on Primary Distribution Feeders", *IEEE Transactions on Power Apparatus and Systems*, Volume PAS 100, Number 1, January 1981, pages 345-352.

[8] J. J. Grainger and S. H. Lee, "Optimum Size and Location of Shunt Capacitors for Reduction of Losses on Distribution Feeders", *IEEE Transactions on Power Apparatus and Systems*, Volume PAS 100, Number 3, March 1981, pages 1105-1118.

[9] R. Baldick, " Co-ordination of Distribution System Capacitors and Regulators: An Application of Integer Quadratic Optimisation", *Control and Dynamic Systems: Analysis and Control System Techniques for Electric Power Systems: Advances in Theory and Applications: Part 2 of 4*, Volume 42, 1991, pages 245-291.

Chapter 2

Literature Review of the Theory of Harmonics in Power Systems

2.1 Introduction

In this chapter the general terminology and the relevant definitions regarding electric power quality and harmonics in the power system in particular, are explained. This theoretical background is necessary, for the understanding of the following chapters.

2.2 Power Quality

Power quality is a very broad area and not clearly defined [1 - 6]. For the purpose of this thesis, the term power quality refers to the measure, analysis and improvement of the bus voltage, usually a load bus voltage. It also refers to maintaining the bus voltage to be a perfect sinusoid, at the rated voltage and frequency [7]. Power quality problems can be divided into synchronous and asynchronous phenomena. Asynchronous refers to aperiodic phenomena and mainly comprise the following:

1. Noise
2. Asynchronous impulses
3. Asynchronous notches
4. Asynchronous sinusoidal waveforms
5. Flicker
6. Inrush currents
7. Geomagnetic disturbances

Synchronous refers to synchronism with the alternating current waveform and therefore implies a periodic steady state condition. Synchronous phenomena are therefore of a periodic nature, where the states are repeated according to the following formula:

$$f(t) = f(t+T) \tag{2.2.1}$$

where: f is a time based periodic function

t is time

T is the period of f

The fundamental period is normally 50 or 60 Hz for power systems, depending on the country that generates the power. In South Africa, the fundamental frequency is 50 Hz. Synchronous phenomena mainly include:

1. Harmonics
2. Synchronous impulses
3. Synchronous notches
4. Magnetising currents

Various indices and methods for quantifying the power quality are in use. The most important of these are mentioned below:

1. Total harmonic distortion
2. Telephone interference factor
3. Bus voltage and telephone influence weight product
4. Line current and telephone influence weight product
5. Distortion index
6. C-message weighted index
7. Flicker factor
8. Bandwidth
9. Maximum frequency
10. Maximum voltage
11. Maximum rate of rise of signal
12. Crest value
13. Area under the frequency response curve
14. Energy

2.3 Harmonics

The term harmonic originates from acoustics, where it refers to the vibration of a string or column of air at a frequency that is a multiple of the basic (fundamental) frequency [8].

In the case of electrical signals, a harmonic is defined as a sinusoidal wave with a frequency given by:

$$f = n \cdot 50 \qquad (2.3.1)$$

where: f is the frequency

n is an integer

Figures 2.3.1 to 2.3.4. show the fundamental harmonic together with its second, third, fourth and fifth harmonic components respectively.

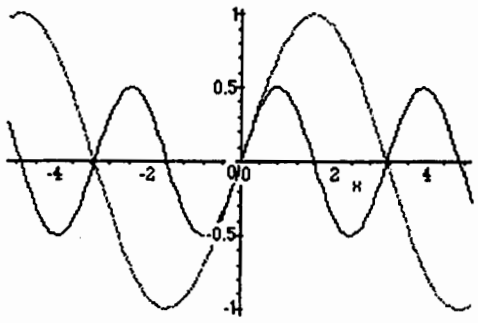

Figure 2.3.1: The fundamental sinusoid with its second harmonic.

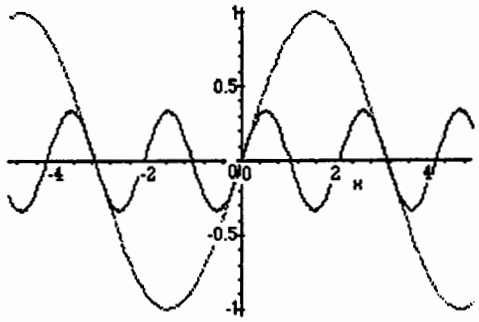

Figure 2.3.2: The fundamental sinusoid with its third harmonic.

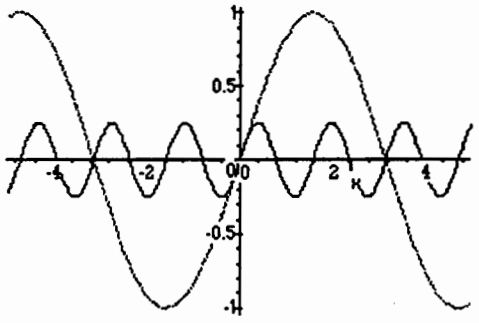

Figure 2.3.3: The fundamental sinusoid with its fourth harmonic.

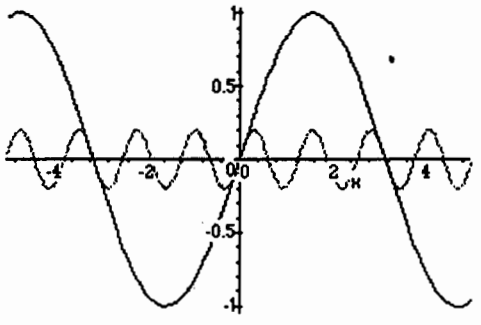

Figure 2.3.4: The fundamental sinusoid with its fifth harmonic.

2.4 Subharmonics

Subharmonics are frequencies that are lower than the fundamental frequency [8]. In equation *(2.3.1)*, f is a subharmonic when n is less than one.

2.5 Interharmonics

Interharmonics are frequencies that are situated between the harmonics [8]. If equation *(2.3.1)* is used, in the case of interharmonics, n would take on values >1 and never equal an integer.

2.6 Characteristic and Non-Characteristic Harmonics

Characteristic or synchronous harmonics are produced when a repetitive distortion pattern arises. In this way the same frequency spectrum arises every time. With the aid of this frequency spectrum specific network elements can be identified. Non-characteristic or asynchronous harmonics result when there are slight variations in the characteristic frequency spectrum, such as the delay of the firing instants in the case of thyristors by one degree [9].

2.7 Fundamental and Harmonic Power

The concepts of power for harmonics are still vague and not clearly defined [10]. However, for the purpose of this thesis, harmonic power is produced according to the following formula:

$$P_h = V_h \cdot I_h \cdot \cos\theta_h \qquad (2.7.1)$$

where:
- P_h is the harmonic power
- V_h is the harmonic voltage
- I_h is the harmonic current
- θ_h is the angle between the harmonic current and voltage
- h denotes the number of the harmonic order

The fundamental current and fundamental voltage, when h=1 in equation *(2.7.1)*, together produce fundamental power.

Fundamental power represents useful power. Harmonic power is normally dissipated as heat or produces other losses of energy, such as negative torques or vibrations [8].

2.8 Composition and Decomposition of Periodic Waves

By using the Fourier transformation, any periodic wave can be obtained by the superposition of sinusoidal waves [11]. This process is shown in figures 2.8.1 and 2.8.2. In figure 2.8.1 the different frequency components are shown, in figure 2.8.2 the two frequency components are added or superimposed and the resultant is shown.

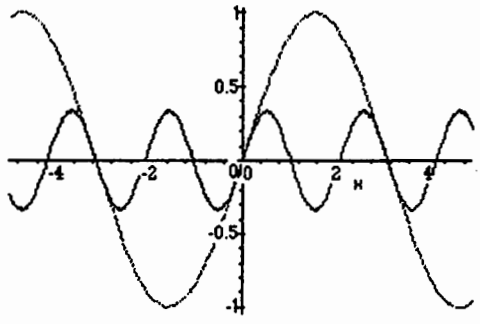

Figure 2.8.1: The fundamental sinusoid and its third harmonic.

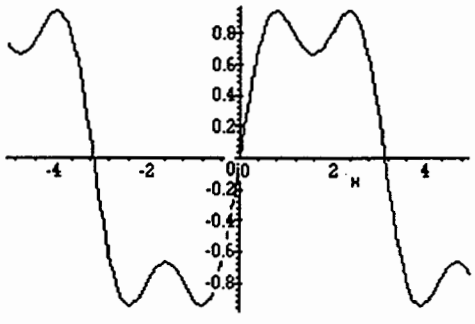

Figure 2.8.2: Superposition of the fundamental sinusoid and its third harmonic.

In a similar way, as shown in figures 2.8.1 and 2.8.2, any periodic wave can be decomposed into its harmonic components, by reversing the procedure [11]. This is demonstrated in figures 2.8.3 and 2.8.4, for a sinusoidal wave.

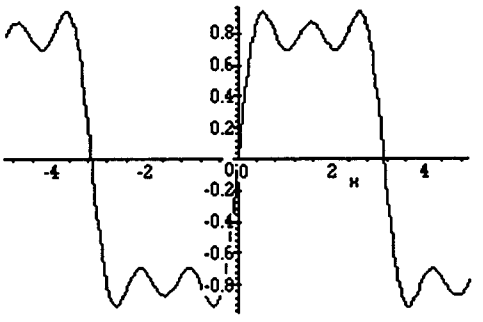

Figure 2.8.3: Superposition of the fundamental sinusoid, its third and fifth harmonic.

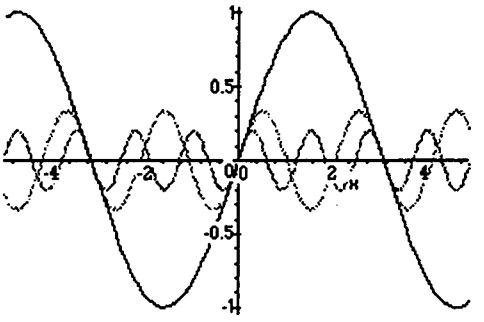

Figure 2.8.4: The fundamental sinusoid, its third and fifth harmonic.

When a Fourier transformation is done on a square wave, many higher order harmonics with lower amplitudes will result, due to the sharp corners of the square wave [11]. This is illustrated in figure 2.8.5 and table 2.8.1. It should be noted, that the Fourier components of a symmetrical square wave consist of odd harmonics with a harmonic amplitude of the inverse of the harmonic order.

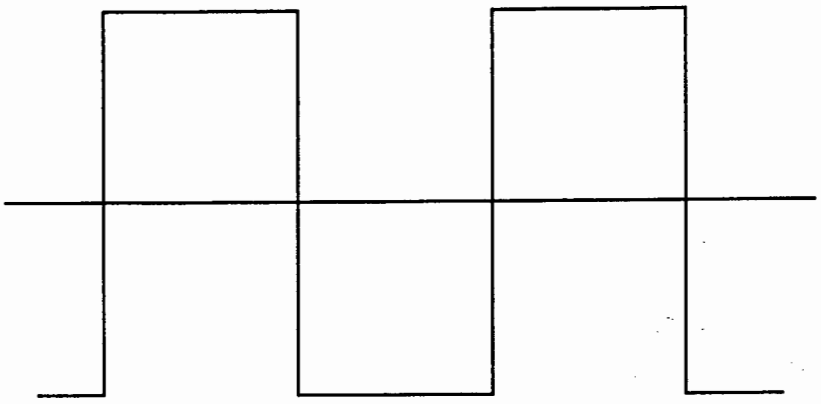

Figure 2.8.5: A square wave.

Harmonic Order	Frequency in Hz	Amplitude in per unit of the Fundamental
1	50	1.0
3	150	1/3
5	250	1/5
7	350	1/7
9	450	1/9
.	.	.
n	50**n*	1/*n*

Table 2.8.1: Fourier components of a square wave.

Other transformations are also often used for the analysis of harmonics in power systems. These are mainly the Laplace transformation, the Walsh transformation [12], as well as the Hartley transformation [13, 14]. However, the Fourier transformation is the most popular and the most widely used.

2.9 Distorted Wave Shapes

When the fundamental and the harmonic waves are superimposed the phase relationship between a harmonic and the fundamental and the amplitude of the harmonic order, determine

the final shape of the resultant wave. Some of the most common distorted wave forms are shown and analysed in [15].

2.10 Harmonics and Sequence Components

When harmonics are injected on a three phase basis, they can also be analysed in terms of sequence components [16]. In a balanced system, where harmonics are a direct result of three phase distortion of positive sequence voltages, the following pattern applies:

Sequence	Positive Sequence	Negative Sequence	Zero Sequence
Harmonic Order	1	2	3
	4	5	6
	7	8	9
	10	11	12
	13	14	15
	.	.	.

Table 2.10.1: Harmonics and their sequence components.

However, table 2.10.1 only applies to a perfectly balanced and symmetrical system, where the same distortion will appear on each of the phases, except for the 120° phase shift between the phases. In this case the harmonic voltage for each phase is given by:

$$V_{ah} = V_h \angle(\beta_h) \qquad (2.10.1)$$

$$V_{bh} = V_h \angle(-120° h + \beta_h) \qquad (2.10.2)$$

$$V_{ch} = V_h \angle(120° h + \beta_h) \qquad (2.10.3)$$

where: V_a is the voltage of phase a

V_b is the voltage of phase b

V_c is the voltage of phase c

h is the harmonic order

β is the voltage phase angle of phase a

If the Fourier fundamental frequency is taken as the principal frequency, h will take on integer values. However, when the period of distortion is greater than the period of the principal frequency, h can have any value >1.

The symmetrical harmonic components of the phasors V_a, V_b and V_c are given by:

$$V_{h0} = \frac{V_h}{3} \cdot [1 + 2 \cdot \cos(2 \cdot \pi \cdot h / 3)] \qquad (2.10.4)$$

$$V_{h+} = \frac{V_h}{3} \cdot [1 + 2 \cdot \cos(2 \cdot \pi \cdot (h-1) / 3)] \qquad (2.10.5)$$

$$V_{h-} = \frac{V_h}{3} \cdot [1 + 2 \cdot \cos(2 \cdot \pi \cdot (h+1) / 3)] \qquad (2.10.6)$$

where: *0* indicates the zero phase sequence components
+ indicates the positive phase sequence components
- indicates the negative phase sequence components

It can now be seen, that more than one sequence may be non-zero at multiple and sub-multiple frequencies of the fundamental, as for:

$$h = 3 \cdot h + 0.5 \qquad (2.10.7)$$

In unbalanced systems a harmonic component must be viewed as a superposition of all three symmetrical components. It can therefore not be concluded that a certain harmonic possesses only a certain sequence in practical systems [16].

In figure 2.10.1, it is shown for all three phases, that the third harmonic is a zero sequence component. It can be seen, that all three phases' third harmonics are in phase, which shows, that they are a zero sequence component.

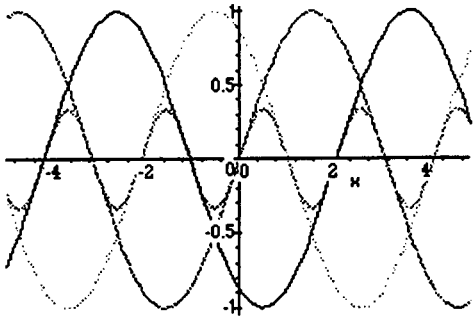

Figure 2.10.1: Balanced three phase voltage or current with the third harmonics.

The same procedure as demonstrated in figure 2.10.1, can be applied to the fifth harmonic, or any other order harmonic. In the case of the fifth harmonic, it will then be seen, that the phase order of the fifth harmonic components is reversed, indicating, that the fifth harmonic is a negative sequence component.

2.11 Causes of Voltage and Current Wave Distortion in Power Systems

2.11.1 Transformers

Transformers with a direct current offset can cause harmonic distortion [17]. The transformer inrush and excitation current also cause some periodic harmonics [18]. These harmonic disturbances are of major concern. With increasing costs and tougher competition transformers are no longer overdesigned, resulting in narrow operating regions, worsening the harmonic distortion problems. For example if the rated voltage is slightly exceeded or if saturation occurs, the core magnetising current is no longer sinusoidal and distortion results; especially the third, fifth, seventh and ninth harmonics are produced. When transformers are only lightly loaded, the voltages in the system rise. This could force some of the transformers into saturation, hence harmonics are once again produced.

Switching transients as well as the Ferranti effect also cause harmonic problems, by increasing the excitation current. However, this is only for a short duration, until the load end breaker of the line is closed. It should be noted though, that switching transients have a negligible effect on transformer saturation.

Previously utilities used star-star transformers grounded on both sides. This minimised the line to ground faultcurrents and ferro-resonance, caused by fuse blowing on the high voltage side. The excitation current of a transformer connected in this way flows into the power system causing distortion on the low voltage side.

Another common practice was to mitigate harmonics through grounded star-delta windings. However, this is not sufficient anymore for the following reasons:

1. Static power converters have increased tremendously recently.
2. Network resonances have increased.
3. Power system equipment and loads are getting increasingly more sensitive to harmonics.

The delta star connection has a low impedance path for all the triplen harmonics. As a result the secondary voltage is not distorted. This is now general practice in industrial plants.

2.11.2 Motors and Generators

Like the transformer, a motor produces third harmonic excitation current on the system, resulting from the magnetic field established in its core. Because of its relatively long airgap the saturation curve of the motor is far more linear, than that of a transformer. The winding pitch of a motor also causes harmonics. Typically motors have five to seven slots per pole. This causes fifth or seventh harmonic currents.

Starters can also produce harmonics, because their control mechanism includes thyristor switching [19 - 21]. Because these devices are used during the starting of motors, this is only of short duration. Once the motor is operating at full speed, these devices are bypassed.

In the case of generators it is practically impossible to distribute the stator windings in such a way, that a perfect sine wave is generated. This causes a dominant third harmonic to flow when the generator is loaded.

Harmonics in rotating machinery can cause vibrations, in particular, negative sequence harmonics cause negative torques, which oppose the fundamental motor force.

2.11.3 Converters and Rectifiers

Converters change the input frequency to a different output frequency. These devices are on the increase and are a major source of distortion in power systems today [22 - 28]. The harmonics generated by converters depend on the power rating, the pulse number and the phase angle control. Rectifiers produce current harmonics on the alternating current side and voltage harmonics on the direct current side. On the alternating current side the dominant harmonics are the fifth, seventh, eleventh and thirteenth harmonics.

2.11.4 Arc Furnaces

During the operation of the arc furnace the current is practically short circuited to ground. As arc furnaces have repetitive cycles of about twenty to sixty minutes, their distortion pattern repeats itself. During one cycle an arc furnace produces zero (direct current), second, fourth and fifth order harmonics.

Typical voltage and current waveforms, produced by an arc furnace, on the bus of common coupling, are shown in figure 2.11.4.1.

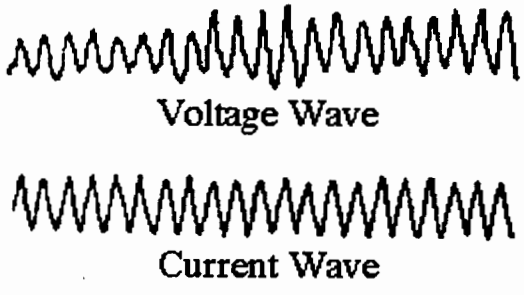

Figure 2.11.4.1: Arc furnace waveshapes, phase current drawn and the resulting voltage on the bus.

2.11.5 Static Volt Ampere Reactive (VAR) Compensators

Static VAR compensators are used for regulating the voltage. VAR compensators can supply and absorb reactive power. These devices are also thyristor controlled and hence also produce harmonics.

2.11.6 Saturated Iron Core Loads

Saturated iron core loads are mainly fluorescent, high pressure sodium, mercury arc and other types of discharge lighting [29 - 31]. Normally a non-linear inductor or ballast is used to prevent overcurrents resulting from their use. This inductor increases the non-linearities, as third harmonic excitation current is required. Saturated iron core loads cause third, fifth and seventh current harmonics.

2.11.7 Other Sources

Battery storage systems, consisting of chargers and batteries also produce harmonics. These are often connected to the power system through converters. Rotating machinery causes harmonics, mainly the third, fifth and seventh harmonics, due to the mechanical design of the machines. Domestic loads or the effect of combined small loads can also give rise to harmonic distortion.

2.12 Harmonic Penetration

For all practical purposes the terminal voltages at generators are pure sinusoids at the fundamental frequency. However, at other busbars the voltage is a perfect sinusoid only if a pure sinusoidal current flows. Loads do not always draw sinusoidal current, the load current is then said to be distorted. This causes non-sinusoidal voltages to appear at remote busses in accordance with Ohm's law [32].

A distorted wave consists of various harmonics. A distorted current will therefore give rise to a distorted voltage, which in turn again gives rise to a distorted current. As shown in figure 2.12.1, distorted currents and voltages will appear throughout the power system.

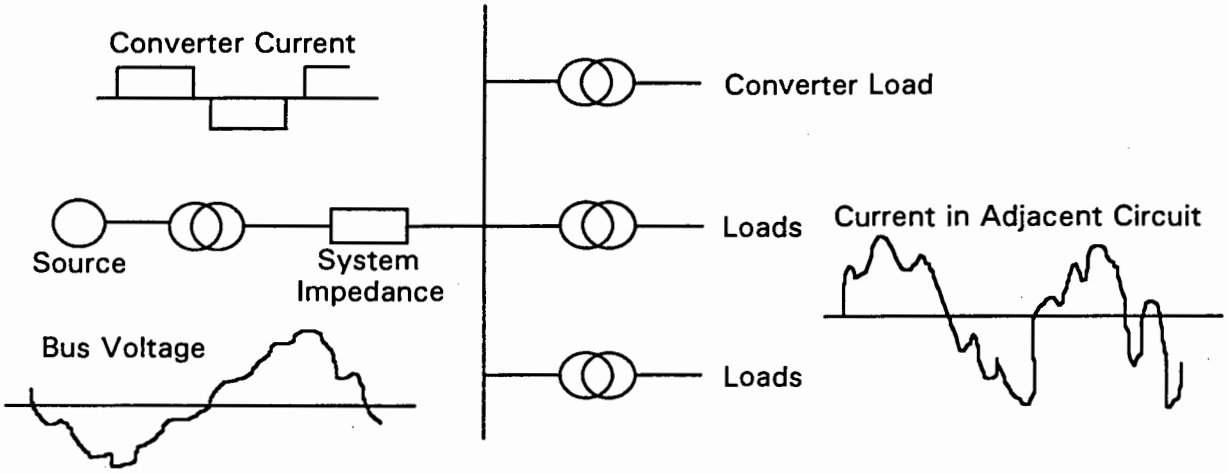

Figure 2.12.1: Propagation of harmonic voltages and currents through a power system.

2.13 Resonance

A power system is especially prone to resonance conditions, particularly because of the common practice of using power factor correction capacitors. These in combination with the inductance of the power system can cause severe harmonic resonance conditions to arise [33, 34].

The resonant frequency is given by:

$$f_r = \frac{1}{2 \cdot \pi \cdot \sqrt{L \cdot C}} \qquad (2.13.1)$$

or:

$$f_r = f_1 \cdot \sqrt{\frac{X_C}{X_L}} \qquad (2.13.2)$$

where: f_r is the resonant frequency

L is the inductance

C is the capacitance

f_1 is the fundamental frequency

X_C is the capacitive reactance

X_L is the inductive reactance

It can be seen from equations *(2.13.1)* and *(2.13.2)*, that there will always be a frequency where X_L is equal to X_C. At this point resonant conditions will arise. Furthermore, increasing the capacitance or decreasing the fault levels will lower the resonant frequency. In both cases a large harmonic current will flow in the system. Generally speaking and because the resistances only have a damping effect, these are neglected, when a frequency response is obtained, thus resulting in a worst case scenario. However, the outlined condition is only applicable, when no series resonance occurs, as in this case, neglecting the resistances results in a larger amplification.

2.13.1 Parallel Resonance

An inductor and a capacitor in parallel cause parallel resonance. Such a combination is also called a tank circuit.

The frequency at which the system impedance appears large is called the resonant frequency. This can cause amplification of harmonic currents close to this frequency. As the *X/R* ratio increases, the harmonic current amplification increasingly worsens. This is typically the case for lower voltage networks.

The load also affects the severity of parallel resonance. As the load increases, so the harmonic current amplification decreases. This is because there are more low impedance paths for the current to flow and there is more resistance to dampen the harmonics.

The above phenomena are demonstrated in figures 2.13.1.1 to 2.13.1.5. An arbitrary plant is chosen. An equivalent circuit is constructed and this circuit is subsequently analysed.

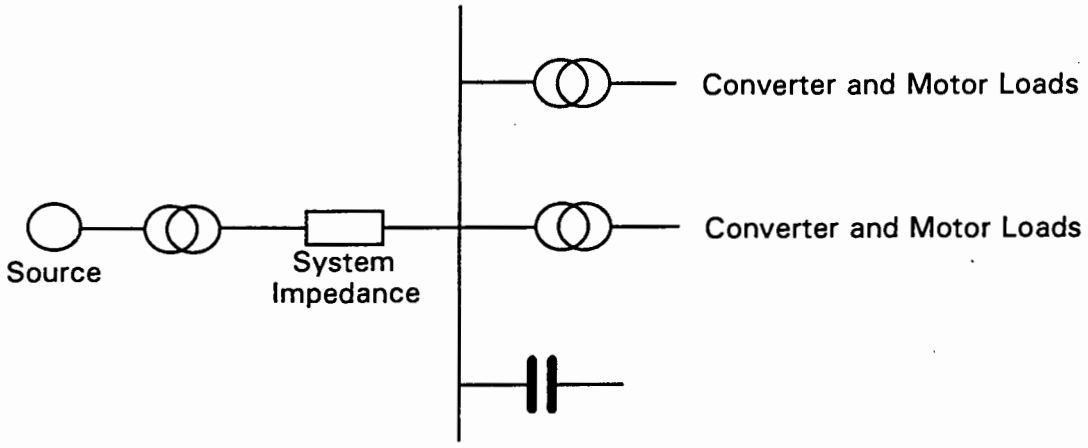

Figure 2.13.1.1: One-line diagram of a plant utilising several static converter motor drives.

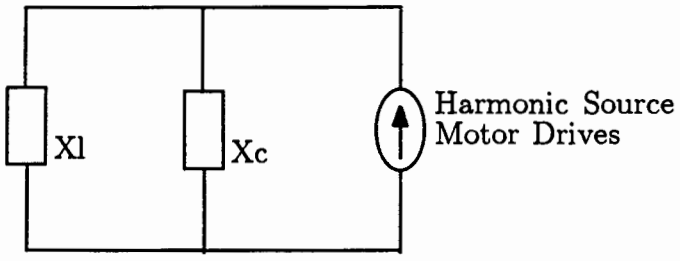

Figure 2.13.1.2: Equivalent circuit of the plant shown in figure 2.13.1.1.

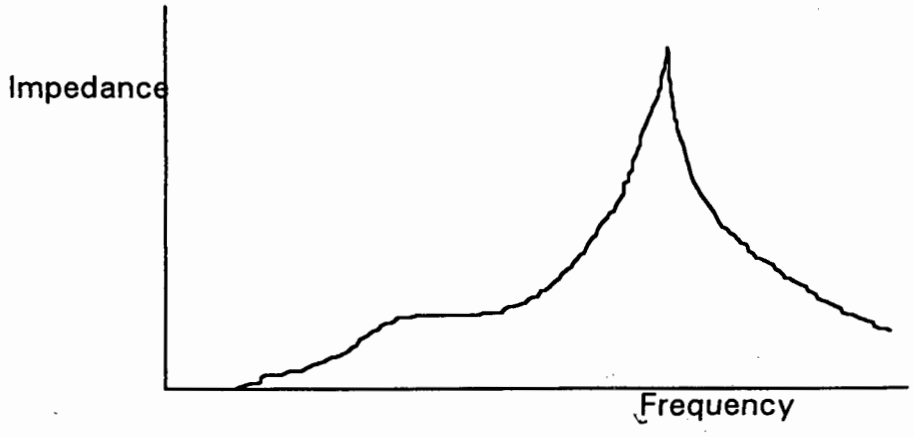

Figure 2.13.1.3: Impedance *versus* frequency curve, for the plant shown in figure 2.13.1.1.

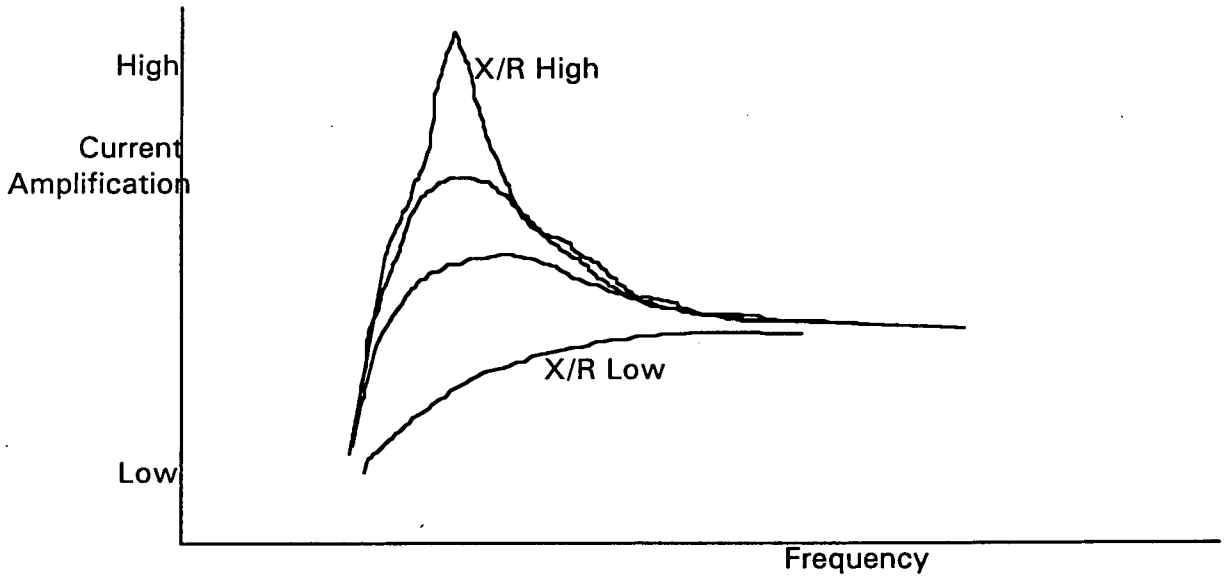

Figure 2.13.1.4: Current amplification *versus* frequency curve for the plant shown in figure 2.13.1.1, illustrating the effect of an increase in the resistance of the tank circuit.

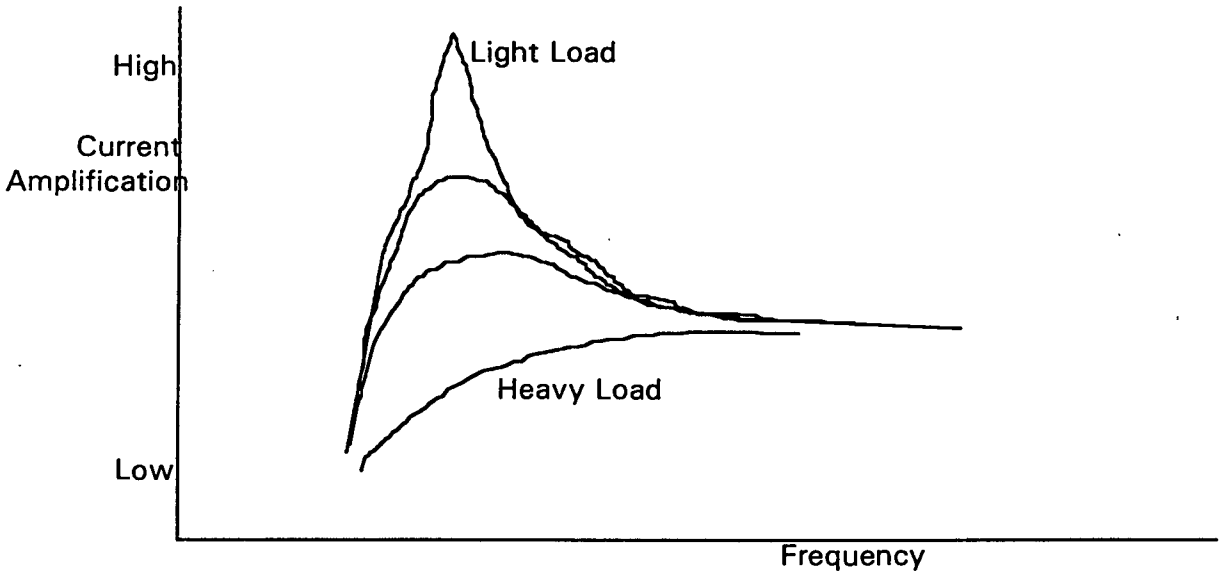

Figure 2.13.1.5: Current amplification *versus* frequency curve for the plant shown in figure 2.13.1.1, illustrating the effect of an increase in the load, due to additional low impedance paths.

2.13.2 Series Resonance

When an inductive and a capacitive element are connected in series, resonance will result at the resonant frequency. In this case however, the impedance at the resonant frequency is much lower. In other words, the circuit will appear as a sharply tuned shunt filter. Harmonic currents are therefore diverted.

An example of a circuit with series resonance is shown in figures 2.13.2.1 to 2.13.2.3.

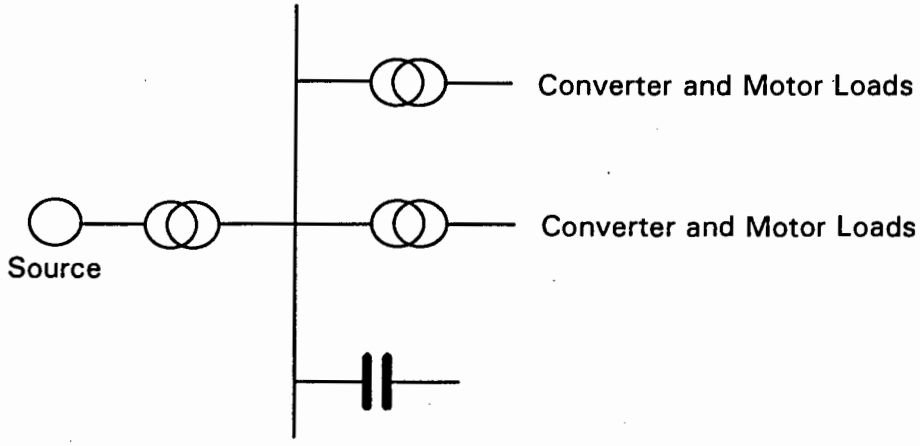

Figure 2.13.2.1: A plant prone to series resonance.

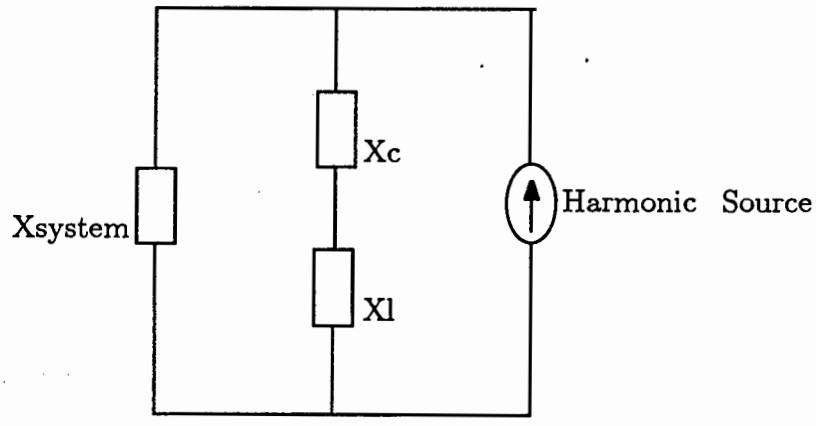

Figure 2.13.2.2: Equivalent circuit for the plant shown in figure 2.13.2.1.

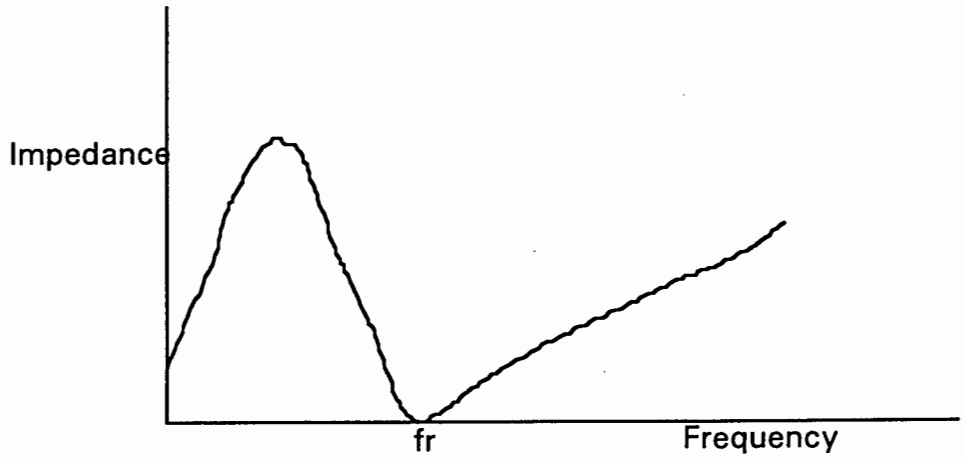

Figure 2.13.2.3: Impedance *versus* frequency curve for the plant shown in figure 2.13.2.1.

2.14 The Effects of Harmonics on Equipment in a Power System

2.14.1 Protective Equipment

False tripping can easily be caused by harmonic overcurrents and overvoltages. If extra zero crossings, caused by the superposition of harmonics on the fundamental sinusoid, are detected, underfrequency detection devices will cause false tripping. False fuse blowing can occur and switchgear can experience severe stress as a result of very high harmonic currents [35, 36].

2.14.2 Underground Cables

Cables are particularly prone to the problems caused by harmonics. Harmonics can cause damaging dielectric heating in underground cables [37], resulting in more severe problems.

2.14.3 Capacitors

If the rated currents or voltages of a capacitor bank are exceeded, the protective fuse can blow or the dielectric medium of the capacitors can be damaged. This can also decrease the life of the capacitor bank. Capacitor bank failure can have severe consequences on the voltage level and the power factor [38, 39].

2.14.4 Measuring Equipment

Most measuring equipment is based on the fundamental frequency. For this reason voltage and current distortion can adversely affect the meter readings.

2.14.5 Line Frequency Controlled Equipment

Line frequency controlled equipment depends on the supply voltage for its operation, in particular the zero crossings or the voltage magnitude at certain instants. Any distortion can therefore cause malfunction of, for example, thyristor firing instants [40].

2.14.6 Neutral Conductors

All the triplen harmonics are of zero sequence. They therefore all add up in the neutral conductor. A conductor with a larger cross sectional area is therefore required, to withstand these currents. For this reason the downsizing of neutral conductors should be discouraged.

2.14.7 Telephone Interference

Electromagnetic coupling between power lines and telephone lines can cause interference. As the human ear is sensitive to frequencies in the 800 Hz region, harmonics close to this value result in disturbances on the telecommunication network [41].

2.14.8 Computer Equipment

Computer equipment or digitally controlled equipment is particularly prone to harmonic disturbances.

2.15 Mitigation or Elimination of Harmonics

To overcome the detrimental effects of harmonics, various strategies are being employed for their mitigation or elimination. The generation of harmonics can be reduced or the harmonic

impedance can be altered amongst others [42 - 46]. In order to do this successfully, an in-depth knowledge of the power system is required. This is normally achieved by doing simulations such as harmonic load flows. Thereafter capacitors can be optimally placed and sized, system extensions can be properly planned and mitigation techniques can be devised.

2.15.1 Shunt Filters

A shunt filter consists of an inductor and a capacitor in parallel with the harmonic source. The characteristic impedance has a minimum value at the tuned frequency. This prevents harmonic currents from spreading to other parts of the system. A shunt filter provides a low impedance path to ground. Double tuned and high pass filters are variations of shunt filters. A double tuned filter only uses one inductor, but two capacitors. There are two advantages of a double tuned shunt filter, namely:

1. The power loss is less at the fundamental frequency.
2. Only one inductor is being used.

The high pass filter is mostly used to filter out higher order harmonics, normally from the eleventh order onwards.

2.15.2 Series Filters

A series filter consists of an inductor in parallel with a capacitor, which is in series with a harmonic source. The impedance of a series filter is very high at the resonant frequency, thereby blocking the path of harmonic currents. A smoothing inductor is often used instead of a series filter. The inductor is also used to smooth out the direct current line ripple.

2.16 References

[1] Eskom Quality of Supply Group, *Eskom Handbook on Quality of Supply*, Revision 1, August 1994.

[2] D. O. Koval, J. Leonard and Z. J. Licsko, "Power Quality of Small Rural Industries", *IEEE Transactions on Industry Applications*, Volume 29, Number 4, July / August 1993, pages 696-700.

[3] K. Price, "Practices for solving End-User Power Quality Problems", *IEEE Transactions on Industry Applications*, Volume 29, Number 6, November / December 1993, pages 1176-1183.

[4] B. M. Hughes, J. S. Chan and D. O. Koval, "Distribution Customer Power Quality Experience", *IEEE Transactions on Industry Applications*, Volume 29, Number 6, November / December 1993, pages 1204-1211.

[5] J. K. Phipps, J. P. Nelson and P. K. Sen, "Power Quality and Harmonic Distortion on Distribution Systems", *IEEE Transactions on Industry Applications*, Volume 30, Number 2, March / April 1994, pages 476-484.

[6] R. D. Henderson and P. J. Rose, "Harmonics - The Effects on Power Quality and Transformers", *IEEE Transactions on Industry Applications*, Volume 30, Number 3, May / June 1994, pages 528-532.

[7] G. T. Heydt, *Electric Power Quality*, Stars in a Circle Publications, West LaFayette, 1991.

[8] R. P. Stratford, M. R. Stambach, J. D. Mountford, T. E. McDermott and D. R. Smith, *Power System Harmonics: Video Training Program Reference Manual*, Power Technologies Incorporated, 1989.

[9] M. Loggini, G. C. Montanari and A. Cavallini, "Generation of Uncharacteristic Harmonics in Electrical Plants with AC / DC Converters", *European Transactions on Electrical Power Engineering*, Volume 4, Number 3, May / June 1994, pages 187-194.

[10] P. S. Filipski, Y. Baghzouz and M. D. Cox, "Discussion of Power Definitions Contained in the IEEE Dictionary", *IEEE Transactions on Power Delivery*, Volume 9, Number 3, July 1994, pages 1237-1244.

[11] F. G. Stremler, *Introduction to Communication Systems*, second edition, Addison-Wesley Publishing Company, Reading, Massachusetts, 1982.

[12] D. J. Kish and G. T. Heydt, "A Generalisation of the Concept of Impedance and a Novel Walsh Domain Immitance", *IEEE Transactions on Power Delivery*, Volume 9, Number 2, April 1994, pages 970-976.

[13] G. T. Heydt, "Systems Analysis using Hartley Impedances", *IEEE Transactions on Power Delivery*, Volume 8, Number 2, April 1993, pages 524-530.

[14] G. T. Heydt and K. J. Olejniczak, "The Hartley Series and its Application to Power Quality Assessment", *IEEE Transactions on Industry Applications*, Volume 29, Number 3, May / June 1993, pages 522-527.

[15] R. L. Smith and R. P. Stratford, "Application Considerations in Handling Effects of SCR Generated Harmonics in Cement Plants", *IEEE Transactions on Industry Applications*, Volume IA-17, Number 1, January / February 1981, pages 63-70.

[16] A. E. Emmanuel, J. A. Orr and D. Cyganski, "Review of Harmonics Fundamentals and Proposal for a Standard Terminology", *Proceedings of the 1988 International Conference on Harmonics in Power Systems*, Nashville, Indiana, United States of America, September / October 1988, pages 2-7.

[17] S. Lu, Y. L. Liu and J. Delaree, "Harmonics Generated from a DC biased Transformer", *IEEE Transactions on Power Delivery*, Volume 8, Number 2, April 1993, pages 725-731.

[18] J. C. Yeh, C. E. Lin, C. L. Huang and C. L. Cgheng, "Calculation and Harmonic Analysis of Transient Inrush Currents in 3-Phase Transformers", *Electric Power Systems Research*, Volume 30, Number 2, July / August 1994, pages 93-102.

[19] L. S. Czarnecki and O. T. Tan, "Evaluation and Reduction of Harmonic Distortion Caused by Solid State Voltage Controllers of Induction Motors", *IEEE Transactions on Energy Conversion*, Volume 9, Number 3, September 1994, pages 528-534.

[20] K. F. Deken, "Dealing with Line Harmonics from PWM Variable Frequency Drives", *Instrumentation and Control Systems*, Volume 66, Number 4, April 1993, pages 71-74.

[21] A. R. Elkoubysi, A. J. Heber and M. M. Morcos, "Harmonics Produced by Variable-Speed Fan Systems", *Transactions of the ASAE*, Volume 37, Number 2, March / April 1994, pages 679-685.

[22] J. Arrillaga, *High Voltage Direct Current Transmission*, Peter Peregrinus IEE Power Engineering Society, Series 6, 1983.

[23] Y. Baghzouz, "An Accurate Solution to Line Harmonic Distortion Produced by AC / DC Converters with Overlap and DC Ripple", *IEEE Transactions on Industry Applications*, Volume 29, Number 3, May / June 1993, pages 536-540.

[24] Y. J. Wang and L. Pierrat, "Probabilistic Modelling of Current Harmonics Produced by an AC / DC Converter Under Voltage Unbalance", *IEEE Transactions on Power Delivery*, Volume 8, Number 4, October 1993, pages 2060-2066.

[25] M. Grotzbach and B. Draxler, "Effect of DC Ripple and Commutation on the Line Harmonics of Current Controlled AC / DC Converters", *IEEE Transactions on Industry Applications*, Volume 29, Number 5, September / October 1993, pages 997-1005.

[26] D. E. Rice, "A Detailed Analysis of 6-Pulse Converter Harmonic Currents", *IEEE Transactions on Industry Applications*, Volume 30, Number 2, March / April 1994, pages 294-304.

[27] A. Cavallini, M. Loggini and G. C. Montanari, "Behaviour of Harmonic Current Vectors Generated by 6-Pulse AC / DC Converters as Function of Plant Parameters", *European Transactions on Electrical Power Engineering*, Volume 4, Number 3, May / June 1994, pages 195-203.

[28] A. Cavallini, M. Loggini and G. C. Montanari, "Comparison of Approximate Methods to Estimate Harmonic Currents Injected by AC / DC Converters", *IEEE Transactions on Industrial Electronics*, Volume 41, Number 2, April 1994, pages 2256-262.

[29] R. R. Verderber, O. C. Morse and W. R. Alling, "Harmonics from Compact Fluorescent Lamps", *IEEE Transactions on Industry Applications*, Volume 29, Number 3, May / June 1993, pages 670-674.

[30] F. V. Topalis, "Efficiency of Energy Saving Lamps and Harmonic Distortion in Distribution Systems", *IEEE Transactions on Power Delivery*, Volume 8, Number 4, October 1993, pages 2038-2042.

[31] J. J. Degroot, H. Houkes, W. Roche and S. Vamvakas, "Triple-U Electronic Compact Fluorescent Lamps with Reduced Harmonics", *Journal of the Illuminating Engineering Society*, Volume 23, Number 1, Winter 1994, pages 45-51.

[32] S. M. Williams, G. T. Brownfield and J. W. Duffus, "Harmonic Propagation on an Electric Distribution System - Field Measurements Compared with Computer Simulation", *IEEE Transactions on Power Delivery*, Volume 8, Number 2, April 1993, pages 547-552.

[33] Eskom Quality of Supply Group, *Power Quality Reference Guide*, Revision 1, March 1994.

[34] W. E. Kazibwe and M. H. Sendaula, *Electric Power Quality Control Techniques*, van Nostrand Reinhold, New York, 1993.

[35] IEEE Tutorial Course, *Power System Harmonics*, Course Text, 84 EH0221-2-PWR, 1984.

[36] J. Arrillaga, D. Bradley and D. Bodger, *Power System Harmonics*, John Wiley & Sons, New York, 1985.

[37] J. A. Palmer, R. C. Degeneff, T. M. Mckernan, T. M. Halleran, "Pipe-Type Cable Ampacities in the Presence of Harmonics", *IEEE Transactions on Power Delivery*, Volume 8, Number 4, October 1993, pages 1689-1695.

[38] G. Benmouyal, H. Bilodeau, S. Chano and G. Sybille, "New Algorithm for Protection of Capacitor Banks exposed to Harmonic Overvoltages", *IEEE Transactions on Power Delivery*, Volume 8, Number 3, July 1993, pages 898-904.

[39] A. A. Girgis, C. M. Fallon, J. C. P. Rubino and R. C. Catoe, "Harmonics and Transient Overvoltages due to Capacitor Switching", *IEEE Transactions on Industry Applications*, Volume 29, Number 6, November / December 1993, pages 1184-1188.

[40] V. E. Wagner, J. C. Balda, T. M. Barnes, A. E. Emmanuel, R. J. Ferraro, D. C. Griffith, D. P. Hartmann, W. F. Horton, W. T. Jewell, A. Mceachern, D. J. Phileggi and W. E. Reid, "Effects of Harmonics on Equipment", *IEEE Transactions on Power Delivery*, Volume 8, Number 2, April 1993, pages 672-680.

[41] M. Kuusaari, "Statistical Evaluation of Telephone Noise Interference caused by AC Power Line Harmonic Currents", *IEEE Transactions on Power Delivery*, Volume 8, Number 2, April 1993, pages 524-530.

[42] K. Mikolajuk and A. Tobola, "A new Method for Reduction of Current and Voltage Harmonic Distortion in Power Systems", *European Transactions on Electrical Power Engineering*, Volume 3, Number 1, January / February 1993, pages 85-89.

[43] J. Arrillaga, L. Yonghe, C. S. Crimp and M. Villablanca, "Harmonic Elimination by DC Ripple Reinjection in Generator Converter Units Operating at Variable Speeds", *IEE Proceedings - C Generation, Transmission and Distribution*, Volume 140, Number 1, January 1993, pages 57-64.

[44] H. L. Jou, H. Y. Chu and J. C. Wu, "A Novel Active Power Filter for Reactive Power Compensation and Harmonic Suppression", *International Journal of Electronics*, Volume 75, Number 3, September 1993, pages 577-587.

[45] W. Lawrance and W. Mielczarski, "Harmonic Current Reduction in Industrial Distribution Networks", *Electric Power Systems Research*, Volume 27, Number 2, July 1993, pages 117-122.

[46] N. Mohan, "A Novel Approach to Minimise Line-Current Harmonics in Interfacing Power Electronics Equipment with 3-Phase Utility Systems", *IEEE Transactions on Power Delivery*, Volume 8, Number 3, July 1993, pages 1395-1401.

Chapter 3

Literature Review of the Theory of Algorithms used for Harmonic Analysis in Power Systems and Comparison thereof

3.1 Introduction

Special algorithms have been developed to solve the harmonic analysis problem in power systems. These are the companion circuit method, the Gauss-Seidel method, the Newton-Raphson method and the current injection method. This chapter is supplementary to the final year BSc (Eng) theses, [1 - 3], that were completed at the University of Cape Town, where the practical usefulness of these algorithms was partly evaluated.

3.2 Companion Circuit Method

The companion circuit method is the most commonly used approach of the time-based algorithms [4, 5]. The companion circuit method is most commonly used for power system transient analysis however, it can also be used for steady state analysis. All power system elements are reduced to simple resistive elements with the use of this method. Correction currents are added to make the resistive circuit elements behave like the real network elements that are being modelled. The resistive element combined with the correction current is called a companion circuit.

The equation that describes an inductor is given by:

$$i_L(t) = \frac{1}{L}\int_0^t v_L(\tau)d\tau \qquad (3.2.1)$$

If the trapezoidal rule of integration is applied, over the time interval from n to $(n+1)$ the following equation results:

$$i_L(n+1) = i_L(n) + \frac{1}{L}(v_L(n+1) + v_L(n))\frac{T}{2} \qquad (3.2.2)$$

After rearranging terms, equation *(3.2.2)* results in:

$$i_L(n+1) = \frac{T}{2L}v_L(n+1) + \left(i_L(n) + \frac{Tv_L(n)}{2L}\right) \qquad (3.2.3)$$

where: i_L is the current through the inductor

v_L is the voltage across the inductor

T is the time step

L is the inductance

n is the lower boundary of the interval

In equation *(3.2.3)* the coefficient to v_L outside the brackets may be regarded as an equivalent conductance and the term in the brackets as a correction current in parallel to the equivalent conductance. In this way an inductor is modelled. This is also shown in figure 3.2.1.

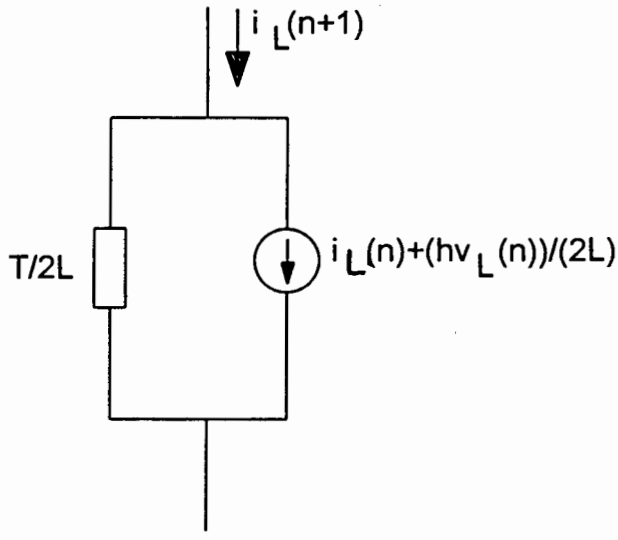

Figure 3.2.1: Companion circuit for an inductor.

In a similar fashion companion circuits can be derived for all the network elements. After the companion circuits have been formed, simple network methods can be used to solve the resistive network at every point in time.

The following steps are necessary to perform a harmonic analysis of a power system, using the companion circuit algorithm [4, 5]:

1. Each individual resistive, inductive and capacitive element is converted into a resistive network of companion circuits.
2. The network conductance matrix is calculated.
3. An LU decomposition is performed.
4. Voltages and currents are initialised.
5. Voltages and currents are found after each time interval.
6. Bus voltages are determined by forward and backward substitution.
7. Non-linear loads and sources are modelled apart from the network as modular sections of the software.
8. The resultant time domain waveforms are obtained by making use of the Fourier Transformation.

3.3 Gauss-Seidel Method

3.3.1 Gauss-Seidel Loadflow at the Fundamental Frequency

In a loadflow study the active and reactive powers at load or generator busses without voltage control, are specified. These are known as PQ busses. At most generator busses the active power and the voltage magnitude are specified. These busses are known as PV busses. One generator bus is known as the swing or slack bus; this is normally the reference bus. The voltage magnitude for this bus is specified and the voltage angle is zero. The power generation at the swing bus is calculated after taking the system losses into consideration. The network topology is specified and the network can therefore be represented by its bus admittance or impedance matrix. The bus voltage profile and the branch active and reactive power flows then need to be determined. This is done with the aid of the following equations:

At the swing bus:

$$V_{swing} = |V_{known}| \angle 0° \qquad (3.3.1.1)$$

At PQ busses:

$$V_i I_i^* = P_i + jQ_i \qquad (3.3.1.2)$$

At PV busses:

$$|V_i| = specified \qquad (3.3.1.3)$$

and

$$\mathrm{Re}\{V_i I_i^*\} = P_i \qquad (3.3.1.4)$$

where:

V_{swing}	is the voltage at the swing bus
V_{known}	is a known voltage
V_i	is the voltage at the i'th bus
I_i	is the current injected into the i'th bus
P_i	is the active power at the i'th bus
Q_i	is the reactive power at the i'th bus

The voltage angle at PV busses can then be determined by:

$$\delta_i = \theta_i + \mathrm{acos}\left(\frac{P_i}{|I_i||V_i|}\right) \qquad (3.3.1.5)$$

where:

δ_i	is the voltage angle at the i'th PV bus
θ_i	is the current angle at the i'th PV bus

For the power network the following equations can be written:

$$V_{bus} = Z_{bus} I_{bus} \qquad (3.3.1.6)$$

or

$$I_{bus} = Y_{bus} V_{bus} \qquad (3.3.1.7)$$

where: V_{bus} is the nodal voltage vector

I_{bus} is the nodal current injection vector

Z_{bus} is the bus impedance matrix

Y_{bus} is the bus admittance matrix

As these equations are all complex they can be split into real and imaginary parts, which each have to balance separately. For an n bus system this results in a system of $4n$ real equations with $4n$ real unknowns, which need to be solved.

The following steps are necessary to perform the Gauss-Seidel algorithm for the fundamental frequency [6 - 10]:

1. The unknown voltages and currents are initialised: Normally the voltages are initialised to one per unit with a phase angle of zero degrees and the currents to the complex conjugate of the specified powers.
2. Equations *(3.3.1.2)* to *(3.3.1.5)* and *(3.3.1.7)*, are solved for a voltage or current.
3. The initial values are used in the first iteration. Thereafter the values are updated. These updated values are used again, if they are needed in another equation in that iteration.
4. The iterations continue using the most recently calculated values as they are required.
5. The iterations stop when a desired accuracy is reached in the solution.

3.3.2 Gauss-Seidel Harmonic Loadflow

The procedure outlined in section 3.3.1 is extended to provide for three phase power systems [11 - 13]. This particular algorithm is explained below:

1. Initialise the unknown voltages and currents at the fundamental frequency.
2. Perform a fundamental loadflow, as discussed in section 3.3.1.
3. For each bus with a harmonic source solve for all the distorted phase currents.
4. Take the Fourier transform of the current for each of these busses.
5. Perform a Gauss-Seidel loadflow for each harmonic.
6. The procedure starts again at step 3. until the solution falls within the specified tolerance level.

As this method has weak convergence properties, and slow execution times, it is not used very often.

3.4 Newton-Raphson Method

3.4.1 Newton-Raphson Loadflow at the Fundamental Frequency

The Newton-Raphson loadflow at the fundamental frequency is used to solve a set of simultaneous equations. Where f and x are vector valued and the mismatch equation formulation can be described by:

$$f(x) = 0 \qquad (3.4.1.1)$$

where: f is the mismatch active and reactive power at each bus except the swing bus
x is the vector of state variables

The state variables in the fundamental frequency loadflow are the voltage magnitudes and voltage angles at each bus. The active and reactive power entering a bus must be the same as the active and reactive power leaving a bus. The power mismatch is the difference between the

power entering and leaving a bus at a certain stage in the solution. When the power mismatch is smaller than a certain tolerancelevel, the solution of the loadflow has been found.

For a bus i, where j refers to a remote bus connected to bus i by an admittance Y_{ij}, the active and reactive power mismatches can be written as shown below:

$$\Delta P_i = P_i - |Y_{ij}| \cdot |v_i| \cdot |v_i| \cdot \cos(-\theta_{ij}) - \sum_{j \neq i} |Y_{ij}| \cdot |v_j| \cdot |v_i| \cdot \cos(-\theta_{ij} - \delta_j + \delta_i) \qquad (3.4.1.2)$$

$$\Delta Q_i = Q_i - |Y_{ij}| \cdot |v_i| \cdot |v_i| \cdot \sin(-\theta_{ij}) - \sum_{j \neq i} |Y_{ij}| \cdot |v_j| \cdot |v_i| \cdot \sin(-\theta_{ij} - \delta_j + \delta_i) \qquad (3.4.1.3)$$

In this case the element of the admittance matrix at row i and column j and the voltages at busses i and j are written in polar form as:

$$|Y_{ij}| \angle \theta_{ij} \qquad (3.4.1.4)$$

$$|v_i| \angle \delta_i \qquad (3.4.1.5)$$

$$|v_j| \angle \delta_j \qquad (3.4.1.6)$$

where:
- ΔP_i is the active power mismatch at bus i
- P_i is the specified active power at bus i
- Y_{ij} is the admittance between busses i and j
- v_i is the voltage at bus i
- θ_{ij} is the admittance angle of the admittance between busses i and j
- v_j is the voltage at bus j
- δ_j is the angle of the voltage at bus j
- δ_i is the angle of the voltage at bus i
- ΔQ_i is the reactive power mismatch at bus i
- Q is the specified reactive power at bus i

The mismatch formula can now be written as:

$$\begin{pmatrix}\Delta P(\delta,V)\\ \Delta Q(\delta,V)\end{pmatrix} = 0 \qquad (3.4.1.7)$$

In this case the mismatch powers are shown at all busses except the swing bus; and the bus voltage magnitudes and angles are shown for all busses except the swing bus.

An initial guess is made for the vector x, which contains the voltage magnitudes and angles of all the busses in the system except the swing bus:

$$x_0 = \begin{pmatrix}\delta_0\\ V_0\end{pmatrix} \qquad (3.4.1.8)$$

The Newton-Raphson update formula, which is derived from the Taylor series expansion, is used to update the solution vector x, until the mismatches are sufficiently small. For the update from iteration k to $(k+1)$, the following formula is used:

$$x_{k+1} = x_k - \left(\frac{\delta f}{\delta x}\bigg|_k\right)^{-1} \cdot f(x_k) \qquad (3.4.1.9)$$

where: k is the number of the current iteration

The update equation, *(3.4.1.9)* uses the partial derivatives of the mismatch equations. The equations for the active power mismatch at each bus, are listed below:

$$\frac{\partial P_i}{\partial \delta_i} = \sum_{j\neq i} |Y_{ij}| \cdot |v_j| \cdot |v_i| \cdot \sin(-\theta_{ij} - \delta_j + \delta_i) \qquad (3.4.1.10)$$

$$\frac{\partial P_i}{\partial \delta_k} = -|Y_{ik}| \cdot |v_k| \cdot |v_i| \cdot \sin(-\theta_{ik} - \delta_k + \delta_i) \qquad i \neq k \qquad (3.4.1.11)$$

$$\frac{\partial P_i}{\partial |v_i|} = -2 \cdot |Y_{ii}| \cdot |v_i| \cdot \cos(-\theta_{ii}) - \sum_{j\neq i} |Y_{ij}| \cdot |v_j| \cos(-\theta_{ij} - \delta_j + \delta_i) \qquad (3.4.1.12)$$

$$\frac{\partial P_i}{\partial |v_k|} = -|Y_{ik}| \cdot |v_i| \cdot \cos(-\theta_{ik} - \delta_k + \delta_i) \qquad i \neq k \qquad (3.4.1.13)$$

Similar equations can be derived for the reactive power at each bus.

A Jacobian matrix containing the partial derivatives is used in solving the update equation *(3.4.1.9)*. This matrix is given by the following expression:

$$J = \begin{pmatrix} \frac{\partial P}{\partial \delta} & \frac{\partial P}{\partial |V|} \\ \frac{\partial Q}{\partial \delta} & \frac{\partial Q}{\partial |V|} \end{pmatrix} \qquad (3.4.1.14)$$

The partial derivatives in the Jacobian matrix need to be calculated for each bus in the system except the swing bus. Hence the Jacobian is made up of four sub-matrices, as shown below:

$$J = \begin{pmatrix} J_1 & J_2 \\ J_3 & J_4 \end{pmatrix} \qquad (3.4.1.15)$$

$[J_1]$ contains the partial derivatives of the active power mismatches taken with respect to the voltage angles for all the busses except the swing bus. $[J_2]$ is the same, except the partial derivatives are taken with respect to the voltage magnitudes. $[J_3]$ and $[J_4]$ contain the partial derivatives of the reactive power mismatches, taken with respect to the voltage angles and voltage magnitudes respectively, for all the busses except the swing bus.

The Jacobian sub-matrix $[J_1]$ has its diagonal and off-diagonal entries given by equations *(3.4.1.10)* and *(3.4.1.11)* respectively. The sub-matrix $[J_2]$ has its diagonal and off-diagonal entries given by equations *(3.4.1.12)* and *(3.4.1.13)* respectively. The sub-matrices $[J_3]$ and $[J_4]$ have their entries given by the corresponding equations for the reactive power.

The following algorithm describes the Newton-Raphson solution [6 - 12], of the mismatch loadflow formulation:

1. Determine the bus admittance matrix.
2. Initialise values for the voltage magnitude and angle for all the busses except the swing bus, in other words initialise the unknown state variable or solution vector x.
3. Using the partial derivative equations calculate the Jacobian matrix J.
4. Calculate the active and reactive power mismatches, the vector f.
5. If the mismatch powers are larger than the tolerance limits, use the Newton-Raphson update formula to calculate new voltage magnitudes and angles for x, otherwise stop the iterations and show the result.
6. Return to step 3.

3.4.2 Newton-Raphson Harmonic Loadflow

The procedure outlined in section 3.4.1 is extended to provide for three phase power systems.

In the fundamental frequency Newton-Raphson loadflow the state variables used are the voltage magnitudes and angles at all the busses in the system, except for the swing bus. In the harmonic loadflow however, the list of state variables must also include each bus voltage *v(t)* and each injected current *i(t)* in full Fourier series form.

The term "linear" refers to a normal power system bus which does not exhibit distorted line current when the bus voltage is sinusoidal. The term "non-linear" refers to busses connected to loads and sources that cause distorted line currents even if the bus voltage is sinusoidal.

Four main power system bus types are considered in the mismatch formulation of the harmonic loadflow:

1. The swing bus which is a single, linear bus for which the voltage is specified.
2. Linear PQ busses at which the active and reactive powers are specified.
3. Linear PV busses at which the active power and the voltage magnitude are specified.
4. Non-linear PQ busses which are connected to converters and other non-linear devices. These are harmonic source busses.

The procedure for solving the harmonic loadflow is much the same as that for the fundamental frequency loadflow. Due to the extra state variables however and the inclusion of mismatch harmonic currents, voltages and active power, the Jacobian matrix is far more complex than for the fundamental loadflow case.

For a linear PQ bus the active and reactive power mismatches are given by the same equations as for the fundamental frequency case, *(3.4.1.2)* and *(3.4.1.3)*. For the harmonic loadflow case there is an additional equation which describes the harmonic current mismatch and an expression for the harmonic voltage mismatch:

$$\Delta I^{(h)} = I_{bus}^{(h)} - Y_{bus}^{(h)} V_{bus}^{(h)} \qquad (3.4.2.1)$$

$$\Delta V^{(h)} = V_i^{(h)} - \bar{z}_i^{(h)} I_i^{(h)} \qquad (3.4.2.2)$$

where:

- ΔI is the current mismatch
- I_{bus} is the bus current
- Y_{bus} is the bus admittance matrix
- V_{bus} is the bus voltage
- h is the harmonic order
- ΔV is the voltage mismatch
- V_i is the voltage at bus i
- $\bar{z}_i$ is the primitive impedance or unconnected equivalent impedance which relates the harmonic voltage at the bus to the injected harmonic current
- I_i is the current through bus i

For a linear PV bus the equations are the same, except that there is no equation for the reactive power mismatch. For a non-linear PQ bus the fundamental active and reactive power mismatch equations still exist, namely equations *(3.4.1.2)* and *(3.4.1.3)*. More equations have to be introduced however, to describe the non-linear characteristic of the bus. If the bus voltage and the phase angle are known, injection currents can be solved in the time domain and decomposed into their Fourier series components. The equations are complex and depend

largely on the type of converter or other non-linear load. The following equation describes this relationship:

$$I_i^{(h)} = f_1(V_i^{(h)}, \alpha) \qquad (3.4.2.3)$$

where: I_i is the injected current at bus i

f is the function that describes the current

V_i is the voltage at bus i

α is the firing angle

h is the harmonic order

The active power at the fundamental frequency for a non-linear bus is also a function of the bus voltage. The firing angle of converters connected to the bus is given by the equation below:

$$P_i^{(1)} = f_2(V_i^{(h)}, \alpha) \qquad (3.4.2.4)$$

where: P_i is the active power at bus i

f is the function describing the power

Equations *(3.4.2.3)* and *(3.4.2.4)* can be rewritten to give the following mismatch equations:

$$\Delta I_c^{(h)} = I_i^{(h)} - f_1(V_i^{(h)}, \alpha_i) \qquad (3.4.2.5)$$

$$\Delta P_c^{(h)} = P_h^{(1)} - f_2(V_i^{(h)}, \alpha_i) \qquad (3.4.2.6)$$

where: ΔI_c is the current mismatch

ΔP_c is the power mismatch

A non-linear PQ bus also has the harmonic current mismatch equation, *(3.4.2.1)*. Hence in total there are six mismatch equations, *(3.4.1.2)*, *(3.4.1.3)*, *(3.4.2.1)*, *(3.4.2.2)*, *(3.4.2.5)* and *(3.4.2.6)*. These six equations give the mismatches of the following six parameters:

$$\Delta P^{(1)},\ \Delta Q^{(1)},\ \Delta I^{(h)},\ \Delta V^{(h)},\ \Delta I_c^{(h)},\ \Delta P_c^{(h)} \qquad (3.4.2.7)$$

There are also seven different state variables:

$$\left|V^{(1)}\right|,\ \delta^{(1)},\ I^{(h)},\ V^{(h)},\ \alpha,\ I^{(1)},\ V^{(1)} \qquad (3.4.2.8)$$

The Jacobian matrix can thus be constructed by taking the partial derivatives of the mismatch equations with respect to the state variables. The Jacobian matrix for the harmonic case, J_h is therefore of the form:

$$J_h = \begin{bmatrix} J_1 & J_2 & J_3 \\ J_4 & J_5 & J_6 \\ J_7 & J_8 & J_9 \end{bmatrix} \qquad (3.4.2.9)$$

Each entry of the Jacobian matrix consists of a Jacobian sub-matrix.

The sub-matrix J_1, refers to linear PQ busses; its rows contain the following mismatch equations for all the linear PQ busses in the system:

$$\Delta P^{(1)},\ \Delta Q^{(1)},\ \Delta I^{(h)},\ \Delta V^{(h)} \qquad (3.4.2.10)$$

The columns of the sub-matrix J_1, consist of partial derivatives and are calculated with respect to the following state variables:

$$\left|V^{(1)}\right|,\ \delta^{(1)},\ I^{(h)},\ V^{(h)} \qquad (3.4.2.11)$$

J_2 and J_3 also refer to the linear PQ busses in the system and hence the same mismatch equations are in the rows with the partial derivatives being calculated for J_2 with respect to:

$$I^{(h)},\ V^{(h)},\ \alpha,\ I^{(1)},\ V^{(1)} \qquad (3.4.2.12)$$

In the case of J_3, the partial derivatives are written with respect to:

$$\delta^{(1)}, \quad I^{(h)}, \quad V^{(h)} \tag{3.4.2.13}$$

Sub-matrices J_4, J_5 and J_6 refer to non-linear PQ busses and the mismatch equations in the rows for all the non-linear PQ busses in the system are:

$$\Delta P^{(1)}, \quad \Delta Q^{(1)}, \quad \Delta I^{(h)}, \quad \Delta I_c^{(h)}, \quad \Delta P_c^{(h)} \tag{3.4.2.14}$$

The partial derivatives for J_4, J_5 and J_6 are calculated with respect to the same state variables as for J_1, J_2 and J_3, respectively.

Sub-matrices J_7, J_8 and J_9 refer to linear PV busses and the mismatch equations in the rows for all the linear PV busses in the system are:

$$\Delta P^{(1)}, \quad \Delta I^{(h)}, \quad \Delta V^{(h)} \tag{3.4.2.15}$$

The partial derivatives for J_7, J_8 and J_9 are calculated with respect to the same state variables as for J_1, J_2 and J_3, respectively.

Each sub-matrix must contain entries for all the busses of that type that exist in the system. In sub-matrices containing harmonic mismatch equations there will be sets of entries for each harmonic order studied.

The following algorithm gives the Newton-Raphson solution [13 - 17], of the harmonic loadflow:

1. Obtain the input data.
2. Initialise the state variables for the fundamental frequency case.
3. Calculate the active and reactive power mismatches for the fundamental frequency case.

4. Go to step 8. if the mismatch is less than the tolerance.
5. Calculate the Jacobian matrix at the fundamental frequency.
6. Update the fundamental voltage magnitudes and angles.
7. Return to step 3..
8. Estimate the harmonic voltages and currents and the firing angle.
9. Solve the converter equations.
10. Return to step 9. if the converter equations do not converge to within the specified tolerance.
11. Calculate the Jacobian matrix for the harmonic loadflow.
12. Order the Jacobian matrix optimally for the harmonic loadflow.
13. Solve the update equation and update the state vector.
14. Calculate the mismatch.
15. Return to step 9. if the mismatch is not less than the specified tolerance.

3.5 Comparison of the Gauss-Seidel and Newton-Raphson Methods

Property	Gauss-Seidel Method	Newton-Raphson Method
Convergence		
Far from solution	Moderate	Fair, may diverge
Near solution	Moderate	Excellent
Typical number of iterations	10-70	2-4
Overall	Moderate	Excellent
Execution Time	Fair	Moderate-Excellent
Memory Requirements	Moderate	Moderate
Ease in Programming	Very easy	Moderate
Modifications	Used as a starting method for Newton-Raphson Solutions	Decoupled Power Flow study Control Equations Gauss-Seidel starting step

Table 3.5.1: Comparison of the Gauss-Seidel and Newton-Raphson methods for the fundamental frequency loadflow [13].

Factor	Fundamental Loadflow	Harmonic Loadflow
Method of Solution		
Iterations	2-4	7-30
Convergence	Rapid	Initialisation / solution of converter equations may degrade convergence
Mismatch Tolerance	Typically 1%	1% at the power frequency, 0.01% at harmonic frequencies
Memory	Moderate, system dependent	Moderate, system dependent
Typical Studies		
External Equivalent	May be required, depends on size of study	Usually required
System Size	Typically 100-10 000 busses	Rarely more than 300 busses
Applications	Operating studies, system planning, voltage regulation and line loading assessment	Interference studies
Input / Output		
Input Data Requirements	Generation, System and Load data	Same as fundamental loadflow, except, non-linear loads are modelled and system components are modelled in more detail
Volume of Output	Moderate, system dependent	About a factor equal to the harmonic order greater than the fundamental loadflow
Ease in Interpreting Results	Moderate	Moderate, more difficult than the fundamental loadflow

Table 3.5.2: Comparison of the Newton-Raphson fundamental loadflow and harmonic loadflow methods [13].

3.6 The Current Injection Method

The current injection method is based on the assumptions that the bus voltages are sinusoidal and that the injected harmonic currents are independent of each other. In many cases converters can be approximated as current injection sources. When the previous assumption is used, the results of the current injection method are fairly accurate for low levels of harmonic distortion and at nearly sinusoidal bus voltages. The relationship between the harmonic currents and voltages is expressed by:

$$V_{Bus}^{h} = Z_{Bus}^{h} \cdot I_{Bus}^{h} \qquad (3.6.1)$$

where: I_{Bus}^{h} is the harmonic current injection vector

V_{Bus}^{h} is the harmonic voltage output vector

Z_{Bus}^{h} is the harmonic bus impedance matrix

h is the harmonic order

The vector I_{Bus}^{h}=0, except at the position which corresponds to the current being injected at the particular bus, which is given by I_{Bus}^{h}. The impedance matrix must be calculated for each frequency. The impedance matrix that is being used must contain the values that are valid for that particular frequency.

The algorithm that is normally used for the application of the current injection method [13 - 15], is outlined below:

1. A base case loadflow, at the fundamental frequency, is done for the network to be studied.
2. All converters are modelled as constant current sources.
3. For each bus a set of harmonic currents is written.
4. Equation *(3.6.1)* is applied to obtain each harmonic voltage.
5. If all the harmonic voltages have not been determined yet, the harmonic order is increased.

6. Calculate the new bus impedance matrix for the new harmonic order and return to step 4.
7. If a time solution is desired, the harmonics calculated for a given bus are superimposed and a Fourier transformation is performed.

The bus impedance matrix does not have to be used in the above equation. Instead, the bus admittance matrix can be used and inverted. This is far more efficient, as the admittance matrix is easier to calculate for each harmonic frequency. This results in the following formula:

$$V_{Bus}^{h} = (Y_{Bus}^{h})^{-1} \cdot I_{Bus}^{h} \qquad (3.6.2)$$

The admittance matrix is not actually inverted as shown in the formula, as this is very computer intensive. Instead, an LU decomposition is performed, the triangular factors of Y_{Bus} are found and the voltages are calculated by forward and backward substitution, with the aid of the following formulas:

$$I_{Bus}^{h} = Y_{Bus}^{h} \cdot V_{Bus}^{h} \qquad (3.6.3)$$

$$I_{Bus}^{h} = L \cdot U \cdot V_{Bus}^{h} \qquad (3.6.4)$$

$$I_{Bus}^{h} = L \cdot W \qquad (3.6.5)$$

$$W = U \cdot V_{Bus}^{h} \qquad (3.6.6)$$

where: L is the lower left triangular factor of the admittance matrix
U is the upper right triangular factor of the admittance matrix
W is solved by forward substitution
V is calculated by backward substitution

This method is very fast and non-iterative and a solution is always obtained. When triangular factorisation is used to calculate the bus voltages, only the triangular factors of the bus

admittance method are needed. These are sparse however, and not much storage space is required. An advantage of the current injection method is, that it is accurate for low total bus voltage and current harmonic distortions. The main disadvantage of the current injection method is, that at harmonics with higher magnitudes the method becomes inaccurate. It is estimated that if the THD level is more than 5%, the method can not be used any longer. The current injection method must not be confused with a harmonic power flow algorithm, as it is a non-iterative procedure.

3.7 Comparison of Harmonic Analysis Methods

	Current Injection	Gauss-Seidel	Newton-Raphson
Solution			
Speed	Very fast	Slow	Slow
Iterations	Non-iterative	50-500	7-30
Memory Requirements	Moderate, using sparsity programming	Moderate, using sparsity programming	Moderate, using sparsity programming
Initialisation	Critical to solution, depends on initialisation	Convergence depends on initialisation	Convergence depends on initialisation
Converter Solution	Done off line	Done on line	Done on line
Input / Output			
Input Data Requirements	Moderate	Moderate	Moderate
Ease of Data Preparation	Moderate	Moderate	Moderate
Volume of Output	Moderate	Moderate	Moderate
Possible Output Features	THD, TIF, C-message index, graphics, standards checking	THD, TIF, C-message index, graphics, standards checking, converter	THD, TIF, C-message index, graphics, standards checking, converter

		solution, resonant conditions	solution, resonant conditions
Accuracy	Accurate only under cases of low THD	Accurate	Accurate
Capabilities			
Three Phase Detail	Possible	Possible	Possible
Variety of Loads	Load current modelled off line	Load models required by program	Load models required by program
Converter Controls	No	Possible	Possible
Hardware for Automatic Data Input	Available	Available	Available
Availability of Software	Readily available commercially, in price range $1000-$15000	Not readily available	Available commercially, in price range $500-$5000

Table 3.7.1: Comparison of the current injection, Gauss-Seidel and Newton-Raphson methods [13].

3.8 Discussion

Harmonic power flow programmes should not be seen as a replacement for conventional fundamental frequency loadflow programmes. This is because harmonic power flow programmes have additional features, such as tap changing, tap limits, reactive power limits at *PV* busses and phase shifter applications. Furthermore, the fundamental loadflow programmes make use of memory allocation techniques, which are based on the sparsity of the Jacobian matrix. For these reasons, it would be unwise to use a harmonic loadflow programme in the place of a fundamental loadflow programme.

The main difference between time domain and frequency domain methods is one of detail. The network elements are modelled in far more detail in the former case. Furthermore, frequency

domain methods are applicable to the steady state of the system, whereas time based methods are for the transient case, as well as the steady state. It would be unwise to expend the effort to compile a time domain simulation case when only the steady state solution is required. In most cases for power systems, the steady state solution is required.

Competition between different harmonic power flow software packages mainly concerns the following:

1. Cost
2. Graphical output
3. Three phase detail capability
4. Modular modelling of loads and sources
5. Long term software support
6. Accuracy of solution
7. Types of errors in modelling
8. Solution speed
9. Maintainability of the software
10. Computer compatibility
11. Data requirements
12. Automatic features

Of increasing importance in harmonic studies for power systems, is the sizing of cables, particularly phase and neutral conductors. This is important because resonance conditions can amplify the currents that flow through the cables. In addition to this, the triplen harmonics do not always cancel each other out in the neutral conductors. They can then add up, resulting in a higher current than what was expected. For this reason the downsizing of neutral conductors should be handled with great care.

3.9 Case Study

In order to illustrate how a typical harmonic study is conducted, a case study is done on a three bus system. This network is shown in figure 3.9.1 and the system data is given in table 3.9.1.

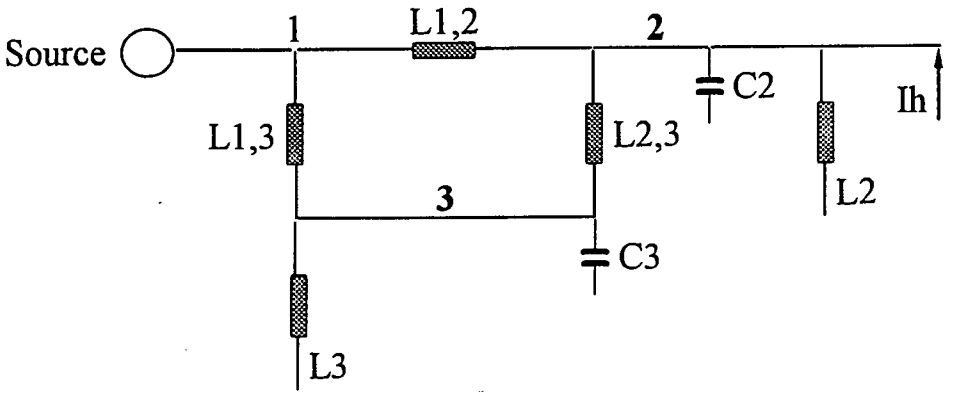

Figure 3.9.1: Three bus network.

Line	Resistance in Per Unit	Inductance in Per Unit
L1,2	0.0581	1.2778
L2,3	3.6780	8.0150
L1,3	0.9870	2.9810
Capacitor	**KV**	**MVA**
C2	44	6
C3	44	6
Loads	**KVA**	**KV**
L2	4500	44
L3	4540	44

Table 3.9.1: Data for the three bus power system.

It can be seen from figure 3.9.1 and table 3.9.1, that there are 2 active devices and 7 passive devices which make up the power system. The line capacitances have been neglected, as these are insignificant to the power capacitors connected to the network. Furthermore, it was assumed, that the fundamental frequency is 60 Hz (as this is used more widely and also consistent with the remainder of the thesis) and that the displacement power factor is 1. In order to analyse the network, SuperHarm was chosen, as this is part of the Harmflo+ Workstation, which is popular amongst EPRI members and because it is based on the current injection method, which is widely used for harmonic analysis of power systems. At first the

admittance matrix is of size *3* × *3* and it is full. However, after the system has been factored and reduced, the size of the matrix is *2* × *2*. During the reduction process no fill in terms were required and the matrix is still full, due to the small size of the network. The harmonic current source *Ih*, connected to bus 2 is swept over all frequencies from 1 to 3000 Hz in steps of 1 Hz. The voltage frequency responses are shown in figures 3.9.2 to 3.9.4.

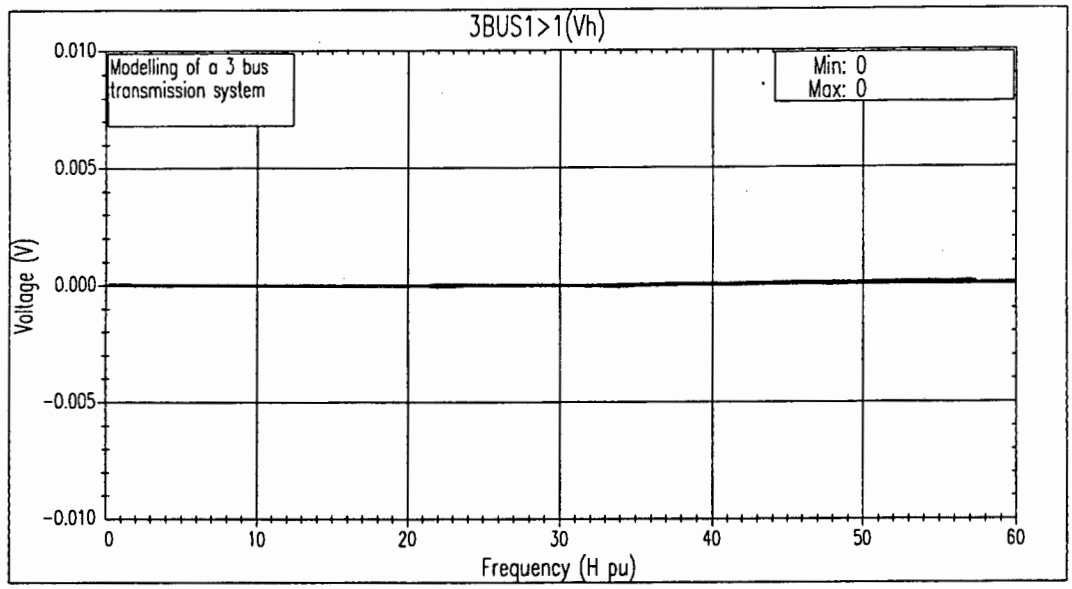

Figure 3.9.2: Voltage frequency response at bus 1.

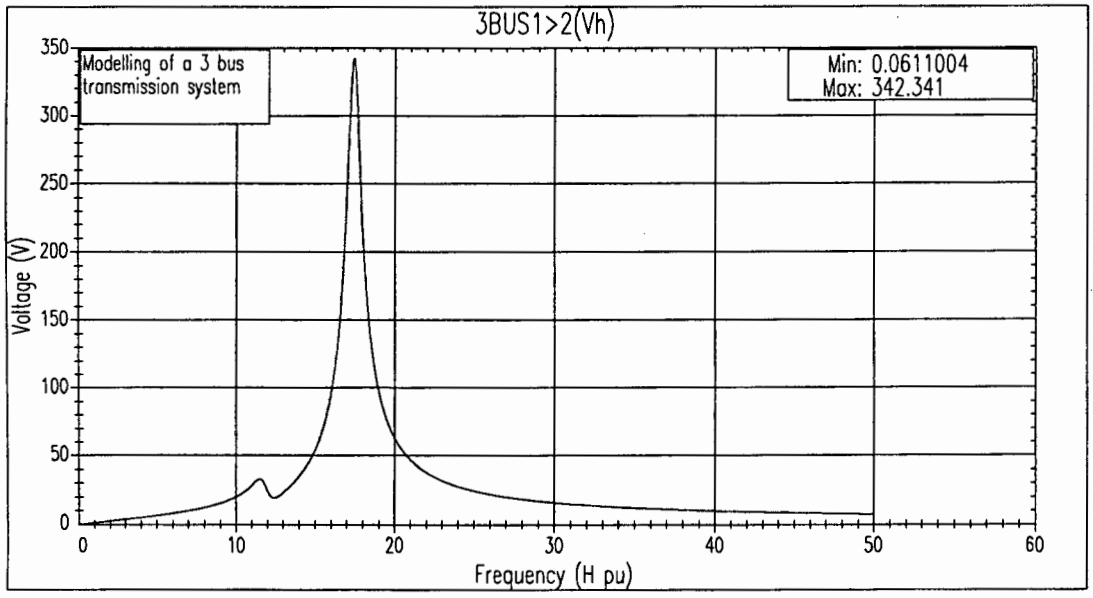

Figure 3.9.3: Voltage frequency response at bus 2.

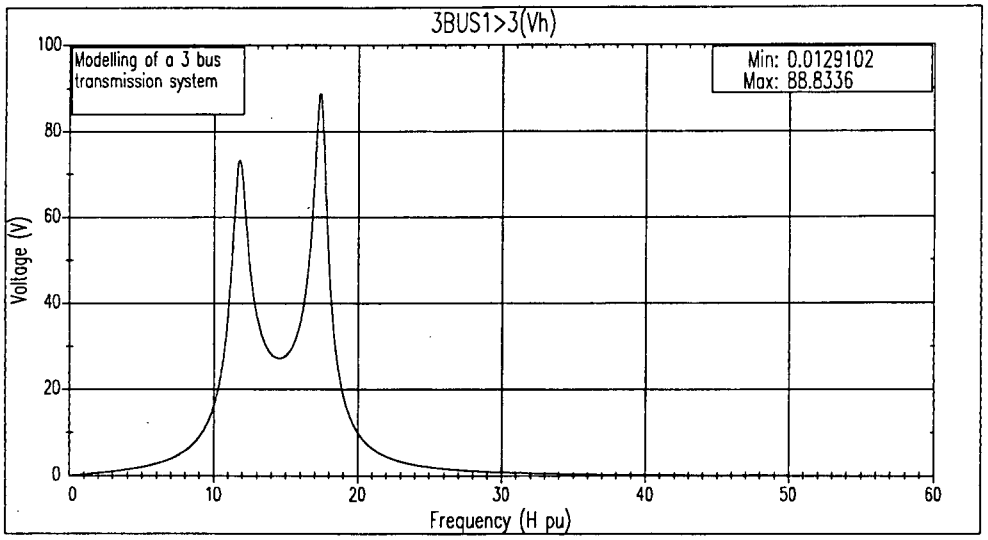

Figure 3.9.4: Voltage frequency response at bus 3.

The voltage response of bus 1 is at 0, since the generator is suppressed for the frequency scan. The voltage at bus 2 shows a high resonant peak at approximately the seventeenth harmonic of about 350 per unit. The voltage at bus 3 indicates two resonant peaks in the vicinity of the twelfth and seventeenth harmonic, of approximate magnitude 70 and 90 per unit respectively.

The current injected by the harmonic current source is shown in figure 3.9.5. It can be seen there, that the current magnitude is 1 per unit over all frequencies. This is characteristic for the current injection method.

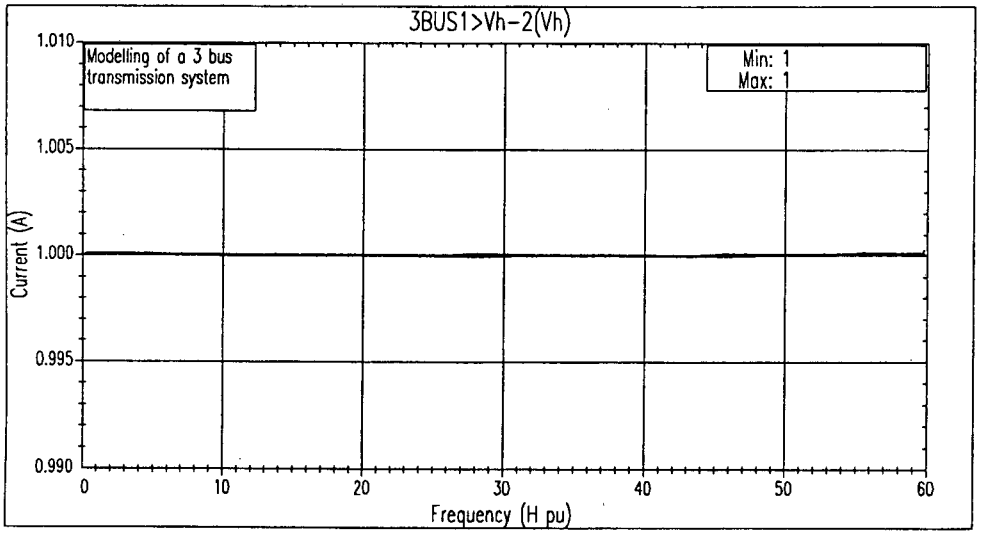

Figure 3.9.5: Current injected by the harmonic current source.

The capacitor currents are shown in figures 3.9.6 and 3.9.7 respectively. It can be seen there, that the current through C2 has a resonant peak close to the seventeenth harmonic, of approximate magnitude 2.7 per unit. The current through C3 has two resonant peaks close to the twelfth and seventeenth harmonic of approximate magnitude 2.7 and 4.8 respectively.

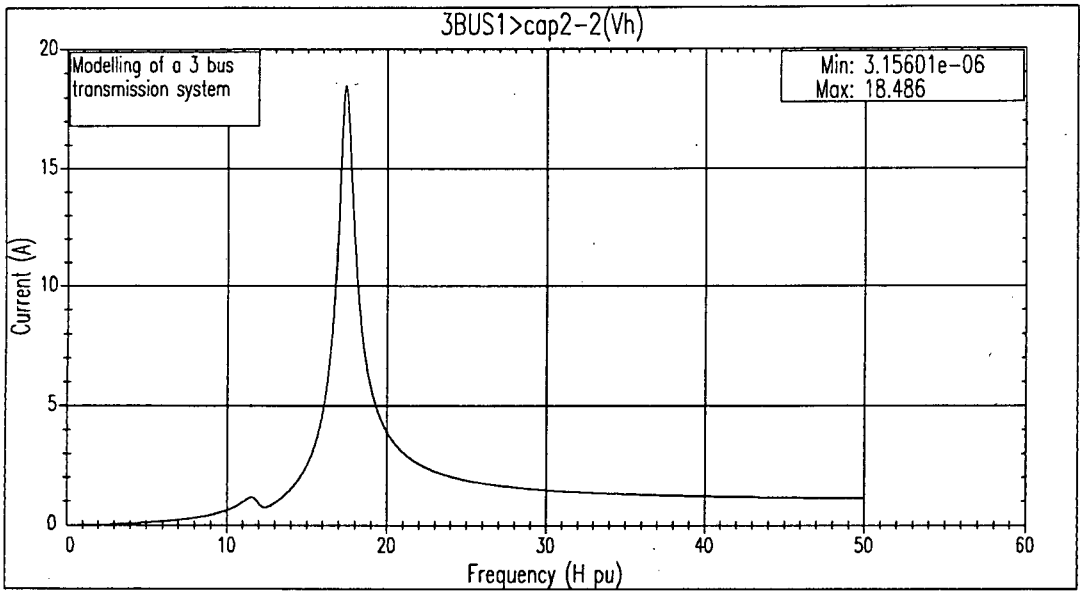

Figure 3.9.6: Current frequency response through C2.

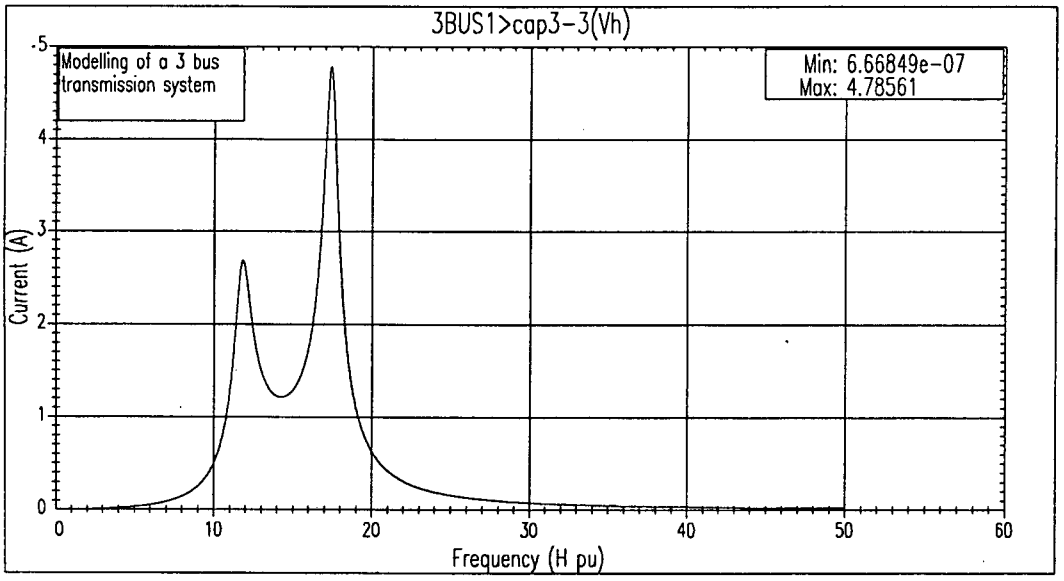

Figure 3.9.7: Current frequency response through C3.

The harmonic currents through the transmission lines are shown in figures 3.9.8 to 3.9.10. It can be seen there, that the current through L1,2 has a resonant peak of about 15 per unit close to the seventeenth harmonic. The current through line L2,3 has two resonant peaks close to the twelfth and seventeenth harmonic of approximate magnitude 2.1 and 1.7 per unit respectively. The current through line L2,3 has a resonant peak in the vicinity of the seventeenth harmonic of approximate magnitude 3 per unit.

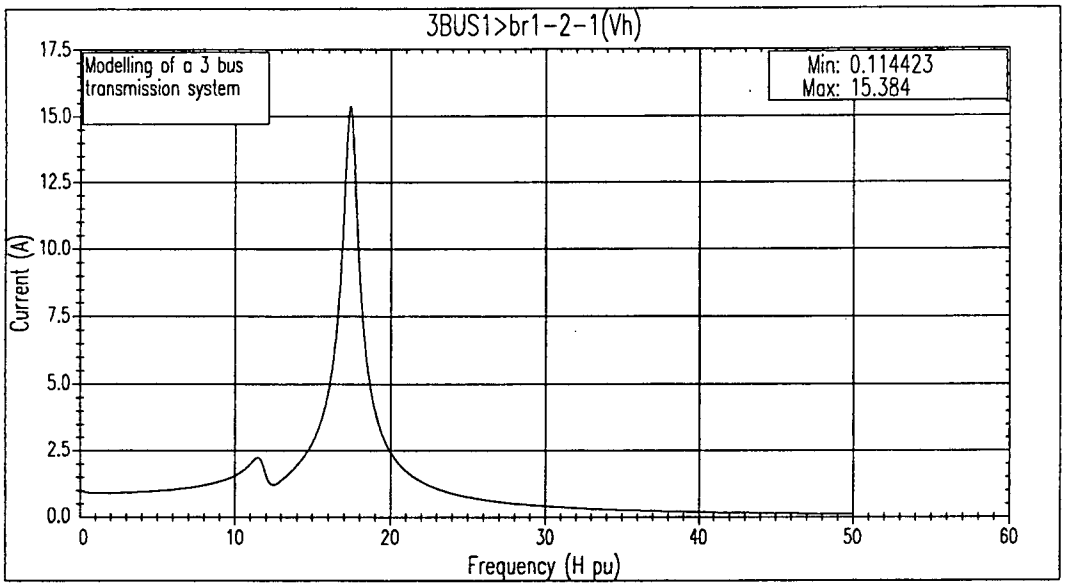

Figure 3.9.8: Current frequency response through L1,2.

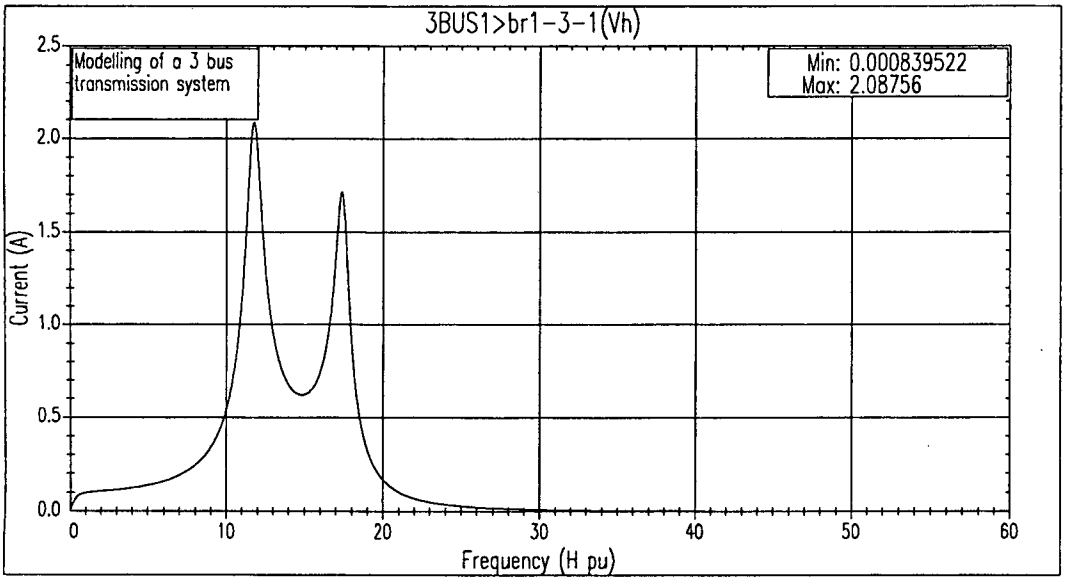

Figure 3.9.9: Current frequency response through L1,3.

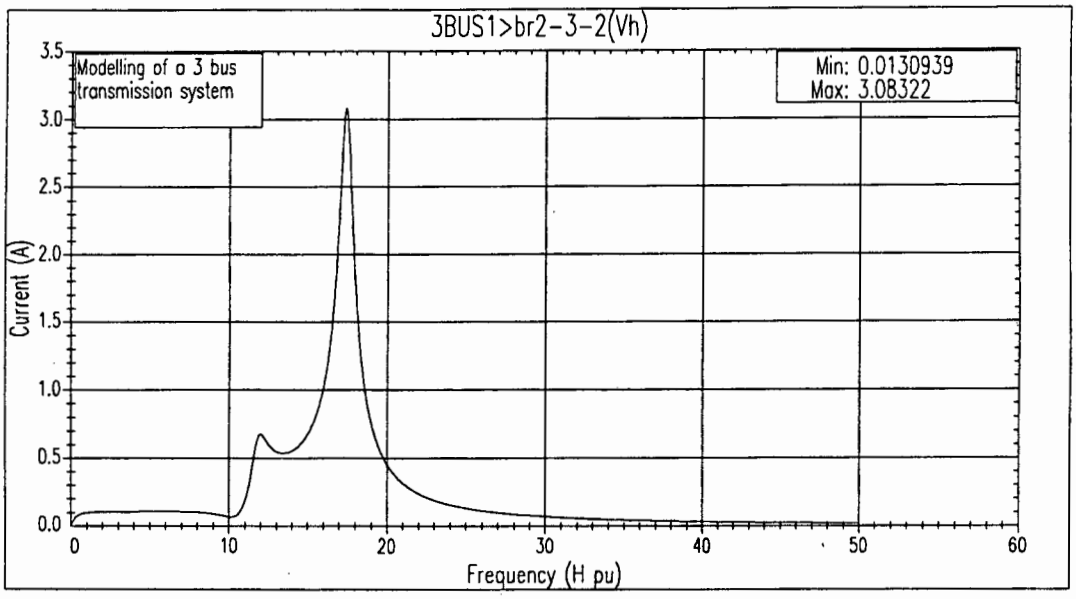

Figure 3.9.10: Current frequency response through L2,3.

The currents through the loads are shown in figures 3.9.11 and 3.9.12. It can be seen there, that the current through L2 has a resonant peak in the vicinity of the seventeenth harmonic of approximate magnitude 0.8. The current through L3 has two resonant peaks close to the twelfth and eighteenth harmonic of about 0.17 and 0.21 per unit respectively.

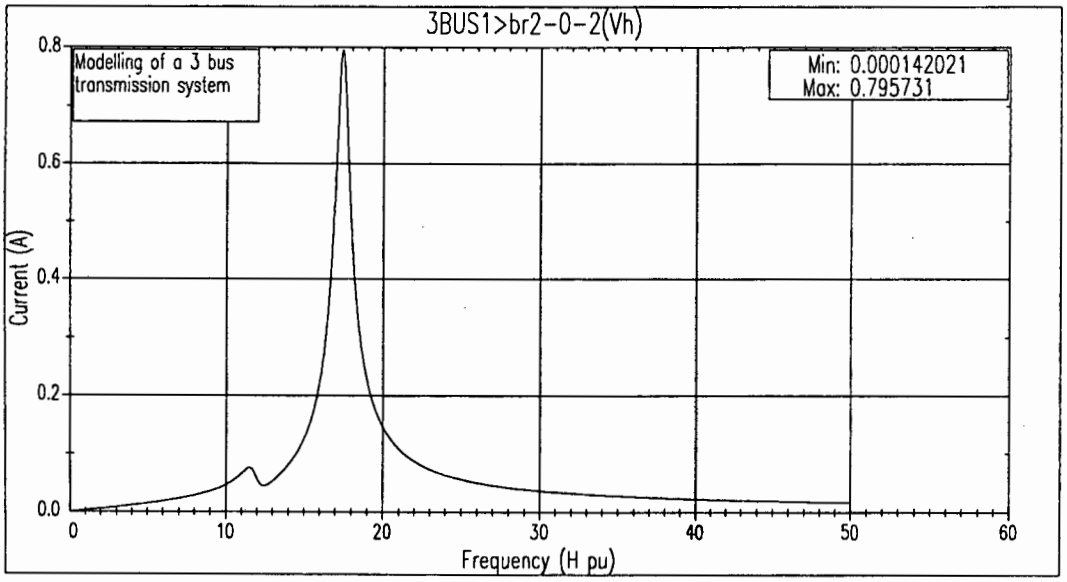

Figure 3.9.11: Current frequency response through L2.

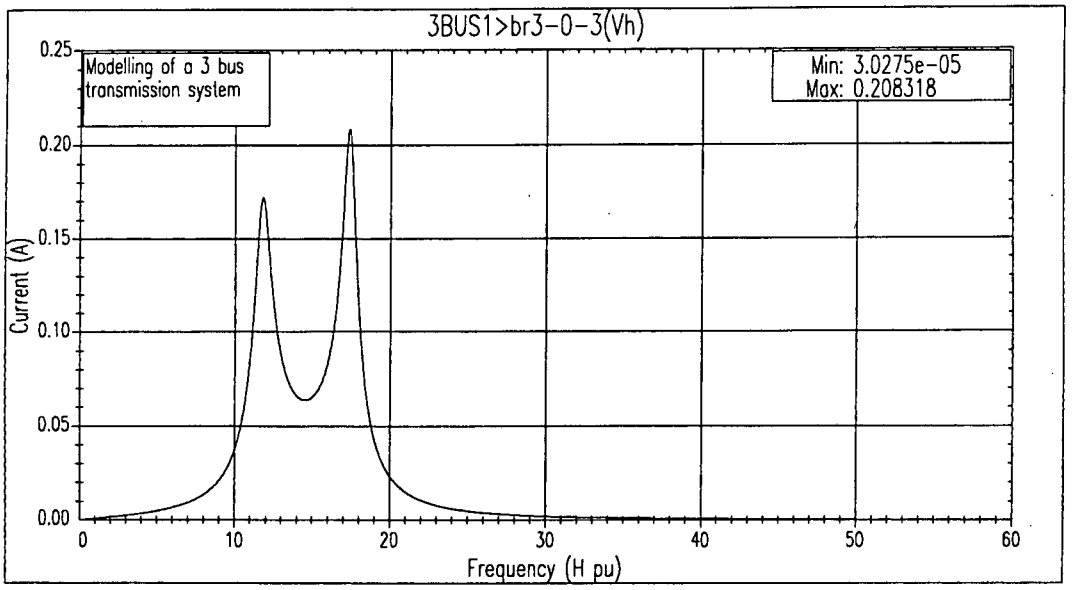

Figure 3.9.12: Current frequency response through L3.

3.10 References

[1] R. Hawkins, "Study of Transformer Modelling in Harmonic Analysis and the Ability of Various Software Packages to Implement the Different Models", *BSc (Eng) Thesis*, University of Cape Town, Republic of South Africa, 1994.

[2] G. W. Rowse, "A Harmonic Parametrical Study of a 22kV Transmission Line using EMTP and V-Harm", *BSc (Eng) Thesis*, University of Cape Town, Republic of South Africa, 1994.

[3] V. Maharaj, "A Harmonic Parametrical Study of a 400kV Transmission Line using Harmonic Simulation Tools", *BSc (Eng) Thesis*, University of Cape Town, Republic of South Africa, 1995.

[4] H. W. Dommel, *Electromagnetic Transients' Program Reference Manual (EMTP Theory Book)*, Printed by the University of British Columbia, Vancouver B. C., Canada, August 1986.

[5] J. J. Allemong, R. J. Bennon and P. W. Selent, "Multiphase Power Flow Solutions Using EMTP and Newton's Method", *IEEE Transactions on Power Systems*, Volume 8, Number 4, November 1993, pages 1455-1462.

[6] S. C. Chapra and R. P. Canale, *Numerical Methods for Engineers with Personal Computer Applications*, New York, McGraw-Hill, 1985.

[7] R. N. Dahr, *Computer Aided Power System Operation and Analysis*, McGraw-Hill.

[8] M. A. Pai, *Computer Techniques in Power System Analysis*, McGraw-Hill, New Delhi, 1979.

[9] G. C. Kusic, *Computer Aided Power Systems Analysis*, Prentice Hall, Englewood Cliffs, 1986.

[10] J. D. Glover and M. Sarma, Power System Analysis and Design with Personal Computer Applications, Second Edition, P. W. S. Publishing Company, Boston, 1994.

[11] J. Arrillaga and C. P. Arnold, *Computer Analysis of Power Systems*, John Wiley and Sons, New York, 1990.

[12] J. Arrillaga, C. P. Arnold and B. J. Harker, *Computer Modelling of Electrical Power Systems*, John Wiley and Sons, New York.

[13] G. T. Heydt, *Electric Power Quality*, West LaFayette: Stars in a Circle Publications, 1991.

[14] Task Force on Harmonics Modelling and Simulation, "Modelling and Simulation of the Propagation of Harmonics in Electric Power Networks Part I: Concepts,

Models and Simulation Techniques", *IEEE Winter Meeting 1995*, Paper 95 WM 264-2 PWRD.

[15] Task Force on Harmonics Modelling and Simulation, "Modelling and Simulation of the Propagation of Harmonics in Electric Power Networks Part II: Sample Systems and Examples", IEEE Winter Meeting 1995, Paper 95 WM 265-9 PWRD.

[16] R. G. Wasley and M. A. Shlash, "Newton-Raphson Algorithm for 3-Phase Load Flow", *Proceedings of the IEE*, Volume 121, Number 7, July 1974, pages 630-638.

[17] W. Xu, J. Marti and H. W. Dommel, "A Multiphase Harmonic Load Flow Solution Technique", *IEEE Transactions on Power Systems*, Volume 6, Number 1, February 1991, pages 174-182.

Chapter 4

Comparison of Harmonic Analysis Software Packages for Power Systems

4.1 Introduction

In order to finally implement an optimisation algorithm to minimise the effect of harmonics in power systems, it was found necessary to investigate existing academic and commercially available software packages for the harmonic analysis of power networks. For this reason and at the request of Eskom's power quality task group, a questionnaire was compiled for the evaluation of the attributes and capabilities of the latest versions of various software packages for harmonic analysis in power systems and to make recommendations on packages to be purchased and used by distribution centres. In this chapter therefore, the questionnaire, the results of the survey and the additional material, demonstration disks, manuals and other relevant literature, that was returned by software developers and suppliers, is discussed. In addition to this, academic software packages and programmes freely available in the public domain, are also elaborated upon. This material is supplementary to the final year BSc (Eng) theses [1 - 3], that were completed at the University of Cape Town.

4.2 Questionnaire on Harmonic Analysis Software Programmes for Power Systems

This questionnaire was compiled in collaboration with Eskom. The questionnaire is attached in appendix A. As can be seen there, the questionnaire comprises seven sections, covering all relevant aspects of harmonic analysis programmes. These seven sections are:

1. Hardware and software requirements: This includes computer or workstation specifications and programmes required.
2. Software interfaces: This covers the operating platforms, the ease of transferring data and whether there are additional programme modules available.

3. Input: This covers items such as graphical user interfaces (GUI's).
4. Output: This includes the way in which the output is displayed.
5. Technical issues: This includes the type of algorithms, the modelling of network elements and the availability of standard models.
6. Additional technical functions: This covers additional functions or capabilities, such as the IEEE or IEC harmonic distortion limits, transformer derating and so forth.
7. General issues: This covers the price, user groups, technical support, manuals and future developments.

This questionnaire was then sent out to various international software developers and suppliers. It was completed by them and then returned. The responses are discussed in section 4.3.

4.3 Evaluation of the Results of the Survey on Harmonic Analysis Programmes for Power Systems

The responses obtained to the questionnaire were very positive. Most respondents completed it as accurately and completely as possible, supplying all the information that was requested.

Responses were obtained on the following packages:

1. Harmflo+
2. V-Harm
3. Hi-Wave
4. Harmonique
5. ETAP
6. CYMHARMO
7. ERACS

The results of this survey are tabulated in appendix B, in such a way, that they can also serve as a guideline for the purchasing of such packages by utilities. However, the main conclusions are as follows:

1. As can be seen in appendix B, most software packages operate from a Microsoft Windows (Windows) platform on an 80386 based computer. This makes the programme very user friendly and allows all the Microsoft Windows facilities to be used, such as multi-tasking and background processing importing and exporting of data and others. Furthermore, these programmes can be operated with a mouse, which makes for ease of use.

2. It can also be seen in appendix B, that mainly the more general power system analysis programmes have GUI's. Harmonique and ERACS are the only packages that can not display the actual waveforms and V-Harm is the only package that can display three dimensional graphs. Otherwise all other standard features are available in all programmes.

3. As regards the technical issues, appendix B shows, that all the listed packages are frequency domain based and make use of the current injection method. The Harmonique and ETAP packages also make use of the Gauss-Seidel algorithm. Only the V-Harm and the CYMHARMO packages provide for unbalanced loads. The Harmonique package, followed by the ETAP package, have the widest range of types of networkelementmodels, such as statistically and probabilistically based models. Batch mode studies are available in Harmflo+, V-Harm and CYMHARMO. Hi-Wave and CYMHARMO have the most standard networkelementmodels available. Harmonique provides for the CIGRE transformer and load models, whereas CYMHARMO includes a CIGRE load model.

4. The programmes with the most additional technical modules available, shown in appendix B, are Harmflo+ and Hi-Wave, followed by Harmonique and ETAP. These additional modules cover items such as filter rating, transformer de-rating, IEEE / IEC distortion limits and such like.

5. In the general section in appendix B it is shown, that the prices of the programmes range widely, depending on the Microsoft Disc Operating System (MS DOS) or Windows versions and the number of additional modules requested. Formal user groups exist for Harmflo+ and ETAP. These groups also operate by e-mail. A group license is not offered for Harmonique.

6. All the programmes are generally fast enough and efficient, making use of sparsity algorithms and such like.

4.4 Harmflo

Harmflo is a software package specifically developed, by G. T. Heydt, at the University of Purdue, USA, for the analysis of harmonics in power systems. It is written in Fortran and operates on the MS DOS platform. Since it has been overtaken by more efficient and user-friendly packages, it is not much in use today any longer [4].

4.5 V-Harm

V-Harm (The Harmonics Verdict) is a module of the Power Verdict Software Series, which is marketed by Cooper Power Systems. It is a power system harmonic simulation and analysis programme, written by E. W. Gunther in collaboration with M. F. McGranaghan and R. C. Dougan. It is a product of the Systems Engineering Department of Cooper Industries, of the McGraw-Edison Power Systems Division in Canonsburg, Pennsylvania [5, 6].

4.5.1 Vendor Reliability and Support

Consulting with the developers, on simulation problems, is available by means of telephone, fax or correspondence. Furthermore, workshops are also organised on an ongoing basis for people interested in harmonics or power quality issues.

4.6 The Harmflo+ Workstation

The Harmflo+ workstation consists of a eight modules [7, 8]. These are:

1. The Datafile editor: This is a text editor used for the preparation of input files.
2. Harmflo+ for Windows: This is a harmonic load flow simulation programme, which is only available for Electric Power Research Institute (EPRI) members. It utilises the Newton-Raphson algorithm.

3. SuperHarm: This is a harmonic simulation programme, utilising the current injection method.
4. TOP: This is the output processor (TOP) for the modules.
5. IEEE519 Verification: This module is used to check, whether a network complies with the IEEE 519 standard. This is only available to EPRI members.
6. Filter Design Spreadsheet: This is a spreadsheet used for the design of filters.
7. Excel Harmonic Workbook: This is a harmonic workbook based on EXCEL.
8. The User Programme: This is a user definable tool. It can be a spreadsheet or even a programme such as the Electromagnetic Transient Programme (EMTP).

Only items 2., 3. and 4. are discussed in the next three subsections, as they are of relevance for the purpose of a software comparison.

4.6.1 Harmflo+

In 1977 L. Fink and G. T. Heydt at the University of Purdue, USA, started investigations into a harmonic analysis programme. In 1981 EPRI approached G. T. Heydt to develop a harmonic load flow programme. His programme is based on the Newton-Raphson algorithm, in which active and reactive powers at all harmonics of the power frequency were forced to zero. G. T. Heydt together with D. Xia worked on this contract. They discarded the mismatch power concept and instead introduced a mismatch current principal. In other words, the current equations were used instead of the power equations in the iteration process. M. Grady also assisted in the project, by rewriting the code and thereby improving many aspects of the programme.

4.6.2 SuperHarm

SuperHarm was developed from V-Harm by the same engineers, mainly E. W. Gunther. The programme is also a product of the Systems Engineering Department of Cooper Industries, of the McGraw-Edison Power Systems Division in Canonsburg, Pennsylvania. SuperHarm is distributed and marketed by Electrotek Concepts Incorporated. SuperHarm uses the current injection method to solve unbalanced multiphase systems of unlimited size. SuperHarm is

available in four versions, Basic (B), Utility (U), Industrial (I) and Advanced (A). The Basic version is distributed automatically with the acquisition of the HarmFlo+ workstation. This version can be easily upgraded at an extra cost. The differences between these four versions are shown in table 4.6.2.1, where an X indicates that the respective device is available in the respective version.

Model	Description	B	U	I	A
BRANCH	Single-phase series impedance with arbitrary frequency dependence.	X	X	X	X
BRANCH3	Three-phase series impedance represented by sequence components.	X	X	X	X
CABLE	A frequency dependent model computed from construction and placement of conductors, insulation jackets and sheaths.		X	X	X
CAPACITOR	Capacitor with optional resistance.	X	X	X	X
CONVERTER	Phase-controlled power converter model, single- or three-phase.			X	X
DOUBLEPI	Single-phase pi representation of a double circuit line, with long line correction.		X		X
DOUBLEPI3	Three-phase DOUBLEPI.		X		X
FREQDEPEQUIV	Creates a frequency dependent network equivalent of a specified portion of the system. Speeds solution without loss of accuracy.				X
INDUCTIONMOTOR	Single-phase induction motor model.			X	X
ISOURCE	Discrete harmonic current source.	X	X	X	X
LINE	A frequency dependent model computed from conductor construction and placement. Includes bundling, earth resistivity, segmented ground wires.		X		X
LINEARLOAD	Linear load model.	X	X	X	X
NONLINEARLOAD	Non-linear load model.	X	X	X	X

PI	Single-phase pi representation of a single circuit line, with long line correction.	X	X	X	X
PI3	Three-phase PI.	X	X	X	X
SERIESFILTER	Series capacitor and reactor, computed from kV, kVAr and tuning frequency.	X	X	X	X
SYNCMOTOR	Synchronous motor model.			X	X
TCR	Thyristor controlled reactor model.		X		X
TRANSFORMER	Single- or three-phase, 2 or 3 winding transformer.	X	X	X	X
VSOURCE	Discrete harmonic voltage source.	X	X	X	X
YPRIMITIVE	Matrix representing a set of node-node and node-ground admittances.		X		X
ZPRIMITIVE	Matrix representing a set of mutually coupled branches.		X		X

Table 4.6.2.1: Device libraries for the different versions of SuperHarm [7].

4.6.3 TOP

TOP was developed by Electrotek Concepts Incorporated. It is a spreadsheet type output processor, specifically designed for the processing of EMTP, V-Harm, Harmflo+ and SuperHarm output files. It is a Windows based programme. This gives it additional flexibility, in that multiple document handling, multi tasking, cutting and pasting of graphs and tables directly into spreadsheets and wordprocessors and the ability to work with more than one graph or table at one time are all possible. It can display quantities in a variety of ways, such as spectra charts, frequency scans, *RX* locus plots, harmonic summary tables and so forth. The programme is also provided with an internal calculator, with which graphs can be manipulated. In this way for example, the powerflow through a branch can be obtained by multiplying the voltage and current wave shapes.

4.6.4 Vendor Reliability and Support

The usergroup for Harmflo+ is cosponsored by Electrotek Concepts Incorporated and EPRI. The group provides a quarterly newsletter, annual meetings, workshops, a library of harmonic case studies and consulting by phone, fax or e-mail. Correspondence with the usergroup is facilitated by a programme called Excalibur, which is supplied with the acquisition of the Harmflo+ workstation. Recently Electrotek Concepts Incorporated also established a site called *PQ* Network on the internet for interested people with access thereto. The address of this site is: http://www.pqnet.electrotek.com/. This can easily be accessed by using programmes such as Mosaic or Netscape.

4.7 Hi_Wave

Hi_Wave (Harmonic Investigation and Analysis Software) is marketed by SKM Systems Analysis Incorporated. This programme is part of a range of software modules, such as modules for loadflow calculations, protection relay grading and so forth. One of these is the well known Distribution Analysis for Power Planning Evaluation and Reporting (DAPPER) package.

4.8 Harmonique

Harmonique is a harmonic analysis programme for power systems. It was developed by Electricite de France (EDF) for their particular requirements. It is extensively used by them to support their improvement of the quality of supply campaign. The programme is as yet only available in French, which makes its use in English speaking countries more difficult.

4.9 ETAP

ETAP is marketed by Operation Technology Incorporated. This programme is a general power system analysis tool, with a capability of analysing harmonics. It is limited at 1000 buses and integrates with any Computer Aided Design (CAD) platform.

4.9.1 Vendor Reliability and Support

Seminars and workshops are organised for interested parties. Newsletters are distributed on a regular basis to members of the user group.

4.10 CYMHARMO

CYME International Incorporated is based in Canada and was established in January 1986. CYME markets a range of power system analysis programmes, amongst others CYMHARMO, which is their harmonics analysis programme.

4.11 PCFLO

PCFLO was developed by M. Grady from the University of Texas at Austin, USA. It is a general power system analysis programme for load flow, short circuit and harmonic analysis.

4.12 ERACS

ERACS is an all over power system analysis and design programme, with a capability for performing harmonic analysis. It is marketed by ERA Technology, which is based in Surrey, England [9].

4.13 Electrical Distribution System Analysis Programs (EDSA)

EDSA is a general power system analysis software package. It is marketed by EDSA Micro Corporation, based in Michigan, USA. According to EDSA Micro Corporation, it is the most comprehensive package of power engineering software ever written for any computer. It is compatible with all CAD platforms and makes use of an extensive library to model real devices. It has a capability to analyse harmonic phenomena in power systems. The programmes are provided with sample longhand calculations and numerous programmes have been verified and validated with the AEP, IEEE, Beeman, Westinghouse, GE, ANSI and IEEE standards sample test files [10].

4.13.1 Hardware and Software Required

For the optimal operation of EDSA, the following minimal requirements are highly recommended:

- An IBM personal computer
- MS DOS 2.0
- 40MB of hard disk space
- 640kB memory
- A VGA or EGA graphic card
- A graphic printer
- A mouse
- A colour plotter

4.13.2 Vendor Reliability and Support

Workshops and seminars are organised by the EDSA Micro Corporation, twice a year for interested persons. On site training is also available upon request. Regular newsletters are sent out and help is also available via fax, regular and toll-free phone calls and e-mail. A 24-hour on-line bulletin board for direct access and down-loading of periodic updates will soon be available.

4.14 DigSilent

DigSilent is a general power system analysis programme. An advance copy was forwarded to the University of Cape Town, for evaluation purposes. The package has a module for the harmonic analysis of power systems. There are programming errors in the source code and these still need to be corrected [11].

4.15 EMTP

The EMTP was developed by the Bonneville Power Administration (BPA) in Portland, Oregon, USA. For fifteen years BPA pioneered work on EMTP. The aim of the development was, that all work was to be kept in the public domain and that everything should be freely available to everyone. However, in 1984 EPRI wanted to terminate their agreement and to market a version commercially. To protect the royalty free contributions of various academics, the Leuven EMTP Centre (LEC) decided to market an Alternative Transient Program (ATP) [12 - 14].

The main purpose of the programme is the simulation of high frequency transients (switching and lightning) in electrical power systems. Very accurate models are used. Harmonic analysis is only possible for two reasons:

1. Diodes, thyristors and other types of switches can be modelled in EMTP. Furthermore, the switching instants can be co-ordinated. In this way the characteristics of a converter can be reproduced. The output response for these types of simulations will be in the time domain. To do harmonic analyses, this will have to be converted to the frequency domain.
2. EMTP has an in-built scanning function, which can determine the frequency response of a network.

4.15.1 DBOS

DBOS is an interface programme between MS DOS and Fortran, the EMTP source code. It is necessary to execute EMTP.

4.15.2 ATP-Draw

At present many GUI's are developed for EMTP. However, ATP-Draw is a GUI for EMTP. It is a freely available graphics front end, where actual one line, or three line diagrams can be constructed and an EMTP file can be automatically compiled and subsequently executed.

4.15.3 TP-Plot and PC-Plot

TP-Plot and PC-Plot are both graphics output processor programmes for EMTP. Both programmes are freely available and can also be obtained with the aid of the file transfer programme (ftp) from an ftp site in north Dakota, USA. The former makes use of a mouse, which makes the operation of the programme much easier.

4.15.4 Hardware and Software Required

In order to execute EMTP, a 386 computer is required. As the output is in eighty column format a special printer or additional software to change the output format is required. A graphics output processor is needed to view the results.

4.15.5 Vendor Reliability and Support

Various usergroups have been established by EMTP users, to provide support to other EMTP users. Some of them are for free, such as the one operated by S. Meyer. Others require a membership fee, such as the one run by Electrotek Concepts Incorporated. Contact with these groups can be established via e-mail. Services provided through these usergroups are amongst others:

1. Quarterly newsletters
2. EMTP and computer support
3. Case studies
4. EMTP models and modules
5. A number hotline
6. Meetings
7. Workshops and training

Regular newsletters and updates of the programme can be easily obtained with the aid of ftp from an ftp site in north Dakota, USA.

4.15.6 Easy Learning and Use

EMTP was developed at a time when Fortran was the best computer language available and when mainframes where in use. As a result the input file is still formatted for the card readers that were in use at that time All input data therefore has to be placed in specific columns. This causes much confusion and also significant errors. The programme is not user-friendly compared to other programmes in use today. For these reasons the programme is very difficult to use and it can take a long time to learn it, if there is no direct help available.

4.16 Matlab

The Matlab programme is mainly used by engineers to solve mathematical type problems. It is not a programme specifically dedicated to the analysis of harmonics in power systems. However, it is possible for an engineer to write his own programmes, which can simulate a given system. In this way the user becomes intimately involved with the modelling and analysis of the system. He can also modify the programme very easily, to achieve something slightly different, such as changing a model. In the case of the other commercially available programmes, mentioned above, changing a model, for example, is not possible, as these are "black boxes" as far as the models and algorithms go. Other programmes are not as flexible as Matlab and in many cases, such as the optimal placement of capacitors, they are of limited use.

Matlab can be executed on any personal computer, under Windows or MS DOS. It is also available for workstations. There are no special hardware or software features required.

Matlab comes with various toolboxes, such as robust control, control, neural networks, optimisation and signal processing. It also comes with Simulink, where actual system blocks can be defined. Input and output data is very easily transferable to programmes such as Maple, C++ and Quatro Pro. EMTP output files can easily be converted to Matlab for postprocessing and any other ASCII type files can be very easily imported. Exporting data is also done in a similar fashion [15 - 22].

4.16.1 Vendor Reliability and Support

Support groups exist for Matlab, these are also readily accessible via e-mail. There are also sites on the internet that can be accessed with programmes such as Mosaic or Trumpet. Some site addresses are: http://www.mathworks.com, or ftp.mathworks.com. Newsgroups also exist, were questions can be mailed to. In addition to this the developers of Matlab are also available on e-mail and can easily be contacted.

4.17 Maple

Maple is a general purpose programme for the symbolic manipulation or analysis of mathematical equations or expressions. It is mainly used by engineers in conjunction with other programmes such as Matlab or Scientific Workplace. Maple is not a dedicated programme for the analysis of harmonics in power systems, but is of tremendous value in an indirect way. It is mainly used to manipulate, develop and analyse equations that can subsequently be used for the modelling of various systems or devices [23, 24].

4.17.1 Vendor Reliability and Support

Various newsgroups exist on the internet, which can easily be accessed with the aid of programmes such as Netscape or Mosaic. Questions of users can be posted there.

4.18 Conclusion and Recommendations

As can be seen from the number of software packages available, power system simulations are becoming increasingly more important. There is also a definite trend towards including a facility for harmonic analysis in these programmes.

Figure 4.18.1 serves as a summary of the different algorithms used by the different programmes. The algorithms mentioned are discussed in chapter 3.

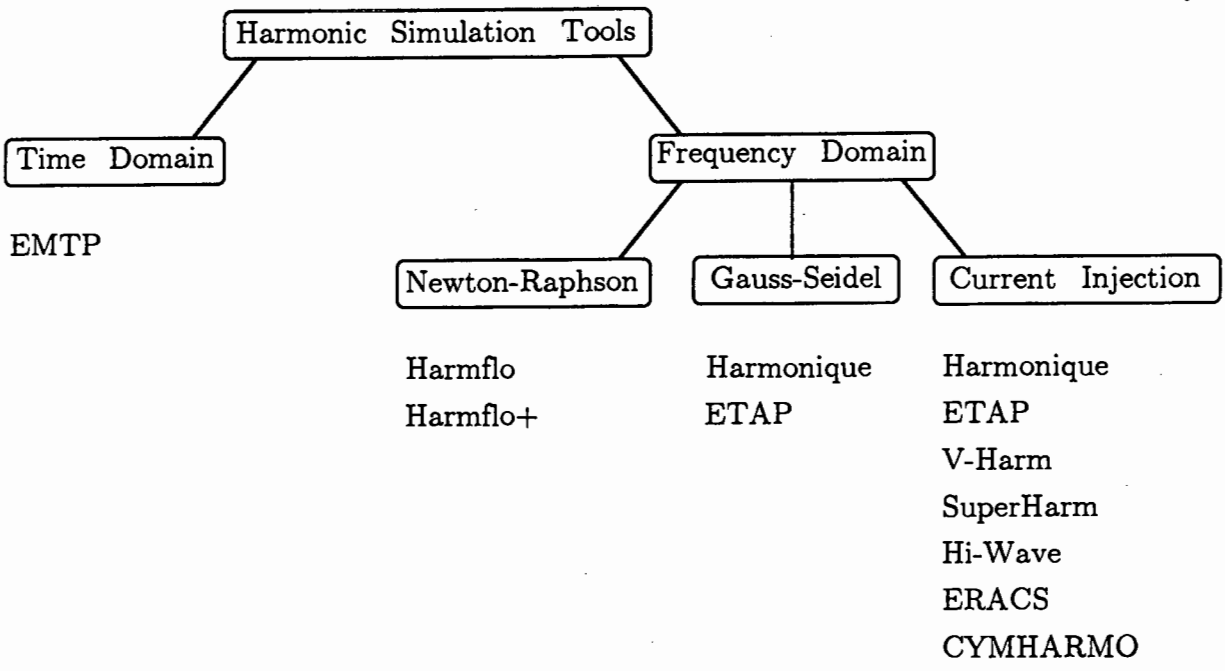

Figure 4.18.1: Overview of algorithms used by the different packages.

It can be seen from figure 4.18.1, that the current injection method is the most popular amongst contemporary power system software packages. This is the case, because the current injection method is effective and efficient. It can also be seen from the previous discussion, that there is a general trend towards a programme that can do everything, from fault calculations and protection grading to harmonic analysis. The reason for this is most likely that customers do not want to buy and study different packages. It is therefore recommended, to use a general power system analysis programme, which has a facility to do harmonic analysis and that the latter should be based on the current injection method. However, should very detailed studies be required, it might be better to use a dedicated three phase harmonic load flow package.

4.19 References

[1] R. Hawkins, " Study of Transformer Modelling in Harmonic Analysis and the Ability of Various Software Packages to Implement the Different Models", *BSc (Eng) Thesis*, University of Cape Town, Republic of South Africa, 1994.

[2] G. W. Rowse, "A Harmonic Parametrical Study of a 22kV Transmission Line using EMTP and V-Harm", *BSc (Eng) Thesis*, University of Cape Town, Republic of South Africa, 1994.

[3] V. Maharaj, "A Harmonic Parametrical Study of a 400kV Transmission Line using Harmonic Simulation Tools", *BSc (Eng) Thesis*, University of Cape Town, Republic of South Africa, 1995.

[4] G. T. Heydt and W. M. Grady, *The Harmflo Code: Version 4.0: User's Guide*, EL-4920-CCM, Research Project 2444-1, Computer Code Manual, Electric Power Research Institute, November 1986.

[5] *V-Harm: The Harmonics Verdict, Power System Harmonics Simulation and Analysis Program: User's Manual*, Cooper Industries, May 1988.

[6] E. W. Gunther and M. F. McGranaghan, "A PC-based Simulation Program for Power System Harmonic Analysis", *Second International Conference on Harmonics in Power Systems*, Winnipeg, Manitoba, October 1986, pages 175-183.

[7] E. W. Gunther and R. Dwyer, *Harmflo+: Harmonic Analysis Workstation: User's Guide: H+: Version 2.0*, February 1995.

[8] E. W. Gunther and R. Dwyer, *Harmonic Analysis Using the Harmflo+ Workstation: Harmflo+ Case Study Workbook: Harmonic Overview*, Electrotek Concepts Incorporated, Harmflo Users Group, April 1994.

[9] ERA Technology, *Electrical Power System Analysis Software (ERACS): User's Manual, Release 11, Version 1.5A*, February 1995.

[10] EDSA Micro Corporation, *Design Master EDSA CAD / CAE*, 1983.

[11] Ingenieurbuero fuer Kybernetik und Energieversorgung, *DigSilent User's Manual: Version 9.0, Release 9.15*

[12] J. M. Van Coller, *An Introduction to EMTP (Electromagnetic Transients Program): Revision 3.0*, University of the Witwatersrand, Department of Electrical Engineering, 1993.

[13] H. W. Dommel, *Electromagnetic Transients Program Reference Manual (EMTP Theory Book)*, Printed by the University of British Columbia, Vancouver B. C., Canada, August 1986.

[14] H. W. Dommel, *Electromagnetic Transients Program Reference Manual (EMTP Rule Book)*, Printed by the University of British Columbia, Vancouver B. C., Canada, August 1986.

[15] The Math Works Incorporated, *Matlab: High Performance Numeric Computation and Visualisation Software: Reference Guide*, October 1992.

[16] The Math Works Incorporated, *Matlab: High Performance Numeric Computation and Visualisation Software: Matlab Notebook Suite: User's Guide: For Microsoft Windows*, September 1994.

[17] The Math Works Incorporated, *Matlab: High Performance Numeric Computation and Visualisation Software: New Features Guide*, March 1993.

[18] The Math Works Incorporated, *Matlab: High Performance Numeric Computation and Visualisation Software: Release Notes*, May 1994.

[19] The Math Works Incorporated, *Matlab: High Performance Numeric Computation and Visualisation Software: Guide to Services, Registration and Subscribing, User Program, Technical Support, Internet Services, Newsletter: For PC and Macintosh Users*, October 1994.

[20] The Math Works Incorporated, *Matlab: High Performance Numeric Computation and Visualisation Software: User's Guide for Microsoft Windows*, August 1992.

[21] The Math Works Incorporated, *Matlab: High Performance Numeric Computation and Visualisation Software: Building Graphical User Interface*, October 1993.

[22] The Math Works Incorporated, *Matlab: High Performance Numeric Computation and Visualisation Software: External Interface Guide*, November 1994.

[23] B. Char, K. O. Geddes, G. H. Gannet, B. L. Leong, M. B. Managan and S. M. Watt, *Maple V: First Leaves: A Tutorial Introduction to Maple V*, Springer Verlag, New York, 1992.

[24] B. Char, K. O. Geddes, G. H. Gannet, B. L. Leong, M. B. Managan and S. M. Watt, *Maple V: Language Reference Manual*, Springer Verlag, New York, 1991.

Chapter 5

Analysis of an Existing State Space Model for Radial Power Systems and the Development of a New State Space Model for Radial and Meshed Power Systems

5.1 Introduction

The solution methods described in chapter 3 are very valuable for the harmonic analysis of power systems. However, none of them provide for control theory methods. This is a significant disadvantage, as the control theory methods are sometimes required and also very valuable for optimisation and contingency studies. For example the case study presented in section 6.4.2 would not be possible, if control theory methods were not available. Other areas where control theory methods would be useful are the analysis of harmonic stability, filter design and robustness amongst others. For this reason it would be advantageous, if the programmes discussed in chapter 4 would include a module for the implementation of control theory methods. However, in order to utilise the control theory methods, a new state space model or system realisation first needs to be developed for the analysis of harmonics in power systems.

5.2 Existing State Space Model for Radial Power Systems

Only one state space model used for power systems of a large size that could be found in the literature is available [1, 2]. The disadvantages of this model or system realisation are significant; these are:

1. The model only applies to radial power systems.
2. There have to be power capacitors at the end of each feeder.
3. The line capacitances are neglected, as they only have a minor effect on the analysis compared to the effect of the power capacitors.

4. The line resistances are also neglected, as they only have a damping effect, resulting in a conservative approach. This assumption is not always true, as in the case of series resonance, where the resistance actually worsens the frequency response.
5. The method makes use of the bus harmonic voltage matrix.
6. A large incidence type matrix and a large impedance type matrix need to be determined and multiplied with each other.
7. A large impedance type matrix needs to be inverted. This is very cumbersome, time consuming and numerical problems may be experienced, particularly for large systems.
8. The input has to be applied at a node with a capacitor.
9. The direct feed through matrix is not considered at all in the model.

According to the method described in [1, 2], the state space model for radial power systems is determined by choosing the independent state variables. These are taken as all the capacitor voltages, and all the nodal current injections at busses with capacitors attached to them. The loop and nodal equations can subsequently be determined. These are then written in the form of matrix equations, as follows:

$$sL \cdot x = A' \cdot x + u \qquad (5.2.1)$$

$$x^T = [I_1, I_2, \ldots I_n, V_1, V_2, \ldots V_n] \qquad (5.2.2)$$

where:
- s is the Laplace operator
- L is a $2n \times 2n$ impedance type matrix
- x is the $2n \times 1$ state vector
- A' is a $2n \times 2n$ incidence type matrix
- u is the $2n \times 1$ harmonic current injection input vector
- n is the number of voltage or current states or the number of power capacitors connected to the network

Rows *0-n* of the L matrix consist of inductances, resulting from the loop equations. Rows *n-2n* of the L matrix consist of single capacitances, which are all located on the diagonal, resulting from the node equations. The elements of A' are either equal to -1 (if the sign of the state

variable is negative), 0 (if the state variable is not present) or 1 (if the sign of the state variable is positive).

The system matrix is given by:

$$A = L^{-1} \cdot A' \tag{5.2.3}$$

Equations *(5.2.1)*, *(5.2.2)* and *(5.2.3)* are then rewritten to yield the familiar state space description for the power system, given below:

$$sx(s) = Ax(s) + Bu(s) \tag{5.2.4}$$

$$y(s) = Cx(s) \tag{5.2.5}$$

$$x^T = [I_1, I_2, \ldots I_n, V_1, V_2, \ldots V_n] \tag{5.2.6}$$

where:

- s is the Laplace operator
- x is the $2n \times 1$ state vector
- A is the $2n \times 2n$ system matrix
- B is the $2n \times 2n$ input coefficient matrix
- u is the $2n \times 1$ harmonic current injection input vector
- y is the $n \times 1$ voltage output vector
- C is the $n \times 2n$ output selection matrix
- I_n is the n'th independent loop current
- V_n is the n'th independent capacitor voltage
- n is the number of voltage or current states or the number of power capacitors connected to the network

Once the state space model has been determined, the parallel resonant frequencies (poles) are obtained by calculating the eigenvalues of the system matrix A.

The system transfer function is given by the following [3]:

$$Z(s) = \frac{y}{u} = C\frac{\text{adj}(sI - A)}{\det(sI - A)}B \qquad (5.2.7)$$

where: $Z(s)$ is the transfer function in the Laplace domain

In the case of a single input, single output (SISO) system, the system impedance can be rewritten as follows:

$$Z = \frac{1}{C_n}\frac{\det(sI - A_n)}{\det(sI - A)} \qquad (5.2.8)$$

where: C_n is the capacitance of the capacitor bank at node n

A_n is a matrix of dimension $(2n\text{-}1) \times (2n\text{-}1)$, obtained by eliminating the row and column of A, corresponding to the output node

Thus the series resonant frequencies (zeros) are determined by calculating the eigenvalues of the matrix A_n.

5.2.1 Case Study Using the Existing State Space Model

A state space model is developed for a two bus radial power system, shown in figure 5.2.1. The procedure as explained in [1, 2] and in section 5.2 is implemented for the particular network.

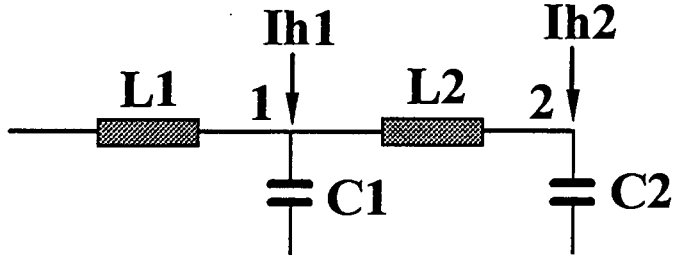

Figure 5.2.1.1: Two bus radial power system.

where: *Ih1* is the harmonic current injected at bus *1*

Ih2 is the harmonic current injected at bus *2*

L1 is an inductor

L2 is an inductor

C1 is a power capacitor

C2 is a power capacitor

At first the circuit equations are written:

$$sL_1 I_1 + V_1 = 0 \qquad (5.2.1.1)$$

$$sL_2 I_2 + V_2 - V_1 = 0 \qquad (5.2.1.2)$$

$$sC_1 V_1 = I_{h1} + I_1 - I_2 \qquad (5.2.1.3)$$

$$sC_2 V_2 = I_{h2} + I_2 \qquad (5.2.1.4)$$

where: I_1 is the current through inductor L_1

I_2 is the current through inductor L_2

These equations are then written in matrix form as follows:

$$s\begin{bmatrix} L_1 & 0 & 0 & 0 \\ 0 & L_2 & 0 & 0 \\ 0 & 0 & C_1 & 0 \\ 0 & 0 & 0 & C_2 \end{bmatrix} \cdot \begin{bmatrix} I_1 \\ I_2 \\ V_1 \\ V_2 \end{bmatrix} = \begin{bmatrix} 0 & 0 & -1 & 0 \\ 0 & 0 & 1 & -1 \\ 1 & -1 & 0 & 0 \\ 0 & 1 & 0 & 0 \end{bmatrix} \cdot \begin{bmatrix} I_1 \\ I_2 \\ V_1 \\ V_2 \end{bmatrix} + \begin{bmatrix} 0 \\ 0 \\ I_{h1} \\ I_{h2} \end{bmatrix} \qquad (5.2.1.5)$$

After applying equation *(5.2.3)* and simplifying, the following matrix results:

$$A = \begin{bmatrix} 0 & 0 & -L_1^{-1} & 0 \\ 0 & 0 & L_2^{-1} & -L_2^{-1} \\ C_1^{-1} & -C_1^{-1} & 0 & 0 \\ 0 & C_2^{-1} & 0 & 0 \end{bmatrix} \qquad (5.2.1.6)$$

Once this A matrix has been determined, it is easy to calculate the eigenvalues, singular values or to apply control theory methods.

5.3 Derivation of a New State Space Model for Radial and Meshed Power Systems

A state space model for radial and meshed power systems does exist [4], however, this method does not seem to be used at all on large networks. In view of the significant disadvantages of the state space model for radial power systems, described in [1, 2] and in section *(5.2)*, a new state space model is developed. The way in which this model is obtained, is easily programmable and applies to radial as well as meshed power systems. At first the branch current equations and nodal voltage equations for the power system are determined. Reduction formulas are then derived, to eliminate unwanted nodal voltages from the set of branch current equations. The reduction formulas are then applied repeatedly, until the voltage vectors of the branch current equations and the nodal voltage equations are the same. Thereafter the two sets of equations are combined into a general hybrid state space model description or system realisation. This system realisation is overspecified and therefore needs to be reduced a second time, to eliminate linearly dependant rows and columns. A minimal realisation of the system is then obtained, now opening the way to control theory methods for the analysis of harmonic current injections in power systems.

5.3.1 Obtaining the Equations

The line capacitances are insignificant compared to the power capacitors connected to the power grid and therefore can be neglected. Since the resistances in a power grid only have a damping effect, when no series resonance occurs, as is generally the case, they are neglected. This results in a conservative approach, providing for a worst case scenario.

At first all the branch current equations, *(5.3.1.1)*, and all the nodal voltage equations, *(5.3.1.2)* [5 - 9], are written for the Laplace domain, giving:

$$s\left[I_1, I_2, \ldots I_n\right]^T = A_2 \cdot \left[V_1, V_2, \ldots V_l\right]^T \qquad (5.3.1.1)$$

$$s[V_1, V_2, \ldots V_m]^T = A_3 \cdot [I_1, I_2, \ldots I_n]^T \qquad (5.3.1.2)$$

where:
- s is the Laplace operator
- I_n is the n'th branch current
- V_l is the l'th nodal voltage for the branch currents
- V_m is the m'th nodal voltage for the nodal voltages
- n is the number of branch currents
- l is the number of all nodes
- m is the number of nodes with capacitors attached to them
- A_2 is the $n \times l$ matrix containing the nodal voltage coefficients
- A_3 is the $m \times n$ matrix containing the branch current coefficients

5.3.2 Reducing Equation *(5.3.1.1)*

It is very likely, that there are some nodal voltages that appear in the branch current equations, but not in the nodal voltage equations, ($l \neq m$). The reason for this is, that these nodes do not have capacitors attached to them.

It is now desirable, that the nodal voltage vectors of equations *(5.3.1.1)* and *(5.3.1.2)* should be the same. For this reason the extra nodal voltage states of the branch current formula, equation *(5.3.1.1)*, need to be eliminated. In order to achieve this, reduction formulas are derived for different cases. By applying the reduction formulas to the voltage and current coefficients of equation *(5.3.1.1)*, redundant nodal voltage states are eliminated.

One row of the matrix equation given by *(5.3.1.1)* is rewritten as a summation as follows:

$$sI_i = \sum_j^l a_{ij} \cdot V_j \qquad (5.3.2.1)$$

where:
- I_i is the i'th branch current
- V_j is the j'th nodal voltage
- i is the row number of the A_2 matrix

j is the column number of the A_2 matrix

a_{ij} is a coefficient in the A_2 matrix, corresponding to the i'th row and the j'th column

5.3.3 Derivation of a Reduction Formula for a Node to be Eliminated, Adjacent to Nodes with Capacitors

For linear time invariant systems under steady state conditions, Kirchhoff's current law can be applied to the changes in currents that flow into or out of the node that is to be eliminated. These changes are then summed and set equal to zero, yielding:

$$\sum_{i}^{n} d_i \cdot sI_i = 0 \qquad (5.3.3.1)$$

where: d_i is the i'th coefficient to the i'th branch current

d can be either equal to -1 (if the change in the branch current flows out of the node), 0 (if the branch current is not connected to the node), or 1 (if the change in the branch current flows into the node).

The corresponding elements are taken out of equation *(5.3.2.1)* and substituted into equation *(5.3.3.1)*, to yield:

$$\sum_{i}^{n}\sum_{j}^{l} d_i \cdot a_{ij} \cdot V_j = 0 \qquad (5.3.3.2)$$

By swapping the summations, taking V_j out of the inner summation, taking the k'th term, corresponding to the k'th column, of the A_2 matrix, out of the summations and solving for V_k, the nodal voltage to be eliminated, gives:

$$V_k = -\frac{\sum_{j\backslash k}^{l} V_j \cdot \sum_{i}^{n} d_i \cdot a_{ij}}{\sum_{i}^{n} d_i \cdot a_{ik}} \qquad (5.3.3.3)$$

Substituting V_k back into equation *(5.3.2.1)* and simplifying, results in:

$$sI_i = \sum_{j\backslash k}^{l} (a_{ij} - \frac{a_{ik} \cdot \sum_{i}^{n} d_i \cdot a_{ij}}{\sum_{i}^{n} d_i \cdot a_{ik}}) \qquad (5.3.3.4)$$

The matrix coefficients, b_{ij}, of the reduced A_2 matrix are then given by:

$$b_{ij} = a_{ij} - \frac{a_{ik} \cdot \sum_{i}^{n} d_i \cdot a_{ij}}{\sum_{i}^{n} d_i \cdot a_{ik}} \qquad (5.3.3.5)$$

5.3.4 Derivation of a Reduction Formula for Two Adjacent Nodes to be Eliminated, Adjacent to Nodes with Capacitors

Once again, as shown in section 5.3.3, the changes in current are summed at the two nodes, that are to be eliminated.

$$\sum_{i}^{n} d_i \cdot sI_i = 0 \qquad (5.3.4.1)$$

$$\sum_{i}^{n} e_i \cdot sI_i = 0 \qquad (5.3.4.2)$$

where: d_i is the i'th coefficient to the i'th branch current

e_i is the i'th coefficient to the i'th branch current

The properties of d, as mentioned in section 5.3.3, are still valid and also apply to e.

The corresponding elements are taken out of equation *(5.3.2.1)* and substituted into equations *(5.3.4.1)* and *(5.3.4.2)*, yielding two equations similar to equation *(5.3.3.2)*. The procedure, as outlined in section *(5.3.3)*, is followed as before. For the one node to be eliminated, the k'th term is taken out of the equation and V_k is then solved for. For the other node to be eliminated, the f'th term is taken out of the equation and V_f is solved for. k and f are the neighbouring nodes to be eliminated and V_k and V_f are the nodal voltages to be eliminated.

$$V_k = -\frac{\sum_{j\backslash k}^{l} V_j \cdot \sum_{i}^{n} d_i \cdot a_{ij}}{\sum_{i}^{n} d_i \cdot a_{ik}} \qquad (5.3.4.3)$$

$$V_f = -\frac{\sum_{j\backslash f}^{l} V_j \cdot \sum_{i}^{n} e_i \cdot a_{ij}}{\sum_{i}^{n} e_i \cdot a_{if}} \qquad (5.3.4.4)$$

These equations are expanded to show the k'th and f'th terms. Equation *(5.3.4.4)* is then substituted into equation *(5.3.4.3)* and *vice versa*. Thereafter V_k and V_f are once again solved for. The resulting equations are then substituted back into equation *(5.3.2.1)*, thereby eliminating the redundant nodes. The new matrix coefficients of the reduced A_2 matrix are then given by:

$$b_{ij} = a_{ij} + a_{ik} \cdot \frac{\frac{\zeta_{k_j} \cdot \zeta_{f_j}}{\psi_k \cdot \psi_f} - \frac{\zeta_{k_j}}{\psi_k}}{1 - \frac{\zeta_{k_j} \cdot \zeta_{f_j}}{\psi_k \cdot \psi_f}} + a_{if} \cdot \frac{\frac{\zeta_{f_j} \cdot \zeta_{k_j}}{\psi_k \cdot \psi_f} - \frac{\zeta_{f_j}}{\psi_f}}{1 - \frac{\zeta_{f_j} \cdot \zeta_{k_j}}{\psi_f \cdot \psi_k}} \qquad (5.3.4.5)$$

$$\zeta_{k_j} = \sum_{i}^{n} d_i \cdot a_{ij} \qquad (5.3.4.6)$$

$$\zeta_{f_j} = \sum_{i}^{n} e_i \cdot a_{ij} \qquad (5.3.4.7)$$

$$\psi_k = \sum_i^n d_i \cdot a_{ik} \qquad (5.3.4.8)$$

$$\psi_f = \sum_i^n e_i \cdot a_{if} \qquad (5.3.4.9)$$

5.3.5 Derivation of a Reduction Formula for Three or More Adjacent Nodes to be Eliminated, Adjacent to Nodes with Capacitors

The above method can easily be expanded to accommodate three or more nodes that have to be eliminated. This is done as shown in section 5.3.4, except that there are more neighbouring nodes.

This elimination of redundant nodal voltage states is repeated until the value of m, the number of nodes with capacitors attached to them, is reached. Equation *(5.3.1.1)* in its reduced form is given by:

$$s\left[I_1, I_2, \ldots I_n\right]^T = A_{2r} \cdot \left[V_1, V_2, \ldots V_m\right]^T \qquad (5.3.5.1)$$

where: A_{2r} is the $n \times m$ reduced A_2 matrix, containing the coefficients determined by equations *(5.3.3.5)*, *(5.3.4.5)* and subsequent ones as determined in section 5.3.4.

It can now be seen that the nodal voltage vectors of equations *(5.3.1.2)* and *(5.3.5.1)* are identical.

5.3.6 Developing the New State Space Model

For a multi-input, multi-output (MIMO) system, the general corresponding state space equations [3, 10, 11], can now be written by inspection as:

$$sx = A \cdot x + B \cdot u \qquad (5.3.6.1)$$

$$y = C \cdot x + D \cdot u \qquad (5.3.6.2)$$

$$x = \left[I_1, I_2, \ldots I_n, V_1, V_2, \ldots V_n\right]^T \qquad (5.3.6.3)$$

where:
- x is the $(n+m) \times 1$ state space vector
- A is the $(n+m) \times (n+m)$ state coefficient matrix
- B is the $(m+n) \times p$ input coefficient matrix
- p is the number of current inputs
- u is the $p \times 1$ current input vector
- y is the $q \times 1$ nodal voltage output vector
- q is the number of nodal output voltages
- C is the $q \times (n+m)$ constant matrix relating the states to the output
- D is the $q \times p$ direct feed through matrix

Equations *(5.3.6.1)*, *(5.3.6.2)* and *(5.3.6.3)* are illustrated by way of a block diagram as shown in figure 5.3.6.1.

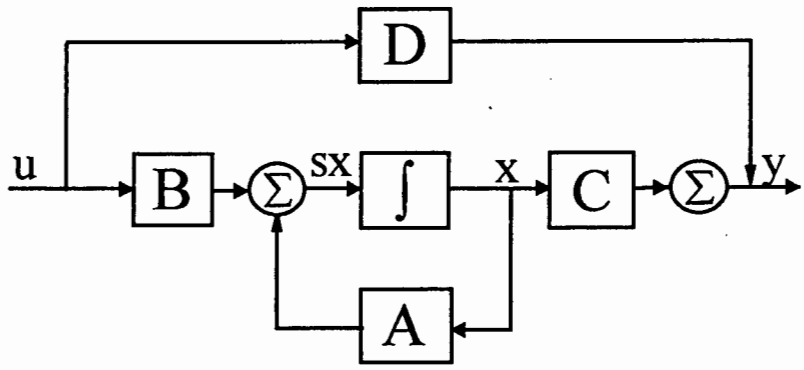

where: Σ denotes a summer

∫ denotes an integrator

Figure 5.3.6.1: Block diagram of the state space model.

Normally the system is strictly proper, and D will be a matrix of zeros. In this case the absolute value of the transfer function will decrease with an increase in frequency. Should the system

not be strictly proper, high frequency terms are fed straight to the output, as they are not attenuated as in the former case. This causes distortion to appear in the output and should therefore be avoided.

By incorporating equations *(5.3.1.1)*, *(5.3.5.1)* and *(5.3.6.3)* into equations *(5.3.6.1)* and *(5.3.6.2)* respectively, and writing the equations in the partitioned form, the final general state space model description, or system realisation is obtained:

$$s\left[I_1,\ldots I_n|V_1,\ldots V_m\right]^T = \left[\begin{array}{c|c} 0 & A_{2r} \\ \hline A_3 & 0 \end{array}\right]\cdot\left[I_1,\ldots I_n|V_1,\ldots V_m\right]^T + \left[\begin{array}{c} B_1 \\ \hline B_2 \end{array}\right]\cdot u \qquad (5.3.6.4)$$

$$y = \left[C_1|C_2\right]\cdot\left[I_1,\ldots I_n|V_1,\ldots V_m\right]^T + D\cdot u \qquad (5.3.6.5)$$

where: A_{2r} is a submatrix of A

A_3 is a submatrix of A

B_1 is the $n \times 1$ submatrix of B

B_2 is the $m \times 1$ submatrix of B

C_1 is the $1 \times n$ submatrix of C

C_2 is the $1 \times m$ submatrix of C

5.3.7 Obtaining a Minimal Realisation of the System

The state space model given by equations *(5.3.6.4)* and *(5.3.6.5)* is overspecified, particularly so for meshed power systems, as there are linearly dependant branch current states. This is undesirable as non-distinct eigenvalues occur, the condition number for matrices is very high and longer calculation times are required for subsequent calculations. To overcome these problems, a minimal realisation of the system needs to be obtained. Once this has been done, the size of the A matrix is normally double the number of capacitors that are connected to the power system.

To obtain this minimal realisation of the system, the A, B and C matrices are transferred to controllability and observability staircase forms. The unobservable and uncontrollable states are

then removed from the equations, thereby eliminating the redundant states. However, different methods are also available to perform a minimal realisation [12 - 14]. Once this has been done in the case of the branch current equations, it is no longer clear what the physical states are. However, the nodal voltage states remain unchanged and the characteristics of the system are preserved.

5.3.8 Flowchart for the Derivation of the State Space Model

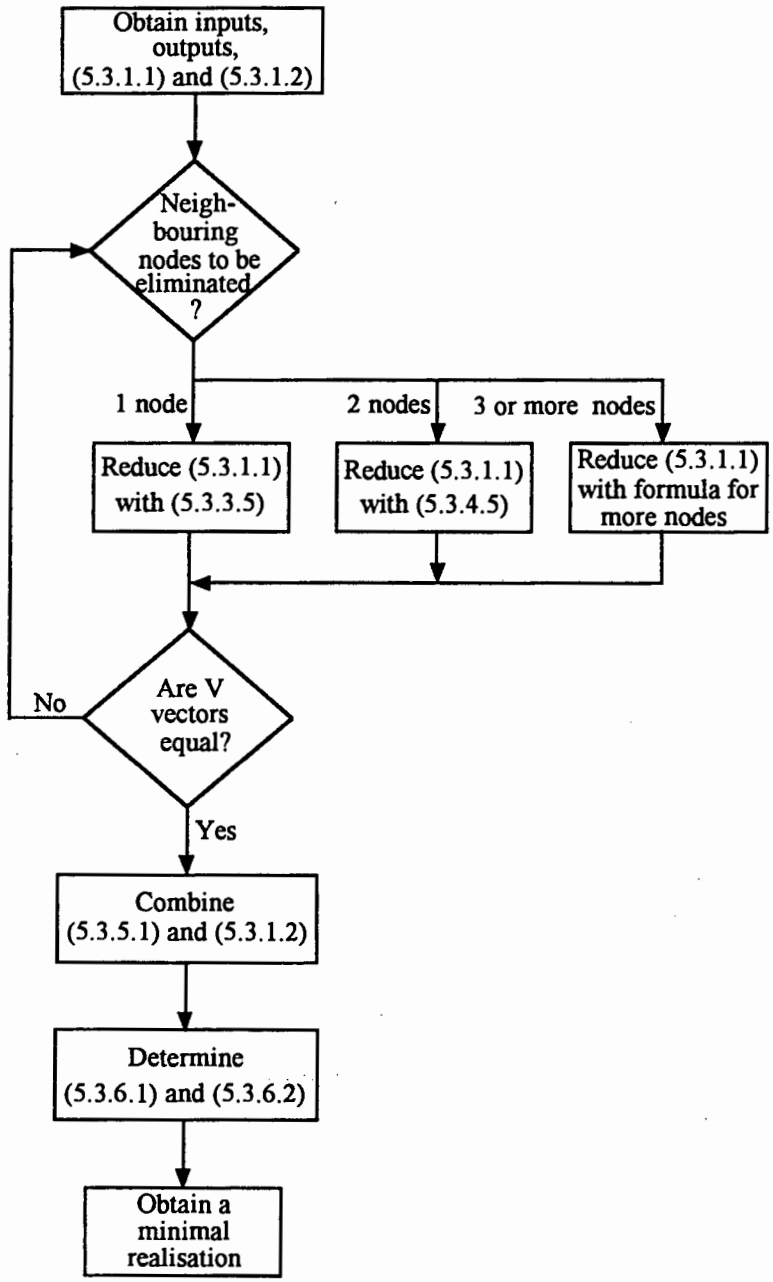

Figure 5.3.8.1: Flowchart for the derivation of the state space model.

The flow chart shown in figure 5.3.8.1, summarises the procedure as outlined in sections (5.3) to (5.3.7). At first the input nodes, output nodes, all the branch current equations, *(5.3.1.1)*, and the nodal voltage equations, *(5.3.1.2)*, are obtained. The branch current equations are then reduced for different cases. Depending on the number of neighbouring nodes to be eliminated, adjacent to nodes with capacitors attached to them, either equation *(5.3.3.5)*, equation *(5.3.4.5)* or a formula for more nodes needs to be used to remove the redundant nodal voltage states, until the voltage vectors of the branch current equations and the nodal voltage equations are the same. Equation *(5.3.1.1)* is thereby reduced to equation *(5.3.4.1)*. Equation *(5.3.1.2)* and equation *(5.3.4.1)* are then combined to form a hybrid matrix equation. The state space equations are subsequently determined by taking this hybrid matrix equation and combining it with the B, C and D matrices which are determined from the input nodes and output nodes. Finally a minimal realisation of the system is obtained, to also eliminate linearly dependant rows and columns of the A matrix.

5.3.9 Case Studies

5.3.9.1 3 Bus, Two Capacitor Meshed Network Example

The procedure of sections 5.3.1 to 5.3.8, is demonstrated analytically on a 3 bus meshed network, shown in figure 5.3.9.1.1.

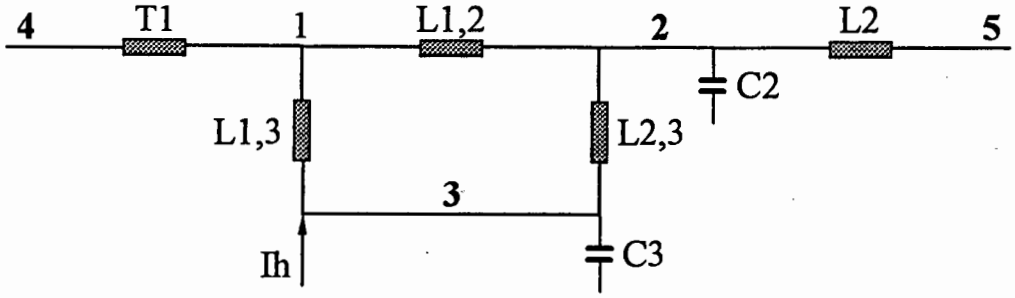

Figure 5.3.9.1.1: 3 bus meshed network.

The branch current equations are given by:

$$-V_1 = sT_1 I_{0,1} \qquad (5.3.9.1.1)$$

$$V_1 - V_2 = sL_{1,2} I_{1,2} \qquad (5.3.9.1.2)$$

$$V_2 - V_3 = sL_{2,3} I_{2,3} \qquad (5.3.9.1.3)$$

$$V_3 - V_1 = sL_{3,1} I_{3,1} \qquad (5.3.9.1.4)$$

$$-V_2 = sL_2 I_{0,2} \qquad (5.3.9.1.5)$$

After rearranging and solving for the branch currents, the equations are brought into the form of equation *(5.3.1.1)*. They are then given by:

$$sI_{0,1} = -\frac{1}{T_1} V_1 \qquad (5.3.9.1.6)$$

$$sI_{1,2} = \frac{1}{L_{1,2}} V_1 - \frac{1}{L_{1,2}} V_2 \qquad (5.3.9.1.7)$$

$$sI_{2,3} = \frac{1}{L_{2,3}} V_2 - \frac{1}{L_{2,3}} V_3 \qquad (5.3.9.1.8)$$

$$sI_{3,1} = -\frac{1}{L_{3,1}} V_1 - \frac{1}{L_{3,1}} V_3 \qquad (5.3.9.1.9)$$

$$sI_{0,2} = -\frac{1}{L_2} V_2 \qquad (5.3.9.1.10)$$

The nodal voltage equations are given by:

$$sC_2 V_2 = I_{1,2} + I_{0,2} + I_{3,2} \qquad (5.3.9.1.11)$$

$$sC_3V_3 = I_{2,3} + I_{1,3} + I_h \qquad (5.3.9.1.12)$$

After rearranging and solving for the voltages, the equations are brought into the form of equation *(5.3.1.2)*. These are given by:

$$sV_2 = \frac{1}{C_2}I_{1,2} + \frac{1}{C_2}I_{0,2} - \frac{1}{C_2}I_{2,3} \qquad (5.3.9.1.13)$$

$$sV_3 = \frac{1}{C_3}I_{2,3} - \frac{1}{C_3}I_{3,1} + \frac{1}{C_3}I_h \qquad (5.3.9.1.14)$$

As V_1 appears in the branch current equations, but not in the nodal voltage equations, it needs to be eliminated. This is done by applying equation *(5.3.3.3)* for V_1.

$$V_1 = \frac{\frac{1}{L_{1,2}}}{\frac{1}{T_1} + \frac{1}{L_{1,2}} + \frac{1}{L_{3,1}}}V_2 + \frac{\frac{1}{L_{3,1}}}{\frac{1}{T_1} + \frac{1}{L_{1,2}} + \frac{1}{L_{3,1}}}V_3 \qquad (5.3.9.1.15)$$

Substituting equation *(5.3.9.1.15)* back into the set of branch current equations *(5.3.1.1)*, and writing them in matrix notation, equations *(5.3.6.4)* and *(5.3.6.5)*, result in the system realisation, with the output being the voltage at node 2. This state space model is given in the following two equations.

$$
s\begin{bmatrix} I_{0,1} \\ I_{1,2} \\ I_{2,3} \\ I_{3,1} \\ I_{0,2} \\ V_2 \\ V_3 \end{bmatrix} = \begin{bmatrix} 0 & 0 & 0 & 0 & 0 & \dfrac{-\dfrac{1}{T_1}\dfrac{1}{L_{1,2}}}{\dfrac{1}{T_1}+\dfrac{1}{L_{1,2}}+\dfrac{1}{L_{3,1}}} & \dfrac{-\dfrac{1}{T_1}\dfrac{1}{L_{3,1}}}{\dfrac{1}{T_1}+\dfrac{1}{L_{1,2}}+\dfrac{1}{L_{3,1}}} \\ 0 & 0 & 0 & 0 & 0 & -\dfrac{1}{L_{1,2}}+\dfrac{\dfrac{1}{L_{1,2}}\dfrac{1}{L_{1,2}}}{\dfrac{1}{T_1}+\dfrac{1}{L_{1,2}}+\dfrac{1}{L_{3,1}}} & \dfrac{\dfrac{1}{L_{1,2}}\dfrac{1}{L_{3,1}}}{\dfrac{1}{T_1}+\dfrac{1}{L_{1,2}}+\dfrac{1}{L_{3,1}}} \\ 0 & 0 & 0 & 0 & 0 & \dfrac{1}{L_{2,3}} & -\dfrac{1}{L_{2,3}} \\ 0 & 0 & 0 & 0 & 0 & \dfrac{-\dfrac{1}{L_{3,1}}\dfrac{1}{L_{1,2}}}{\dfrac{1}{T_1}+\dfrac{1}{L_{1,2}}+\dfrac{1}{L_{3,1}}} & \dfrac{1}{L_{3,1}}-\dfrac{\dfrac{1}{L_{3,1}}\dfrac{1}{L_{3,1}}}{\dfrac{1}{T_1}+\dfrac{1}{L_{1,2}}+\dfrac{1}{L_{3,1}}} \\ 0 & 0 & 0 & 0 & 0 & -\dfrac{1}{L_2} & 0 \\ 0 & \dfrac{1}{C_2} & -\dfrac{1}{C_2} & 0 & \dfrac{1}{C_2} & 0 & 0 \\ 0 & 0 & \dfrac{1}{C_3} & -\dfrac{1}{C_3} & 0 & 0 & 0 \end{bmatrix} \cdot \begin{bmatrix} I_{0,1} \\ I_{1,2} \\ I_{2,3} \\ I_{3,1} \\ I_{0,2} \\ V_2 \\ V_3 \end{bmatrix} + \begin{bmatrix} 0 \\ 0 \\ 0 \\ 0 \\ 0 \\ 0 \\ \dfrac{1}{C_3} \end{bmatrix} \cdot I_h
$$

(5.3.9.1.16)

$$V_2 = \begin{bmatrix} 0 & 0 & 0 & 0 & 0 & 1 & 0 \end{bmatrix} \cdot \begin{bmatrix} I_{0,1} \\ I_{1,2} \\ I_{2,3} \\ I_{3,1} \\ I_{0,2} \\ V_2 \\ V_3 \end{bmatrix} \qquad (5.3.9.1.17)$$

The coefficients of the A matrix are also given by equation *(5.3.3.5)*.

5.3.9.2 3 Bus, One Capacitor Meshed Network Example

The above mentioned procedure is again demonstrated analytically on a 3 bus meshed network, shown in figure 5.3.9.2.1. In this case there is one less capacitor connected to the power system.

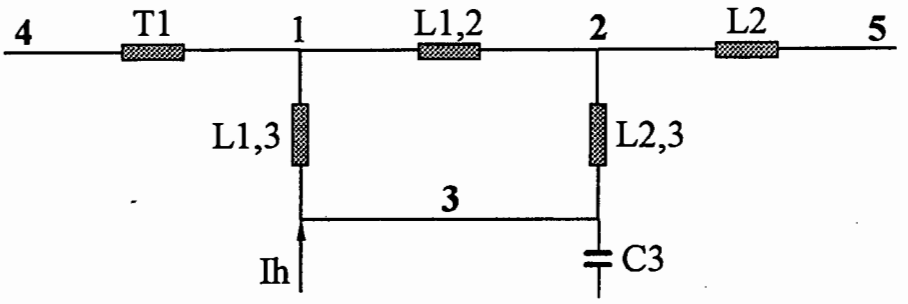

Figure 5.3.9.2.1: 3 bus meshed network.

The branch current equations are the same as in the previous example, equations *(5.3.9.1.1)* to *(5.3.9.1.5)*. Once again these are brought into the form of equation *(5.3.1.1)*, giving the same set of equations as before, namely: equations *(5.3.9.1.6)* to *(5.3.9.1.10)*.

However, since the capacitor configuration has changed, there is now only one nodal voltage equation, i. e. *(5.3.9.1.12)*. This equation is brought into the form of equation *(5.3.1.2)*, resulting in equation *(5.3.9.1.14)*.

V_1 and V_2 now need to be eliminated, as they appear in the branch current equations, but not in the nodal voltage equations. By applying equations *(5.3.4.3)* and *(5.3.4.4)*, the following equations result:

$$V_1 = \frac{\frac{1}{L_{1,2}}}{\frac{1}{T_1}+\frac{1}{L_{1,2}}+\frac{1}{L_{3,1}}}V_2 + \frac{\frac{1}{L_{3,1}}}{\frac{1}{T_1}+\frac{1}{L_{1,2}}+\frac{1}{L_{3,1}}}V_3 \qquad (5.3.9.2.1)$$

$$V_2 = -\frac{\frac{1}{L_{1,2}}}{\frac{1}{L_{1,2}}+\frac{1}{L_{2,3}}+\frac{1}{L_2}}V_1 - \frac{\frac{1}{L_{2,3}}}{\frac{1}{L_{1,2}}+\frac{1}{L_{2,3}}+\frac{1}{L_2}}V_3 \qquad (5.3.9.2.2)$$

Substituting equation *(5.3.9.2.2)* into equation *(5.3.9.2.1)* and simplifying, results in:

$$V_1 = \varsigma V_3 \qquad (5.3.9.2.3)$$

$$\varsigma = \frac{\frac{\frac{1}{L_{1,2}}}{\frac{1}{T_1}+\frac{1}{L_{1,2}}+\frac{1}{L_{3,1}}}\cdot\frac{\frac{-1}{L_{2,3}}}{\frac{1}{L_{1,2}}+\frac{1}{L_{2,3}}-\frac{1}{L_2}} + \frac{\frac{1}{L_{3,1}}}{\frac{1}{T_1}+\frac{1}{L_{1,2}}-\frac{1}{L_{3,1}}}}{1-\frac{\frac{1}{L_{1,2}}}{\frac{1}{T_1}+\frac{1}{L_{1,2}}+\frac{1}{L_{3,1}}}\cdot\frac{\frac{-1}{L_{1,2}}}{\frac{1}{L_{1,2}}+\frac{1}{L_{2,3}}-\frac{1}{L_2}}} \qquad (5.3.9.2.4)$$

Substituting equation *(5.3.9.2.1)* into equation *(5.3.9.2.2)* and simplifying, results in:

$$V_2 = \tau V_3 \qquad (5.3.9.2.5)$$

$$\tau = \frac{\dfrac{-\dfrac{1}{L_{1,2}}}{\dfrac{1}{L_{1,2}}+\dfrac{1}{L_{2,3}}-\dfrac{1}{L_2}} \cdot \dfrac{\dfrac{1}{L_{3,1}}}{\dfrac{1}{T_1}+\dfrac{1}{L_{1,2}}+\dfrac{1}{L_{3,1}}} + \dfrac{-\dfrac{1}{L_{2,3}}}{\dfrac{1}{L_{1,2}}+\dfrac{1}{L_{2,3}}-\dfrac{1}{L_2}}}{1+\dfrac{\dfrac{1}{L_{1,2}}}{\dfrac{1}{L_{1,2}}+\dfrac{1}{L_{2,3}}-\dfrac{1}{L_2}} \cdot \dfrac{\dfrac{1}{L_{1,2}}}{\dfrac{1}{T_1}+\dfrac{1}{L_{1,2}}+\dfrac{1}{L_{3,1}}}} \qquad (5.3.9.2.6)$$

Substituting equations *(5.3.9.2.3)* to *(5.3.9.2.6)* back into the set of branch current equations *(5.3.1.1)*, and writing them in matrix notation, equations *(5.3.6.4)* and *(5.3.6.5)*, result in the system realisation, with the output being the voltage at node 2. This state space model is given in equations *(5.3.9.2.7)* and *(5.3.9.2.8)*.

$$s\begin{bmatrix} I_{0,1} \\ I_{1,2} \\ I_{2,3} \\ I_{3,1} \\ I_{0,2} \\ V_3 \end{bmatrix} = \begin{bmatrix} 0 & 0 & 0 & 0 & 0 & -\dfrac{\varsigma}{T_1} \\ 0 & 0 & 0 & 0 & 0 & \dfrac{\varsigma}{L_{1,2}} - \dfrac{\tau}{L_{1,2}} \\ 0 & 0 & 0 & 0 & 0 & \dfrac{\tau}{L_{2,3}} - \dfrac{1}{L_{2,3}} \\ 0 & 0 & 0 & 0 & 0 & \dfrac{1}{L_{3,1}} - \dfrac{\varsigma}{L_{3,1}} \\ 0 & 0 & 0 & 0 & 0 & -\dfrac{\tau}{L_2} \\ 0 & 0 & \dfrac{1}{C_3} & -\dfrac{1}{C_3} & 0 & 0 \end{bmatrix} \cdot \begin{bmatrix} I_{0,1} \\ I_{1,2} \\ I_{2,3} \\ I_{3,1} \\ I_{0,2} \\ V_3 \end{bmatrix} + \begin{bmatrix} 0 \\ 0 \\ 0 \\ 0 \\ 0 \\ \dfrac{1}{C_3} \end{bmatrix} \cdot I_h \qquad (5.3.9.2.7)$$

$$V_2 = \begin{bmatrix} 0 & 0 & 0 & 0 & 0 & 1 \end{bmatrix} \cdot \begin{bmatrix} I_{0,1} \\ I_{1,2} \\ I_{2,3} \\ I_{3,1} \\ I_{0,2} \\ V_3 \end{bmatrix} \qquad (5.3.9.2.8)$$

5.3.9.3 Comparison of Case Studies 5.3.9.1 and 5.3.9.2 with SuperHarm

The numerical values for the network components for the case studies of sections 5.3.9.1 and 5.3.9.2 are given in table 5.3.9.3.1. The inductance of transformers T1 is 50. The inductance of load L2 is 50.

Line	Resistance	Inductance
L1,2	0.0581	1.2778
L2,3	3.6780	8.0150
L1,3	0.9870	2.9810
Capacitor	**KV**	**MVA**
C2	44	6
C3	44	6

Table 5.3.9.3.1: Numerical data for the case studies in sections 5.3.9.1 and 5.3.9.2.

The frequency base is 60 Hz and the magnitude of the harmonic current source, which is swept from 60 Hz to 3000 Hz in increments of 30 Hz, is 1 per unit at a phase angle of 0 degrees.

The graphs shown in figures 5.3.9.3.1 to 5.3.9.3.3, refer to the case study in section 5.3.9.1. It can be seen from these graphs, that there is one significant harmonic peak and another minor harmonic peak. Furthermore, the voltage profiles of the three different busses does not differ very much.

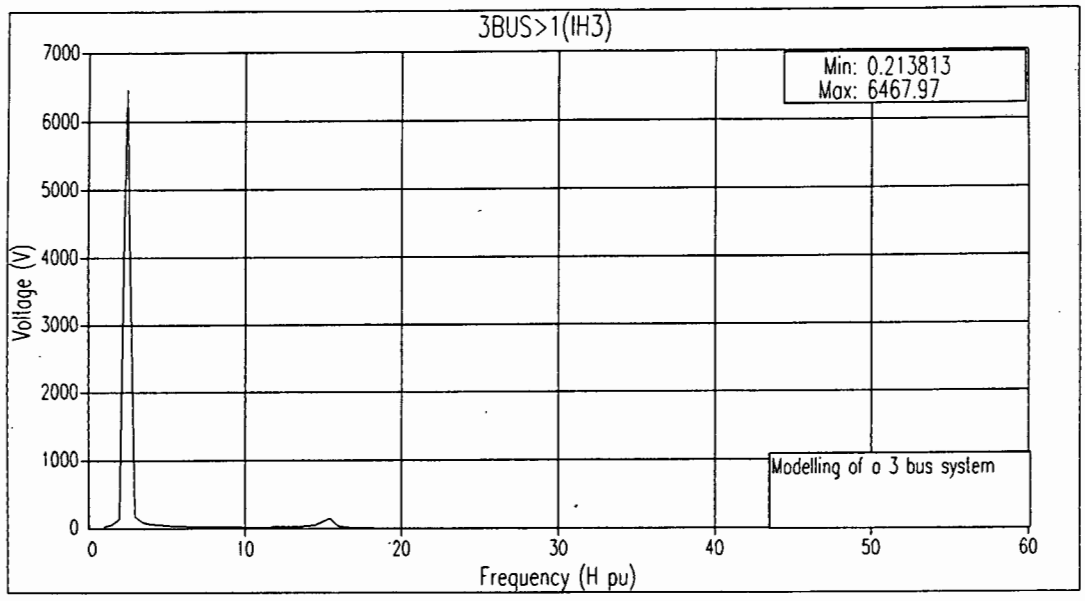

Figure 5.3.9.3.1: Output voltage at bus 1.

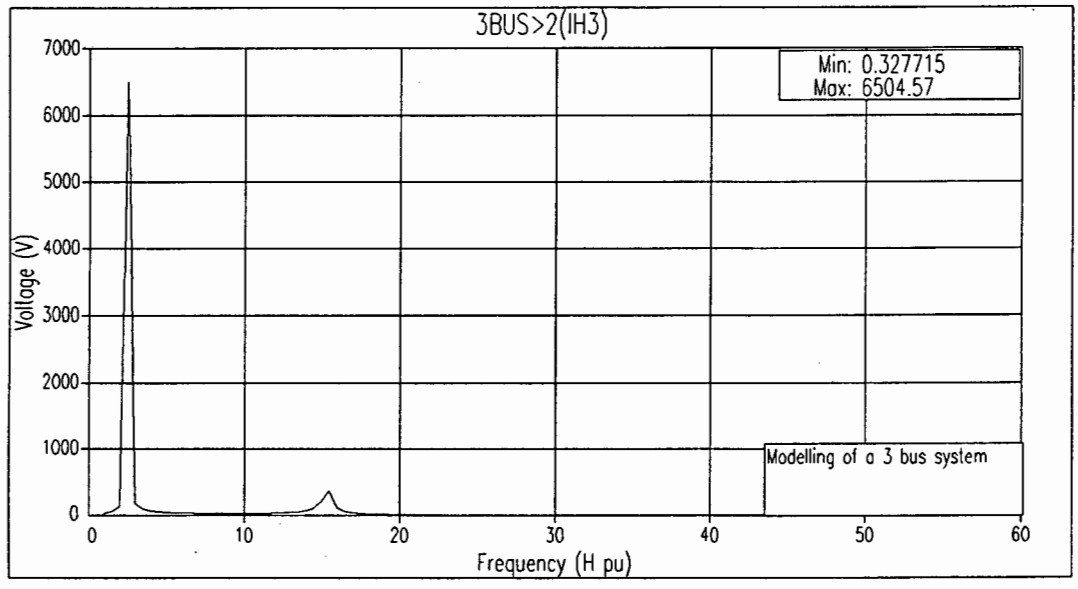

Figure 5.3.9.3.2: Output voltage at bus 2.

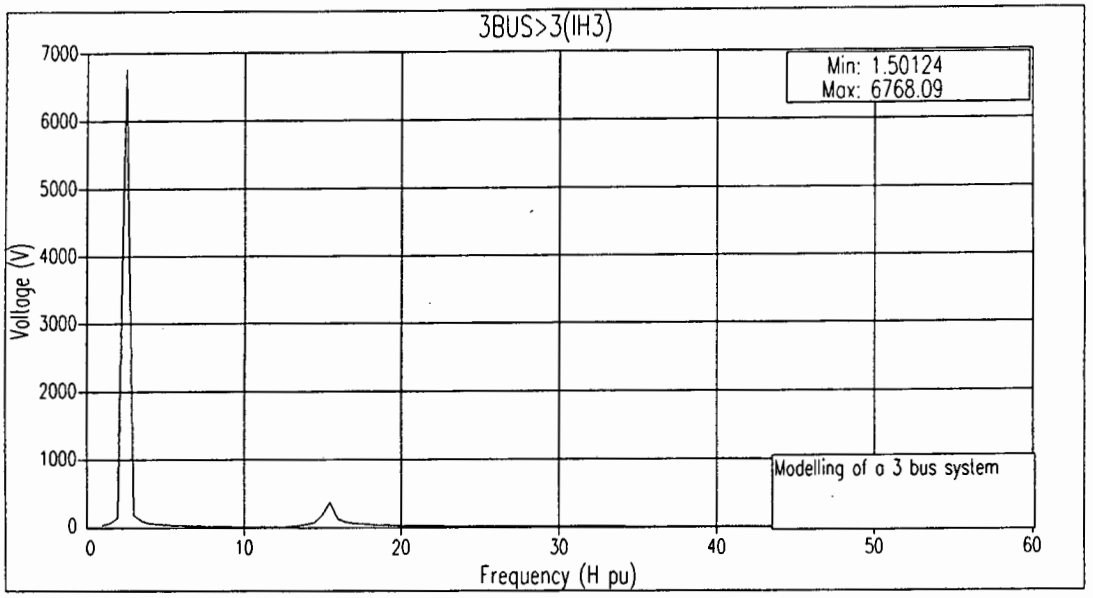

Figure 5.3.9.3.3: Output voltage at bus 3.

The graphs shown in figures 5.3.9.3.4 to 5.3.9.3.6, refer to the case study in section 5.3.9.2. It can be seen from these graphs, that there is now only one significant harmonic peak, which was caused by the removal of capacitor C2. In addition, the voltage profiles of the three different busses does not differ very much.

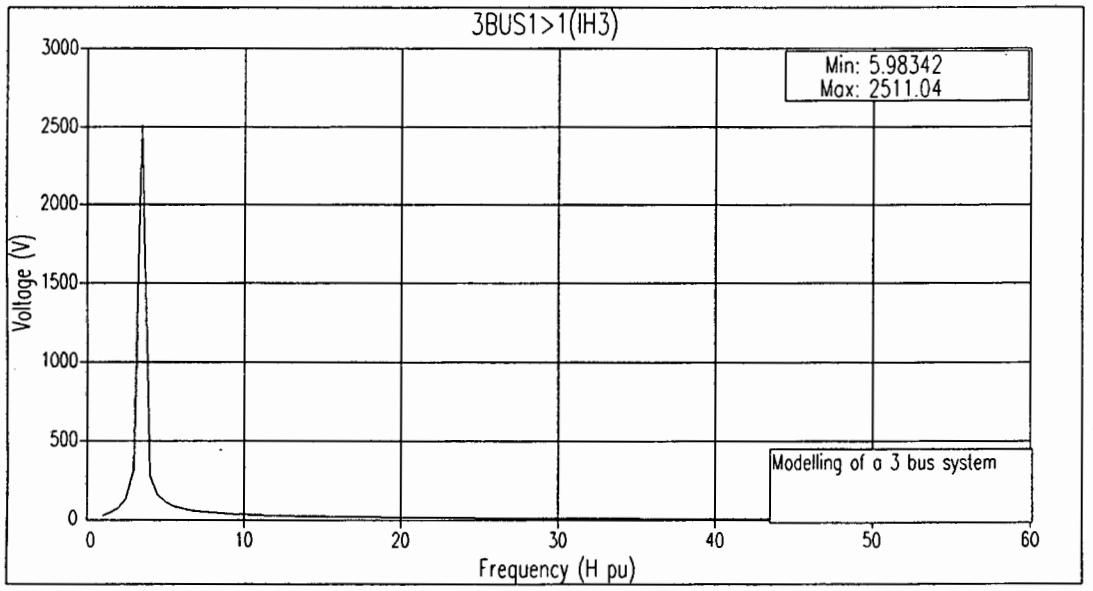

Figure 5.3.9.3.4: Output voltage at bus 1.

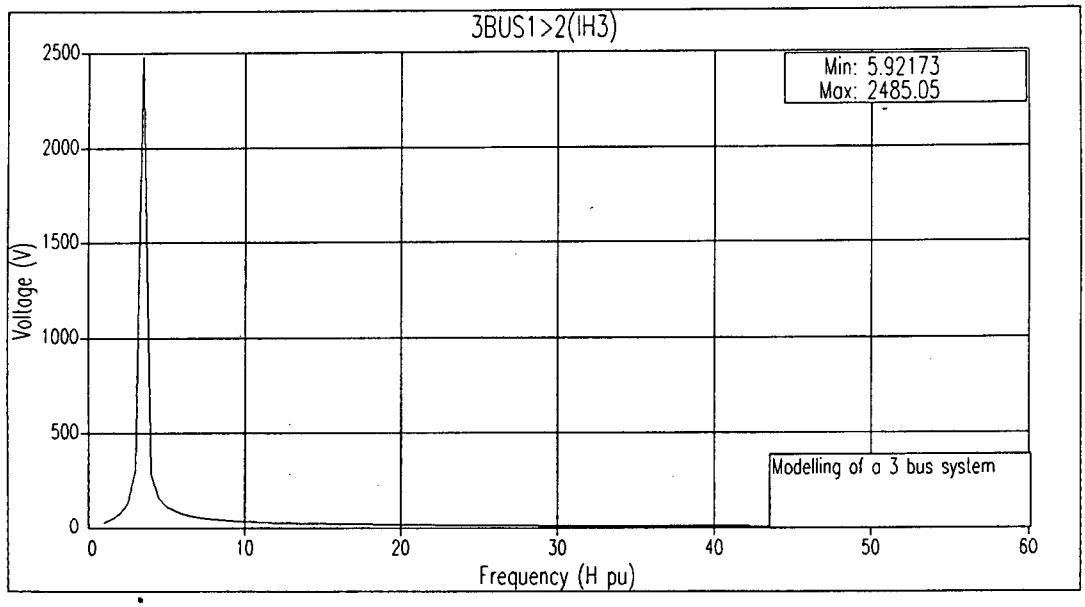

Figure 5.3.9.3.5: Output voltage at bus 2.

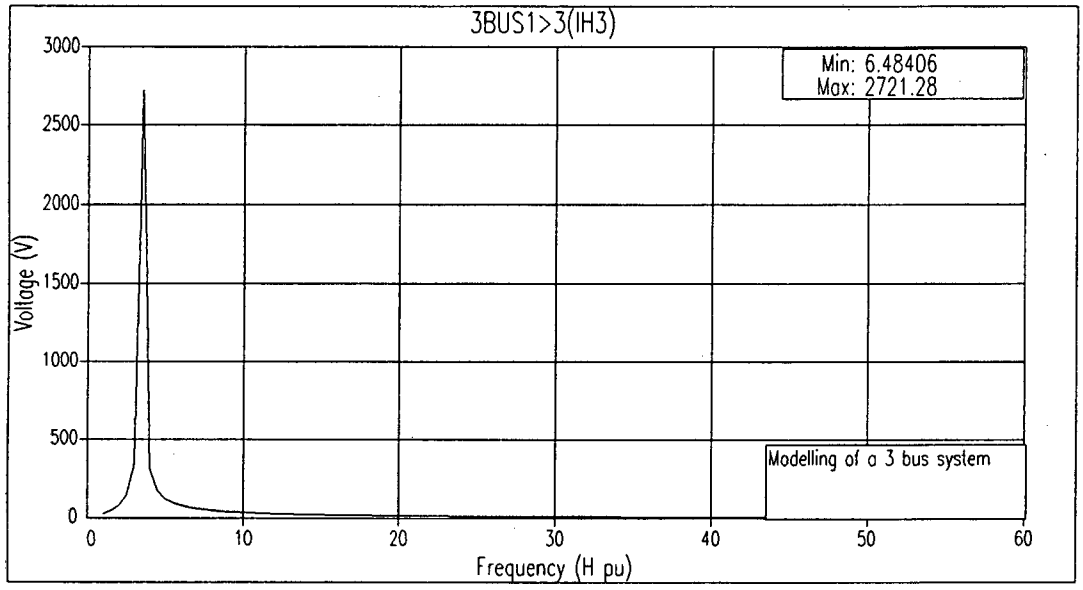

Figure 5.3.9.3.6: Output voltage at bus 3.

By comparing the two case studies, it is shown, that the removal of a capacitor causes the number of resonant peaks to decrease, however, the remaining harmonic peak has not changed very much, which was to be expected.

5.3.9.4 16 Bus Multi-Input, Multi-Output (MIMO) Meshed Network Example

A programme was written in Matlab to implement the above procedure on a 16 bus meshed network [15, 16], which is given in figure 5.3.9.4.1. The relevant data in per unit is given in tables 5.3.9.4.1, 5.3.9.4.2, 5.3.9.4.3 and 5.3.9.4.4.

Generator	Inductance in per unit
G1	1.7000
G2	2.0086
G3	2.7618

Table 5.3.9.4.1: Generator data in per unit for the 16 bus network.

Transformer	Inductance in per unit
T1	0.0625
T2	0.0650
T3	0.0600
T4	0.0570
T5	0.0625

Table 5.3.9.4.2: Transformer data in per unit for the 16 bus network.

Line	Inductance in per unit
L1	0.007580340
L2	0.015160680
L3	0.026531190
L4	0.022741020
L5	0.025015122
L6	0.023705103
L7	0.035296143
L8	0.043904958

L9	0.025441919
L10	0.058826905
L11	0.058826905
L12	0.016676748
L13	0.022741020
L14	0.007580340

Table 5.3.9.4.3: Line data in per unit for the 16 bus network.

Capacitor	Capacitance in per unit
C7	0.3
C8	0.3
C9	0.3
C11	0.3
C15	0.3

Table 5.3.9.4.4: Capacitor data in per unit for the 16 bus network.

The loads of the system have been neglected for this case study, as the aim is to demonstrate the method. However, should loads be incorporated, they can simply be modelled as a transmission line or the load impedance can be added to the existing transmission lines.

For a MIMO system, two harmonic injections are applied and there are two output nodes being two bus voltages. As there are five capacitors connected to the power grid, the final A matrix should be of dimension 10×10.

Harmonic current injections are applied to busses 8 and 9. The output is also obtained at these nodes, thereby making it a square problem (2 inputs and 2 outputs). The final minimal realisation of the A, B, C and D system matrices, after 18 redundant states have been removed, is given in tables 5.3.9.4.5, 5.3.9.4.6, 5.3.9.4.7 and 5.3.9.4.8.

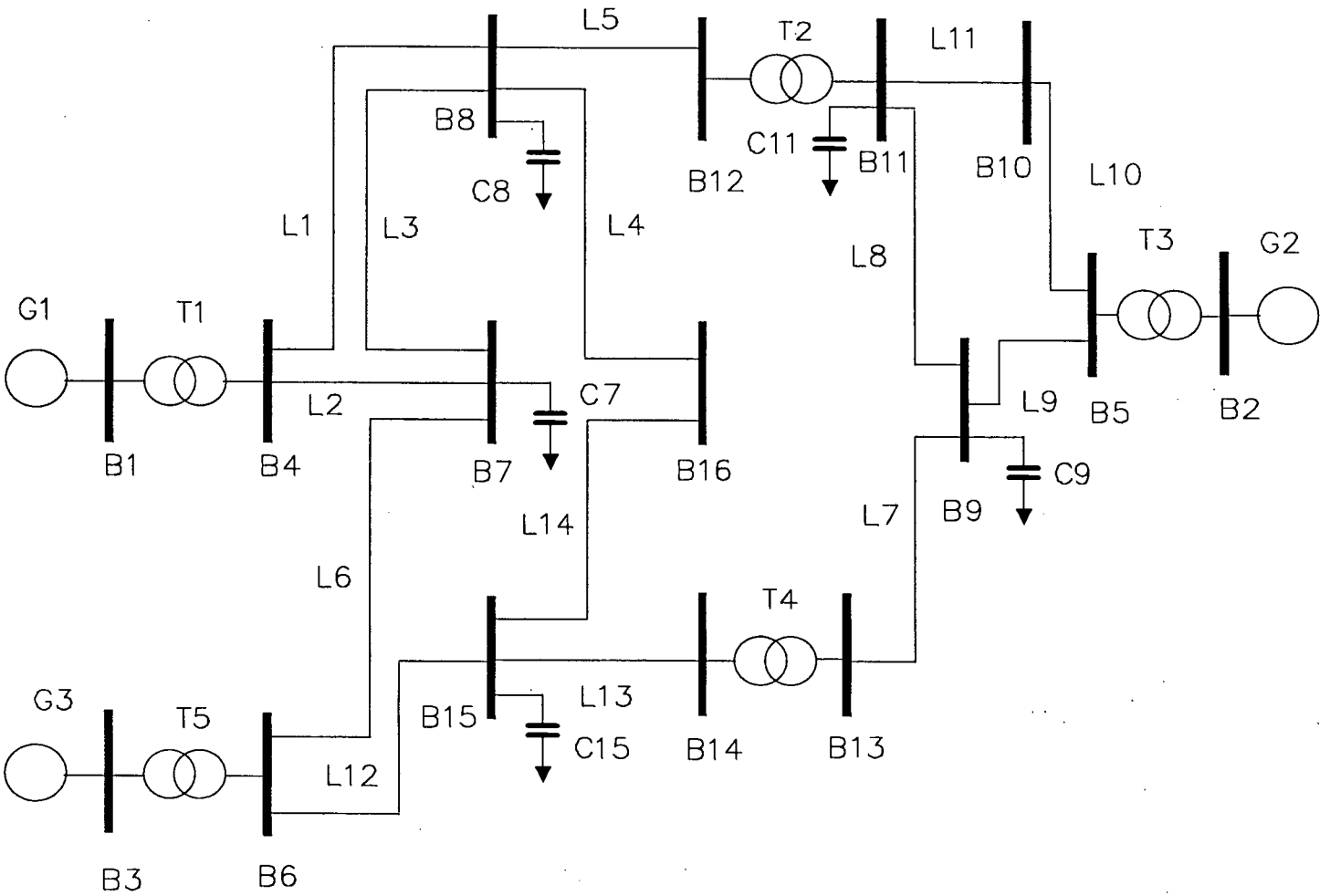

Figure 5.3.9.4.1: 16 bus meshed network.

Column 1	Column 2	Column 3	Column 4	Column 5	Column 6	Column 7	Column 8	Column 9	Column 10
0.0000	-51.6935	0.0000	0.0000	10.5190	-16.5941	0.0000	0.0000	1.6902	-1.8693
4.8789	0.0000	-1.7981	0.0701	0.0000	0.0000	0.7340	0.1796	0.0000	0.0000
0.0000	16.1301	0.0000	0.0000	3.1453	10.2979	0.0000	0.0000	-5.9043	-6.0667
0.0000	22.9333	0.0000	0.0000	-28.7995	42.4719	0.0000	0.0000	3.8039	-34.6010
0.0000	0.0000	-1.5330	3.6204	0.0000	0.0000	-3.1559	0.6423	0.0000	0.0000
0.0000	0.0000	-2.2816	-2.4324	0.0000	0.0000	-1.4432	2.4487	0.0000	0.0000
0.0000	0.0000	0.0000	0.0000	18.3715	17.2447	0.0000	0.0000	-24.9836	-16.4459
0.0000	0.0000	0.0000	0.0000	6.5110	-48.6576	0.0000	0.0000	-4.4101	70.7273
0.0000	0.0000	0.0000	0.0000	0.0000	0.0000	4.9702	1.1557	0	0
0.0000	0.0000	0.0000	0.0000	0.0000	0.0000	1.0070	-5.7044	0	0

Table 5.3.9.4.5: Coefficients of the A matrix.

Column 1	0	0	0	0	0	0	0	0	0	3.3333
Column 2	0	0	0	0	0	0	0	0	3.3333	0

Table 5.3.9.4.6: Coefficients of the *B* matrix transposed.

Row 1	0	0	0	0	0	0	0	0	0	1
Row 2	0	0	0	0	0	0	0	0	1	0

Table 5.3.9.4.7: Coefficients of the *C* matrix.

Row 1	0	0
Row 2	0	0

Table 5.3.9.4.8: Coefficients of the *D* matrix.

5.3.9.5 16 Bus Single-Input, Single-Output (SISO) Meshed Network Example

The same network as used for section 5.3.9.4 is taken. In this case the above method is compared to the current injection method. For a SISO system, a one per unit harmonic current injection is applied to bus 8 on the network. The voltage at the output is obtained at bus 9. A magnitude *versus* frequency diagram is obtained and shown in figure 5.3.9.5.1.

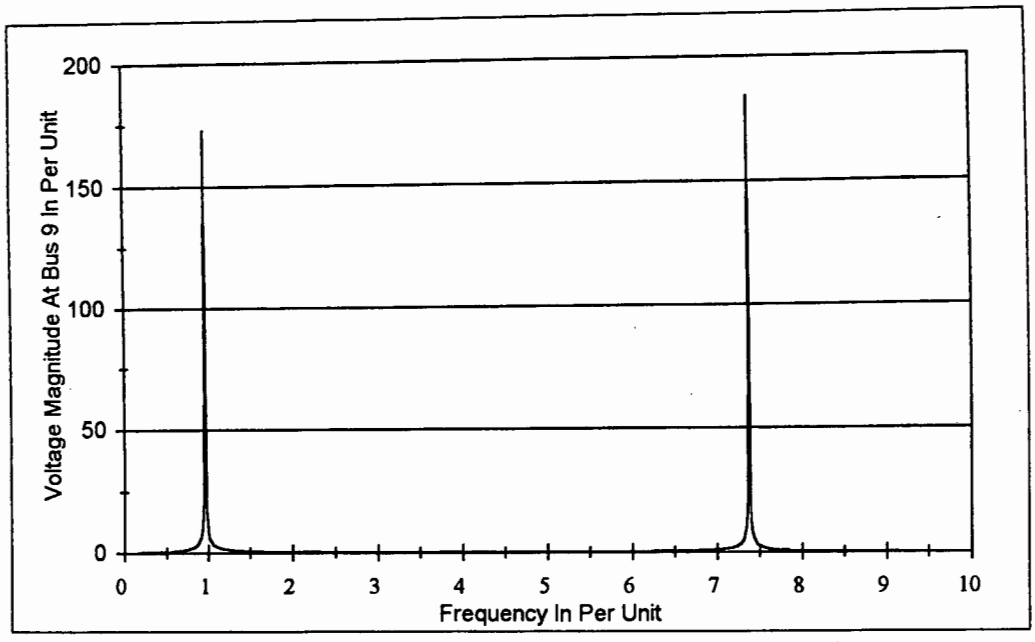

Figure 5.3.9.5.1: Magnitude *versus* frequency diagram of the voltage at bus 9.

Figure 5.3.9.5.1 shows that there are resonant peaks at just below the first harmonic and between the seventh and eighth harmonics, with a magnitude of about 175.

In order to verify the results of the state space model approach, another different programme was written in Matlab, to implement the current injection method for the same network. The algorithm for the particular current injection method programme is given in section 3.6 and the corresponding programme listing is shown in appendix G. A magnitude *versus* frequency diagram of the voltage at bus 9 was once again obtained. This diagram is identical to the one shown in figure 5.3.9.5.1. The two methods produce the same results.

5.4 References

[1] T. H. Ortmeyer and K. Zehar, "Distribution System Harmonic Design", *IEEE Transactions on Power Delivery*, Volume 6, Number 1, January 1991, pages 289-294.

[2] H. V. Hitzeroth and A. Petroianu, "Optimal Capacitor Placement on Radial Distribution Systems to Minimise Harmonic Distortion", *Proceedings of the Fifth South African Universities Power Engineering Conference 1995*, pages 9-12.

[3] B. Friedland, *Control System Design: An Introduction to State - Space Methods*, McGraw-Hill, 1987.

[4] D. A. Calahan, *Computer Aided Network Design*, Mc Graw-Hill, 1968.

[5] R. B. Shipley, *Introduction to Matrices and Power Systems*, John Wiley and Sons, New York.

[6] G. W. Stagg and A. H. El-Abiad, *Computer Methods in Power System Analysis*, McGraw-Hill, London, 1968.

[7] I. Vago, *Studies in Electrical and Electronic Engineering 15: Graph Theory: Application to the Calculation of Electrical Networks*, Elsevier, Amsterdam, 1985.

[8] H. H. Happ, *Piecewise Methods and Applications to Power Systems*, John Wiley and Sons, New York, 1980.

[9] H. E. Brown, *Solution of Large Networks by Matrix Methods*, second edition, John Wiley and Sons, New York, 1985.

[10] C. T. Chen, *Linear System Theory And Design*, Holt, Rinehart and Winston, New York, 1970.

[11] T. Kailath, *Linear Systems*, Prentice-Hall, Englewood Cliffs, 1980.

[12] B. W. Dickinson, M. Morf and T. Kailath, "A minimal realisation algorithm for matrix sequences", *IEEE Transactions on Automatic Control*, Volume AC-19, Number 1, February 1974, pages 31-38.

[13] B. C. Moore, "Principal Component Analysis in Linear Systems: Controllability, Observability and Model Reduction", *IEEE Transactions on Automatic Control*, Volume AC 26, Number 1, February 1981, pages 17-32.

[14] R. V. Patel, "Computation of minimal-order state-space realisations and observability indices using orthogonal transformations", *International Journal of Control*, Volume 33, Number 2, 1981, pages 227-246.

[15] A. Petroianu, S. I. Darie and E. Johnson, "Teaching Power Systems through Projects Work", *Proceedings of the Fourth South African Universities Power Engineering Conference 1994*, pages 376-378.

[16] P. Mangang, S. S. Ahmed and A. Petroianu, "Sequential use of Optimal Power Flow for improving the Static Voltage Stability Margin", *Proceedings of the Stockholm Power Technology Conference 1995*, pages 203-208.

Chapter 6

New Methods of Mitigating or Eliminating Harmonics by Optimal Capacitor Placement

6.1 Introduction

In order to optimally place capacitors, to minimise harmonic distortion and penetration, optimisation methods need to be applied. For this purpose the state space models of chapter 5 were used in conjunction with an exhaustive search, greedy search, neighbourhood search and simulated annealing. These optimisation procedures are explained in this chapter. The simulated annealing algorithm is discussed in greater detail than the others, as it proved to give the best results. Case studies are also presented, demonstrating the application and implementation of the optimisation methods.

For all practical purposes, a minimisation procedure is the same as a maximisation procedure, as the sign of the objective function only needs to be negated. Throughout this thesis therefore, the two methods serve the same purpose.

6.2 Configuration Space

The configuration space is the space spanning all possible combinations of configurations [1]. This would be defined by the number of all permutations of capacitors and nodes. The larger the power system, the greater this number will be.

6.3 Move Set

A move set is the change from one configuration to the next [1]. For the placement of capacitors this would be reassigning them, to a new set of nodes. By disconnecting a capacitor

from one node and connecting it to a different node, a two bit change results. This is also called a move set.

6.4 Objective Function or Cost Function

The objective function expresses some kind of measure, that is used for the evaluation of the system configuration. It would be a measure, whereby the goodness or badness of the harmonic response is expressed [1]. Two objective functions with constraints were developed for the purpose of this thesis. These are discussed in sections 6.4.1 and 6.4.2.

As harmonic resonance problems are usually dealt with as a second - order phenomenon, their mitigation is formulated in terms of an objective function, which should be minimised. The primary requirements, such as voltage regulation (maintaining the voltage profile between 95% and 105% of 1 per unit), distribution system losses, the cost of for example power factor correction capacitors and the limiting of harmonic voltage magnitudes are therefore formulated as constraints.

6.4.1 Case Study 1

In order to minimise the effect of the harmonic distortion problem, specifications can be placed on the poles and zeros of the system. To obtain the best frequency response, the zeros should be located close to and poles should be far from harmonic frequencies, unless there is a zero between that pole and the harmonic frequency in question. Furthermore, poles and zeros should be close to each other.

These requirements are formulated as an objective function as follows:

$$\underset{CS}{\text{maximise}}(J = \min_{i}(\min_{j}|H_i - P_j|)) \qquad (6.4.1.1)$$

subject to the constraint:

$$C = \min_i(\min_j|H_i - Z_j|) < \gamma \qquad (6.4.1.2)$$

where: H_i is the i'th harmonic frequency injected by the harmonic source

P_j is the j'th system pole

Z_j is the j'th system zero

CS is the configuration space or feasibility set

J is the value of the objective function

C is the value of the constraint for the zeros

γ is the limit of the constraint for the zeros

The formulation of equations *(6.4.1.1)* and *(6.4.1.2)* is chosen, since it is desirable to have the poles far away from a harmonic frequency, in order to avoid resonance effects. Furthermore, by choosing γ=1, it is ensured, that there is a zero in the vicinity of a harmonic frequency. This is desirable, as it mitigates the undesirable dominant effects of the harmonic frequency.

6.4.2 Case Study 2

The objective function of section 6.4.1 has certain shortcomings. The main disadvantage being, that situations where there is a zero between the relevant pole and the harmonic frequency in question can not be adequately evaluated. This is due to the fact, that the objective function does not take the pole / zero cancellation effects into account. For this reason an improved objective function is developed.

This objective function makes use of the principles of the H_2 and H_∞ norms [2 - 5]. The objective function forces the magnitude of the frequency response curve down over all frequencies, thereby improving the system performance over all frequencies. This is subject to specific constraints. These constraints ensure that the harmonic resonant peaks are limited to certain values, typically the standards set by the industry. Thereby they also ensure the robustness of the power system at the particular harmonic frequencies. This objective function with its constraints is given by the following equations:

$$\underset{CS}{\text{minimise}}\left(J = \sum_{f=1}^{h} |V(f)|\right) \qquad (6.4.2.1)$$

subject to the constraints:

$$C_1 = \sum_{f=\text{odd harmonics}}^{h} |V(f)| < \alpha \qquad (6.4.2.2)$$

$$C_2 = \sum_{f=\text{even harmonics}}^{h} |V(f)| < \beta \qquad (6.4.2.3)$$

$$C_3 = \sum_{f=\text{inter harmonics}}^{h} |V(f)| < \chi \qquad (6.4.2.4)$$

$$C_4 = \sum_{f=14 \text{ to } 25 \text{ harmonic}}^{h} |V(f)| < \delta \qquad (6.4.2.5)$$

$$C_5 = \sum_{f=>25 \text{ harmonic}}^{h} |V(f)| < \varepsilon \qquad (6.4.2.6)$$

where:

CS	is the configuration space
h	is the harmonic order
f	is the frequency
V	is the voltage
J	is the objective function
C_1	is the first constraint
C_2	is the second constraint
C_3	is the third constraint
C_4	is the fourth constraint
C_5	is the fifth constraint
α	is the value of the first constraint
β	is the value of the second constraint
χ	is the value of the third constraint
δ	is the value of the fourth constraint

ε is the value of the fifth constraint

This objective function takes pole / zero cancellation effects into consideration and therefore better behaviour and results are achieved.

6.5 Exhaustive Search

Normally, when an optimisation algorithm is applied, there exist many combinations or possibilities, which need to be eliminated, in order to arrive at the optimal solution. The exhaustive search however, does not do this. It tests every possibility, the whole configuration space, making use of a brute force approach. In other words any information obtained from testing a specific configuration is disregarded [1]. This method guarantees the global optimal solution, but it is very time consuming and computer intensive, particularly for large power systems.

6.6 Greedy Search

A greedy search is an optimisation algorithm that can not do any uphill climbing. In other words, it will find a local minimum in the objective function, which might coincide with the global minimum, but most likely not. In order to arrive at a global minimum, the initialisation values need to be chosen very carefully [1]. All configuration space elements that do not improve the value of the objective function are therefore discarded. The greedy search method is very practical for initialising other optimisation routines, or to obtain initial guesses.

6.7 Neighbourhood Search

A neighbourhood search results when only one capacitor at a time is switched on to another bus, thereby changing two bits in the configuration space. In other words the new capacitor assignment is not done completely randomly, but only one capacitor is chosen randomly and switched on to another randomly determined bus [1]. In this way, information regarding the objective function, from the configurations is utilised in the optimisation procedure.

6.7.1 Case Study 3

Figure 6.7.1.1 shows a flowchart of the procedure that is used to obtain a solution to the optimisation problem as posed in section 6.4.1, with the use of a neighbourhood search algorithm.

After a random initial assignment of capacitors the state space model is generated and the system poles and zeros are calculated. The constraint for the zeros is then checked. If it is not satisfied, a new configuration space element is chosen by changing the position of one capacitor, resulting in a neighbourhood search. If the constraint is satisfied, the value of the objective function is calculated and compared to the previous one.

If $J_i<J_{(i-1)}$, a new configuration space element is chosen as explained above. The objective function is once again evaluated and compared to the original value. If $J_i<J_{(i-1)}$, then the current configuration space element is taken as the feasible capacitor assignment.

If $J_i>J_{(i-1)}$, the feasible configuration space element is updated. The process repeats itself until the stop criterion is met. The stop criterion states that if two iterations have not produced an improvement in the objective function value, the algorithm terminates.

The distribution system shown in figure 6.7.1.2 was studied [6]. The system is an 18 bus radial power system consisting of three feeders connected to a transformer.

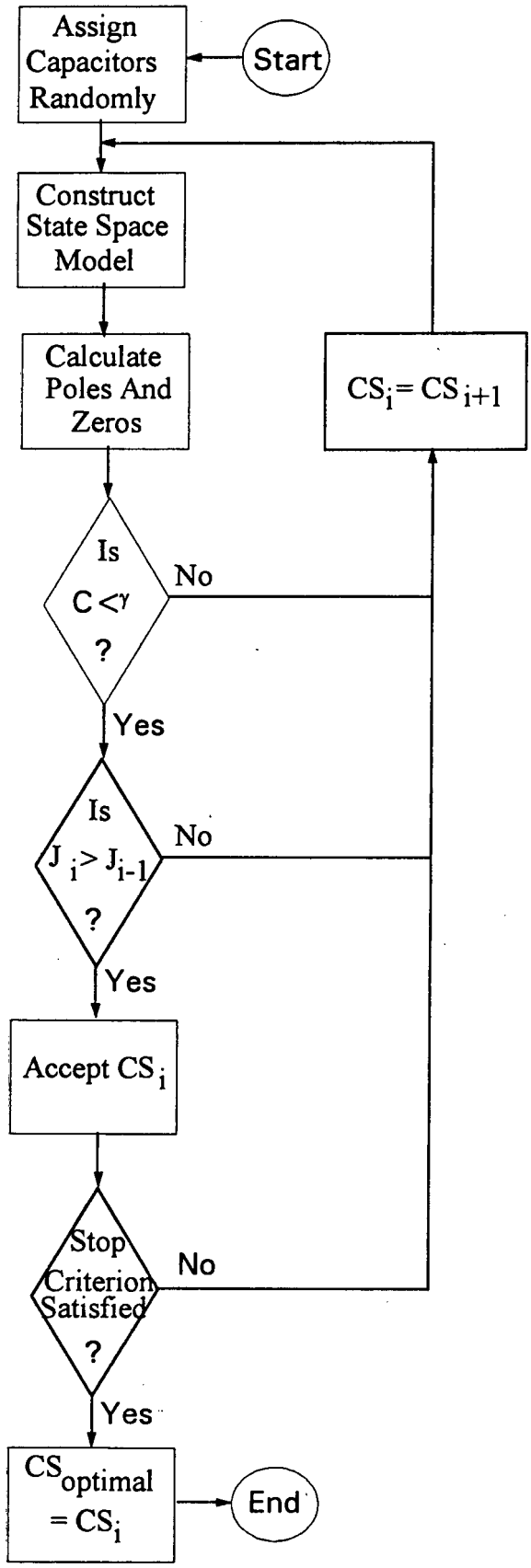

Figure 6.7.1.1: Flowchart of the neighbourhood search optimisation algorithm.

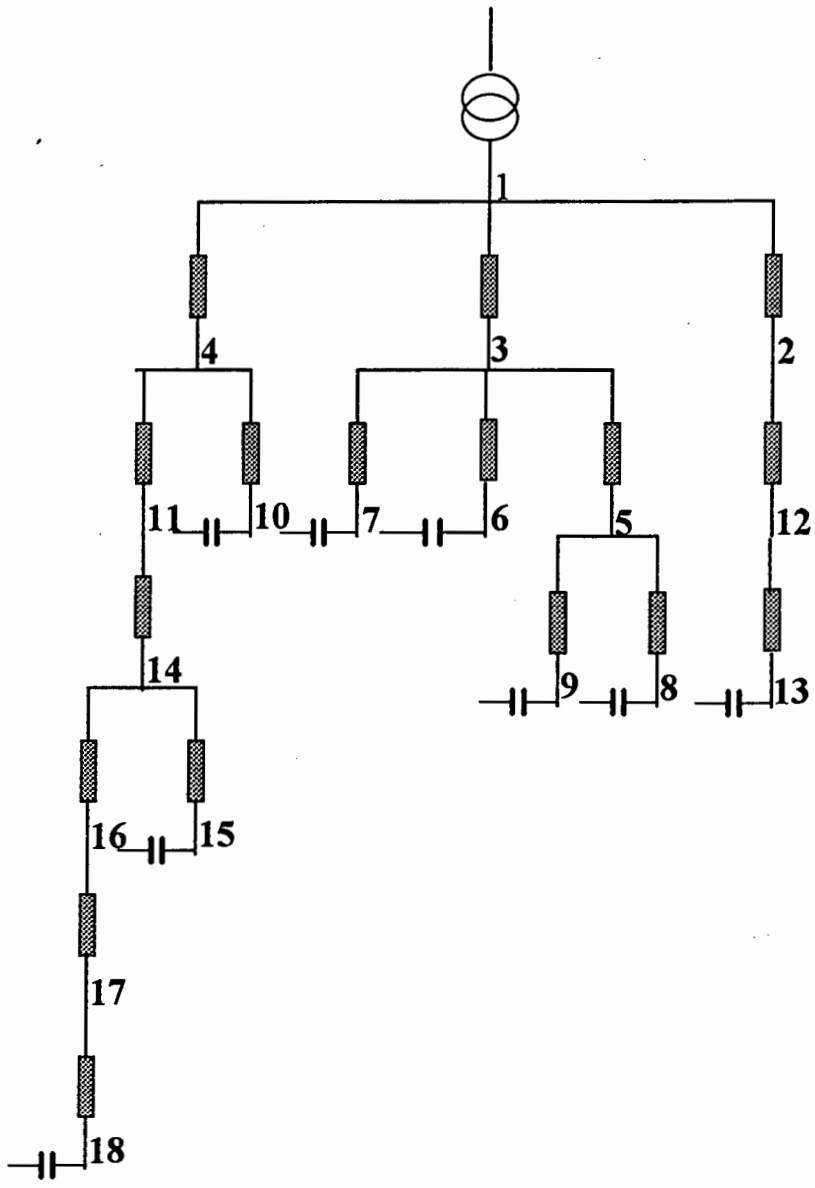

Figure 6.7.1.2: Positive sequence representation of the 18 bus radial network.

The system bases are 1 MVA, 13.2 kV and 377 rad/s. The line data as well as the transformer data is given in Table 6.7.1.1.

Line	Inductance in percent of per unit	Line	Inductance in percent of per unit
1-2	0.174	1-4	0.278
2-12	0.246	4-10	0.096
12-13	0.107	4-11	0.171
1-3	1.209	11-14	0.045
3-5	2.968	14-15	0.164
3-6	0.160	14-16	0.251
3-7	2.282	16-17	0.354
5-8	0.055	17-18	0.134
5-9	0.127	Transformer	0.532

Table 6.7.1.1: Line and transformer data in percent of per unit for the 18 bus network.

The capacitor values are all 0.5 per unit. The line resistances and the loads are neglected in the study, as they only have minimal effects on the system poles and zeros, thus resulting in a more conservative design. The shunt line capacitances were ignored, as they are negligible compared to the power capacitor banks connected to the power system.

A 1 MVA 6 pulse converter is connected to bus 18. Only the 5th and 7th harmonics are injected.

The poles and zeros, listed in table 6.71.2, were calculated by using Matlab. Furthermore, the system response shown in figure 6.7.1.3, was obtained by using V-Harm. The V-Harm simulation was done by injecting a 0.3 per unit current over all frequencies up to the tenth harmonic.

Poles	Zeros
±j15.3027	±j35.2219
±j9.18034	±j33.3099
±j7.47741	±j30.0978
±j4.11069	0

Table 6.7.1.2: Lower system poles and zeros in per unit before the optimisation.

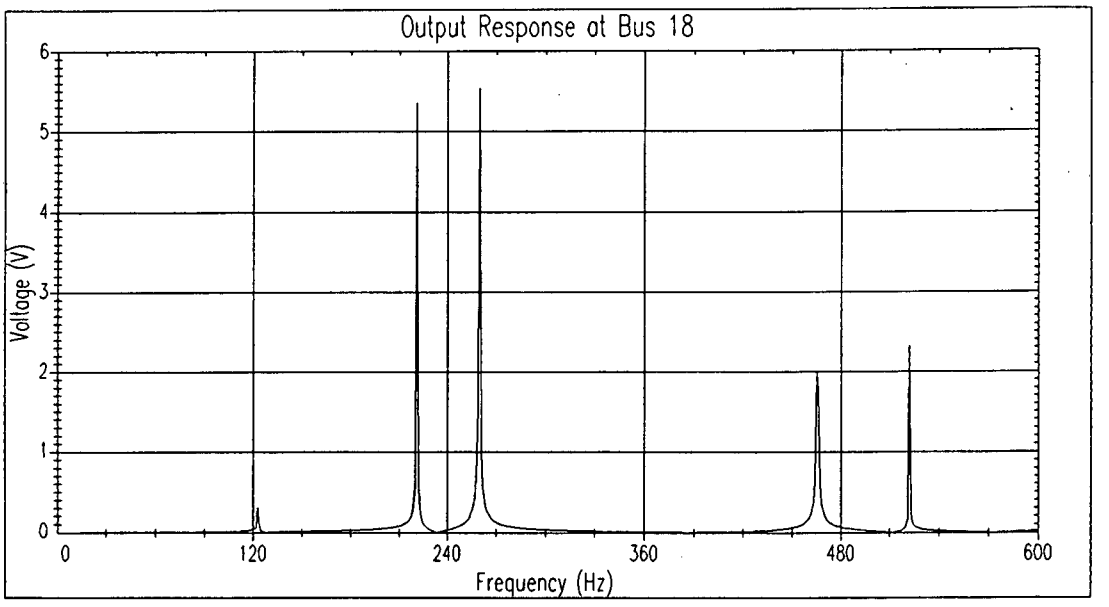

Figure 6.7.1.3: V-Harm output response before the optimisation.

From table 6.7.1.2 it can be seen that all the zeros are far from the fifth and seventh harmonics. Furthermore, the poles are very close to these frequencies. This indicates that there will be a harmonic distortion problem in the network if no countermeasures are applied. This is confirmed by figure 6.7.1.3, which shows that there are very high resonant peaks in the vicinity of the fifth and seventh harmonic. The magnitudes for the fifth and seventh harmonic are 0.0344074 per unit and 0.0127801 per unit respectively.

In order to minimise the voltage distortion that is produced by the converter, four additional capacitors of 0.5 per unit each are at first randomly placed at the network buses. The A matrix and the poles and zeros for the output response at bus 18 are calculated. The optimisation

algorithm as shown in figure 6.7.1.1 is applied, resulting in a neighbourhood search over the configuration space.

Figure 6.7.1.4 shows the value of the objective function for each iteration. It can be seen that the value of the objective function increases with each iteration, which is also characteristic of a maximisation optimisation procedure. The optimal capacitor assignment is obtained after five iterations. The maximum value of the objective function is 0.96337 per unit. For this example the optimal response at bus 18 is obtained when additional capacitors are connected to the following buses: 2, 12, 16 and 17.

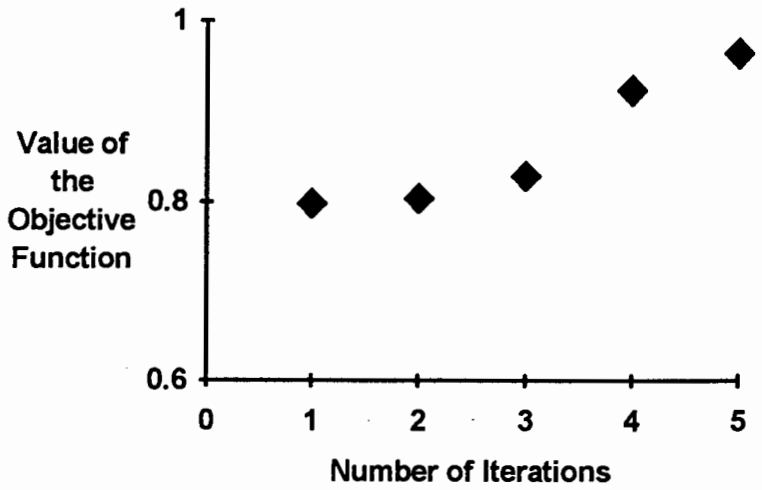

Figure 6.7.1.4: Value of the objective function for each iteration.

The poles and zeros for the optimal configuration are shown in table 3. The output response is shown in figure 6.7.1.5.

Poles	Zeroes
±j16.6779	±j16.8447
±j11.2373	±j16.4566
±j7.98704	±j7.99356
±j5.96337	±j4.59542
±j3.96613	0

Table 6.7.1.3: Lower system poles and zeros in per unit with the optimal capacitor assignment.

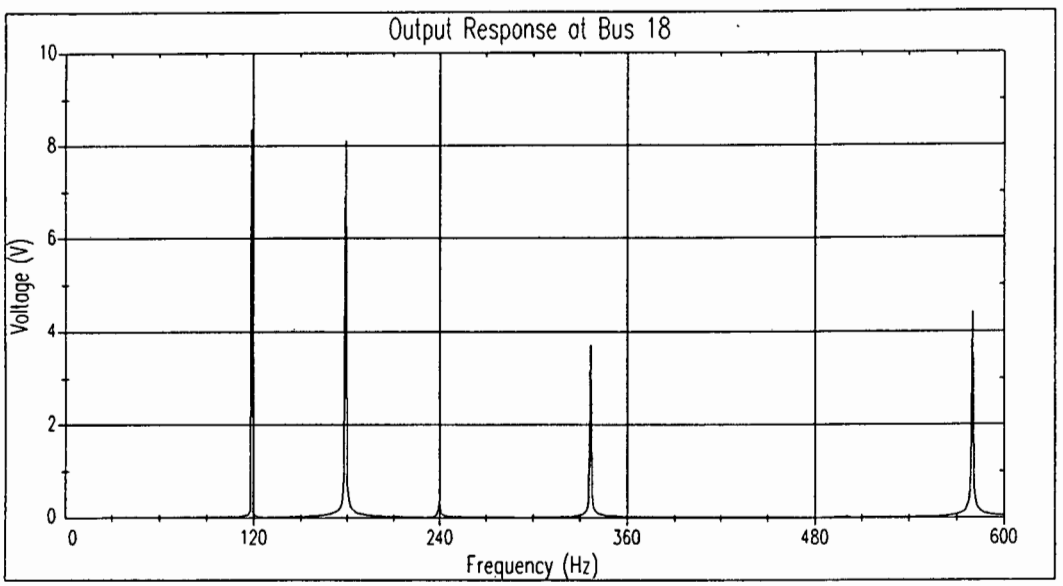

Figure 6.7.1.5: V-Harm output response with the optimal capacitor assignment.

From Table 6.7.1.3 it can be seen that the nearest poles to the fifth and seventh harmonic are at 5.96337 and 7.98704 respectively. The frequency response of the simulation performed in V-Harm also confirms the significant improvement over the original system. The magnitudes of the fifth and seventh harmonic are 0.00222821 per unit and 0.00708988 per unit respectively. This is an improvement by a factor of about 15 and 2 respectively. The new network configuration is therefore better than the original distribution system in terms of harmonic distortion.

6.8 Simulated Annealing

The simulated annealing algorithm was first introduced in 1983 [7]. Since then it became a popular method for solving combinatorial and travelling salesman type problems. It has been successfully used in optimisation type problems, addressing network configurations [8, 9], least cost distribution planning and unit commitment [10] and in other fields [11 - 14].

Annealing is the physical process whereby a solid is heated up until melting point and then slowly cooled down, until it crystallises into a state with a perfect lattice. The temperature prescribed by the cooling schedule is directly related to the freedom with which the particles can move around.

The simulated annealing algorithm is an analogy to the physical annealing process, used for the crystallisation process in physical systems [15]. The cooling schedule is predefined. It is normally chosen as a geometric series, according to which the temperature is lowered. This is given by:

$$T_n = pT_o \qquad (6.8.1)$$

where: T_n is the new temperature
p is the geometric series scaling factor
T_o is the old temperature

At the beginning of the optimisation procedure, due to the characteristics of the annealing process, the system is in a state of high entropy. The temperature is then gradually lowered, until the system "crystallises". At this point the "crystallised" or "frozen" system configuration will be equal to the lowest energy in the system or equal to the lowest value of the cost function or objective function [16].

At each value of the temperature the Metropolis algorithm, derived from statistical physics principles, is used to simulate the system [15]. A set of moves is then selected, according to which the system can change from one state to the next. These moves are selected randomly. If

a move causes an increase in the cost function, it is called an uphill move. If the move causes a decrease in the cost function, it is called a downhill move.

In the simulated annealing algorithm, the information, regarding the objective function, obtained from the various configurations is utilised better than in other optimisation methods. For this reason, all downhill moves are accepted as possible feasible solutions. However, uphill moves are also accepted, but with a probability equal to the Boltzmann factor and then only if this is greater than a random number uniformly distributed between 0 and 1 [7]. The Boltzmann factor is given by:

$$e^{\left(\frac{-\Delta C}{T}\right)} > r \qquad (6.8.2)$$

where: ΔC is the increase in the cost

T is the temperature

r is a uniformly chosen random number from the interval 0 to 1

Due to this criterion, equation *(6.8.2)* and the fact that the Boltzmann factor is very small, the simulated annealing algorithm accepts all moves at high temperatures. Many uphill moves therefore occur in addition to the normal downhill moves. Through this a broad search through the configuration space is achieved. As the temperature is lowered, the value of the Boltzmann factor increases and the algorithm does not accept uphill moves as easily as before. Mainly downhill moves are accepted. At this stage the algorithm behaves like a greedy search. Due to the probabilistic selection rule, the optimisation routine will always be able to get out of a local minimum and proceed to the desired global minimum.

The simulated annealing algorithm guarantees the globally optimal solution, as the number of iterations tends to infinity [15]. This optimisation method is very useful, but it requires a large number of iterations and is therefore very computer intensive.

The following steps are necessary to implement the simulated annealing algorithm [8 - 10]:

1. Select sufficiently high initial values for the temperature and the objective function.
2. Perform a constant number of iterations in which feasible trial points are generated randomly and accepted with a probability equal to the Boltzmann factor given in equation *(6.8.2)*.
3. Decrement the temperature according to a cooling schedule, normally a geometric series.
4. If the algorithm has not converged yet, go back to step 2., otherwise stop.

6.8.1 Case Study 4

The 16 bus meshed network as shown in section 5.3.9.3, is analysed. Three one per unit current injection sources, swept from 1/60 to 30 per unit frequency, are applied to buses 8, 9, and 15. The output voltage is obtained at bus 10. The loads have been neglected, which will cause unrealistically high resonant peaks. At first no voltage support capacitors are applied to the power system, giving an undesirable response. It can be seen from figures 6.8.1.1 and 6.8.1.2, that there is a high harmonic voltage peak of approximately 1200 per unit magnitude close to the second harmonic. There is another harmonic voltage peak close to the eleventh harmonic of approximately 50 per unit magnitude. This is a highly undesirable situation, as this will result in harmonic problems on the power system.

In order to improve the problem situation, the simulated annealing algorithm, as explained in section 6.8, is applied together with the objective function, of section 6.4.2. This procedure is illustrated by way of a flowchart, which is shown in figure 6.8.1.3.

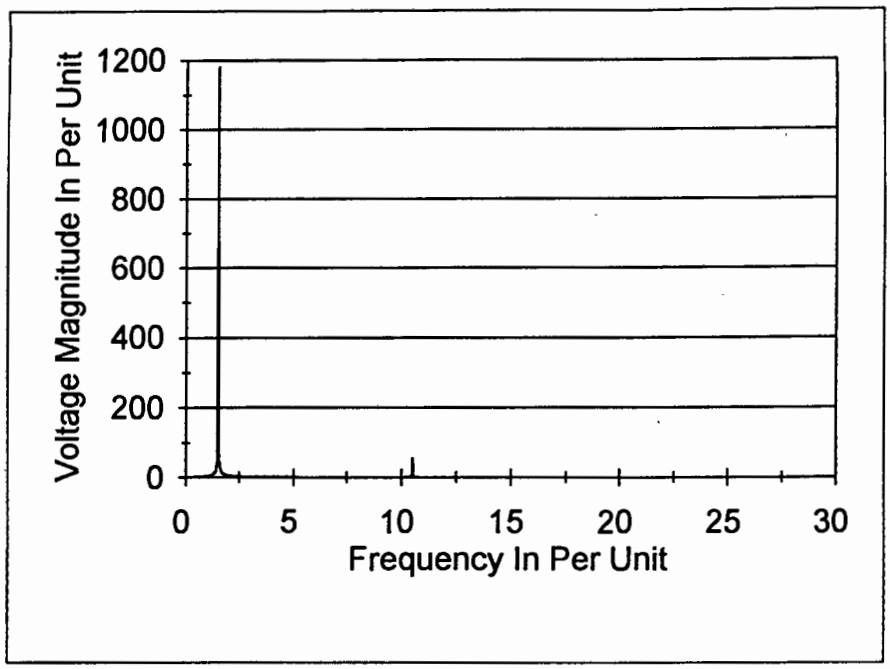

Figure 6.8.1.1: Linear frequency response of the 16 bus network before the optimal placement of capacitors.

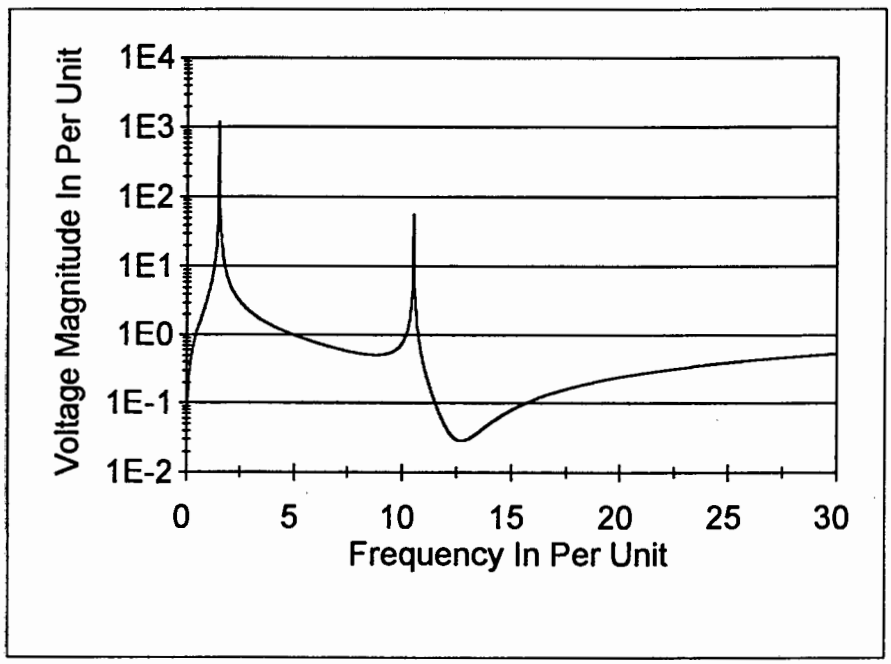

Figure 6.8.1.2: Logarithmic frequency response of the 16 bus network before the optimal placement of capacitors.

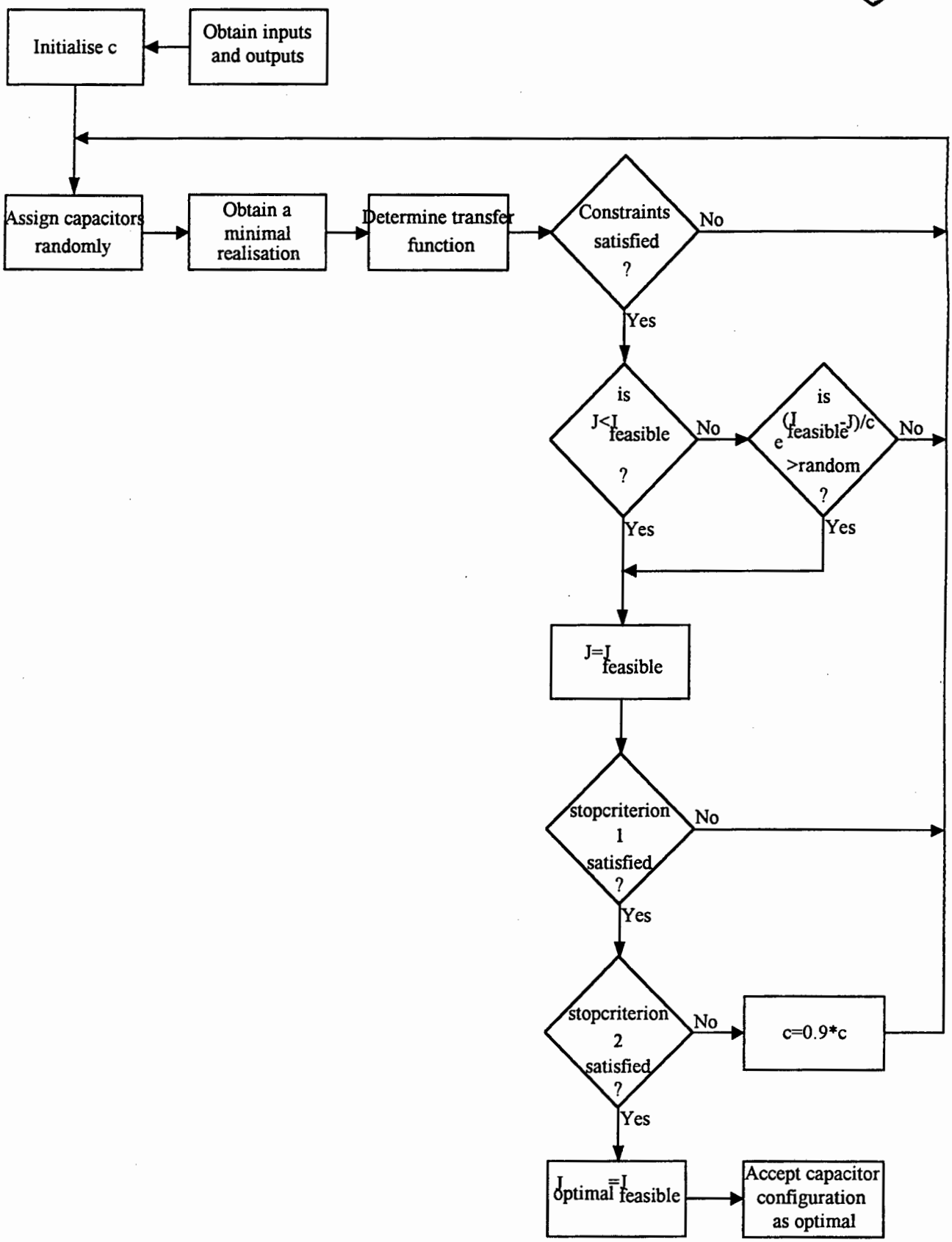

Figure 6.8.1.3: Flowchart of the simulated annealing algorithm.

At first five power capacitors of 0.3 per unit each are randomly connected to the network. The algorithm shown in figure 6.8.1.3 is now applied, to determine the optimal locations on the network, for these power capacitors. The minimum value of the objective function for this example is 1166.9 per unit. The optimal frequency response at bus 10 is obtained when five additional capacitors of 0.3 per unit are connected to the following buses: 7, 10, 14, 15 and 16. The optimal frequency response is subsequently obtained and shown in figures 6.8.1.4 and 6.8.1.5.

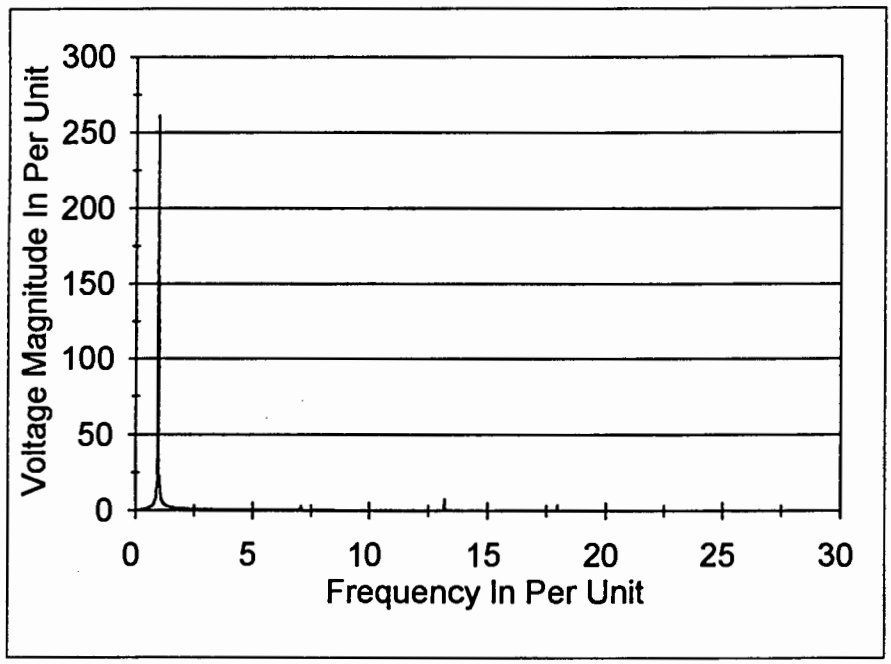

Figure 6.8.1.4: Linear frequency response of the 16 bus network after the optimal placement of capacitors.

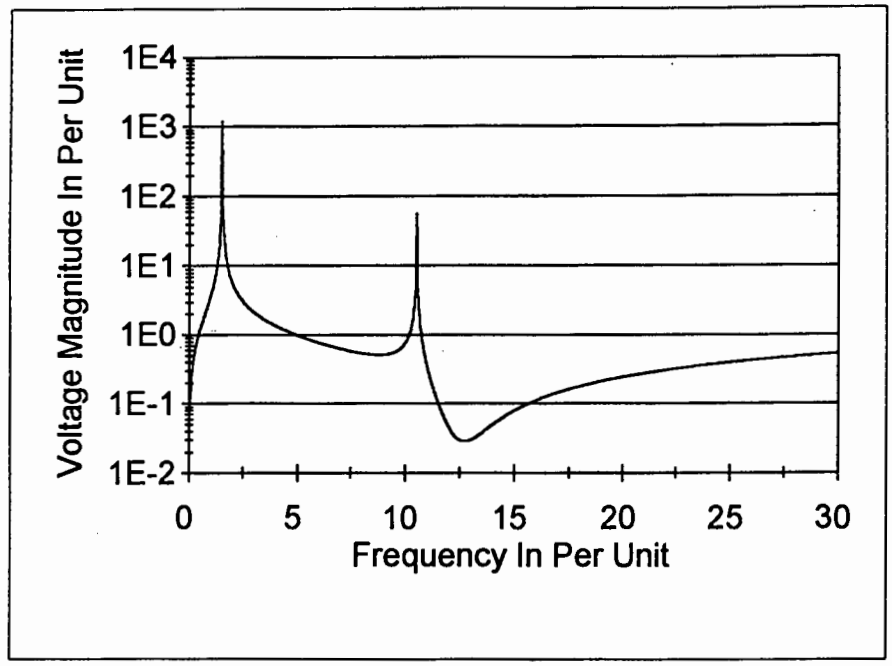

Figure 6.8.1.5: Logarithmic frequency response of the 16 bus network after the optimal placement of capacitors.

It can be seen from figures 6.8.1.4 and 6.8.1.5, that there is now only one significant resonant peak. This is located at the first harmonic and has a magnitude of approximately 250 per unit. This is far more desirable than a few resonant peaks located at the lower order harmonics, as shown in figures 6.8.1.1 and 6.8.1.2.

6.9 References

[1] R. Fletcher, *Practical Methods of Optimisation*, second edition, John Wiley and Sons, Chichester, 1987.

[2] B. A. Francis, *Lecture Notes in Control and Information Sciences: A Course in $H\infty$ Control Theory*, Springer Verlag, Berlin, 1987.

[3] S. P. Boyd and C. H. Barratt, *Linear Controller Design: Limits of Performance*, Prentice Hall, Englewood Cliffs, 1991.

[4] M. Green and D. J. N. Limebeer, *Linear Robust Control*, Prentice Hall, Englewood Cliffs, 1995.

[5] M. Morari, *Robust Process Control*, Prentice Hall, Englewood Cliffs, 1989.

[6] T. H. Ortmeyer and K. Zehar, "Distribution System Harmonic Design" *IEEE Transactions on Power Delivery*, Volume 6, Number 1, January 1991, pages 289-294.

[7] S. Kirkpatrick, C. D. Gelatt and M. P. Vecchi, "Optimisation by Simulated Annealing", *Science*, Volume 220, Number 4598, May 1983, pages 671-680.

[8] H. D. Chiang and R. Jean-Jumeau, "Optimal Network Reconfigurations in Distribution Systems: Part I: A New Formulation and Solution Methodology", *IEEE Transactions on Power Delivery*, Volume 5, Number 4, November 1990, pages 1902-1908.

[9] H. D. Chiang and R. Jean-Jumeau, "Optimal Network Reconfigurations in Distribution Systems: Part II: Solution Algorithm and Numerical Results", *IEEE Transactions on Power Delivery*, Volume 5, Number 3, July 1990, pages 1568-1574.

[10] F. Zhuang and F. D. Galina, "Unit Commitment by Simulated Annealing", *IEEE Transactions on Power Systems*, Volume 5, Number 1, February 1990, pages 311-318.

[11] M. Piccioni, "A Combined Multistart - Annealing Algorithm for Continuos Global Optimisation", *Computers and Mathematics with Applications*, Volume 21, 1991, pages 173-179.

[12] Y. G. Saab and V. B. Rao, "Combinatorial Optimisation by Stochastic Evolution", *IEEE Transactions on Computer Aided Design*, Volume 10, April 1991, pages 525-535.

[13] C. L. Chen and Y. Y. Hsu, "An efficient algorithm for the design of decentralised output feedback power system stabilisers", *IEEE Transactions on Power Systems*, Volume 3, August 1988, pages 999-1004.

[14] F. Ronnie, S. M. Chu, J. C. Wang and H. D. Chiang, "Strategic Planning of LC Compensators in Nonsinusoidal Distribution Systems", *IEEE Transactions on Power Delivery*, Volume 9, Number 3, July 1994, pages 1558-1563.

[15] E. Aarts and J. Korst, *Simulated Annealing and Boltzmann Machines: A Stochastic Approach to Combinatorial Optimisation and Neural Computing*, John Wiley and Sons, Chichester, 1989.

[16] A. Toern and A. Zilinskas, *Lecture Notes in Computer Science: Global Optimisation*, Springer Verlag, 1989.

Chapter 7

Conclusions and Future Research

The quality of the power supply will become increasingly more important in power system planning and operation. The power system is constantly expanding and the loads are steadily increasing and also cause power quality problems. Resonance conditions will occur more frequently and their associated losses will increase. Injection contracts are already being negotiated at present and these will definitely increase in number. Because of the trends outlined above, a general awareness of power quality is necessary and active measures should be taken to improve the scenario.

Of the harmonic analysis methods that are investigated, it was found, that the current injection method is the most popular and most widely used. This is followed by the Newton - Raphson method and then the Gauss - Seidel - and companion circuit methods.

The investigation of software packages used for the harmonic analysis of power systems revealed, that the most popular package for this purpose is the Harmflo+ Workstation, which consists of two solution modules, Harmflo+ and SuperHarm. However, it was found that none of the available packages utilises a state space model. This is a disadvantage, since a state space model is very useful for harmonic stability, optimisation, filter design and robustness amongst others.

The existing state space models for power systems are only applicable to radial systems with capacitors at the end of each feeder, or they are not widely used amongst others. For this reason a new state space model is developed. This model is applicable to radial and meshed networks and overcomes most of the disadvantages of the existing models. The state space model approach was implemented on a 16 bus meshed network example and also compared to the current injection method. It is shown that the two methods produce identical results.

The state space model approach is used together with the simulated annealing algorithm to optimally place capacitors on a meshed power network. This is done by keeping the voltage profile at all busses within ±5% of one per unit and limiting the harmonic peaks, while also minimising the total frequency response curve over all frequencies. This ensures improved performance and robustness of the power system.

It is recommended, that future research should be done along the lines of using an $H\infty$ and H_2 norm for the optimal placement of capacitors. These norms lend themselves to be taken as objective functions and constraints. Especially since they can be applied to state space models. By applying the $H\infty$ norm to certain harmonics as a constraint, the robustness of the system can be improved. In addition to this, the H_2 norm can be used as an objective function, by which the performance of the system over all frequencies can be improved. This procedure can also be combined with other additional requirements, such as minimising the cost of the power factor correction capacitors, optimally sizing the capacitors, and keeping the voltage profile within ±5% of one per unit.

It is recommended that these norms be used in conjunction with specific different optimisation routines, in particular simulated annealing, a genetic algorithm, a taboo search and a neural network type method amongst others. In this way capacitors can be utilised effectively and efficiently for power factor correction and harmonic mitigation or elimination.

Appendices

Appendix A

Questionnaire on Harmonic Analysis Programmes for Power Systems

UNIVERSITY OF CAPE TOWN

Department of Electrical Engineering

University Private Bag · Rondebosch 7700 · South Africa
Telex: 5-21439 · Telephone (021) 650-2811
Telefax: (021) 650-3465

QUESTIONNAIRE ON HARMONIC ANALYSIS PROGRAMS FOR POWER SYSTEMS

Eskom is the national electricity supply utility in South Africa with an installed capacity of 36 000 MW and annual electricity sales of 150 GWh. The Eskom management board has recently established a power quality task group with the directive ensuring that Eskom is well placed to meet future power quality needs. One of the tasks of this group is to investigate software packages for harmonic analysis of power systems and to make recommendations on packages to be used by distribution centers. For this reason a questionnaire was compiled in collaboration with the University of Cape Town. The purpose of the survey is to establish the attributes and capabilities of the latest versions of various software packages used for harmonic analysis in power systems. It will be much appreciated if you could kindly complete the questionnaire and return it as soon as possible, together with any literature, brochures, or demonstration disks to the following address:

Mr. H.V. Hitzeroth
c/o Prof. A. Petroainu
Department of Electrical Engineering
University of Cape Town
Private Bag
Rondebosch
7700
Cape Town
REPUBLIC OF SOUTH AFRICA

Fax No.: 27 (21) 650 3465

Please note that the questions below do not reflect an Eskom specification requirement but are aimed at providing a general survey of available software tools.

Please indicate with a tick in the appropriate space where applicable.

1. HARDWARE AND SOFTWARE REQUIRED:

1.1. Does the harmonic simulation program operate on a PC?

Yes ☐ No ☐

1.2. Does the harmonic simulation program operate on a workstation?

Yes ☐ No ☐

1.3. What other hardware is required to operate the harmonic simulation program?.....
.....
.....

1.4. What other software is required to operate the harmonic simulation program?.....
.....
.....

2. SOFTWARE INTERFACES:

2.1. Does the harmonic simulation program operate under Windows?

Yes ☐ No ☐

2.2. Does the harmonic simulation program operate under DOS?

Yes ☐ No ☐

2.3. Can data be imported from other software programs?

Yes ☐ No ☐

2.4. Can data be exported to other software programs?

Yes ☐ No ☐

2.5. In which format can data be imported or exported?.....
.....
.....

2.6. To which other programs can data be exported?.....
.....
.....

2.7. From which other programs can data be imported?.....
.....
.....

2.8. Does the harmonics simulation program form part of a package with a module for short circuit calculations?

Yes ☐ No ☐

2.9. Does the harmonics simulation program form part of a package with a module for load flow calculations?

Yes ☐ No ☐

2.10. Which other modules does the harmonic simulation program provide for?.....
.....
.....

3. INPUT:

3.1. Does the harmonic simulation program have a graphic user interface which allows single line diagrams to be generated?

Yes ☐ No ☐

4. OUTPUT:

4.1. Can the harmonic simulation program display the network impedance magnitude versus frequency on a two dimensional graph?

Yes ☐ No ☐

4.2. Can the harmonic simulation program display the voltage or current magnitude versus frequency on a two dimensional graph?

Yes ☐ No ☐

4.3. Can the harmonic simulation program display the voltage or current phase versus frequency on a two dimensional graph?

Yes ☐ No ☐

4.4. Can the harmonic simulation program display the voltage or current waveforms?

Yes ☐ No ☐

4.5. Can the harmonic simulation program display three dimensional plots?

Yes ☐ No ☐

4.6. Which items can be displayed on the three dimensional plots?.....
.....
.....

4.7. Are the simulation results available in a table?

Yes ☐ No ☐

4.8. Are there other items that the harmonic simulation program can display?
.....
.....

5. TECHNICAL ISSUES:

5.1. Is the harmonic simulation program time domain based?

Yes ☐ No ☐

5.2. Is the harmonic simulation program frequency domain based?

Yes ☐ No ☐

5.3. Does the harmonic simulation program use the Gauss-Seidel method of solution?

Yes ☐ No ☐

5.4. Does the harmonic simulation program use the Newton-Raphson method of solution?

Yes ☐ No ☐

5.5. Does the harmonic simulation program use the current injection method of solution?

Yes ☐ No ☐

5.6. Is the modelling of unbalanced three-phase systems included in the program?

Yes ☐ No ☐

5.7. Does the harmonic simulation program do a frequency scan?

Yes ☐ No ☐

5.8. Is statistical modelling implemented on linear loads?

Yes ☐ No ☐

5.9. Is statistical modelling implemented on harmonic sources?

Yes ☐ No ☐

5.10. Is statistical modelling implemented on network elements (e.g. line parameters)?

Yes ☐ No ☐

5.11. Is probabilistic modelling implemented on linear loads?

Yes ☐ No ☐

5.12. Is probabilistic modelling implemented on harmonic sources?

Yes ☐ No ☐

5.13. Is probabilistic modelling implemented on network elements (e.g. line parameters)?

Yes ☐ No ☐

5.14. Can batch-mode studies (i.e. various input files) be implemented by the harmonic simulation program?

Yes ☐ No ☐

5.15. Does the program provide a standard arc furnace load model?

Yes ☐ No ☐

5.16. Does the program provide a standard uncontrolled converter model?

Yes ☐ No ☐

5.17. Does the program provide a standard controlled converter model?

Yes ☐ No ☐

5.18. Does the program provide a standard thyristor controlled reactor model?

Yes ☐ No ☐

5.19. Does the program provide a standard cyclo converter model?

Yes ☐ No ☐

5.20. Does the program provide a standard linear motor model?

Yes ☐ No ☐

5.21. Does the program provide a standard lumped load model?

Yes ☐ No ☐

5.22. Are any other standard models provided?.....
.....
.....

5.23. Which transmission line models are used in the program?.....
.....
.....

5.24. Do the transmission line models include the skin effect?

Yes ☐ No ☐

5.25. Do the transmission line models include a frequency dependent ground return path?

Yes ☐ No ☐

5.26. Is the CIGRE transformer model contained in the program?

Yes ☐ No ☐

5.27. Is a constant X/R ratio transformer model contained in the program?

Yes ☐ No ☐

5.28. Is a variable X/R ratio transformer model contained in the program?

Yes ☐ No ☐

5.29. Are there any other standard transformer models contained in the program?.....
.....
.....

6. ADDITIONAL TECHNICAL FUNCTIONS:

6.1. Does the program include a module for harmonic filter design rating?

Yes ☐ No ☐

6.2. Does the program include a module for transformer de-rating?

Yes ☐ No ☐

6.3. Does the program include a module to compare the simulated results with the IEEE / IEC distortion limits?

Yes ☐ No ☐

6.4. Does the program include a module for the calculation of IEEE / IEC values?

Yes ☐ No ☐

6.5. Does the program include any other such modules?.....
.....
.....

7. GENERAL ISSUES:

7.1. What is the name of the harmonic simulation program?.....
.....
.....

7.2. What is the price of the software package?.....
.....
.....

7.3. Can a demonstration disk of the program be supplied?

Yes ☐ No ☐

7.4. At what cost can a demonstration disk of the program be supplied?.....
.....
.....

7.5. Does a user group for the program exist?

Yes ☐ No ☐

7.6. Does the user group communicate by e-mail?

Yes ☐ No ☐

7.7. Does the user group send out newsletters?

Yes ☐ No ☐

7.8. What is the cost for joining the user group?.....
.....
.....

7.9. Can theory books on the program be supplied (i.e. information on how network elements are modeled, algorithms used, etc.)?

Yes ☐ No ☐

7.10. Can a user reference manual be supplied?

Yes ☐ No ☐

7.11. Is a group license offered?

Yes ☐ No ☐

7.12. When will the next version of the harmonic simulation program be released?.....
.....
.....

7.13. Which improvements will be included in a new release?.....

7.14. Additional comments:.....

Appendix B

Results of the Survey of Harmonic Analysis Programmes for Power Systems

The fields left blank in table B.1, indicate that the item is not applicable, or that the person who completed the questionnaire did not specify an answer. Fields marked by a √ or X, show that the answer is positive or negative respectively.

Harmonic Analysis Programmes	Harmflo+	V-Harm	Hi-Wave	Harmonique	ETAP	CYMHARMO	ERACS
Hardware and software requirements							
Does the harmonic simulation programme operate on a PC?	√	√	√	√	√	√	√
Does the harmonic simulation programme operate on a workstation?	√	X	X	X	√	X	X
What other hardware is required to operate the harmonic simulation programme?	minimum: 80286, numeric coprocessor, 2MB RAM, about 10MB harddisk space		minimum: 80286, numeric coprocessor, about 120MB hard disk space, VGA screen	minimum: 80386, 8MB RAM	minimum: DOS version: 80286, numeric coprocessor, 560kB RAM, 20 MB hard disk space, Windows version: 486 DX, 20MB	minimum: 80386, numeric coprocessor, 2MB RAM	

					RAM, 100MB hard disk space, 800X760, SVGA monitor		
What other software is required to operate the harmonic simulation programme?	minimum: Windows 3.1	V-Graph	minimum: DOS 5 or later	minimum: Windows 3.1	minimum: DOS version: DOS 5.0 Windows version: Windows NT 3.5		ERACS loadflow
Software interfaces							
Does the harmonic simulation programme operate under Windows?	√	√	X in future	√	√	X	√
Does the harmonic simulation programme operate under DOS?	X	√	√	√	√	√	√
Can data be imported from other software programmes?	X	√	√	X	√	√	X in future

Can data be exported to other software programmes?	√ with TOP	X	√	√	√	X	X in future
In which format can data be imported or exported?	exported to other windows with clipboard	ASCII	ASCII	ASCII		ASCII	SQL in future
To which other programmes can data be exported?	EXCEL and Word			EXCEL and Word	ASCII and DBase	ASCII	SQL compatible in future
From which other programmes can data be imported?		Cooper Power Systems "Verdict Programs"			DAPPER and ELMS	CYMFLO	ICL DINIS programme
Does the harmonics simulation programme form part of a package with a module for short circuit calculations?	X	√ V-Net	√	X	√	X	√
Does the harmonics simulation programme form part of a package with a module for load flow	X	√ V-Flow	√	X	√	√	√

calculations?							
Which other modules does the harmonic simulation programme provide for?	load flow	data input (V-Graph), over current protection (V-Pro), capacitor application (V-Cap)	transient stability, motor starting, fault analysis, protection co-ordination	calculation of ripple control emitted by voltage - series: emiHors	load flow, short circuit, motor starting, transient stability	transmission line parameters, voltage induced on a communication line	transient stability, protection co-ordination, AVR and govenor modelling
Input							
Does the harmonic simulation programme have a graphic user interface which allows single line diagrammes to be generated?	X	√ V-Graph	√ Dapper	√	√	X in future	√
Output							
Can the harmonic simulation programme display the network impedance magnitude *versus* frequency on a two dimensional graph?	√	√	√	√	√	√	√

Can the harmonic simulation programme display the voltage or current magnitude *versus* frequency on a two dimensional graph?	√	√	√	√	√	√	X in future
Can the harmonic simulation programme display the voltage or current phase *versus* frequency on a two dimensional graph?	√	√	√	√	√	√	X in future
Can the harmonic simulation programme display the voltage or current waveforms?	√	√	√	X	√	√	X in future
Can the harmonic simulation programme display three dimensional plots?	X	√	X	X	X	X	X
Which items can be displayed on the three dimensional plots?		Magnitude *versus* frequency *versus* location					

Are the simulation results available in a table?	√	√	√	√	√	√	√
Are there other items that the harmonic simulation programme can display?		spectrum plots, *RX* plots, bode plots	combined waveform and current / voltage phase *versus* frequency or harmonic order, TIF			harmonic voltage *versus* variation of admittance, induced voltage on communication line *versus* distance along line, total voltage induced on communication line *versus* frequency	detailed harmonic current flows, THD, TIF
Technical issues							
Is the harmonic simulation programme time domain based?	X	X	X	X	X	X	X

Is the harmonic simulation programme frequency domain based?	√	√	√	√	√	√	√
Does the harmonic simulation programme use the Gauss-Seidel method of solution?	X	X	X	√	√ at fundamental	X	X
Does the harmonic simulation programme use the Newton-Raphson method of solution?	X	X	X	X	X	X	
Does the harmonic simulation programme use the current injection method of solution?	√	√	√	√	√	√	√
Is the modelling of unbalanced three-phase systems included in the programme?	X	√	X	X	X	√	X
Does the harmonic simulation programme do a frequency scan?	√	√	√	√	√	√	√
Is statistical modelling	X	X	X	√	√	X	√

implemented on linear loads?							
Is statistical modelling implemented on harmonic sources?	X	X	X	√	√	X	X
Is statistical modelling implemented on network elements (e.g. line parameters)?	X	X	X	√	√	X	X
Is probabilistic modelling implemented on linear loads?	X	X	X	√ with HAZAR	X	X	X
Is probabilistic modelling implemented on harmonic sources?	X	X	X	√ with HAZAR	X	X	X
Is probabilistic modelling implemented on network elements (e.g. line parameters)?	X	X	X	√ with HAZAR	X	X	X
Can batch-mode studies (i.e. various input files) be implemented by the harmonic	√	√	X	X	X	√	X in future

simulation programme?							
Does the programme provide a standard arc furnace load model?	X in future	X	√	√	X in future	√	X
Does the programme provide a standard uncontrolled converter model?	X in future	√	√	√	√	√	√
Does the programme provide a standard controlled converter model?	X in future	X	√	X	√	√	√
Does the programme provide a standard thyristor controlled reactor model?	X in future	√	√	X	X in future	√	X
Does the programme provide a standard cyclo converter model?	X in future	X	√	X	√	X	X
Does the programme provide a standard linear motor model?	√	√	√	√	√	√	X
Does the program provide a	√	√	√	√	√	√	√

standard lumped load model?							
Are any other standard models provided?	machines	machines, cables	non-linear frequency dependent cables	CIGRE load	cables, breakers, motors	CIGRE type C load, filters: single-, double tuned, C-type, high pass damped, mutually coupled *RL* branch, branch with user defined impedance spectrum	converters
Which transmission line models are used in the programme?	frequency dependent *RL* branch, Pi, longline, model based on line geometry	frequency dependant *RL* branch, model based on Carson equations, skin effect,	non-linear, frequency dependent, model based on first three terms of Carson's		short line, in future: long line, distributed parameter model	Pi, distributed parameter (hyperbolic), transposed or not, with or without skin effect,	equivalent Pi with skin effect

		transpositions, tower geometry	equations			balanced, mutually coupled	
Do the transmission line models include the skin effect?	√	√	√	√	√	√	√
Do the transmission line models include a frequency dependent ground return path?	√	X but a frequency dependent neutral	√	√	X	√	X
Is the CIGRE transformer model contained in the programme?	X	X	X	√	X	X	
Is a constant *X/R* ratio transformer model contained in the programme?	√	√	√	√	X	X	X
Is a variable *X/R* ratio transformer model contained in the programme?	√	√	X	X	√	√	√
Are there any other standard	X	1 or 3 phase,	3 winding,		2, 3 winding	single phase,	X

transformer models contained in the programme?		star, delta, grounded star	non-linear, frequency dependent		transformers	three phase, star-star, star-delta, star-delta-star, single phase two port	
Additional technical functions							
Does the programme include a module for harmonic filter design rating?	√	X	√	√	√	√	X
Does the programme include a module for transformer de-rating?	√	X	√		X	X	X
Does the programme include a module to compare the simulated results with the IEEE / IEC distortion limits?	√	X user can put in limits and have violations highlighted	√	√	√	X	X
Does the programme include a module for the calculation of IEEE / IEC values?	√ voltage, current	X	√	X	√	√ HDF, KV-T, I*T, VTIF,	X

	distortion limits					ITIF	
Does the programme include any other such modules?	X				RMS value, absolute arithmetic simulation, TIF value for voltage, current		THD, TIF
General issues							
What is the price of the software package?	$2900 for non EPRI members, $2500 for EPRI members, free to universities, providing they provide technical	$7200	$4750 100 Bus, $5600 1000 Bus	FF20000		DOS version: $8000, DOS extended version: $9500	loadflow: £5950, harmonics: £3830, multiple copy discounts, academic discounts

	articles for distribution						
Can a demonstration disk of the programme be supplied?	X in future	√	√	√	√	√	√
At what cost can a demonstration disk of the programme be supplied?		no charge	no charge	no charge	no charge	no charge	no charge
Does a usergroup for the programme exist?	√	X	X	X	√	X	X
Does the usergroup communicate by e-mail?	√				√		
Does the usergroup send out newsletters?	√						
What is the cost for joining the usergroup?	$2900 first year, $1800/$1200 thereafter, free for universities				no charge		
Can theory books on the	X	X	X	√	√	X	X

programme be supplied (i.e. information on how network elements are modelled, algorithms used, etc.)?							
Can a user reference manual be supplied?	√	X	√	√	√, extra ones can be bought for $150	√	√
Is a group license offered?	√	√	√	X	√	√	√
When will the next version of the harmonic simulation programme be released?		mid 1995	end 1995	1996		end 1995	end 1995
Which improvements will be included in a new release?	More advanced models	Interface directly with V-Graph	Windows, graphical one line interface, custom phase shift specification	3 phase description	improved models, unbalanced three phase models	Windows, graphical I/O, addition of IEEE519 or IEC 77 limits considered	short circuit programme, DC power systems,non-linear loads, SVC's

Table B.1: Results of the questionnaire that was sent out to various software developers and suppliers.

Appendix C

Paper submitted to the 1996 Power Systems Computation Conference, Dresden, Federal Republic of Germany, August 1996

A STATE SPACE MODEL FOR HARMONIC ANALYSIS OF MESHED AND RADIAL POWER SYSTEMS

Helmuth Victor Hitzeroth
e-mail: helmuth@eleceng.uct.ac.za

Alexander Petroianu
e-mail: apetroianu@eleceng.uct.ac.za

Department of Electrical Engineering, University of Cape Town
University Private Bag, Rondebosch 7700, South Africa

KEYWORDS

Distribution systems, harmonic analysis, system realisation.

ABSTRACT

A novel approach for harmonic analysis and design of meshed and radial power systems is presented. Redundant nodal voltages are eliminated from the branch current equations. A system realisation is derived from the remaining equations and the nodal voltage equations. This is reduced to a minimal realisation. A flow chart of the procedure is presented and two case studies are performed. A frequency scan is done and compared to the current injection method, yielding the same result. The state space model opens the way to the application of a wide variety of control theory methods for the analysis of power system harmonics.

1 INTRODUCTION

Harmonic distortion in power systems is becoming an increasingly important issue in transmission / distribution system design and operation. Not only are harmonic levels increasing in distribution systems, but consumer loads are also becoming far more sensitive to harmonic distortion [1]. Particularly recently, with the increasing awareness of the quality of supply, and the introduction of freemarket elements into the electricity industry, new momentum was given to this field, by a movement towards penalties for injected harmonics (harmonic injection contracts) [2].

Harmonics are generated by a variety of sources, ranging from arc furnaces, drives, transformers to lighting and computers. Most of these sources inject harmonic currents into the power system. These currents in turn result in harmonic voltage drops across various network elements. In this way harmonics can propagate throughout the power system to buses remote from the harmonic source, thereby causing various problems in the power system [3]. These are amongst others resonant conditions, telephone interference, capacitor bank failures, overheating of motors, vibrations and false tripping of equipment [4].

Various methods are presently in use for the harmonic or frequency analysis of power systems. Time based methods [5, 6], methods that make use of a loadflow (Newton-Raphson, Gauss-Seidel type algorithms) at different discrete frequencies (harmonic load flow) [5, 7] and finally the current injection method are used. The latter is the most popular, as it makes use of the bus admittance matrix, as shown below:

$$[V] = [Y(\varpi)]^{-1} \cdot [I] \tag{1}$$

where: V is the $r \times 1$ nodal voltage vector
r is the number of nodes
Y is the $r \times r$ bus admittance matrix
ϖ is the frequency in radians per second
I is the $r \times 1$ nodal current injection vector

The bus admittance matrix is recalculated for each frequency under investigation. Of all the methods the current injection method is the fastest, as it is a non-iterative process [8].

However, a significant disadvantage of the above procedures, is that none allow the implementation of state space theory methods.

In [9] a method is used to develop a state space model, by making use of graph theory and a proper tree. This method does not seem to be widely used on large power systems though.

In view of these circumstances a state space model description was recently developed and used for radial networks [10]. However, the method only applies to radial power systems and furthermore, there have to be power

capacitors at the end of each feeder. In addition to this, once the equations that describe the network are determined, the state coefficient matrix is obtained by calculating the inverse of an impedance type matrix and multiplying this with a matrix similar to an incidence matrix. This is very cumbersome and time consuming, especially when the process has to be done everytime the network configuration changes, as is necessary for contingency and some optimisation studies.

In this paper an improved minimal state space model description (minimal system realisation) is developed for the harmonic analysis of power systems. This approach provides for the analysis of radial and meshed networks and furthermore, the inverse of a matrix does not have to be calculated. Once this model is obtained, the field to control theory methods is available. At first the branch current equations and nodal voltage equations for the system are determined. Reduction formulas, applicable to different cases, are then derived, to eliminate unwanted nodal voltages from the set of branch current equations. This is done until the voltage vectors of the branch current equations and the nodal voltage equations are equal. Thereafter the two sets of equations are combined into a general hybrid state space model description (system realisation). A minimal realisation of the system is then obtained, opening the way to control theory methods for the analysis of harmonic current injections in power systems.

The procedure is implemented on a 16 bus meshed network and also compared to the current injection method, yielding identical results.

2 OBTAINING THE EQUATIONS

The line capacitances can be neglected, as they are insignificant compared to the power capacitors connected to the grid. Since the resistances in a power grid only have a damping effect, when no series resonance occurs, they are neglected here, resulting in a conservative approach, providing for a worst case scenario.

At first all the branch current equations, (2), and all the nodal voltage equations, (3), are written for the Laplace domain, giving:

$$s\left[I_1, I_2, \ldots I_n\right]^T = A_2 \cdot \left[V_1, V_2, \ldots V_l\right]^T \quad (2)$$

$$s\left[V_1, V_2, \ldots V_m\right]^T = A_3 \cdot \left[I_1, I_2, \ldots I_n\right]^T \quad (3)$$

where: s is the Laplace operator
I_n is the n'th branch current
V_l is the l'th nodal voltage for the branch currents
V_m is the m'th nodal voltage for the nodal voltages
n is the number of branch currents
l is the number of all nodes
m is the number of nodes with capacitors attached to them
A_2 is the $n \times l$ matrix containing the nodal voltage coefficients
A_3 is the $m \times n$ matrix containing the branch current coefficients

3 REDUCING EQUATION (2)

It is very likely, that there are some nodal voltages that appear in the branch current equations, but not in the nodal voltage equations ($l \neq m$). The reason for this is, that these nodes do not have capacitors attached to them.

It is now desirable, that the nodal voltage vectors of equations (2) and (3) should be the same. For this reason the extra nodal voltage states of the branch current formula, equation (2), need to be eliminated. In order to achieve this, reduction formulas are derived for different cases, by manipulating the voltage and current coefficients of equation (2).

One row of the matrix equation given by (2) is rewritten as a summation as follows:

$$sI_i = \sum_j^l a_{ij} \cdot V_j \quad (4)$$

where: I_i is the i'th branch current
V_j is the j'th nodal voltage
i is the row number of the A_2 matrix
j is the column number of the A_2 matrix
a_{ij} is a coefficient in the A_2 matrix, corresponding to the i'th row and the j'th column

3.1 For a Node to be eliminated, adjacent to Nodes with Capacitors

For linear time invariant systems under steady state conditions, Kirchhoff's current law can now be applied to the changes in currents that flow into or out of the node that is to be eliminated. These changes are added and set equal to 0, yielding:

$$\sum_{i}^{n} d_i \cdot sI_i = 0 \qquad (5)$$

where: d_i is the i'th coefficient to the i'th branch current

d can be either -1 (if the change in the branch current flows out of the node), 0 (if the branch current is not connected to the node at all), or 1 (if the change in the branch current flows into the node).

The corresponding elements are now taken out of equation (4) and substituted into equation (5), to yield:

$$\sum_{i}^{n}\sum_{j}^{l} d_i \cdot a_{ij} \cdot V_j = 0 \qquad (6)$$

By swapping the summations, taking V_j out of the inner summation, taking the k'th term, corresponding to the k'th column, of the A_2 matrix, out of the summations and solving for V_k, the nodal voltage to be eliminated, gives:

$$V_k = -\frac{\sum_{j\backslash k}^{l} V_j \cdot \sum_{i}^{n} d_i \cdot a_{ij}}{\sum_{i}^{n} d_i \cdot a_{ik}} \qquad (7)$$

Substituting V_k back into equation (4) and simplifying, results in:

$$sI_i = \sum_{j\backslash k}^{l} \left(a_{ij} - \frac{a_{ik} \cdot \sum_{i}^{n} d_i \cdot a_{ij}}{\sum_{i}^{n} d_i \cdot a_{ik}}\right) \qquad (8)$$

The matrix coefficients, b_{ij}, of the reduced A_2 matrix are then given by:

$$b_{ij} = a_{ij} - \frac{a_{ik} \cdot \sum_{i}^{n} d_i \cdot a_{ij}}{\sum_{i}^{n} d_i \cdot a_{ik}} \qquad (9)$$

3.2 For two adjacent Nodes to be eliminated, adjacent to Nodes with Capacitors

Once again the changes in the branchcurrents are summed at the two nodes, that are to be eliminated.

$$\sum_{i}^{n} d_i \cdot sI_i = 0 \qquad \sum_{i}^{n} e_i \cdot sI_i = 0 \qquad (10, 11)$$

where: d_i is the i'th coefficient to the i'th branch current

e_i is the i'th coefficient to the i'th branch current

The properties of d as mentioned in section 3.1 are still valid and also apply to e.

The corresponding elements are taken out of equation (4) and substituted into equations (10) and (11), yielding two equations similar to equation (6). The procedure is followed as before. In the first case the k'th term is taken out of the equation and V_k is then solved for. In the second case the f'th term is taken out of the equation and V_f is solved for. k and f are the neighbouring nodes to be eliminated and V_k and V_f are the nodal voltages to be eliminated.

$$V_k = -\frac{\sum_{j\backslash k}^{l} V_j \cdot \sum_{i}^{n} d_i \cdot a_{ij}}{\sum_{i}^{n} d_i \cdot a_{ik}} \qquad (12)$$

$$V_f = -\frac{\sum_{j\backslash f}^{l} V_j \cdot \sum_{i}^{n} e_i \cdot a_{ij}}{\sum_{i}^{n} e_i \cdot a_{if}} \qquad (13)$$

These equations are expanded to show the k'th and f'th terms. Equation (13) is then substituted into equation (12) and *vice versa*. Thereafter V_k and V_f are once again solved for. The resulting equations are then substituted back into equation (4), thereby eliminating the redundant nodes. The new matrix coefficients of the reduced A_2 matrix are then given by:

$$b_{ij} = a_{ij} + a_{ik} \cdot \frac{\frac{\zeta_{k_j} \cdot \zeta_{f_j}}{\psi_k \cdot \psi_f} - \frac{\zeta_{k_j}}{\psi_k}}{1 - \frac{\zeta_{k_j} \cdot \zeta_{f_j}}{\psi_k \cdot \psi_f}} + a_{if} \cdot \frac{\frac{\zeta_{f_j} \cdot \zeta_{k_j}}{\psi_k \cdot \psi_f} - \frac{\zeta_{f_j}}{\psi_f}}{1 - \frac{\zeta_{f_j} \cdot \zeta_{k_j}}{\psi_f \cdot \psi_k}} \qquad (14)$$

where: $\zeta_{k_j} = \sum_i^n d_i \cdot a_{ij}$ $\zeta_{f_j} = \sum_i^n e_i \cdot a_{ij}$ (15, 16)

$$\psi_k = \sum_i^n d_i \cdot a_{ik} \quad \psi_f = \sum_i^n e_i \cdot a_{if} \quad (17, 18)$$

3.3 For three or more adjacent Nodes to be eliminated, adjacent to Nodes with Capacitors

The above method is easily expanded to accommodate three or more nodes that have to be eliminated. This is done as shown in section 3.2, except that there are more neighbouring nodes.

This elimination procedure is repeated until the value of *m*, the number of nodes with capacitors attached to them, is reached. The nodal voltage vectors of equations (3) and (19) are now identical *(l=m)*. Equation (2) in its reduced form is now given by:

$$s\left[I_1, I_2, \ldots I_n\right]^T = A_{2r} \cdot \left[V_1, V_2, \ldots V_m\right]^T \quad (19)$$

where: A_{2r} is the $n \times m$ reduced A_2 matrix, containing the coefficients determined by equations *(9)*, *(14)* and subsequent ones, as determined in section 3.2.

4 DEVELOPING THE STATE SPACE MODEL

For a multi-input, multi-output (MIMO) system, the general corresponding state space equations can now be written by inspection as:

$$sx = A \cdot x + B \cdot u \quad (20)$$

$$y = C \cdot x + D \cdot u \quad (21)$$

$$x = \left[I_1, I_2, \ldots I_n, V_1, V_2, \ldots V_n\right]^T \quad (22)$$

where: x is the $(n+m) \times 1$ state space vector
A is the $(n+m) \times (n+m)$ state coefficient matrix
B is the $(m+n) \times p$ input coefficient matrix
p is the number of current inputs
u is the $p \times 1$ current input vector
y is the q $\times$ *1* nodal voltage output vector
q is the number of nodal output voltages
C is the $q \times (n+m)$ constant matrix relating the states to the output
D is the $q \times p$ direct feed through matrix

These equations are illustrated by way of a block diagram as shown in figure 1.

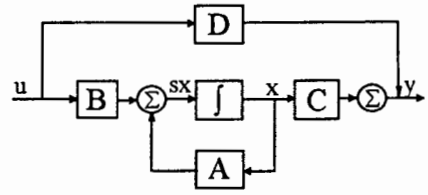

where: Σ is a summer $\int$ is an integrator

Figure 1: Block diagram of the state space model.

Normally the system is strictly proper, and D will be a matrix of zeros. In this case the absolute value of the transfer function will decrease with an increase in frequency. Should the system not be strictly proper, high frequency terms are fed straight to the output, as they are not attenuated as in the former case. This is undesirable, as distortion results.

By incorporating equations (2), (19) and (22) into equations (20) and (21) and writing the equations in the partitioned form, the final general state space model description, or system realisation is obtained:

$$s\left[I_1, \ldots I_n | V_1, \ldots V_m\right]^T = \left[\begin{array}{c|c} 0 & A_{2r} \\ \hline A_3 & 0 \end{array}\right] \cdot \left[I_1, \ldots I_n | V_1, \ldots V_m\right]^T + \left[\begin{array}{c} B_1 \\ \hline B_2 \end{array}\right] \cdot u \quad (23)$$

$$y = \left[C_1 | C_2\right] \cdot \left[I_1, \ldots I_n | V_1, \ldots V_m\right]^T + D \cdot u \quad (24)$$

where: A_{2r} is a submatrix of A
A_3 is a submatrix of A
B_1 is the $n \times 1$ submatrix of B
B_2 is the $m \times 1$ submatrix of B
C_1 is the $1 \times n$ submatrix of C
C_2 is the $1 \times m$ submatrix of C

5 OBTAINING A MINIMAL REALISATION OF THE SYSTEM

The state space model given by equations (23) and (24) is overspecified, particularly so for meshed power systems, as there are extra branch current states. This is undesirable as non-distinct eigenvalues occur, problems are experienced with the matrix conditioning and longer calculation times are required for subsequent calculations. To overcome these problems, a minimal realisation of the system needs to be obtained. Once this has been done,

the size of the A matrix is normally double the number of capacitors that are connected to the power system.

To obtain this minimal realisation of the system, the A, B and C matrices are transferred to controllability and observability staircase forms. The unobservable and uncontrollable states are then removed from the equations, thereby eliminating the redundant states. However, other methods are also available [11]. Once this has been done, in the case of the branch current equations, it is no longer clear what the physical states are. However, the nodal voltage states remain unchanged and the characteristics of the system are preserved.

6 FLOW CHART FOR THE DERIVATION OF THE STATE SPACE MODEL

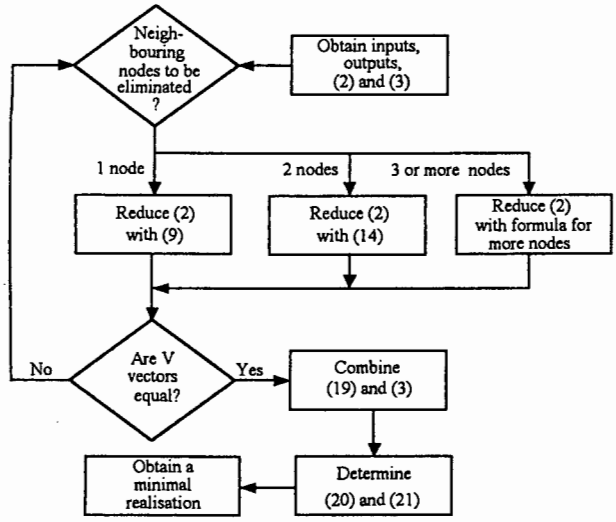

Figure 2: Flow chart for the derivation of the state space model.

The flow chart shown in figure 2, summarises the procedure as outlined above. At first the inputnodes, outputnodes, all the branch current equations (2), and the nodal voltage equations (3), are obtained. The branch current equations are then reduced with the aid of equation (9), until the voltage vectors of the branch current equations and the nodal voltage equations are the same. Equation (2) is thereby reduced to equation (10). Equation (3) and equation (10) are then combined to form a hybrid matrix equation. The state space equations are subsequently determined by taking this hybrid matrix equation and combining it with the B, C and D matrices which are determined from the inputnodes and outputnodes. Finally a minimal realisation of the system is obtained.

7 16 BUS MESHED NETWORK EXAMPLE

A program was written in Matlab™ to implement the above procedure. Two case studies were then done on a 16 bus meshed network [12], which is given in figure 4, in the appendix. The relevant data in per unit is given in tables 5, 6, 7 and 8, also in the appendix.

7.1 Case Study 1

In the first case, for a multi-input, multi-output (MIMO) system, two harmonic current injections are applied and there are two outputnodes, two bus voltages. As there are five capacitors connected to the power grid, the final A matrix should be of dimension 10×10.

Harmonic current injections are applied to buses 8 and 9. The output is also obtained at these nodes, thereby making it a square problem. However, the output could just as well have been from different nodes. The final minimal realisation of the A, B, C and D system matrices, after 18 redundant states have been removed, is given in tables 1, 2, 3 and 4.

Table 1: Coefficients of the A matrix.

0.0000	-51.6935	0.0000	0.0000	10.5190	-16.5941	0.0000	0.0000	1.6902	-1.8693
4.8789	0.0000	-1.7981	0.0701	0.0000	0.0000	0.7340	0.1796	0.0000	0.0000
0.0000	16.1301	0.0000	0.0000	3.1453	10.2979	0.0000	0.0000	-5.9043	-6.0667
0.0000	22.9333	0.0000	0.0000	-28.7995	42.4719	0.0000	0.0000	3.8039	-34.6010
0.0000	0.0000	-1.5330	3.6204	0.0000	0.0000	-3.1559	0.6423	0.0000	0.0000
0.0000	0.0000	-2.2816	-2.4324	0.0000	0.0000	-1.4432	2.4487	0.0000	0.0000
0.0000	0.0000	0.0000	0.0000	18.3715	17.2447	0.0000	0.0000	-24.9836	-16.4459
0.0000	0.0000	0.0000	0.0000	6.5110	-48.6576	0.0000	0.0000	-4.4101	70.7273
0.0000	0.0000	0.0000	0.0000	0.0000	0.0000	4.9702	1.1557	0	0
0.0000	0.0000	0.0000	0.0000	0.0000	0.0000	1.0070	-5.7044	0	0

Table 2: Coefficients of the *B* matrix transposed.

0	0	0	0	0	0	0	0	3.3333
0	0	0	0	0	0	0	3.3333	0

Table 3: Coefficients of the *C* matrix.

0	0	0	0	0	0	0	0	0	1
0	0	0	0	0	0	0	0	1	0

Table 4: Coefficients of the *D* matrix.

0	0
0	0

7.2 Case Study 2

In the second case the above method is compared to the current injection method. For a single-input, single-output (SISO) system, a one per unit harmonic current injection is applied to bus 8 on the network. The voltage at the output is obtained at bus 9. A magnitude *versus* frequency diagram is obtained and shown in figure 3.

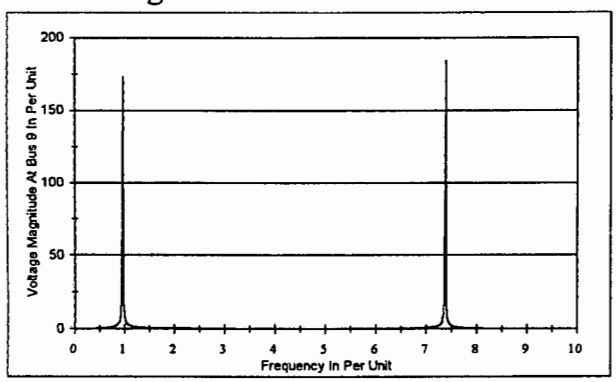

Figure 3: Magnitude *versus* frequency diagram of the voltage at bus 9.

Figure 3 shows that there are resonant peaks at just below the first harmonic and between the seventh and eighth harmonics, with a magnitude of about 175 per unit.

In order to verify the results of the state space model approach, a program was written in Matlab™, to implement the current injection method for the same network. A magnitude *versus* frequency diagram of the voltage at bus 9 was once again obtained. This diagram is identical to the one shown in figure 3. The two methods produce the same results.

8 CONCLUSION

It has been shown in this paper, that a state space model can be developed for the harmonic analysis of large meshed as well as radial power systems. This is done by first obtaining the branch current equations as well as the nodal voltage equations. Thereafter the former set of equations is reduced to get rid of unwanted nodal voltages. The two are then combined to form a hybrid matrix equation. Once the input and output nodes have been determined and combined with the hybrid equation, the state space model can be determined. Finally a minimal realisation of the system is obtained. This opens the field to control theory methods for the harmonic analysis of power systems.

A flow chart of the procedure is given to present a clear picture of the method.

Programs were written in Matlab™, to implement the above method, as well as the current injection method. The procedure was then demonstrated on a 16 bus meshed power system. The state space model method was then compared with the current injection method, yielding identical results.

9 APPENDIX

The 16 bus network is given in figure 4. The relevant input data is given in tables 5, 6, 7 and 8.

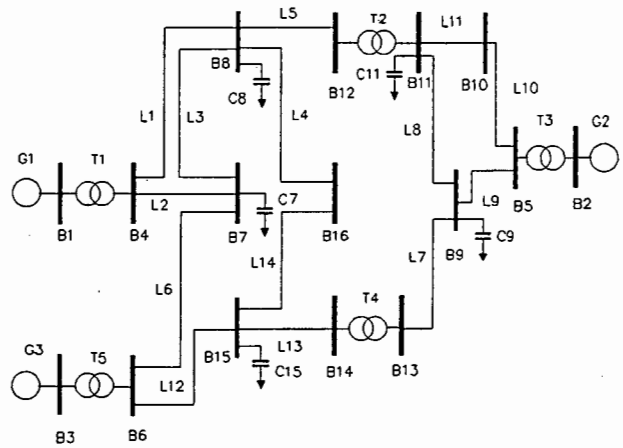

Figure 4: 16 bus meshed network.

Table 5: Generator data in per unit for the 16 bus network.

Generator	Inductance
G1	1.7000
G2	2.0086
G3	2.7618

Table 6: Transformer data in per unit for the 16 bus network.

Transformer	Inductance
T1	0.0625
T2	0.0650
T3	0.0600
T4	0.0570
T5	0.0625

Table 7: Line data in per unit for the 16 bus network.

Line	Inductance
L1	0.007580340
L2	0.015160680
L3	0.026531190
L4	0.022741020
L5	0.025015122
L6	0.023705103
L7	0.035296143
L8	0.043904958
L9	0.025441919
L10	0.058826905
L11	0.058826905
L12	0.016676748
L13	0.022741020
L14	0.007580340

Table 8: Capacitor data in per unit for the 16 bus network.

Capacitor	Capacitance
C7	0.3
C8	0.3
C9	0.3
C11	0.3
C15	0.3

10 REFERENCES

[1] IEEE Tutorial Course, *Power System Harmonics*, Course Text, 84 EH0221-2-PWR, 1984, pp. 1-31.

[2] IEEE Working Group on Non-sinusoidal Situations, "A survey of North American Electric Utility Concerns Regarding Non-sinusoidal Waveforms", IEEE Winter Meeting 1995, Paper 95 WM 036-4 PWRD.

[3] J. Arrillaga, D. Bradley and D. Bodger, *Power System Harmonics*, New York: John Wiley & Sons, 1985, pp. 215-295.

[4] IEEE Task Force on the Effects of Harmonics on Equipment, "Effects of Harmonics on Equipment", *IEEE Transactions on Power Delivery*, Vol. 8, No. 2, April 1993, pp. 672-680.

[5] J. J. Allemong, R. J. Bennon and P. W. Selent, "Multiphase Power Flow Solutions Using EMTP and Newton's Method", *IEEE Transactions on Power Systems*, Vol. 8, No. 4, November 1993, pp 1455-1462.

[6] H. W. Dommel, *Electromagnetic Transients Program Reference Manual (EMTP Theory Book)*, Printed by the University of British Columbia: Vancouver B. C., Canada, August 1986.

[7] W. Xu, J. Marti and H. W. Dommel, "A Multiphase Harmonic Load Flow Solution Technique", *IEEE Transactions on Power Systems*, Vol. 6, No. 1, February 1991.

[8] G. T. Heydt, *Electric Power Quality*, West LaFayette: Stars in a Circle Publications, 1991, pp. 346-353.

[9] D. A. Calahan, *Computer Aided Network Design*, McGraw-Hill, 1968, pp. 203-211.

[10] T. H. Ortmeyer and K. Zehar, "Distribution System Harmonic Design", *IEEE Transactions on Power Delivery*, Vol. 6, No. 1, January 1991, pp. 289-294.

[11] B. W. Dickinson, M. Morf and T. Kailath, "A minimal realisation algorithm for matrix sequences", *IEEE Transactions on Automatic Control*, AC-19, 1974, pp. 31-38.

[12] P. Mangang, S. S. Ahmed and A. Petroianu, "Sequential use of Optimal Power Flow for improving the Static Voltage Stability Margin", *Proceedings of the 1995 Stockholm Power Technology Conference*, pp. 203-208.

Appendix D

Summary and Paper to be submitted to the 1996 IEEE Summer Meeting and Transactions, Denver, United States of America, July 1996

A STATE SPACE MODEL FOR HARMONIC ANALYSIS OF MESHED AND RADIAL POWER SYSTEMS

Helmuth Victor Hitzeroth

e-mail: helmuth@eleceng.uct.ac.za
Department of Electrical Engineering
University of Cape Town
University Private Bag
Rondebosch 7700
South Africa

Alexander Petroianu

e-mail: apetroianu@eleceng.uct.ac.za
Department of Electrical Engineering
University of Cape Town
University Private Bag
Rondebosch 7700
South Africa

SUMMARY:

BACKGROUND AND STATE OF THE ART:

Harmonic distortion in power systems is becoming increasingly more important in power system design and operation. Harmonics are generated by a variety of sources. These inject harmonic currents into the power system, which cause harmonic voltage drops across various network elements. In this way harmonics can propagate throughout the power system, to busses remote from the source, thereby causing various problems in the system.

Various methods are presently in use for the harmonic or frequency analysis of power systems. Time based methods, methods that make use of a loadflow at different discrete frequencies and finally the current injection method are used. The latter is the most popular, as it is non-iterative and makes use of the bus admittance matrix. However, a significant disadvantage of the above procedures is, that none allow the implementation of control theory methods, with the aid of state space models. In view of these requirements a state space model description was recently developed and used for radial networks. However, this method only applies to radial power systems and furthermore, power capacitors have to be at the end of each feeder. In addition to this, once the equations that describe the network are determined, the state coefficient matrix is obtained by calculating the inverse of a matrix and multiplying this with a matrix similar to an incidence matrix. This is very cumbersome and time consuming. A different method is also used to develop state space models, by making use of graph theory and a proper tree. However, this method does not seem to be widely used on large power systems though.

NEW CONTRIBUTION:

In this paper an improved minimal state space model description (minimal system realisation) is developed for the harmonic analysis of power systems. This approach provides for the analysis of radial as well as meshed power systems and furthermore, the inverse of a matrix does not have to be calculated. Once this model has been obtained, the field to control theory methods is laid open. At first the branch current equations and nodal voltage equations for the power system are determined. Reduction formulas, applicable for different cases, are then derived, to reduce the set of branch current equations, thereby eliminating redundant nodal voltages. This reduction is repeated, until the voltage vectors of the branch current equations and the nodal voltage equations are the same. Thereafter the two sets of equations are combined into a general hybrid state space model description (system realisation), resulting in the familiar set of equations. Subsequently a minimal realisation of the system is obtained, by eliminating the unobservable and uncontrollable states. Finally a flow chart of the procedure is depicted and explained.

APPLICATION AND RESULTS:

A program was written in Matlab™ to implement the above procedure. Two case studies were done on a 16 bus meshed network. At first, two harmonic injections are applied to a MIMO system. The A, B, C and D system matrices are obtained for two outputs, two bus voltages on the network. Subsequently, the state space model method is compared with the current injection method. For this purpose a program was also written in Matlab™. For a SISO system, a harmonic injection is applied to a bus on the network and the gain is plotted for the voltage at the output bus. This was then once again obtained, by using the current injection method, and compared to the previous graph. The two methods were found to be identical, as the same graphs were obtained.

CONCLUSION:

A general state space model description for the analysis of harmonics in meshed as well as radial power systems is obtained. The method is easily programmable and opens the field to various control theory methods. A flow chart of the procedure is presented and the procedure is applied to a 16 bus meshed network. The A, B, C and D matrices are obtained for a MIMO system and the procedure is compared to the current injection method. These results were found to be identical, showing that the state space model approach is indeed valid.

A STATE SPACE MODEL FOR HARMONIC ANALYSIS OF MESHED AND RADIAL POWER SYSTEMS

Helmuth Victor Hitzeroth

e-mail: helmuth@eleceng.uct.ac.za
Department of Electrical Engineering
University of Cape Town
University Private Bag
Rondebosch 7700
South Africa

Alexander Petroianu

e-mail: apetroianu@eleceng.uct.ac.za
Department of Electrical Engineering
University of Cape Town
University Private Bag
Rondebosch 7700
South Africa

ABSTRACT:

This paper presents a novel approach to the harmonic analysis and design of meshed as well as radial power systems. From the branch current equations and the nodal voltage equations of the power grid, a state space model is obtained. From the former set of equations, redundant nodal voltages are eliminated and the equations are then developed into a system realisation, which is then reduced to a minimal realisation. A flow chart of the procedure is presented and finally two case studies are done for a 16 bus meshed network. The state space model approach is also compared with the current injection method, giving the same result. The state space model opens the way to the application of a wide variety of control theory methods for the analysis of power system harmonics.

KEYWORDS:

Power systems, quality of supply, harmonic analysis, state space model, system realisation, minimal realisation.

1. INTRODUCTION:

Harmonic distortion in the power system is becoming an increasingly important issue in transmission / distribution system design and operation. Not only are harmonic levels increasing in distribution systems, but consumer loads are also becoming far more sensitive to harmonic distortion [1]. Particularly recently, with the increasing awareness of the quality of supply, as well as the introduction of freemarket elements into the electricity industry, new momentum was given to this field, by a movement towards penalties for injected harmonics (harmonic injection contracts) [2].

Harmonics are generated by a variety of sources, ranging from arc furnaces, drives, transformers to lighting and computers. Most of these sources inject harmonic currents into the power system. These currents in turn result in harmonic voltage drops across various network elements. In this way harmonics can propagate throughout the power system to buses remote from the harmonic source, thereby causing various problems in the system [3]. These are amongst others resonant conditions, telephone interference, capacitor bank failures, overheating of motors, vibrations as well as false tripping of equipment [4].

Various methods are presently in use for the harmonic or frequency analysis of power systems. Time based methods [5, 6], methods that make use of a loadflow (Newton-Raphson, Gauss-Seidel type algorithms) at different discrete frequencies (harmonic load flow) [5, 7] and finally the current injection method are used. The latter is the most popular, as it makes use of the bus admittance matrix, as shown below:

$$[V] = [Y(\varpi)]^{-1} \cdot [I] \qquad (1)$$

where: V is the $r \times 1$ nodal voltage vector
r is the number of nodes
Y is the $r \times r$ bus admittance matrix
ϖ is the frequency in radians per second
I is the $r \times 1$ nodal current injection vector

The bus admittance matrix is recalculated for each frequency under investigation. Of all the methods the current injection method is the fastest, as it is a non-iterative process [8].

However, a significant disadvantage of the above procedures, is that none allow the implementation of control theory methods.

In view of these circumstances a state space model description was recently developed and used for radial networks [9]. However, the method only applies to radial power systems and furthermore, there have to be power

capacitors at the end of each feeder. In addition to this, once the equations that describe the network are determined, the state coefficient matrix is obtained by calculating the inverse of an impedance type matrix and multiplying this with a matrix similar to an incidence matrix. This is very cumbersome and time consuming, especially when the process has to be done everytime the network configuration changes, as is necessary for contingency- and some optimisation studies.

In this paper an improved minimal state space model description (minimal system realisation) is developed for the harmonic analysis of power systems. This approach provides for the analysis of radial as well as meshed networks and furthermore, the inverse of a matrix does not have to be calculated. Once this model is obtained, the field to control theory methods is available.

In [10], a different method is used to develop the state space model, by making use of graph theory and a proper tree. However, this method does not seem to be widely used on large power systems though.

In this paper a new approach is developed. At first the branch current equations and nodal voltage equations for the system are determined. Reduction formulas, applicable to different cases, are then derived, to eliminate unwanted nodal voltages from the set of branch current equations. This is done until the voltage vectors of the branch current equations and the nodal voltage equations are the same. Thereafter the two sets of equations are combined into a general hybrid state space model description (system realisation). A minimal realisation of the system is then obtained, opening the way to control theory methods for the analysis of harmonic current injections in power systems.

The procedure is implemented on a 16 bus meshed network and also compared to the current injection method, yielding identical results.

2. OBTAINING THE EQUATIONS:

The line capacitances can be neglected, as they are insignificant compared to the power capacitors connected to the grid. Since the resistances in a power grid only have a damping effect, when no series resonance occurs, they are neglected here, resulting in a conservative approach, providing for a worst case scenario.

At first all the branch current equations, *(2)*, and all the nodal voltage equations, *(3)*, are written for the Laplace domain, giving:

$$s[I_1, I_2, \ldots I_n]^T = A_2 \cdot [V_1, V_2, \ldots V_l]^T \qquad (2)$$

$$s[V_1, V_2, \ldots V_m]^T = A_3 \cdot [I_1, I_2, \ldots I_n]^T \qquad (3)$$

where: s is the Laplace operator
I_n is the n'th branch current
V_l is the l'th nodal voltage for the branch currents
V_m is the m'th nodal voltage for the nodal voltages
n is the number of branch currents
l is the number of all nodes
m is the number of nodes with capacitors attached to them
A_2 is the $n \times l$ matrix containing the nodal voltage coefficients
A_3 is the $m \times n$ matrix containing the branch current coefficients

3. REDUCING EQUATION *(2)*:

It is very likely, that there are some nodal voltages that appear in the branch current equations, but not in the nodal voltage equations ($l \neq m$). The reason for this is, that these nodes do not have capacitors attached to them.

It is now desirable, that the nodal voltage vectors of equations *(2)* and *(3)* should be the same. For this reason the extra nodal voltage states of the branch current formula, equation *(2)*, need to be eliminated. In order to achieve this, reduction formulas are derived for different cases, by manipulating the voltage and current coefficients of equation *(2)*.

One row of the matrix equation given by *(2)* is rewritten as a summation as follows:

$$sI_i = \sum_j^l a_{ij} \cdot V_j \qquad (4)$$

where: I_i is the i'th branch current
V_j is the j'th nodal voltage
i is the row number of the A_2 matrix
j is the column number of the A_2 matrix
a_{ij} is a coefficient in the A_2 matrix, corresponding to the i'th row and the j'th column

3.1. FOR A NODE TO BE ELIMINATED, ADJACENT TO NODES WITH CAPACITORS:

For linear time invariant systems under steady state conditions, Kirchhoff's current law can now be applied to the changes in currents that flow into or out of the node that is to be eliminated. These changes are then summed and set equal to 0, yielding:

$$\sum_i^n d_i \cdot sI_i = 0 \qquad (5)$$

where: d_i is the i'th coefficient to the i'th branch current

d can be either -1, if the change in the branch current flows out of the node, 0, if the branch current is not connected to the node at all, or 1, if the change in the branch current flows into the node.

The corresponding elements are now taken out of equation *(4)* and substituted in to equation *(5)*, to yield:

$$\sum_{i}^{n}\sum_{j}^{l} d_i \cdot a_{ij} \cdot V_j = 0 \qquad (6)$$

By swapping the summations, taking V_j out of the inner summation, taking the k'th term, corresponding to the k'th column, of the A_2 matrix, out of the summations and solving for V_k, the nodal voltage to be eliminated, gives:

$$V_k = -\frac{\sum_{j\backslash k}^{l} V_j \cdot \sum_{i}^{n} d_i \cdot a_{ij}}{\sum_{i}^{n} d_i \cdot a_{ik}} \qquad (7)$$

Substituting V_k back into equation *(4)* and simplifying, results in:

$$sI_i = \sum_{j\backslash k}^{l} \left(a_{ij} - \frac{a_{ik} \cdot \sum_{i}^{n} d_i \cdot a_{ij}}{\sum_{i}^{n} d_i \cdot a_{ik}}\right) \qquad (8)$$

The matrix coefficients, b_{ij}, of the reduced A_2 matrix are then given by:

$$b_{ij} = a_{ij} - \frac{a_{ik} \cdot \sum_{i}^{n} d_i \cdot a_{ij}}{\sum_{i}^{n} d_i \cdot a_{ik}} \qquad (9)$$

3.2. FOR TWO ADJACENT NODES TO BE ELIMINATED, ADJACENT TO NODES WITH CAPACITORS:

Once again the changes in the branchcurrents are summed at the two nodes, that are to be eliminated.

$$\sum_{i}^{n} d_i \cdot sI_i = 0 \qquad \sum_{i}^{n} e_i \cdot sI_i = 0 \qquad (10), (11)$$

where: d_i is the i'th coefficient to the i'th branch current
e_i is the i'th coefficient to the i'th branch current

The properties of d as mentioned in section 3.1. are still valid and also apply to e.

The corresponding elements are taken out of equation *(4)* and substituted in to equations *(10)* and *(11)*, yielding two equations similar to equation *(6)*. The procedure is followed as before. In the first case the k'th term is taken out of the equation and V_k is then solved for. In the second case the f'th term is taken out of the equation and V_f is solved for. k and f are the neighbouring nodes to be eliminated and V_k and V_f are the nodal voltages to be eliminated.

$$V_k = -\frac{\sum_{j\backslash k}^{l} V_j \cdot \sum_{i}^{n} d_i \cdot a_{ij}}{\sum_{i}^{n} d_i \cdot a_{ik}} \qquad V_f = -\frac{\sum_{j\backslash f}^{l} V_j \cdot \sum_{i}^{n} e_i \cdot a_{ij}}{\sum_{i}^{n} e_i \cdot a_{if}} \qquad (12), (13)$$

These equations are expanded to show the k'th and f'th terms. Equation *(13)* is then substituted into equation *(12)* and vice versa. Thereafter V_k and V_f are once again solved for. The resulting equations are then substituted back into equation *(4)*, thereby eliminating the redundant nodes. The new matrix coefficients of the reduced A_2 matrix are then given by:

$$b_{ij} = a_{ij} + a_{ik} \cdot \frac{\frac{\zeta_{k_j} \cdot \zeta_{f_j}}{\psi_k \cdot \psi_f} - \frac{\zeta_{k_j}}{\psi_k}}{1 - \frac{\zeta_{k_j} \cdot \zeta_{f_j}}{\psi_k \cdot \psi_f}} + a_{if} \cdot \frac{\frac{\zeta_{f_j} \cdot \zeta_{k_j}}{\psi_k \cdot \psi_f} - \frac{\zeta_{f_j}}{\psi_f}}{1 - \frac{\zeta_{f_j} \cdot \zeta_{k_j}}{\psi_f \cdot \psi_k}} \qquad (14)$$

where: $\zeta_{k_j} = \sum_{i}^{n} d_i \cdot a_{ij}$ $\qquad \zeta_{f_j} = \sum_{i}^{n} e_i \cdot a_{ij}$ $\qquad (15), (16)$

$$\psi_k = \sum_{i}^{n} d_i \cdot a_{ik} \qquad \psi_f = \sum_{i}^{n} e_i \cdot a_{if} \qquad (17), (18)$$

3.3. FOR THREE OR MORE ADJACENT NODES TO BE ELIMINATED, ADJACENT TO NODES WITH CAPACITORS:

The above method is easily expanded to accommodate three or more nodes that have to be eliminated. This is done as shown in section 3.2., except that there are more neighbouring nodes.

This elimination procedure is repeated until the value of m, the number of nodes with capacitors attached to them, is reached *(l=m)*. Equation *(2)* in its reduced form is now given by:

$$s\left[I_1, I_2, \ldots I_n\right]^T = A_{2r} \cdot \left[V_1, V_2, \ldots V_m\right]^T \qquad (19)$$

where: A_{2r} is the $n \times m$ reduced A_2 matrix, containing the coefficients determined by equations *(9)*, *(14)* and subsequent ones

It can now be seen that the nodal voltage vectors of equations *(3)* and *(19)* are identical *(l=m)*.

4. DEVELOPING THE STATE SPACE MODEL:

For a multi-input, multi-output (MIMO) system, the general corresponding state space equations can now be written by inspection as:

$$sx = A \cdot x + B \cdot u \qquad (20)$$

$$y = C \cdot x + D \cdot u \qquad (21)$$

$$x = \left[I_1, I_2, \ldots I_n, V_1, V_2, \ldots V_n\right]^T \qquad (22)$$

where: x is the $(n+m) \times 1$ state space vector
A is the $(n+m) \times (n+m)$ state coefficient matrix
B is the $(m+n) \times p$ input coefficient matrix
p is the number of current inputs
u is the $p \times 1$ current input vector
y is the q $\times$ *1* nodal voltage output vector
q is the number of nodal output voltages

C is the $q \times (n+m)$ constant matrix relating the states to the output

D is the $q \times p$ direct feed through matrix

These equations are illustrated by way of a block diagram as shown in figure 1..

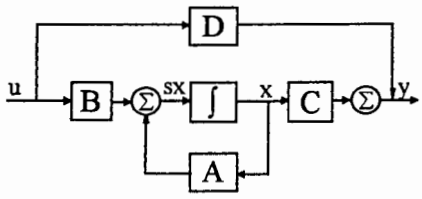

where: Σ denotes a summer

$\int$ denotes an integrator

Figure 1.: Block diagram of the state space model.

Normally the system is strictly proper, and D will be a matrix of zeros. In this case the absolute value of the transfer function will decrease with an increase in frequency. Should the system not be strictly proper, high frequency terms are fed straight to the output, as they are not attenuated as in the former case. This is undesirable, as distortion results.

By incorporating equations *(2)*, *(19)* and *(22)* into equations *(20)* and *(21)* and writing the equations in the partitioned form, the final general state space model description, or system realisation is obtained:

$$s\left[I_1,\ldots I_n \middle| V_1,\ldots V_m\right]^T = \left[\begin{array}{c|c} 0 & A_{2r} \\ \hline A_3 & 0 \end{array}\right] \cdot \left[I_1,\ldots I_n \middle| V_1,\ldots V_m\right]^T + \left[\frac{B_1}{B_2}\right] \cdot u \qquad (23)$$

$$y = \left[C_1 \middle| C_2\right] \cdot \left[I_1,\ldots I_n \middle| V_1,\ldots V_m\right]^T + D \cdot u \qquad (24)$$

where: A_{2r} is a submatrix of A

A_3 is a submatrix of A

B_1 is the $n \times 1$ submatrix of B

B_2 is the $m \times 1$ submatrix of B

C_1 is the $1 \times n$ submatrix of C

C_2 is the $1 \times m$ submatrix of C

5. OBTAINING A MINIMAL REALISATION OF THE SYSTEM:

The state space model given by equations *(23)* and *(24)* is overspecified, particularly so for meshed power systems, as there are extra branch current states. This is undesirable as nondistinct eigenvalues occur, problems are experienced with the matrix conditioning and longer calculation times are required for subsequent calculations. To overcome these problems, a minimal realisation of the system needs to be obtained. Once this has been done, the size of the A matrix is normally double the number of capacitors that are connected to the power system.

To obtain this minimal realisation of the system, the A, B and C matrices are transferred to controllability and observability staircase forms. The unobservable and uncontrollable states are then removed from the equations, thereby eliminating the redundant states. However, other methods are also available [11]. Once this has been done, in the case of the branch current equations, it is no longer clear what the physical states are. However, the nodal voltage states remain unchanged and the characteristics of the system are preserved.

6. FLOW CHART FOR THE DERIVATION OF THE STATE SPACE MODEL:

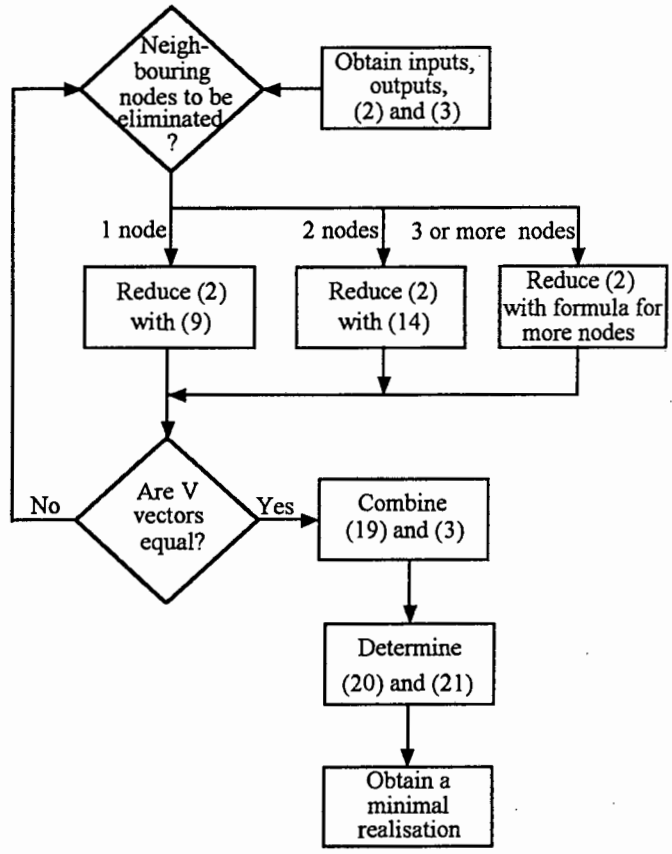

Figure 2.: Flow chart for the derivation of the state space model.

The flow chart shown in figure 2., summarises the procedure as outlined above. At first the inputnodes, outputnodes, all the branch current equations, *(2)*, and the nodal voltage equations, *(3)*, are obtained. The branch current equations are then reduced with the aid of equation *(9)*, until the voltage vectors of the branch current equations and the nodal voltage equations are the same. Equation *(2)* is thereby reduced to equation *(10)*. Equation *(3)* and equation *(10)* are then combined to form a hybrid matrix equation. The state space equations are subsequently determined by taking this hybrid matrix equation and combining it with the B, C and D matrices which are

determined from the inputnodes and outputnodes. Finally a minimal realisation of the system is obtained.

7. 16 BUS MESHED NETWORK EXAMPLE:

A program was written in Matlab™ to implement the above procedure. Two case studies were then done on a 16 bus meshed network [12], which is given in figure 4., in the appendix. The relevant data in per unit is given in tables 5., 6., 7. and 8., also in the appendix.

7.1. CASE STUDY 1:

In the first case, for a multi-input, multi-output (MIMO) system, two harmonic current injections are applied and there are two outputnodes, two bus voltages. As there are five capacitors connected to the power grid, the final A matrix should be of dimension $10 X 10$.

Harmonic current injections are applied to buses 8 and 9. The output is also obtained at these nodes, thereby making it a square problem. However, the output could just as well have been from different nodes. The final minimal realisation of the A, B, C and D system matrices, after 18 redundant states have been removed, is given in tables 1., 2., 3. and 4..

Table 1.: Coefficients of the A matrix.

Column 1	Column 2	Column 3	Column 4	Column 5
0.0000	-51.6935	0.0000	0.0000	10.5190
4.8789	0.0000	-1.7981	0.0701	0.0000
0.0000	16.1301	0.0000	0.0000	3.1453
0.0000	22.9333	0.0000	0.0000	-28.7995
0.0000	0.0000	-1.5330	3.6204	0.0000
0.0000	0.0000	-2.2816	-2.4324	0.0000
0.0000	0.0000	0.0000	0.0000	18.3715
0.0000	0.0000	0.0000	0.0000	6.5110
0.0000	0.0000	0.0000	0.0000	0.0000
0.0000	0.0000	0.0000	0.0000	0.0000

Column 6	Column 7	Column 8	Column 9	Column 10
-16.5941	0.0000	0.0000	1.6902	-1.8693
0.0000	0.7340	0.1796	0.0000	0.0000
10.2979	0.0000	0.0000	-5.9043	-6.0667
42.4719	0.0000	0.0000	3.8039	-34.6010
0.0000	-3.1559	0.6423	0.0000	0.0000
0.0000	-1.4432	2.4487	0.0000	0.0000
17.2447	0.0000	0.0000	-24.9836	-16.4459
-48.6576	0.0000	0.0000	-4.4101	70.7273
0.0000	4.9702	1.1557	0	0
0.0000	1.0070	-5.7044	0	0

Table 2.: Coefficients of the B matrix transposed.

Column 1	0	0	0	0	0	0	0	0	0	3.3333
Column 2	0	0	0	0	0	0	0	0	3.3333	0

Table 3.: Coefficients of the C matrix.

Row 1	0	0	0	0	0	0	0	0	0	1
Row 2	0	0	0	0	0	0	0	0	1	0

Table 4.: Coefficients of the D matrix.

Row 1	0	0
Row 2	0	0

7.2. CASE STUDY 2:

In the second case the above method is compared to the current injection method. For a single-input, single-output (SISO) system, a one per unit harmonic current injection is applied to bus 8 on the network. The voltage at the output is obtained at bus 9. A magnitude versus frequency diagram is obtained and shown in figure 3..

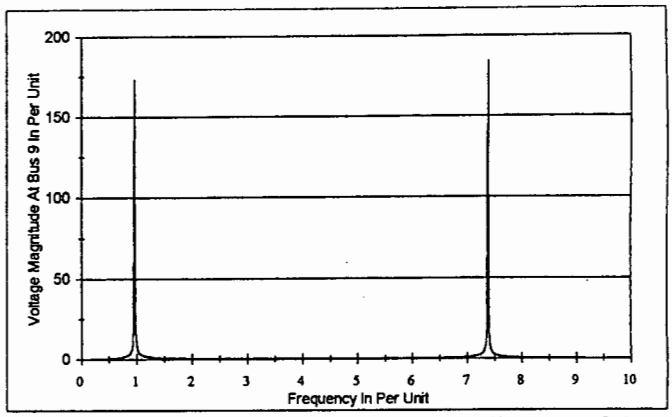

Figure 3.: Magnitude versus frequency diagram of the voltage at bus 9.

Figure 3. shows that there are resonant peaks at just below the first harmonic and between the seventh and eighth harmonics, with a magnitude of about 175 per unit.

In order to verify the results of the state space model approach, a program was written in Matlab™, to implement the current injection method for the same network. A magnitude versus frequency diagram of the voltage at bus 9 was once again obtained. This diagram is identical to the one shown in figure 3. The two methods produce the same results.

8. CONCLUSION:

It has been shown in this paper, that a state space model can be developed for the harmonic analysis of large meshed as well as radial power systems. This is done by first obtaining the branch current equations as well as the nodal voltage equations. Thereafter the former set of equations is reduced to get rid of unwanted nodal voltages. The two are then combined to form a hybrid matrix equation. Once the input and output nodes have been determined and combined with the hybrid equation, the state space model can be determined. Finally a minimal realisation of the system is obtained. This opens the field to control theory methods for the harmonic analysis of power systems.

A flow chart of the procedure is given to present a clear picture of the method.

Programs were written in Matlab™, to implement the above method, as well as the current injection method. The procedure was then demonstrated on a 16 bus meshed power system. The state space model method was then compared with the current injection method, yielding identical results.

9. APPENDIX:

The 16 bus network is given in figure 4.. The relevant input data is given in tables 5., 6., 7. and 8..

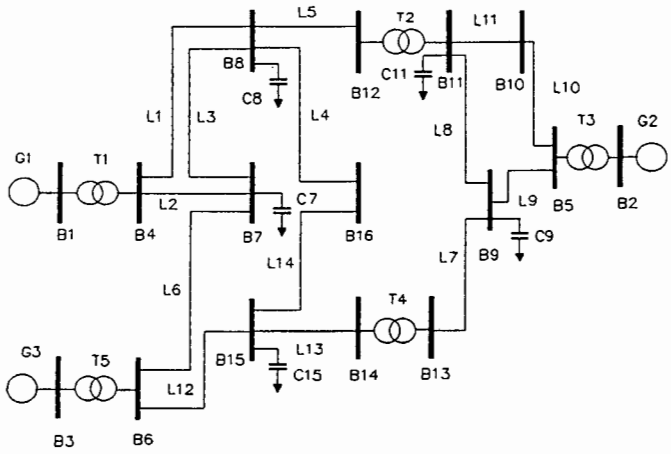

Figure 4.: 16 bus meshed network.

Table 5.: Generator data in per unit for the 16 bus network.

Generator	Inductance in per unit
G1	1.7000
G2	2.0086
G3	2.7618

Table 6.: Transformer data in per unit for the 16 bus network.

Transformer	Inductance in per unit
T1	0.0625
T2	0.0650
T3	0.0600
T4	0.0570
T5	0.0625

Table 7.: Line data in per unit for the 16 bus network.

Line	Inductance in per unit
L1	0.007580340
L2	0.015160680
L3	0.026531190
L4	0.022741020
L5	0.025015122
L6	0.023705103
L7	0.035296143
L8	0.043904958
L9	0.025441919
L10	0.058826905
L11	0.058826905
L12	0.016676748
L13	0.022741020
L14	0.007580340

Table 8.: Capacitor data in per unit for the 16 bus network.

Capacitor	Capacitance in per unit
C7	0.3
C8	0.3
C9	0.3
C11	0.3
C15	0.3

10. REFERENCES:

[1] IEEE Tutorial Course, *Power System Harmonics*, Course Text, 84 EH0221-2-PWR, 1984, pp. 1-31.

[2] IEEE Working Group on Non-sinusoidal Situations, "A survey of North American Electric Utility Concerns Regarding Non-sinusoidal Waveforms", IEEE Wintermeeting 1995, Paper 95 WM 036-4 PWRD.

[3] J. Arrillaga, D. Bradley and D. Bodger, *Power System Harmonics*, New York: John Wiley & Sons, 1985, pp. 215-295.

[4] IEEE Task Force on the Effects of Harmonics on Equipment, "Effects of Harmonics on Equipment", *IEEE Transactions on Power Delivery*, Vol. 8, No. 2, April 1993, pp. 672-680.

[5] J. J. Allemong, R. J. Bennon and P. W. Selent, "Multiphase Power Flow Solutions Using EMTP and Newton's Method", *IEEE Transactions on Power Systems*, Vol. 8, No. 4, November 1993, pp 1455-1462.

[6] H. W. Dommel, *Electromagnetic Transients Program Reference Manual (EMTP Theory Book)*, Printed by the University of British Columbia: Vancouver B. C., Canada, August 1986.

[7] W. Xu, J. Marti and H. W. Dommel, "A Multiphase Harmonic Load Flow Solution Technique", *IEEE Transactions on Power Systems*, Vol. 6, No. 1, February 1991.

[8] G. T. Heydt, *Electric Power Quality*, West LaFayette: Stars in a Circle Publications, 1991, pp. 346-353.

[9] T. H. Ortmeyer and K. Zehar, "Distribution System Harmonic Design", *IEEE Transactions on Power Delivery*, Vol. 6, No. 1, January 1991, pp. 289-294.

[10] D. A. Calahan, *Computer Aided Network Design*, Mc Graw-Hill, 1968, pp. 203-211.

[11] B. W. Dickinson, M. Morf and T. Kailath, "A minimal realisation algorithm for matrix sequences", *IEEE Transactions on Automatic Control*, AC-19, 1974, pp. 31-38.

[12] P. Mangang, S. S. Ahmed and A. Petroianu, "Sequential use of Optimal Power Flow for improving the Static Voltage Stability Margin", *Proceedings of the 1995 Stockholm Power Technology Conference*, pp. 203-208.

11. BIOGRAPHIES:

Helmuth Victor Hitzeroth was born in Freiburg, in Germany. He obtained his BIng. (cum laude) in Electronic Engineering at the University of Pretoria, in the Republic of South Africa. During 1991 he completed his compulsory military training in the South African Navy. Subsequently, 1992-1993, he worked for SASOL, in the petro-chemical industry, as an electrical engineer. Thereafter he went to further his studies in electrical engineering at the University of Cape Town, in the Republic of South Africa. He is presently completing his MSc. (Eng) in Power Systems at the University of Cape Town. His interests are Power Systems, Quality of Supply, Control Systems, and Optimisation Techniques for Power Systems.

Alexander Petroianu was born in Romania. He obtained his Diploma in Electrical Engineering in 1955 from the Power Polytechnical Institute-Ivanowo (Russian Federation) and his Doctoral Degree in Engineering in 1969 from the Polytechnical Institute of Bucharest. From 1956 to 1975 he worked with the National Control Center of the Romanian Power System, concurrently he held academic tasks at the Polytechnical Institute in Bucharest and Cluj. He joined Brown Boveri and ASEA Brown Boveri (Germany)-Network Control Division, being involved in SCADA/EMS software development, from 1976 to 1988. Since 1989 he is professor at the University of Cape Town and a consultant engineer for ESKOM. His research interests include Computer Applications in Power System Analysis, Operation and Control and Power Dispatch Control Center Technology. He is a member of SAIEE, VDE, CIGRE and a Senior Member of IEEE.

Appendix E

Paper presented at the South African Universities Power Engineering Conference, Pretoria, Republic of South Africa, January 1995

OPTIMAL CAPACITOR PLACEMENT ON RADIAL DISTRIBUTION SYSTEMS TO MINIMISE HARMONIC DISTORTION

H V Hitzeroth
University of Cape Town

A Petroianu
University of Cape Town

Abstract
This paper describes a new method to determine the optimal locations of shunt compensation capacitors for radial distribution systems with harmonic distortion. The state space equations for a network are derived and the network poles and zeros are obtained. The solution to the harmonic resonance problem is formulated as a discrete optimisation problem in terms of pole and zero locations. Optimal capacitor locations are determined by means of a neighbourhood search algorithm. The procedure is demonstrated on an 18 bus radial distribution network. Furthermore, it is shown that the algorithm does provide optimal harmonic attenuation.

1. Introduction

Harmonic distortion in the power system is becoming an increasingly important issue in distribution system planning, design and operation. Not only are harmonic levels increasing in distribution systems but consumer loads are also becoming more sensitive to harmonic distortion [1].

Harmonics are generated by a variety of sources, ranging from arc furnaces, drives, transformers to lighting and computers. Most of these sources inject harmonic currents into the power system. These currents in turn result in harmonic voltage drops across various network elements. In this way harmonics can propagate throughout the power system to buses remote from the harmonic source [2].

If these harmonics are ignored, they can cause harmonic problems such as resonant conditions, telephone interference, capacitor bank failures, overheating of motors, vibrations as well as false tripping of equipment [1].

One way of solving the harmonic distortion problem (HDP) is by making use of sensitivity analysis methods [3, 4]. However, this requires much computational effort since all the system eigenvalues and eigenvectors need to be calculated. In addition, the sensitivity methods rely on a step by step method of analysis, whereby the sensitivity factors have to be analysed for each proposed system configuration.

Recently, the HDP was formulated as an optimisation problem [5]. However, the proposed method requires the solution of a three phase load flow at each iteration. This makes the computation cumbersome.

In this paper the HDP is formulated as a discrete optimisation problem. The objective function and its constraint are formulated in terms of distances from poles and zeros to the harmonic frequencies. A simple neighbourhood search is used to obtain the optimal solution. The method is tested on an 18 bus radial distribution network and the results are presented.

2. Mathematical Formulation of the HDP

2.1. State Space Model

In this study two types of radial distribution systems are considered, namely systems that have a capacitor at the end of each feeder and systems ending with a line on each feeder. The second case can be modelled in the same way as the first case, by modelling the line as part of the load.

In order to derive the state space model for such distribution systems, the independent state variables need to be chosen. These are taken as all the capacitor voltages, as well as all the nodal current injections at buses with capacitors attached to them. The loop and node equations can then be determined and expressed in the familiar state space form:

$$sx=Ax+Bu \quad (1)$$

$$y=Cx \quad (2)$$

$$x^t=[I_1\, I_2 \ldots I_n\, V_1\, V_2 \ldots V_n] \quad (3)$$

where: s is the Laplace operator
x is the $2n \times 1$ state space vector containing the n independent line currents as well as the n independent capacitor voltages
A is the $2n \times 2n$ state coefficient matrix
B is the $2n \times m$ input coefficient matrix
m is the number of harmonic current sources
u is the $m \times 1$ input vector of harmonic source currents
y is the $p \times 1$ voltage output vector
p is the number of nodal output voltages
C is the $p \times 2n$ constant matrix relating the states to the output
I_n is the current injected into node n
V_n is the voltage at node n

Once the state space model has been determined, the parallel resonant frequencies (poles) are obtained by calculating the eigenvalues of the matrix A.

It is well known, that the system transfer function is given by the following [6]:

$$Z(s) = \frac{y}{u} = C\frac{\text{adj}(sI - A)}{\det(sI - A)}B \qquad (4)$$

where: $Z(s)$ is the transfer function in the Laplace domain

In the case of a single input, single output system (SISO), where the input is applied at a capacitor node, the system impedance can be rewritten as follows [3]:

$$Z = \frac{1}{C_n}\frac{\det(sI - A_n)}{\det(sI - A)} \qquad (5)$$

where: C_n is the capacitance of the capacitor bank at node n
A_n is obtained by eliminating the row and column of A, corresponding to the output node

Thus the series resonant frequencies (zeros) are determined by calculating the eigenvalues of the matrix A_n, which is of dimension *(2n-1) x (2n-1)*.

2.2. Formulation of the HDP as an Optimisation Problem

In order to minimise the effect of the HDP, specifications can be placed on the poles and zeros of the system. The zeros should be close to harmonic frequencies and poles should be far from harmonic frequencies unless there is a zero between that pole and the harmonic frequency in question. Furthermore, poles and zeros should be close to each other.

These requirements are formulated as an objective function as follows:

$$\underset{CS}{\text{maximise}}\left(J = \min_i\left(\min_j\left|H_i - P_j\right|\right)\right) \qquad (6)$$

subject to the constraint:

$$C = \min_i\left(\min_j\left|H_i - Z_j\right|\right) < \gamma \qquad (7)$$

where: H_i is the ith harmonic frequency injected by the harmonic source
P_j is the jth system pole
Z_j is the jth system zero
CS is the configuration space or feasibility set [4]
J is the value of the objective function
C is the value of the constraint for the zeros
γ is the limit of the constraint

The configuration space is given by all the possible combinations of capacitor locations. A neighbourhood search results when only one capacitor at a time is switched on to another bus, thereby changing two bits in the configuration space.

The formulation of (6) and (7) was chosen, since it is desirable to have the poles far away from a harmonic frequency in order to avoid resonance effects. Furthermore, by choosing $\gamma=1$ it is ensured, that there is a zero in the vicinity of a harmonic frequency. This is desirable, as it mitigates the dominance of the harmonic frequency.

2.3. Method of Solution

Figure 1 shows a flowchart of the procedure that was used to obtain a solution to the optimisation problem as posed in *(6)* and *(7)*.

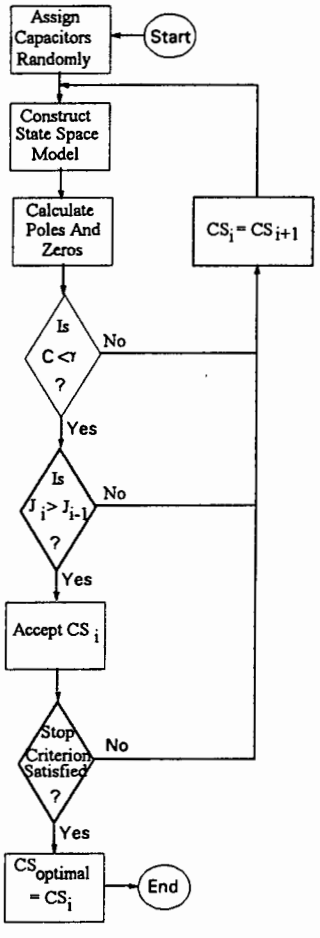

Figure 1: Flowchart of the optimisation algorithm.

After a random initial assignment of capacitors the state space model is generated and the system poles and zeros are calculated. The constraint for the zeros is then checked. If it is not satisfied, a new configuration space element is chosen by changing the position of one capacitor, resulting in a neighbourhood search. If the constraint is satisfied,

the value of the objective function is calculated and compared to the previous one.

If $J_i<J_{(i-1)}$, a new configuration space element is chosen as explained above. The objective function is once again evaluated and compared to the original value. If $J_i<J_{(i-1)}$, then CS_i is taken as the feasible capacitor assignment.

If $J_i>J_{(i-1)}$, the feasible configuration space element is updated. The process repeats itself until the stop criterion is met. The stop criterion states that if two iterations have not produced an improved J value, the algorithm terminates.

3. Case Study

The distribution system shown in Figure 2 was studied [3]. The system consists of three feeders connected to a transformer.

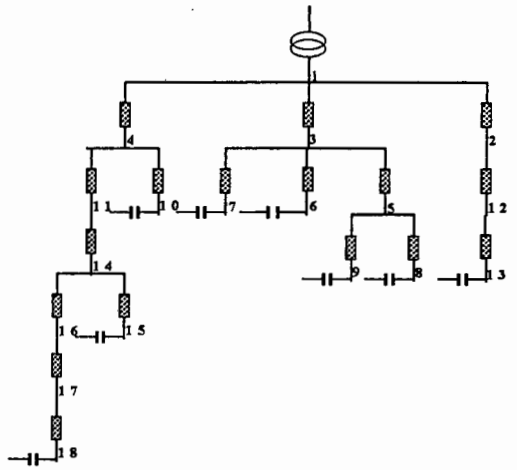

Figure 2: Positive sequence representation of the example network.

The system bases are 1 MVA, 13.2 kV and 377 rad/s. The line data as well as the transformer data is given in Table 1. The capacitor values are all 0.5 per unit. The line resistance and the loads were neglected in the study, as they only have minimal effects on the system poles and zeros thus resulting in a more conservative design. The shunt line capacitance was ignored, as it is negligible compared to the capacitor banks connected to the system.

A 1 MVA 6 pulse converter is connected to bus 18. Only the 5th and 7th harmonic are injected.

The poles and zeros, listed in Table 2, were calculated by using Matlab®. Furthermore, the system response shown in Figure 3, was obtained by using V-Harm®, which was developed by Cooper Industries specifically for harmonic analysis of power systems [8]. The V-Harm® simulation was done by injecting a 0.3 per unit current over all frequencies up to the 10th harmonic.

Line	L	Line	L
Transformer	0.532	5-9	0.127
1-2	0.174	1-4	0.278
2-12	0.246	4-10	0.096
12-13	0.107	4-11	0.171
1-3	1.209	11-14	0.045
3-5	2.968	14-15	0.164
3-6	0.160	14-16	0.251
3-7	2.282	16-17	0.354
5-8	0.055	17-18	0.134

Table 1: Line and transformer data in percent of per unit values.

Poles	Zeros
±j15.3027	±j35.2219
±j9.18034	±j33.3099
±j7.47741	±j30.0978
±j4.11069	0

Table 2: Lower system poles and zeros in per unit before the optimisation.

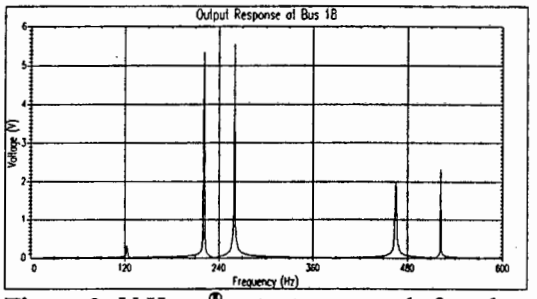

Figure 3: V-Harm® output response before the optimisation.

From Table 2 it can be seen that all the zeros are far from the 5th and 7th harmonic. Furthermore, the poles are very close to these frequencies. This indicates that there will be a harmonic distortion problem in the network if no countermeasures are applied. This is confirmed by Figure 3 which shows that there are very high resonant peaks in the vicinity of the 5th and 7th harmonic. The magnitudes for the 5th and 7th harmonic are 0.0344074 per unit and 0.0127801 per unit respectively.

In order to minimise the voltage distortion that is produced by the converter, four additional capacitors of 0.5 per unit each are at first randomly placed at the network buses. The A matrix and the poles and zeros for the output response at bus 18 are calculated. The optimisation algorithm as described in section 2.3. is applied, resulting in a neighbourhood search over the configuration space.

Figure 4 shows the value of the objective function for each iteration. It can be seen that J increases with each iteration. The optimal capacitor assignment is obtained after five iterations. The maximum value of J is 0.96337 per unit. For this example the optimal response at bus 18 is obtained when additional capacitors are connected to the following buses: 2, 12, 16 and 17.

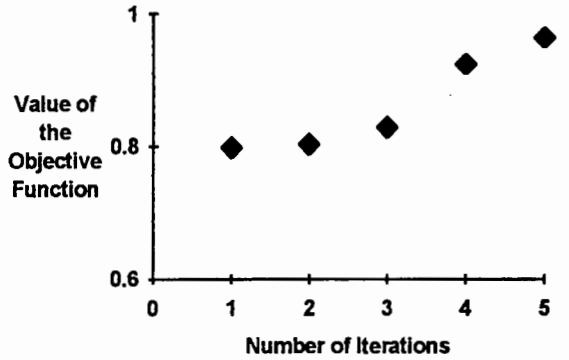

Figure 4: Value of the objective function for each iteration.

The poles and zeros for the optimal configuration are shown in Table 3. The output response is shown in Figure 5.

Poles	Zeroes
±j16.6779	±j16.8447
±j11.2373	±j16.4566
±j7.98704	±j7.99356
±j5.96337	±j4.59542
±j3.96613	0

Table 3: Lower system poles and zeros in per unit with the optimal capacitor assignment.

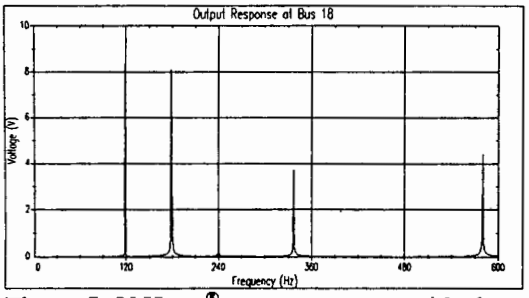

Figure 5: V-Harm® output response with the optimal capacitor assignment.

From Table 3 it can be seen that the nearest poles to the 5th and 7th harmonic are at 5.96337 and 7.98704 respectively. The frequency response of the simulation performed in V-Harm® also confirms the significant improvement over the original system. The magnitudes of the 5th and 7th harmonic are 0.00222821 per unit and 0.00708988 per unit respectively. This is an improvement by a factor of about 15 and 2 respectively.
The new network configuration is therefore better than the original distribution system in terms of harmonic distortion.

4. Conclusion

It has been shown in this paper, that the HDP can be formulated in terms of an optimisation problem. The objective function and its constraint can be expressed in terms of differences between poles, zeros and harmonic current injections. The optimisation algorithm was successfully applied to an 18 bus example network and the validity of the method was confirmed by V-Harm® simulations.

5. References

[1] Arrillaga, J., Bradley, D. and Bodger, D.: *Power System Harmonics*, John Wiley & Sons, New York 1985.

[2] IEEE Tutorial Course: "Power System Harmonics" Course Text, 84 EH0221-2-PWR, 1984.

[3] Ortmeyer, T.H. and Zehar, K.: "Distribution System Harmonic Design" *IEEE Transactions on Power Delivery*, Vol. 6, No. 1, pp. 289-294, January 1991.

[4] Wickramasekara, M.G. and Lubekeman, D.: "Application of Sensitivity Factors for the Harmonic Analysis of Distribution System Reconfiguration and Capacitor Problems" *Proceedings of the Third International Conference on Harmonics in Power Systems"*, pp. 141-148, Purdue, September 1988.

[5] Grady, W.M., Samotyj, M.J. and Noyola, A.H.: "The Application of Network Objective Functions for Actively Minimising the Impact of Voltage Harmonics in Power Systems" *IEEE Transactions on Power Delivery*, Vol. 7, No. 3, pp. 1379-1386, July 1992.

[6] Friedland, B.: *Control System Design*, McGraw-Hill, New York, 1987.

[7] Fletcher, R.: *Practical Methods of Optimisation*, John Wiley & Sons, Chichester, 1987.

[8] V-Harm Users Manual: Power System Harmonics Simulation and Analysis Program, McGraw-Edison, Cooper Industries, May 1988.

6. Acknowledgements

We would like to thank Mr. S.S. Ahmed for his constructive contributions to this project.

Appendix F

Summary of the paper submitted to the South African Universities Power Engineering Conference, Johannesburg, Republic of South Africa, January 1996

OPTIMAL CAPACITOR PLACEMENT ON POWER SYSTEMS TO MINIMISE HARMONIC DISTORTION, BY SIMULATED ANNEALING

Helmuth Victor Hitzeroth

e-mail: helmuth@eleceng.uct.ac.za
Department of Electrical Engineering
University of Cape Town
University Private Bag
Rondebosch 7700
South Africa

Alexander Petroianu

e-mail: apetroianu@eleceng.uct.ac.za
Department of Electrical Engineering
University of Cape Town
University Private Bag
Rondebosch 7700
South Africa

SUMMARY:

Harmonic distortion in the power system is becoming an increasingly important issue in transmission / distribution system design and operation. Not only are harmonic levels increasing in distribution systems but consumer loads are also becoming more sensitive to harmonic distortion. Particularly recently with the increasing awareness of the quality of supply and the introduction of freemarket elements into the electricity industry, new momentum was given to this field, by a movement towards penalties for injected harmonics (harmonic injection contracts).

In this paper a novel approach to the placement problem of shunt power factor correction capacitors on power systems is developed. This would serve to improve the quality of supply on the power grid, by limiting the harmonics.

The solution to the harmonic resonance problem is formulated as a discrete optimisation problem in terms of an objective function subject to constraints. The objective function is used to obtain a measure of the area under the general frequency response curve. By minimising this, the overall performance is improved. The constraints limit the sizes of various categories of harmonics, the harmonic magnitudes. This improves the robustness of the system. In addition to this, the voltage profile is kept within ±5% of one per unit at every bus. In this way, the power factor as well as the quality of supply is improved.

The simulated annealing optimisation algorithm is used for the determination of the optimal capacitor locations. The algorithm ensures, that the procedure will not get stuck in a local minimum, thereby guaranteeing a global optimal solution.

The current injection method is subsequently used to obtain the frequency response of the power system.

The method is designed to mitigate AC side current harmonics produced by converters or other harmonic sources. The procedure is demonstrated on a 16 bus meshed distribution network. Furthermore, it is shown that the algorithm does provide optimal harmonic attenuation.

CASE STUDY:

A 16 bus meshed power system is analysed. Three one per unit current injection sources, swept from 1/60 to 30 per unit frequency, are applied to buses 8, 9, and 15 and the output voltage is obtained at bus 10. At first no voltage support capacitors are applied to the grid, giving an undesirable response, as there are unwanted resonant peaks close to harmonic frequencies.

After the capacitors have been connected to their optimal locations, the frequency response is obtained and shown in figure 1.

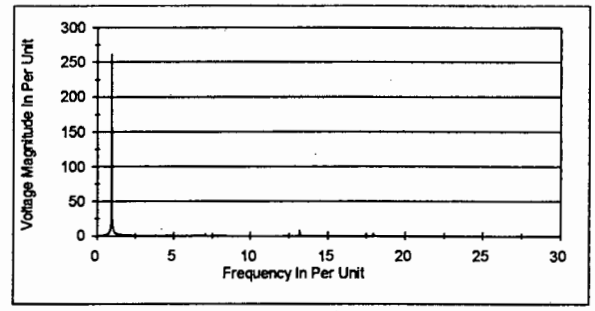

Figure 1: Output response at bus 10, with capacitors connected to their optimal locations.

It can be seen from figure 1, that there is now only one resonant peak, this is located at the first harmonic. This is far more desirable than a few resonant peaks located at the lower order harmonics.

Appendix G

Matlab Programmes written for this Thesis

```
K=7

% Variables used:
% K=
% C=
% l1=
% l4=
% astar2=
% I=
% G,H=
% astar=
% l=
% ap=
% az=
% V,D=
% W,E=
% AP=
% BP=
% AZ=
% BZ=

% line inductances in per unit corrected for per cent per unit
L0Z1  =0.532/100;

L1Z2  =0.174/100;
L2Z12 =0.246/100;
L12Z13=0.107/100;

L1Z3  =1.209/100;
L3Z5  =2.968/100;
L3Z6  =0.160/100;
L3Z7  =2.282/100;   %was 2.282   4.1076
L5Z8  =0.055/100;
L5Z9  =0.127/100;

L1Z4  =0.278/100;
L4Z10 =0.096/100;
L4Z11 =0.171/100;
L11Z14=0.045/100;
L14Z15=0.164/100;
L14Z16=0.251/100;
L16Z17=0.354/100;
L17Z18=0.134/100;

% capacitance in per unit
C2 =0.5;        %0.300;
C6 =0.5;        %0.600;
C7 =0.5;        %1.125;
C8 =0.5;        %0.300;
C9 =0.5;        %0.600;
C10=0.5;        %0.300;
C11=0.5;        %0.300;
C12=0.5;        %0.300;
C13=0.5;        %0.300;
C15=0.5;        %0.300;
C16=0.5;        %0.300;
C17=0.5;        %0.300;
C18=0.5;        %0.300;
```

```
% get an initial K
%K=10;
% get an initial L
%L=[11 11 11 11 11 11 11 8 9 10];
% get an initial distold
%distold=100;
% get an initial dist
%dist=99;
% get an initial C
%C=[0 0 0 0 0 0 0 0 0 0 0 0 0 0 0 0 0 0 0 0 0];

%disp('outside while top');
%pause;

% start optimisation
%while dist<=distold,

%  disp('inside while');
%  pause;

%  if ((K==0) | (K==L(1)) | (K==L(2)) | (K==L(3)) | (K==L(4)) | (K==L(5)) | (K==L(6)) | (K==L(7)) |
(K==L(8)) | (K==L(9)) | (K==L(10))),
%     K=round(rand*10);
%     K=1;

%     K
%     pause;

%  end

%  disp('outside K loop');
%  pause;

%  Cold=C;

% assign configuration spaces
  if K==1,
%       1  2  3  4  5  6  7  8  9 10 11 12 13 14 15 16 17 18
    C=[0  1  0  0  0  1  1  1  1  1  1  1  1  0  1  1  1  1];
    L(1)=1;
  end
  if K==2,
    C=[0  0  0  0  0  1  1  1  1  1  1  1  1  0  1  1  1  1];
    L(2)=2;
  end
  if K==3,
    C=[0  1  0  0  0  1  1  1  1  1  1  0  1  0  1  1  1  1];
    L(3)=3;
  end
  if K==4,
    C=[0  1  0  0  0  1  1  1  1  1  0  1  1  0  1  1  1  1];
    L(4)=4;
  end
  if K==5,
    C=[0  1  0  0  0  1  1  1  1  1  1  1  1  0  1  0  1  1];
    L(5)=5;
  end
```

```
  if K==6,
    C=[0 1 0 0 0 1 1 1 1 1 1 1 1 0 1 1 0 1];
    L(6)=6;
  end
  if K==7,
    C=[0 0 0 0 0 1 1 1 1 1 0 0 1 0 1 0 0 1];
    L(7)=7;
  end

% call the file matrix.m
  matrix;

% call the file calcpz.m
  calcpz;

% calculate distances from harmonics to poles and zeroes
%  for G=1:I,
%     DP5(G)=abs(5-P(G));
%     DP7(G)=abs(7-P(G));
%  end

%  distold=dist;

% get minimum distances
%  if min(DP5)<=min(DP7),
%     dist=min(DP5);
%     M=5;
%     else,
%        dist=min(DP7);
%        M=7;
%     end
%  end

%  Cold=C;
%  distold=dist;

%end

%disp('outside while bottomn');
%pause;

% calculate values for optimal solution
%C=cold;

% call the file matrix.m
%matrix;

% call the file calcpz.m
%calcpz;

% call the file display.m
display;

% call the file store.m
store;

% initialise astar
astar=zeros((2*I),(2*I));
```

```
% put 2nd submatrix for astar in right place
for G=1:I,
  for H=((I+1):(2*I)),
    astar(G,H)=astar2(G,(H-I));
  end
end

% calculate the 3rd submatrix for astar
for G=((I+1):(2*I)),
  for H=1:I,
    astar(G,H)=(-1)*astar2(H,(G-I));
  end
end

% initialise l
l=zeros((2*I),(2*I));

% put 1st submatrix for l in right place
for G=1:I,
  for H=1:I,
    l(G,H)=l1(G,H);
  end
end

% put 4th submatrix for l in right place
for G=((I+1):(2*I)),
  for H=((I+1):(2*I)),
    l(G,H)=l4((G-I),(H-I));
  end
end

ap=(inv(l))*astar;

% calculate az
for G=1:(2*I-1),
  for H=1:(2*I-1),
    az(G,H)=ap(G,H);
  end
end

% to obtain poles
% calculate eigenvalues and eigenvectors of ap
% D has eigenvalues of ap on the diagonal
% V's collumns are the corresponding eigenvectors of ap
[V,D]=eig(ap);

% to obtain zeros
% calculate eigenvalues and eigenvectors of az
% E has eigenvalues of az on the diagonal
% W's collumns are the corresponding eigenvectors of az
[W,E]=eig(az);

% get + poles
DA=imag(D);
J=find(DA>0);
P=DA(J);
```

```
% get + zeroes
EA=imag(E);
J=find(EA>0);
Z=EA(J);

% this file contains all the display routines

% display astar
%disp('now showing astar')
%pause;
%disp('astar collumn 1 - 9, row 1 - 9')
%astar(1:9,1:9)
%pause;
%disp('astar collumn 10 - 18, row 1 - 9')
%astar(1:9,10:18)
%pause;
%disp('astar collumn 19 - 26, row 1 - 9')
%astar(1:9,19:26)
%pause;

%disp('astar collumn 1 - 9, row 10 -18')
%astar(10:18,1:9)
%pause;
%disp('astar collumn 10 - 18, row 10 - 18')
%astar(10:18,10:18)
%pause;
%disp('astar collumn 19 - 26, row 10 - 18')
%astar(10:18,19:26)
%pause;

%disp('astar collumn 1 - 9, row 19 - 26')
%astar(19:26,1:9)
%pause;
%disp('astar collumn 10 - 18, row 19 - 26')
%astar(19:26,10:18)
%pause;
%disp('astar collumn 19 - 26, row 19 - 26')
%astar(19:26,19:26)
%pause;

% display l
%disp('now showing l')
%pause;
%disp('l collumn 1 - 9, row 1 - 9')
%l(1:9,1:9)
%pause;
%disp('l collumn 10 - 18, row 1 - 9')
%l(1:9,10:18)
%pause;
%disp('l collumn 19 - 26, row 1 - 9')
%l(1:9,19:26)
%pause;

%disp('l collumn 1 - 9, row 10 -18')
%l(10:18,1:9)
%pause;
%disp('l collumn 10 - 18, row 10 - 18')
%l(10:18,10:18)
```

```
%pause;
%disp('l collumn 19 - 26, row 10 - 18')
%l(10:18,19:26)
%pause;

%disp('l collumn 1 - 9, row 19 - 26')
%l(19:26,1:9)
%pause;
%disp('l collumn 10 - 18, row 19 - 26')
%l(19:26,10:18)
%pause;
%disp('l collumn 19 - 26, row 19 - 26')
%l(19:26,19:26)
%pause;

% display ap
%disp('now showing ap')
%pause;
%disp('ap collumn 1 - 9, row 1 - 9')
%ap(1:9,1:9)
%pause;
%disp('ap collumn 10 - 18, row 1 - 9')
%ap(1:9,10:18)
%pause;
%disp('ap collumn 19 - 26, row 1 - 9')
%ap(1:9,19:26)
%pause;

%disp('ap collumn 1 - 9, row 10 -18')
%ap(10:18,1:9)
%pause;
%disp('ap collumn 10 - 18, row 10 - 18')
%ap(10:18,10:18)
%pause;
%disp('ap collumn 19 - 26, row 10 - 18')
%ap(10:18,19:26)
%pause;

%disp('ap collumn 1 - 9, row 19 - 26')
%ap(19:26,1:9)
%pause;
%disp('ap collumn 10 - 18, row 19 - 26')
%ap(19:26,10:18)
%pause;
%disp('ap collumn 19 - 26, row 19 - 26')
%ap(19:26,19:26)
%pause;

% display az
%disp('now showing az')
%pause;
%disp('az collumn 1 - 9, row 1 - 9')
%az(1:9,1:9)
%pause;
%disp('az collumn 10 - 18, row 1 - 9')
%az(1:9,10:18)
%pause;
%disp('az collumn 19 - 25, row 1 - 9')
```

```
%az(1:9,19:25)
%pause;

%disp('az collumn 1 - 9, row 10 -18')
%az(10:18,1:9)
%pause;
%disp('az collumn 10 - 18, row 10 - 18')
%az(10:18,10:18)
%pause;
%disp('az collumn 19 - 25, row 10 - 18')
%az(10:18,19:25)
%pause;

%disp('az collumn 1 - 9, row 19 - 25')
%az(19:25,1:9)
%pause;
%disp('az collumn 10 - 18, row 19 - 25')
%az(19:25,10:18)
%pause;
%disp('az collumn 19 - 25, row 19 - 25')
%az(19:25,19:25)
%pause;

% display the eigenvalues
%disp('now showing poles')
%pause;
%diag(D)
%pause;

% display the eigenvalues
%disp('now showing zeros')
%pause;
%diag(E)
%pause;

% this file contains all the if statements for various network configurations

% all capacitors in place
%     1  2  3  4  5  6  7  8  9 10 11 12 13 14 15 16 17 18
if C==[0  1  0  0  0  1  1  1  1  1  1  1  1  0  1  1  1  1],
  disp('in 1st if')
  pause;
  l1=[(L0Z1+L1Z2) L0Z1          L0Z1          L0Z1             L0Z1             L0Z1          L0Z1
0   0    0          0          0    0      % 2
    L0Z1      (L0Z1+L1Z3+L3Z6) (L0Z1+L1Z3)    (L0Z1+L1Z3)      (L0Z1+L1Z3)      L0Z1
L0Z1          0   0    0          0          0    0      % 6
    L0Z1      (L0Z1+L1Z3)    (L0Z1+L1Z3+L3Z7) (L0Z1+L1Z3)      (L0Z1+L1Z3)      L0Z1
L0Z1          0   0    0          0          0    0      % 7
    L0Z1      (L0Z1+L1Z3)    (L0Z1+L1Z3)    (L0Z1+L1Z3+L3Z5+L5Z8) (L0Z1+L1Z3+L3Z5)    L0Z1
L0Z1          0   0    0          0          0    0      % 8
    L0Z1      (L0Z1+L1Z3)    (L0Z1+L1Z3)    (L0Z1+L1Z3+L3Z5)    (L0Z1+L1Z3+L3Z5+L5Z9) L0Z1
L0Z1          0   0    0          0          0    0      % 9
    L0Z1      L0Z1          L0Z1          L0Z1             L0Z1             (L0Z1+L1Z4+L4Z10)
(L0Z1+L1Z4)    0   0    0          0          0    0      %10
    L0Z1      L0Z1          L0Z1          L0Z1             L0Z1             (L0Z1+L1Z4)
(L0Z1+L1Z4+L4Z11) 0   0    0          0          0    0      %11
    0         0          0          0          0          0          0          L2Z12 0    0
0          0    0      %12
```

```
    0       0          0          0             0             0          0          0   L12Z13 0
0          0    0       %13
    0       0          0          0             0             0          0          0   0
(L11Z14+L14Z15) L11Z14        0    0       %15
    0       0          0          0             0             0          0          0   0    L11Z14
(L11Z14+L14Z16) 0     0       %16
    0       0          0          0             0             0          0          0   0    0
0          L16Z17 0       %17
    0       0          0          0             0             0          0          0   0    0
0          0    L17Z18]; %18

%    2       6          7          8             9             10         11         12   13   15
16         17     18

  l4=[(C2) 0    0    0    0    0    0    0    0    0    0    0    0     % 2
     0   (C6) 0    0    0    0    0    0    0    0    0    0    0     % 6
     0    0   (C7) 0    0    0    0    0    0    0    0    0    0     % 7
     0    0    0   (C8) 0    0    0    0    0    0    0    0    0     % 8
     0    0    0    0   (C9) 0    0    0    0    0    0    0    0     % 9
     0    0    0    0    0   (C10) 0    0    0    0    0    0    0     %10
     0    0    0    0    0    0   (C11) 0    0    0    0    0    0     %11
     0    0    0    0    0    0    0   (C12) 0    0    0    0    0     %12
     0    0    0    0    0    0    0    0   (C13) 0    0    0    0     %13
     0    0    0    0    0    0    0    0    0   (C15) 0    0    0     %15
     0    0    0    0    0    0    0    0    0    0   (C16) 0    0     %16
     0    0    0    0    0    0    0    0    0    0    0   (C17) 0     %17
     0    0    0    0    0    0    0    0    0    0    0    0   (C18)]; %18

%    2    6    7    8    9    10   11   12   13   15   16   17   18

% astar 2nd submatrix
  astar2=[-1  0  0  0  0  0  0  0  0  0  0  0  0  % 2
        0 -1  0  0  0  0  0  0  0  0  0  0  0  % 6
        0  0 -1  0  0  0  0  0  0  0  0  0  0  % 7
        0  0  0 -1  0  0  0  0  0  0  0  0  0  % 8
        0  0  0  0 -1  0  0  0  0  0  0  0  0  % 9
        0  0  0  0  0 -1  0  0  0  0  0  0  0  %10
        0  0  0  0  0  0 -1  0  0  0  0  0  0  %11
        1  0  0  0  0  0  0 -1  0  0  0  0  0  %12
        0  0  0  0  0  0  0  1 -1  0  0  0  0  %13
        0  0  0  0  0  0  0  1  0  0 -1  0  0  %15
        0  0  0  0  0  0  0  1  0  0  0 -1  0  %16
        0  0  0  0  0  0  0  0  0  0  0  1 -1  0  %17
        0  0  0  0  0  0  0  0  0  0  0  0  1 -1]; %18

%         2  6  7  8  9 10 11 12 13 15 16 17 18

  I=13;
end

% capacitor at node 2 is out
%     1  2  3  4  5  6  7  8  9 10 11 12 13 14 15 16 17 18
if C==[0  0  0  0  0  1  1  1  1  1  1  1  1  0  1  1  1  1],
  disp('in 2nd if')
  pause;
  l1=[(L0Z1+L1Z3+L3Z6) (L0Z1+L1Z3)     (L0Z1+L1Z3)        (L0Z1+L1Z3)        L0Z1          L0Z1
L0Z1           0     0           0           0     0       % 6
```

```
    (L0Z1+L1Z3)    (L0Z1+L1Z3+L3Z7) (L0Z1+L1Z3)       (L0Z1+L1Z3)       L0Z1          L0Z1
L0Z1          0    0          0          0    0      %7
    (L0Z1+L1Z3)    (L0Z1+L1Z3)    (L0Z1+L1Z3+L3Z5+L5Z8) (L0Z1+L1Z3+L3Z5)    L0Z1
L0Z1          L0Z1          0    0          0          0    0      %8
    (L0Z1+L1Z3)    (L0Z1+L1Z3)    (L0Z1+L1Z3+L3Z5)    (L0Z1+L1Z3+L3Z5+L5Z8) L0Z1
L0Z1          L0Z1          0    0          0          0    0      %9
    L0Z1          L0Z1          L0Z1          L0Z1          (L0Z1+L1Z4+L4Z10) (L0Z1+L1Z4)
L0Z1          0    0          0          0    0      %10
    L0Z1          L0Z1          L0Z1          L0Z1          (L0Z1+L1Z4)    (L0Z1+L1Z4+L4Z11)
L0Z1          0    0          0          0    0      %11
    L0Z1          L0Z1          L0Z1          L0Z1          L0Z1          L0Z1
(L0Z1+L1Z2+L2Z12) 0    0          0          0    0      %12
    0          0          0          0          0          0          0          L12Z13 0
0          0    0      %13
    0          0          0          0          0          0          0          0
(L11Z14+L14Z15) L11Z14       0    0      %15
    0          0          0          0          0          0          0          0    L11Z14
(L11Z14+L14Z16) 0    0      %16
    0          0          0          0          0          0          0          0    0
0          L16Z17 0      %17
    0          0          0          0          0          0          0          0    0
0          0    L17Z18]; %18

%    6          7          8          9          10          11          12          13    15
16          17    18

  14=[(C6) 0    0    0    0    0    0    0    0    0    0    0      %6
    0    (C7) 0    0    0    0    0    0    0    0    0    0      %7
    0    0    (C8) 0    0    0    0    0    0    0    0    0      %8
    0    0    0    (C9) 0    0    0    0    0    0    0    0      %9
    0    0    0    0    (C10) 0    0    0    0    0    0    0      %10
    0    0    0    0    0    (C11) 0    0    0    0    0    0      %11
    0    0    0    0    0    0    (C12) 0    0    0    0    0      %12
    0    0    0    0    0    0    0    (C13) 0    0    0    0      %13
    0    0    0    0    0    0    0    0    (C15) 0    0    0      %15
    0    0    0    0    0    0    0    0    0    (C16) 0    0      %16
    0    0    0    0    0    0    0    0    0    0    (C17) 0      %17
    0    0    0    0    0    0    0    0    0    0    0    (C18)]; %18

%    6    7    8    9    10    11    12    13    15    16    17    18

% astar 2nd submatrix
  astar2=[-1  0  0  0  0  0  0  0  0  0  0  0  0  %6
        0 -1  0  0  0  0  0  0  0  0  0  0  0  %7
        0  0 -1  0  0  0  0  0  0  0  0  0  0  %8
        0  0  0 -1  0  0  0  0  0  0  0  0  0  %9
        0  0  0  0 -1  0  0  0  0  0  0  0  0  %10
        0  0  0  0  0 -1  0  0  0  0  0  0  0  %11
        0  0  0  0  0  0 -1  0  0  0  0  0  0  %12
        0  0  0  0  0  0  1 -1  0  0  0  0  0  %13
        0  0  0  0  0  1  0  0 -1  0  0  0  0  %15
        0  0  0  0  0  1  0  0  0 -1  0  0  0  %16
        0  0  0  0  0  0  0  0  0  1 -1  0  0  %17
        0  0  0  0  0  0  0  0  0  0  1 -1 -1]; %18

%        6  7  8  9 10 11 12 13 15 16 17 18

  I=12;
```

```
end

% capacitor at node 12 is out
%     1 2 3 4 5 6 7 8 9 10 11 12 13 14 15 16 17 18
if C==[0 1 0 0 0 1 1 1 1 1 1 1 0 1 0 1 1 1 1],
  disp('in 3rd if')
  pause;
  l1=[(L0Z1+L1Z2) L0Z1          L0Z1          L0Z1          L0Z1          L0Z1          L0Z1
0          0          0          0    0      % 2
    L0Z1      (L0Z1+L1Z3+L3Z6) (L0Z1+L1Z3)    (L0Z1+L1Z3)       (L0Z1+L1Z3)       L0Z1
L0Z1          0          0          0          0    0      % 6
    L0Z1      (L0Z1+L1Z3)    (L0Z1+L1Z3+L3Z7) (L0Z1+L1Z3)       (L0Z1+L1Z3)       L0Z1
L0Z1          0          0          0          0    0      % 7
    L0Z1      (L0Z1+L1Z3)    (L0Z1+L1Z3)    (L0Z1+L1Z3+L3Z5+L5Z8) (L0Z1+L1Z3+L3Z5)    L0Z1
L0Z1          0          0          0          0    0      % 8
    L0Z1      (L0Z1+L1Z3)    (L0Z1+L1Z3)    (L0Z1+L1Z3+L3Z5)    (L0Z1+L1Z3+L3Z5+L5Z9) L0Z1
L0Z1          0          0          0          0    0      % 9
    L0Z1      L0Z1          L0Z1          L0Z1          L0Z1          (L0Z1+L1Z4+L4Z10)
(L0Z1+L1Z4)    0          0          0          0    0      %10
    L0Z1      L0Z1          L0Z1          L0Z1          L0Z1          (L0Z1+L1Z4)
(L0Z1+L1Z4+L4Z11) 0          0          0          0    0      %11
    0         0          0          0          0          0          0          (L2Z12+L12Z13) 0
0          0    0      %13
    0         0          0          0          0          0          0          0
(L11Z14+L14Z15) L11Z14       0    0      %15
    0         0          0          0          0          0          0          0          L11Z14
(L11Z14+L14Z16) 0    0      %16
    0         0          0          0          0          0          0          0          0
0          L16Z17 0      %17
    0         0          0          0          0          0          0          0          0
0          0    L17Z18]; %18

%    2         6          7          8          9          10          11          13          15
16          17     18

  l4=[(C2) 0    0    0    0    0    0    0    0    0    0    0      % 2
     0   (C6) 0    0    0    0    0    0    0    0    0    0      % 6
     0    0   (C7) 0    0    0    0    0    0    0    0    0      % 7
     0    0    0   (C8) 0    0    0    0    0    0    0    0      % 8
     0    0    0    0   (C9) 0    0    0    0    0    0    0      % 9
     0    0    0    0    0   (C10) 0    0    0    0    0    0      %10
     0    0    0    0    0    0   (C11) 0    0    0    0    0      %11
     0    0    0    0    0    0    0   (C13) 0    0    0    0      %13
     0    0    0    0    0    0    0    0   (C15) 0    0    0      %15
     0    0    0    0    0    0    0    0    0   (C16) 0    0      %16
     0    0    0    0    0    0    0    0    0    0   (C17) 0      %17
     0    0    0    0    0    0    0    0    0    0    0   (C18)]; %18

%    2    6    7    8    9    10    11    13    15    16    17    18

% astar 2nd submatrix
  astar2=[-1 0 0 0 0 0 0 0 0 0 0 0  % 2
        0 -1 0 0 0 0 0 0 0 0 0 0  % 6
        0 0 -1 0 0 0 0 0 0 0 0 0  % 7
        0 0 0 -1 0 0 0 0 0 0 0 0  % 8
        0 0 0 0 -1 0 0 0 0 0 0 0  % 9
        0 0 0 0 0 -1 0 0 0 0 0 0  %10
        0 0 0 0 0 0 -1 0 0 0 0 0  %11
```

```
        1 0 0 0 0 0 0 -1 0 0 0 0  %13
        0 0 0 0 0 0 1 0 -1 0 0 0  %15
        0 0 0 0 0 0 1 0 0 -1 0 0  %16
        0 0 0 0 0 0 0 0 0 1 -1 0  %17
        0 0 0 0 0 0 0 0 0 0 1 -1]; %18

%       2 6 7 8 9 10 11 13 15 16 17 18

  I=12;
end

% capacitor at node 11 is out
%    1 2 3 4 5 6 7 8 9 10 11 12 13 14 15 16 17 18
if C==[0 1 0 0 0 1 1 1 1 1 0 1 1 0 1 1 1 1],
  disp('in 4th if')
  pause;
  l1=[(L0Z1+L1Z2) L0Z1          L0Z1          L0Z1          L0Z1          L0Z1          0   0
L0Z1                  L0Z1                  0   0      % 2
    L0Z1      (L0Z1+L1Z3+L3Z6) (L0Z1+L1Z3)    (L0Z1+L1Z3)       (L0Z1+L1Z3)       L0Z1
0   0   L0Z1                  L0Z1                  0   0      % 6
    L0Z1      (L0Z1+L1Z3)     (L0Z1+L1Z3+L3Z7) (L0Z1+L1Z3)       (L0Z1+L1Z3)       L0Z1
0   0   L0Z1                  L0Z1                  0   0      % 7
    L0Z1      (L0Z1+L1Z3)     (L0Z1+L1Z3)     (L0Z1+L1Z3+L3Z5+L5Z8) (L0Z1+L1Z3+L3Z5)    L0Z1
0   0   L0Z1                  L0Z1                  0   0      % 8
    L0Z1      (L0Z1+L1Z3)     (L0Z1+L1Z3)     (L0Z1+L1Z3+L3Z5)    (L0Z1+L1Z3+L3Z5+L5Z9) L0Z1
0   0   L0Z1                  L0Z1                  0   0      % 9
    L0Z1      L0Z1          L0Z1          L0Z1          L0Z1          (L0Z1+L1Z4+L4Z10) 0   0
(L0Z1+L1Z4)           (L0Z1+L1Z4)           0   0      %10
    0       0         0         0         0         0         L2Z12 0   0
0                 0   0      %12
    0       0         0         0         0         0         0   L12Z13 0
0                 0   0      %13
    L0Z1      L0Z1          L0Z1          L0Z1          L0Z1          (L0Z1+L1Z4)     0   0
(L0Z1+L1Z4+L4Z11+L11Z14+L14Z15) (L0Z1+L1Z4+L4Z11+L11Z14)     0   0      %15
    L0Z1      L0Z1          L0Z1          L0Z1          L0Z1          (L0Z1+L1Z4)     0   0
(L0Z1+L1Z4+L4Z11+L11Z14)      (L0Z1+L1Z4+L4Z11+L11Z14+L14Z16) 0   0      %16
    0       0         0         0         0         0         0   0   0                 0
L16Z17 0      %17
    0       0         0         0         0         0         0   0   0                 0
0    L17Z18]; %18

%   2       6         7         8         9         10        12  13  15
16                17  18

  l4=[(C2) 0   0   0   0   0   0   0   0   0   0   0     % 2
    0   (C6) 0   0   0   0   0   0   0   0   0   0     % 6
    0   0   (C7) 0   0   0   0   0   0   0   0   0     % 7
    0   0   0   (C8) 0   0   0   0   0   0   0   0     % 8
    0   0   0   0   (C9) 0   0   0   0   0   0   0     % 9
    0   0   0   0   0   (C10) 0   0   0   0   0   0     %10
    0   0   0   0   0   0   (C12) 0   0   0   0   0     %12
    0   0   0   0   0   0   0   (C13) 0   0   0   0     %13
    0   0   0   0   0   0   0   0   (C15) 0   0   0     %15
    0   0   0   0   0   0   0   0   0   (C16) 0   0     %16
    0   0   0   0   0   0   0   0   0   0   (C17) 0     %17
    0   0   0   0   0   0   0   0   0   0   0   (C18)]; %18

%   2   6   7   8   9   10  12  13  15  16  17  18
```

```
% astar 2nd submatrix
  astar2=[-1  0  0  0  0  0  0  0  0  0  0  0  % 2
          0 -1  0  0  0  0  0  0  0  0  0  0  % 6
          0  0 -1  0  0  0  0  0  0  0  0  0  % 7
          0  0  0 -1  0  0  0  0  0  0  0  0  % 8
          0  0  0  0 -1  0  0  0  0  0  0  0  % 9
          0  0  0  0  0 -1  0  0  0  0  0  0  %10
          1  0  0  0  0  0 -1  0  0  0  0  0  %12
          0  0  0  0  0  0  1 -1  0  0  0  0  %13
          0  0  0  0  0  0  0  0 -1  0  0  0  %15
          0  0  0  0  0  0  0  0  0 -1  0  0  %16
          0  0  0  0  0  0  0  0  0  1 -1  0  %17
          0  0  0  0  0  0  0  0  0  0  1 -1]; %18

%         2  6  7  8  9 10 12 13 15 16 17 18

  I=12;
end

% capacitor at node 16 is out
%     1  2  3  4  5  6  7  8  9 10 11 12 13 14 15 16 17 18
if C==[0  1  0  0  0  1  1  1  1  1  1  1  1  0  1  0  1  1],
  disp('in 5th if')
  pause;
  l1=[(L0Z1+L1Z2) L0Z1          L0Z1          L0Z1             L0Z1             L0Z1          L0Z1
0    0    0          0             0       % 2
    L0Z1      (L0Z1+L1Z3+L3Z6) (L0Z1+L1Z3)    (L0Z1+L1Z3)      (L0Z1+L1Z3)      L0Z1
L0Z1          0    0    0          0             0       % 6
    L0Z1      (L0Z1+L1Z3)     (L0Z1+L1Z3+L3Z7) (L0Z1+L1Z3)      (L0Z1+L1Z3)      L0Z1
L0Z1          0    0    0          0             0       % 7
    L0Z1      (L0Z1+L1Z3)     (L0Z1+L1Z3)     (L0Z1+L1Z3+L3Z5+L5Z8) (L0Z1+L1Z3+L3Z5)    L0Z1
L0Z1          0    0    0          0             0       % 8
    L0Z1      (L0Z1+L1Z3)     (L0Z1+L1Z3)     (L0Z1+L1Z3+L3Z5)    (L0Z1+L1Z3+L3Z5+L5Z9) L0Z1
L0Z1          0    0    0          0             0       % 9
    L0Z1      L0Z1          L0Z1          L0Z1             L0Z1             (L0Z1+L1Z4+L4Z10)
(L0Z1+L1Z4)     0    0    0          0             0       %10
    L0Z1      L0Z1          L0Z1          L0Z1             L0Z1             (L0Z1+L1Z4)
(L0Z1+L1Z4+L4Z11) 0    0    0          0             0       %11
    0         0             0             0                0                0             0             L2Z12 0     0
0               0       %12
    0         0             0             0                0                0             0             0    L12Z13 0
0               0       %13
    0         0             0             0                0                0             0             0    0
(L11Z14+L14Z15) L11Z14          0       %15
    0         0             0             0                0                0             0             0    0    L11Z14
(L11Z14+L14Z16+L16Z17) 0        %17
    0         0             0             0                0                0             0             0    0    0
0               L17Z18]; %18

%    2         6             7             8                9                10            11            12   13   15
17              18

  l4=[(C2) 0    0    0    0    0    0    0    0    0    0    0      % 2
     0   (C6) 0    0    0    0    0    0    0    0    0    0      % 6
     0    0   (C7) 0    0    0    0    0    0    0    0    0      % 7
     0    0    0   (C8) 0    0    0    0    0    0    0    0      % 8
     0    0    0    0   (C9) 0    0    0    0    0    0    0      % 9
```

```
    0   0   0   0   0   (C10) 0   0   0   0   0   0     %10
    0   0   0   0   0   0   (C11) 0   0   0   0   0     %11
    0   0   0   0   0   0   0   (C12) 0   0   0   0     %12
    0   0   0   0   0   0   0   0   (C13) 0   0   0     %13
    0   0   0   0   0   0   0   0   0   (C15) 0   0     %15
    0   0   0   0   0   0   0   0   0   0   (C17) 0     %17
    0   0   0   0   0   0   0   0   0   0   0   (C18)]; %18

%   2   6   7   8   9   10  11  12  13  15  17  18

% astar 2nd submatrix
  astar2=[-1  0 0 0 0 0 0 0 0 0 0 0  % 2
        0 -1  0 0 0 0 0 0 0 0 0 0  % 6
        0 0 -1  0 0 0 0 0 0 0 0 0  % 7
        0 0 0 -1  0 0 0 0 0 0 0 0  % 8
        0 0 0 0 -1  0 0 0 0 0 0 0  % 9
        0 0 0 0 0 -1  0 0 0 0 0 0  %10
        0 0 0 0 0 0 -1  0 0 0 0 0  %11
        1 0 0 0 0 0 0 -1  0 0 0 0  %12
        0 0 0 0 0 0 0 1 -1  0 0 0  %13
        0 0 0 0 0 0 1 0 0 -1  0 0  %15
        0 0 0 0 0 0 1 0 0 0 -1  0  %17
        0 0 0 0 0 0 0 0 0 0 1 -1]; %18

%       2 6 7 8 9 10 11 12 13 15 17 18

  I=12;
end

% capacitor at node 17 is out
%    1 2 3 4 5 6 7 8 9 10 11 12 13 14 15 16 17 18
if C==[0  1 0 0 0 1 1 1 1 1 1 1 1 0 1 1 0  1],
  disp('in 6th if')
  pause;
  l1=[(L0Z1+L1Z2) L0Z1          L0Z1          L0Z1            L0Z1            L0Z1          L0Z1
0   0   0           0           0           % 2
    L0Z1      (L0Z1+L1Z3+L3Z6) (L0Z1+L1Z3)    (L0Z1+L1Z3)       (L0Z1+L1Z3)       L0Z1
L0Z1          0   0   0           0           0           % 6
    L0Z1      (L0Z1+L1Z3)     (L0Z1+L1Z3+L3Z7) (L0Z1+L1Z3)       (L0Z1+L1Z3)       L0Z1
L0Z1          0   0   0           0           0           % 7
    L0Z1      (L0Z1+L1Z3)     (L0Z1+L1Z3)     (L0Z1+L1Z3+L3Z5+L5Z8) (L0Z1+L1Z3+L3Z5)     L0Z1
L0Z1          0   0   0           0           0           % 8
    L0Z1      (L0Z1+L1Z3)     (L0Z1+L1Z3)     (L0Z1+L1Z3+L3Z5)    (L0Z1+L1Z3+L3Z5+L5Z9) L0Z1
L0Z1          0   0   0           0           0           % 9
    L0Z1      L0Z1          L0Z1          L0Z1            L0Z1            (L0Z1+L1Z4+L4Z10)
(L0Z1+L1Z4)     0   0   0           0           0           %10
    L0Z1      L0Z1          L0Z1          L0Z1            L0Z1            (L0Z1+L1Z4)
(L0Z1+L1Z4+L4Z11) 0   0   0           0           0           %11
    0         0           0           0           0           0           0           L2Z12 0     0
0           0           %12
    0         0           0           0           0           0           0           0   L12Z13 0
0           0           %13
    0         0           0           0           0           0           0           0   0
(L11Z14+L14Z15) L11Z14        0           %15
    0         0           0           0           0           0           0           0   0   L11Z14
(L11Z14+L14Z16) 0           %16
    0         0           0           0           0           0           0           0   0   0
0           L16Z17+L17Z18]; %18
```

```
%    2        6          7          8              9              10          11          12   13    15
16          18

  l4=[(C2) 0    0    0    0    0    0    0    0    0    0    0      % 2
     0    (C6) 0    0    0    0    0    0    0    0    0    0      % 6
     0    0    (C7) 0    0    0    0    0    0    0    0    0      % 7
     0    0    0    (C8) 0    0    0    0    0    0    0    0      % 8
     0    0    0    0    (C9) 0    0    0    0    0    0    0      % 9
     0    0    0    0    0    (C10) 0    0    0    0    0    0      %10
     0    0    0    0    0    0    (C11) 0    0    0    0    0      %11
     0    0    0    0    0    0    0    (C12) 0    0    0    0      %12
     0    0    0    0    0    0    0    0    (C13) 0    0    0      %13
     0    0    0    0    0    0    0    0    0    (C15) 0    0      %15
     0    0    0    0    0    0    0    0    0    0    (C16) 0      %16
     0    0    0    0    0    0    0    0    0    0    0    (C18)]; %18

%    2    6    7    8    9    10   11   12   13   15   16   18

% astar 2nd submatrix
  astar2=[-1  0  0  0  0  0  0  0  0  0  0  0  % 2
        0 -1  0  0  0  0  0  0  0  0  0  0  % 6
        0  0 -1  0  0  0  0  0  0  0  0  0  % 7
        0  0  0 -1  0  0  0  0  0  0  0  0  % 8
        0  0  0  0 -1  0  0  0  0  0  0  0  % 9
        0  0  0  0  0 -1  0  0  0  0  0  0  %10
        0  0  0  0  0  0 -1  0  0  0  0  0  %11
        1  0  0  0  0  0  0 -1  0  0  0  0  %12
        0  0  0  0  0  0  0  1 -1  0  0  0  %13
        0  0  0  0  0  0  1  0  0 -1  0  0  %15
        0  0  0  0  0  0  1  0  0  0 -1  0  %16
        0  0  0  0  0  0  0  0  0  0  1 -1]; %18

%         2  6  7  8  9 10 11 12 13 15 16 18

  I=12;
end

% all capacitors out
%     1  2  3  4  5  6  7  8  9 10 11 12 13 14 15 16 17 18
if C==[0  0  0  0  0  1  1  1  1  1  0  0  1  0  1  0  0  1],
  disp('in 7th if')
  pause;
  l1=[(L0Z1+L1Z3+L3Z6) (L0Z1+L1Z3)     (L0Z1+L1Z3)        (L0Z1+L1Z3)        L0Z1          L0Z1
L0Z1                  L0Z1                                  % 6
     (L0Z1+L1Z3)     (L0Z1+L1Z3+L3Z7) (L0Z1+L1Z3)        (L0Z1+L1Z3)        L0Z1          L0Z1
L0Z1                  L0Z1                                  % 7
     (L0Z1+L1Z3)     (L0Z1+L1Z3)     (L0Z1+L1Z3+L3Z5+L5Z8) (L0Z1+L1Z3+L3Z5)     L0Z1
L0Z1              L0Z1                  L0Z1                                  % 8
     (L0Z1+L1Z3)     (L0Z1+L1Z3)     (L0Z1+L1Z3+L3Z5)     (L0Z1+L1Z3+L3Z5+L5Z9) L0Z1
L0Z1              L0Z1                  L0Z1                                  % 9
     L0Z1          L0Z1          L0Z1            L0Z1            (L0Z1+L1Z4+L4Z10) L0Z1
(L0Z1+L1Z4)              L0Z1+L1Z4                                 %10
     L0Z1          L0Z1          L0Z1            L0Z1            L0Z1
(L0Z1+L1Z2+L2Z12+L12Z13) L0Z1                  L0Z1                                  %13
     L0Z1          L0Z1          L0Z1            L0Z1            (L0Z1+L1Z4)      L0Z1
(L0Z1+L1Z4+L4Z11+L11Z14+L14Z15) (L0Z1+L1Z4+L4Z11+L11Z14)                              %15
```

```
    L0Z1        L0Z1        L0Z1          L0Z1          (L0Z1+L1Z4)    L0Z1            0
(L0Z1+L1Z4+L4Z11+L11Z14+L14Z16+L16Z17+L17Z18)]; %18

%   6         7         8            9           10         13            15
18

% l 4th submatrix for all capacitors in place
  l4=[(C6) 0   0   0   0   0   0   0     % 6
     0   (C7) 0   0   0   0   0   0     % 7
     0   0   (C8) 0   0   0   0   0     % 8
     0   0   0   (C9) 0   0   0   0     % 9
     0   0   0   0   (C10) 0   0   0     %10
     0   0   0   0   0   (C13) 0   0     %13
     0   0   0   0   0   0   (C15) 0     %15
     0   0   0   0   0   0   0   (C18)]; %18

%   6   7   8   9   10   13   15   18

% astar 2nd submatrix
  astar2=[-1  0  0  0  0  0  0  0   % 6
        0 -1  0  0  0  0  0  0   % 7
        0  0 -1  0  0  0  0  0   % 8
        0  0  0 -1  0  0  0  0   % 9
        0  0  0  0 -1  0  0  0   %10
        0  0  0  0  0 -1  0  0   %13
        0  0  0  0  0  0 -1  0   %15
        0  0  0  0  0  0  0 -1]; %18

%       6  7  8  9 10 13 15 18

  I=8;
end

% calculate distances from harmonics to poles and zeroes
for G=1:I,
  DP5(G)=abs(5-P(G));
  DP7(G)=abs(7-P(G));
end

% get minimum distances
if min(DP5)<=min(DP7),
  dist5=min(DP5);
  M=5;
  else,
    dist7=min(DP7);
    M=7;
  end
end

L=round(rand*10);
while (L==0) | (L==8) | (L==9) | (L==10) | (L==K),
  L=round(rand*10);
end
  K=L;

end
% calculate distances from harmonics to poles and zeroes
  for G=1:(2*I),
```

```
    AP(I)=abs(5-abs(D(I,I)));
    BP(I)=abs(7-abs(D(I,I)));
    AZ(I)=abs(5-abs(E(I,I)));
    BZ(I)=abs(7-abs(E(I,I)));
  end

  if (min(AP)>=0.05) & (min(BP)>=0.05) & (min(AZ)==0) & (min(BZ)==0),
    K=0;
    elseif (min(AP)>=0.05) & (min(BP)>=0.05) & (min(AZ)==0) & (min(BZ)<=0.05),
      K=0;
      elseif (min(AP)>=0.05) & (min(BP)>=0.05) & (min(AZ)==0.05) & (min(BZ)<=0.05),
        K=0;
        elseif (min(AP)>=0.05) & (min(BP)>=0.05) & (min(AZ)==0.05) & (min(BZ)<=0),
          K=0;
          else,
            K=round(rand*10);
            while (K==0) | (K==8) | (K==9) | (K==10),
              K=round(rand*10);
            end
          end
        end
      end
    end
  end

end

% save results to file out.m
%for G=1:18,
%  fprintf('out.m','configuration space %10g\n',C(G));
%end
%fprintf('out.m','\n');
for G=1:I,
  fprintf('out.m','poles  %10g\n',P(G));
end
fprintf('out.m','\n');
for G=1:(I-1),
  fprintf('out.m','zeroes %10g\n',Z(G));
end
fprintf('out.m','\n');
%fprintf('out.m','minimum distance from harmonic to pole %10g\n',dist);
%fprintf('out.m','\n');
%fprintf('out.m','harmonic in question %10g\n',M);
%fprintf('out.m','\n');

% initialise the loop variables
c=100/0.9;
e=[0 0 0 0 0 0 0 0 0 0 0 0 0 0 0 0 0];
h=30;
row=0;
count2=1;
summag=0;
summagfeas=Inf;
magfeas=Inf;
freqfeas=Inf;

% the frequency is in per unit from 1Hz (1/60) to the h'th harmonic
w=1/60;
```

```
% current injections in per unit on nodes 8, 9 and 15
I=[0 0 0 0 0 0 0 1 1 0 0 0 0 0 1 0]';

% select the nodes for the output voltages,
% check nodes 10, 7 or 16
V=[0 0 0 0 0 0 0 0 0 1 0 0 0 0 0 0]';

% start the temperature loop for the optimisation
while c>0
  c=0.9*c

  % start the inner loop for the optimisation
  while row<20

    % do the first iteration for the inner loop
    if row==0

      % generate a random e vector for the first capacitor assignment
      while sum(e)<5
        f=round(rand*10)+6;
        % get equal probabilities for node 16
        if f==6
          f=16;
        end
        e(f)=1;
      end

      % write the first e to eused
      row=row+1;
      eused(row,:)=e;

      % get the indices for the 1's in e
      g=find(e);

      % calculate the magnitude for each frequency, start the frequency loop
      while w<=h

        % call ybusim without capacitors on
        [ymat,C]=ybusim(w,g);

        % calculate the correct y-bus for each capacitor assignment
        for i=1:5
          ymat(g(i),g(i))=ymat(g(i),g(i))+C(g(i));
        end

        % calculate the transfer function vector
        t=inv(ymat)*I;

        % select the correct voltages from the transfer function vector
        t1=t(V,:);

        % store the frequency and magnitude in matrices
        mag(count2)=abs(t1);
        freq(count2)=w;

        % add the magnitudes and store them in summag
        summag=summag+mag(count2);
```

```
        % change the loop variables
        w=w+1/60;
        count2=count2+1;
      end

      % calculate the constraints
      odd=max([mag(3),mag(5),mag(7),mag(9),mag(11),mag(13)]);
      even=max([mag(2),mag(4),mag(6),mag(8),mag(10),mag(12)]);

x14to25=max([mag(14),mag(15),mag(16),mag(17),mag(18),mag(19),mag(20),mag(21),mag(22),mag(23),mag(
24),mag(25)]);
      x26toh=max([mag(26),mag(27),mag(28),mag(29),mag(30)]);

      % update the objective function
      if summag<summagfeas & odd<1.5 & even<1.5 & x14to25<1.5 & x26toh<1.5
        summagfeas=summag;
        magfeas=mag;
        freqfeas=freq;
        efeas=e;
        disp('in 1')
      elseif exp((summagfeas-summag)/c)>random & odd<1.5 & even<1.5 & x14to25<1.5 & x26toh<1.5
        summagfeas=summag;
        magfeas=mag;
        freqfeas=freq;
        efeas=e;
        disp('in 2')
      else
        disp('in 3')
      end

      % update the loop variables
      count2=1;
      w=1/60;
      e=[0 0 0 0 0 0 0 0 0 0 0 0 0 0 0 0];
      summag=0;

    % do the other iterations for the inner loop
    else

      % generate subsequent e vectors for the capacitor assignments
      while sum(e)<5
        f=round(rand*10)+6;
        % get equal probabilities for node 16
        if f==6
          f=16;
        end
        e(f)=1;
        for i=1:row
          if e==eused(i,:)
            e=[0 0 0 0 0 0 0 0 0 0 0 0 0 0 0 0];
          end
        end
      end

      % write the e vectors to eused
      row=row+1;
      eused(row,:)=e;
```

```
% get the indices for the 1's in e
g=find(e);

% calculate the magnitude for each frequency, start the frequency loop
while w<=h

  % call ybusim without capacitors on
  [ymat,C]=ybusim(w,g);

  % calculate the correct y-bus for each capacitor assignment
  for i=1:5
    ymat(g(i),g(i))=ymat(g(i),g(i))+C(g(i));
  end

  % calculate the transfer function vector
  t=inv(ymat)*I;

  % select the correct voltages from the transfer function vector
  t1=t(V,:);

  % store the frequency and magnitude in matrices
  mag(count2)=abs(t1);
  freq(count2)=w;

  % add the magnitudes and store them in summag
  summag=summag+mag(count2);

  % change the loop variables
  w=w+1/60;
  count2=count2+1;
end

% calculate the constraints
odd=max([mag(3),mag(5),mag(7),mag(9),mag(11),mag(13)]);
even=max([mag(2),mag(4),mag(6),mag(8),mag(10),mag(12)]);

x14to25=max([mag(14),mag(15),mag(16),mag(17),mag(18),mag(19),mag(20),mag(21),mag(22),mag(23),mag(
24),mag(25)]);
x26toh=max([mag(26),mag(27),mag(28),mag(29),mag(30)]);

% update the objective function
if summag<summagfeas & odd<1.5 & even<1.5 & x14to25<1.5 & x26toh<1.5
  summagfeas=summag;
  magfeas=mag;
  freqfeas=freq;
  efeas=e;
  disp('in 1')
elseif exp((summagfeas-summag)/c)>random & odd<1.5 & even<1.5 & x14to25<1.5 & x26toh<1.5
  summagfeas=summag;
  magfeas=mag;
  freqfeas=freq;
  efeas=e;
  disp('in 2')
else
  disp('in 3')
end
```

```
      % update the loop variables
      count2=1;
      w=1/60;
      e=[0 0 0 0 0 0 0 0 0 0 0 0 0 0 0 0 0 0];
      summag=0;
    end
  end

  % reset variables
  row=0;
  eused=zeros(size(eused));
end

% write freqfeas and magfeas to 2 files
for i=1:1800
  fid=fopen('freq.txt','a');
  fprintf(fid,'\n %f',freqfeas(i));
  status=fclose(fid);
  fid=fopen('mag.txt','a');
  fprintf(fid,'\n %f',magfeas(i));
  status=fclose(fid);
end

% plot the data
%system_dependent(14, 'on');
plot(freqfeas,magfeas)
xlabel('Frequency In Per Unit')
ylabel('Voltage Magnitude At Bus 9 In Per Unit')
%system_dependent(14, 'off');



% initialise the loop variables
c=100/0.9;
e=[0 0 0 0 0 0 0 0 0 0 0 0 0 0 0 0 0 0];
h=30;
row=0;
count2=1;
summag=0;
summagfeas=Inf;
magfeas=Inf;
freqfeas=Inf;

% the frequency is in per unit from 1Hz (1/60) to the h'th harmonic
w=1/60;

% current injections in per unit on nodes 8, 9 and 15
I=[0 0 0 0 0 0 0 1 1 0 0 0 0 0 1 0]';

% select the nodes for the output voltages,
% check nodes 10, 7 or 16
V=[0 0 0 0 0 0 0 0 0 1 0 0 0 0 0 0]';

% start the temperature loop for the optimisation
while c>0
  c=0.9*c

  % start the inner loop for the optimisation
```

```
while row<20

  % do the first iteration for the inner loop
  if row==0

    % generate a random e vector for the first capacitor assignment
    while sum(e)<5
      f=round(rand*10)+6;
      % get equal probabilities for node 16
      if f==6
        f=16;
      end
      e(f)=1;
    end

e=[0 0 0 0 0 0 0 1 0 0 0 0 1 0 0 0];

    % write the first e to eused
    row=row+1;
    eused(row,:)=e;

    % get the indices for the 1's in e
    g=find(e);

    % calculate the magnitude for each frequency, start the frequency loop
    while w<=h

      % call ybusim without capacitors on
      [ymat,C]=ybusim(w,g);

      % calculate the correct y-bus for each capacitor assignment
      for i=1:2
        ymat(g(i),g(i))=ymat(g(i),g(i))+C(g(i));
      end

      % calculate the transfer function vector
      t=inv(ymat)*I;

      % select the correct voltages from the transfer function vector
      t1=t(V,:);

      % store the frequency and magnitude in matrices
      mag(count2)=abs(t1);
      freq(count2)=w;

      % add the magnitudes and store them in summag
      summag=summag+mag(count2);

      % change the loop variables
      w=w+1/60;
      count2=count2+1;
    end

    % calculate the constraints
    odd=max([mag(3),mag(5),mag(7),mag(9),mag(11),mag(13)]);
    even=max([mag(2),mag(4),mag(6),mag(8),mag(10),mag(12)]);
```

```
x14to25=max([mag(14),mag(15),mag(16),mag(17),mag(18),mag(19),mag(20),mag(21),mag(22),mag(23),mag(
24),mag(25)]);
      x26toh=max([mag(26),mag(27),mag(28),mag(29),mag(30)]);

      % update the objective function
      if summag<summagfeas & odd<1.5 & even<1.5 & x14to25<1.5 & x26toh<1.5
        summagfeas=summag;
        magfeas=mag;
        freqfeas=freq;
        efeas=e;
        disp('in 1')
      elseif exp((summagfeas-summag)/c)>random & odd<1.5 & even<1.5 & x14to25<1.5 & x26toh<1.5
        summagfeas=summag;
        magfeas=mag;
        freqfeas=freq;
        efeas=e;
        disp('in 2')
      else
        disp('in 3')
      end

      % update the loop variables
      count2=1;
      w=1/60;
      e=[0 0 0 0 0 0 0 0 0 0 0 0 0 0 0 0 0 0];
      summag=0;

disp('now')
pause

    % do the other iterations for the inner loop
    else

      % generate subsequent e vectors for the capacitor assignments
      while sum(e)<5
        f=round(rand*10)+6;
        % get equal probabilities for node 16
        if f==6
          f=16;
        end
        e(f)=1;
        for i=1:row
          if e==eused(i,:)
            e=[0 0 0 0 0 0 0 0 0 0 0 0 0 0 0 0 0 0];
          end
        end
      end

      % write the e vectors to eused
      row=row+1;
      eused(row,:)=e;

      % get the indices for the 1's in e
      g=find(e);

      % calculate the magnitude for each frequency, start the frequency loop
      while w<=h
```

```
        % call ybusim without capacitors on
        [ymat,C]=ybusim(w,g);

        % calculate the correct y-bus for each capacitor assignment
        for i=1:5
          ymat(g(i),g(i))=ymat(g(i),g(i))+C(g(i));
        end

        % calculate the transfer function vector
        t=inv(ymat)*I;

        % select the correct voltages from the transfer function vector
        t1=t(V,:);

        % store the frequency and magnitude in matrices
        mag(count2)=abs(t1);
        freq(count2)=w;

        % add the magnitudes and store them in summag
        summag=summag+mag(count2);

        % change the loop variables
        w=w+1/60;
        count2=count2+1;
      end

      % calculate the constraints
      odd=max([mag(3),mag(5),mag(7),mag(9),mag(11),mag(13)]);
      even=max([mag(2),mag(4),mag(6),mag(8),mag(10),mag(12)]);

x14to25=max([mag(14),mag(15),mag(16),mag(17),mag(18),mag(19),mag(20),mag(21),mag(22),mag(23),mag(
24),mag(25)]);
      x26toh=max([mag(26),mag(27),mag(28),mag(29),mag(30)]);

      % update the objective function
      if summag<summagfeas & odd<1.5 & even<1.5 & x14to25<1.5 & x26toh<1.5
        summagfeas=summag;
        magfeas=mag;
        freqfeas=freq;
        efeas=e;
        disp('in 1')
      elseif exp((summagfeas-summag)/c)>random & odd<1.5 & even<1.5 & x14to25<1.5 & x26toh<1.5
        summagfeas=summag;
        magfeas=mag;
        freqfeas=freq;
        efeas=e;
        disp('in 2')
      else
        disp('in 3')
      end

      % update the loop variables
      count2=1;
      w=1/60;
      e=[0 0 0 0 0 0 0 0 0 0 0 0 0 0 0];
      summag=0;
    end
```

```
  end

  % reset variables
  row=0;
  eused=zeros(size(eused));
end

% write freqfeas and magfeas to 2 files
for i=1:1800
  fid=fopen('freq.txt','a');
  fprintf(fid,'\n %f',freqfeas(i));
  status=fclose(fid);
  fid=fopen('mag.txt','a');
  fprintf(fid,'\n %f',magfeas(i));
  status=fclose(fid);
end

% plot the data
%system_dependent(14, 'on');
plot(freqfeas,magfeas)
xlabel('Frequency In Per Unit')
ylabel('Voltage Magnitude At Bus 9 In Per Unit')
%system_dependent(14, 'off');



function [rndm] = random
f=1;
while f==1
  f=rand;
end
rndm=f;



function[ymat,C]=ybusim(w,g)

% sepecify the values of all the input variables for the
% 16 bus network in admittances and with frequency for the y bus
% only the imaginary parts

% generators
% bases
% G1: Zb=18k*18k/270M=1.2
% G2: Zb=14.4k*14.4k/245M=0.846367346
% G3: Zb=15k*15k/260M=0.865384615
% G=1/(0+jwX)
G1 =1/(0          +i*2.04/1.2          *w);
G2 =1/(0          +i*1.70/0.846367346  *w);
G3 =1/(0          +i*2.39/0.865384615  *w);

% transformers
% bases
% Zb=230k*230k/270M=
% Zb=230k*230k/400M=
% Zb=132k*132k/250M=
% Zb=230k*230k/400M=
% Zb=230k*230k/260M=
```

```
% T=1/(0+jwX)
T1 =1/(0                +i*6.25/100    *w);
T2 =1/(0                +i*6.50/100    *w);
T3 =1/(0                +i*6.00/100    *w);
T4 =1/(0                +i*5.70/100    *w);
T5 =1/(0                +i*6.25/100    *w);

% transmission lines
% bases
% Zb=230K*230K/100M=529
% Zb=132k*132K/100M=174.24
% L=1/(l*(0+jwX))
L1 =1/(0                +i*0.401*10/529      *w);
L2 =1/(0                +i*0.401*20/529      *w);
L3 =1/(0                +i*0.401*35/529      *w);
L4 =1/(0                +i*0.401*30/529      *w);
L5 =1/(0                +i*0.401*33/529      *w);
L6 =1/(0                +i*0.418*30/529      *w);
L7 =1/(0                +i*0.410*15/174.24   *w);
L8 =1/(0                +i*0.450*17/174.24   *w);
L9 =1/(0                +i*0.403*11/174.24   *w);
L10=1/(0                +i*0.410*25/174.24   *w);
L11=1/(0                +i*0.410*25/174.24   *w);
L12=1/(0                +i*0.401*22/529      *w);
L13=1/(0                +i*0.401*30/529      *w);
L14=1/(0                +i*0.401*10/529      *w);

% capacitors
% bases
% Zb=230K*230K/100M=529
% Zb=132k*132K/100M=174.24
% C=0-jwX
C7 =-1*(0       -i*0.3      *w);
C8 =-1*(0       -i*0.3      *w);
C16=-1*(0       -i*0.3      *w);
C15=-1*(0       -i*0.3      *w);
C12=-1*(0       -i*0.3      *w);
C14=-1*(0       -i*0.3      *w);
C11=-1*(0       -i*0.3      *w);
C9 =-1*(0       -i*0.3      *w);
C13=-1*(0       -i*0.3      *w);
C10=-1*(0       -i*0.3      *w);

% initialise the y bus
ymat=zeros(16,16);

% write the actual values to the y bus
ymat( 1, 1)=G1+T1;
ymat( 1, 4)=-T1;
ymat( 2, 2)=G2+T3;
ymat( 2, 5)=-T3;
ymat( 3, 3)=G3+T5;
ymat( 3, 6)=-T5;
ymat( 4, 1)=-T1;
ymat( 4, 4)=T1+L1+L2;
ymat( 4, 7)=-L2;
ymat( 4, 8)=-L1;
ymat( 5, 2)=-T3;
```

```
ymat( 5, 5)=T3+L9+L10;
ymat( 5, 9)=-L9;
ymat( 5,10)=-L10;
ymat( 6, 3)=-T5;
ymat( 6, 6)=T5+L6+L12;
ymat( 6, 7)=-L6;
ymat( 6,15)=-L12;
ymat( 7, 4)=-L2;
ymat( 7, 6)=-L6;
ymat( 7, 7)=L2+L6+L3;
ymat( 7, 8)=-L3;
ymat( 8, 4)=-L1;
ymat( 8, 7)=-L3;
ymat( 8, 8)=L1+L3+L5+L4;
ymat( 8,12)=-L5;
ymat( 8,16)=-L4;
ymat( 9, 5)=-L9;
ymat( 9, 9)=L9+L8+L7;
ymat( 9,11)=-L8;
ymat( 9,13)=-L7;
ymat(10, 5)=-L10;
ymat(10,10)=L10+L11;
ymat(10,11)=-L11;
ymat(11, 9)=-L8;
ymat(11,10)=-L11;
ymat(11,11)=L8+L11+T2;
ymat(11,12)=-T2;
ymat(12, 8)=-L5;
ymat(12,11)=-T2;
ymat(12,12)=L5+T2;
ymat(13, 9)=-L7;
ymat(13,13)=L7+T4;
ymat(13,14)=-T4;
ymat(14,13)=-T4;
ymat(14,14)=T4+L13;
ymat(14,15)=-L13;
ymat(15, 6)=-L12;
ymat(15,14)=-L13;
ymat(15,15)=L12+L13+L14;
ymat(15,16)=-L14;
ymat(16, 8)=-L4;
ymat(16,15)=-L14;
ymat(16,16)=L4+L14;

C=[0 0 0 0 0 0 C7 C8 C9 C10 C11 C12 C13 C14 C15 C16];
```